AQUEOUS CHEMISTRY OF MOLYBDENUM AT ELEVATED

TEMPERATURES AND PRESSURES

WITH APPLICATIONS TO

PORPHYRY MOLYBDENUM DEPOSITS

by

Robert W. Smith

Aqueous Chemistry of Molybdenum at Elevated
Temperatures and Pressures
with Applications to
Porphyry Molybdenum Deposits

Robert W. Smith
May 1983

## ABSTRACT

The principle of corresponding states has been extended to include techniques which allow the accurate prediction of partial molal quantities for anions at elevated temperatures and pressures. In addition, the same relationships have been demonstrated for entropies of dissociation for fluoride and hydroxide complexes and oxy-acids. The use of the correspondence principle and equations of state for ions and aqueous dissociation reactions which explicitly account for electrostatic and nonelectrostatic contributions to thermodynamic behavior, allow the thermodynamic properties of reactions and ions to be predicted at temperatures and pressures up to 600°C and 5000 bars.

These techniques were used to estimate the dissociation constants for 26 fluoride complexes of alkaline earth ions, divalent first-row transition ions, divalent tin and lead, and iron (III) and aluminum at temperatures up to 300°C in steam saturated water. Evaluation of the stability of these complexes in hydrothermal and geothermal fluids indicates that fluoride complexing is not important in the transport of divalent metals at elevated temperatures. However, fluoride complexes of aluminum are important in the transport of this ion at elevated temperatures.

Theoretical calculations of the thermodynamic properties of the molybdate ion coupled with reported thermodynamic properties of molybdenum minerals allow calculations of equilibrium constants for

reactions involving the molybdate ion at temperatures and pressures of up to 600°C and 5000 bars. In addition, predicted dissociation constants of hydrolysis species and chloride complexes of molybdenum (V) and (VI) as well as fluoride and sulfide complexes of molybdenum (VI) allow the calculation of mineral solubilities which are consistent with experimental measurements.

Calculations of molybdenum speciation at elevated temperatures and pressures indicate that at neutral pH's the bimolybdate ion predominates. However, $MoO_3F^-$ becomes the predominate solution species if the fugacity of hydrogen fluoride exceeds $10^{-1.5}$. Chloride complexes and cationic species of molybdenum (VI) are not important in the transport of molybdenum. In acid solutions molybdenum (V) species become significant. Sulfide complexes may be significant if the molality of hydrogen sulfide exceeds $10^{-1.5}$.

Light, stable-isotope and fluid inclusion studies of the 23 million year old Questa molybdenite deposit located in the Sangre de Cristo Mountains of northern Toas County, New Mexico have been done. The results of these studies indicate that early, high-temperature (+550°C), hypersaline (40 to 70 eq. wt. % sodium chloride), magmatic fluids ($\delta^{18}O$ = +7.7 per mil) with KCl/NaCl ratios of greater than 0.20 were derived from a shallow (1000 to 1600 meters deep) crystallizing granite intrusive. The reactions of these fluids with the andesite volcanic rocks produced barren quartz and quartz-biotite veins. In addition, fluorine-rich biotite and molybdenite ("clotty-moly") mineralization resulted from wall rock reactions involving the early fluids and the andesites. Later, quartz-molybdenite vein mineralization occurred as a

result of adiabatic decompression of lower-temperature (350 to 450°C), halite-saturated fluids with KCl/NaCl ratios of less than 0.20 and hydrogen sulfide concentrations of 0.03 molal. These fluids were mixtures of magmatic and meteoric water (40 to 70 % magmatic) and had compositions which were consistent with potassic alteration. Pyrite-quartz±molybdenite vein mineralization associated with sericitic alteration was deposited from hydrogen sulfide rich (0.4 molal) fluids at temperatures of less than 350°C. The oxygen-18 composition of these fluids was similar to the fluids associated with the quartz-molybdenite mineralization. This similarity implies that the two fluids were derived from a similar source, but underwent different chemical histories.

Isotopic disequilibrium between quartz and K-feldspar, as well as low $\delta D$ values (approximately -115 per mil) for hydrothermal biotites, indicate a late influx of surface-derived meteoric waters into the hydrothermal system. This influx may have been the result of hydrothermal activity associated with the Deep Granite system which postdates the mineralization studied.

Theoretical calculations indicate that the reactions of potassium- and fluoride-rich fluids with the andesities to produce fluorine-rich biotite would result in molybdenite mineralization due to a decrease in fluoride activity and a destablization of molybdenum fluoride complexes. Furthermore, calculations indicate that molybdenite solubility is retrograde above approximately 450°C which means that mineralization resulting from a temperature decrease, such as the quartz-molybdenite veins, would occur only at temperatures of less than 450°C. The

calculated solubility of molybdenite is 800 ppm molybdenum at 400°C in fluids such as those associated with the quartz-molybdenite veins, while fluids such as those associated with pyrite-quartz veins have calculated solubilities of less than 1 ppm molybdenum.

The results of this study indicate that models describing the thermodynamic properties of aqueous species can be used with confidence in evaluating the transport and deposition of molybdenum from fluids associated with porphyry molybdenum deposits. Furthermore, these techniques can be used for calculations in other hydrothermal and geothermal systems for which appropriate experimental measurements are not available.

# ACKNOWLEDGMENT

# TABLE OF CONTENTS

## LIST OF FIGURES

x

LIST OF TABLES

CHAPTER 1

SOLUTION CHEMISTRY OF MOLYBDENUM

SIGNIFICANCE OF THE PROBLEM

PURPOSE

The formation of geochemical anomalies known as ore deposits involves complex geologic and geochemical processes. These geochemical processes may conveniently be divided into three parts. These are:

1)  Source of the metals. Where did the metals of interest come from? Are they derived from a pluton, leached from surrounding rocks, or from some other source?

2)  Transport of metals. How did the metal get from the source to the location of the deposit? In the class of deposits, which can loosely be defined as 'hydrothermal', the metals were transported in an aqueous fluid. The question then becomes, what complexes were important to the transport?

3)  Deposition of metals. What physico-chemical processes brought about ore mineral deposition? What were the effects of pressure and temperature changes? What was the role of boiling or wall rock reactions?

The thrust of this study was to evaluate numbers two and three listed above for porphyry molybdenum deposits.

STATEMENT OF PROBLEM

The primary use of molybdenum is in metallurgical applications for steels, cast irons and high alloy steels. As of 1978, 90% of molybdenum consumption was for metallurgical applications, with the remaining

consumption in chemical and non-metallurgical applications (Elevatorski, 1979). Production figures for the year 1978 indicated that 50% (Elevatorski, 1981) of world molybdenum production was from porphyry deposits in which molybdenum was the primary recoverable metal. Another 46% of world molybdenum production was as a byproduct of porphyry copper production, with the remaining 4% as a byproduct of lead-zinc production and Mo-bearing tactites recovered primarily for tungsten (Elevatorski, 1981).

In North America, which accounts for 74% of world production, over 99% of the production was from porphyry deposits. Because of the great importance of porphyry deposits, this study is devoted exclusively to the evaluation of molybdenum transport in hydrothermal solutions associated with porphyry deposits.

Porphyry molybdenum deposits may be conveniently classified based on the rock type. The first group are the granite or Climax-type deposits. These deposits are associated with hypabyssal granites, aplites and rhyolite porphyries. In addition, multiple mineralizing events are commonly recognized in these deposits. Futhermore, these rocks are rich in fluorine, as evidenced by the abundance of fluorine bearing phases. The second group is referred to as quartz monzonite type deposits. This group has also been classified as calc-alkalic-type deposits (Westra and Keith, 1981). Westra and Keith (1981) presented trace element and other data which suggests that the quartz monzonite-type deposits are molybdenum-rich end members of a continuum of deposits which range from porphyry molybdenum to porphyry copper deposits. The quartz monzonite-type deposits are characterized by quartz monzonites, granodiorites and granites. The fluorine content, as

well as the molybdenum grades are lower for the quartz monzonite-type deposits. Multiple ore events are not common for this type of deposit.

Climax-type porphyry molybdenum deposits, unlike porphyry copper-molybdenum deposits, are characterized by significant amounts of fluorine-rich mineralization including fluorite, topaz and fluorine-rich micas. Gunow et al. (1980) have determined the log $f_{H_2O}/f_{HF}$ ratios for hydrothermal solutions associated with the Henderson, CO molybdenite deposit from the fluorine content of micas. Their work suggests a steep gradient of the log $f_{H_2O}/f_{HF}$ ratio, with the most fluorine rich solutions being associated with the highest grade molybdenite minerali-zation. Furthermore, Munoz (1980) concluded that $f_{HF}/f_{HCl}$ ratios of hydrothermal fluids associated with the Henderson deposit were ten times higher than for fluids associated with the Santa Rita, NM porphyry copper deposit. Thus, assuming $f_{HCl}$ similar for both deposits, these results suggest that hydrothermal solutions associated with porphyry molybdenum mineralization may be richer in fluorine than fluids associated with porphyry copper mineralization.

Although porphyry copper-molybdenum and Climax-type porphyry molybdenum deposits appear to be similar in some respects (e.g., association with intrusive rocks, possibly temperature of formation), they are undoubtedly different in others. Most importantly here is the mechanism of hydrothermal transport. The apparent continuum between porphyry copper deposits and quartz monzonite-type porphyry molybdenum deposits does not require that the transport mechanism for molybdenum and copper be the same. The chemistries of copper and molybdenum are sufficiently different so as to suggest that aqueous speciation of these elements will not be similarly affected by similar processes. For

example, copper typically exists in solution as a cation (with or without complexing ligands) at low temperatures, whereas molybdenum (VI) exists as an oxy-acid ($MoO_4^{2-}$, $HMoO_4^-$, etc.). The anionic nature of molybdenum (VI) is not consistent with the formation of chloride complexes, except in extremely acid solutions (Griffith and Wickins, 1967). In contrast, however, chloride complexes of copper have been shown to be the most important mechanism by which copper is transported in hydrothermal fluids.

Crerar and Barnes (1976) have provided the experimental work necessary to better understand the conditions most favorable for copper transport and precipitation in hydrothermal solutions. These data can be integrated with appropriate field measurements to yield useful information on the mechanism of copper mineralization in, for example, a porphyry copper terrain. Analogous data for the molybdenum system, however, are not available. Thus, numerous, relatively unconstrained models have been proposed to account for the transport of aqueous molybdenum species in hydrothermal fluids. For example, sulfide complexes (Arutyunyan, 1966), silica complexes (Khitarov et al., 1965), fluoride and hydroxide complexes (Smith et al., 1980) and chloride complexes (Westrich, 1974) have all been proposed as important mechanisms of molybdenum transport in high temperature aqueous electrolyte solutions.

APPROACH

The use of equilibrium thermodynamics to evaluate the mechanism of water-rock interactions currently represents one of the most useful methods to determine how metals are transported in solutions. Helgeson

and Aagaard (1979) have indicated that at temperatures greater than 200°C, equilibrium between an aqueous phase and minerals is on the order of hours or days, instantaneous compared to the length of tens of thousands of years (Norton and Knight, 1977) for a hydrothermal event associated with magmatism. However, in order to use equilibrium thermodynamics, a complete knowledge of the standard thermodynamic functions for all solid, aqueous and gaseous phases and species is required. In addition, the intensive variables (typically temperature and pressure) must also be defined.

The thermodynamic properties of a large number of common gases and minerals have been determined over a wide temperature range (e.g., Robie et al., 1978). However, the coverage of aqueous ions and solution species is much more limited. In order to fully evaluate the role of the aqueous phase in metal transport and precipitation, the thermodynamic properties of solution species must be determined. These properties may be determined by several methods. Some of these methods are:

1) Experimentally determining the partial molal heat capacities and volumes of aqueous electrolytes. This information, coupled with the thermodynamic relationships among volume, entropy, heat capacity, and Gibbs free energy, allows the desired information to be derived.

2) Potentiometric titrations.

3) Solubility studies of sparingly soluble salt in solutions of a complexing ligand.

4) Conductivity measurements of solutions of weak electrolytes.

5) Estimation of the property of interest using a model with valid assumptions.

The first four methods outlined above allow the determination of the thermodynamic properties of interest from experimental measurements. Methods based on careful experimental work are much better than estimates. However, no one experimental method can be used to determine all the thermodynamic parameters for an aqueous solution. For example, the partial molal volume and heat capacity of an ion may be determined from density and heat of solution measurements, whereas the Gibbs free energy of an ion is determined from solubility measurements. As a consequence, several different types of experimental measurements must be made to determine the thermodynamic properties of a single ion. The only method which has the potential to allow the derivation of a large amount of thermodynamic data over the temperature and pressure range of hydrothermal ore deposits is the use of estimates. Helgeson (1964) demonstrated the validity of the approach for several systems of geologic interest. Furthermore, a through theoretical evaluation of a hydrothermal system may indicate which complexes are significant in the transport of metals. This knowledge can be used to plan experimental hydrothermal solubility studies.

The approach chosen in this study of molybdenum solution species is the use of estimates based on theoretical evaluations of the behavior of aqueous electrolyte solutions. For a system such as molybdenum, where very little experimental work has been done, estimates prove to be the most valuable technique to derive the large amount of thermodynamic data needed for a study of this type. During this study, the dissociation constants for over 40 aqueous species at elevated temperatures were determined. Although these estimates may require some revision as experimental results become available, the results presented here allow

significant conclusions to be made about the role of both molybdenum and fluoride complexes in hydrothermal solutions.

ORGANIZATION

This work may be broken into two parts. The first portion, covering Chapters 2 through 7, deals with the derivation of the thermodynamic properties of molybdenum minerals and solution species of both molybdenum and fluorine. Also presented is an evaluation of the transport of molybdenum in hydrothermal solutions associated with porphyry molybdenum deposits. Presented in the second portion of this dissertation (Chapter 8) are the results of a preliminary fluid inclusion, light, stable-isotope and gas study of Molycorp's Questa mine. Information derived from the observations of Questa material, along with pertinent chemical information for porphyry molybdenum deposits presented in the literature, allows modeling of hydrothermal solutions which are consistent with geologic observations.

# CHAPTER 2

## REVIEW OF THERMODYNAMIC RELATIONSHIPS

### STANDARD STATES

The thermodynamic properties of minerals, gases and ions can be calculated at elevated temperatures and pressures from the relationships among volume, pressure, temperature and the energetics of the system. In addition, a clear definition of the standard states for ion, gases, minerals and water is necessary.

### MINERALS

The standard state for minerals and solids of stoichiometric composition is defined as unit activity for the phase at all temperatures and pressures.

### GASES

The standard state for a gas is defined in terms of ideal gas law behavior at one bar pressure and any temperature. This differs from solids in that the effects of pressure are not implicitly incorporated into the standard state definition.

### IONS AND ELECTROLYTES

A hypothetical one molal solution with properties at infinite dilution at any temperature and pressure is defined to have unit activity. In addition, all thermodynamic properties for the hydrogen ion are defined as zero at all temperatures and pressures.

WATER

The standard state for water chosen in this study is liquid water at all pressures above or on the boiling curve. Pure water is defined as having unit activity at all temperatures and pressures. Water could alternately be defined in terms of a gas (see above).


APPARENT AND STANDARD FUNCTIONS

Throughout this study, apparent Gibbs free energies and enthalpies are used at all temperatures and pressures other than 298.15 K and 1 bar. Apparent functions differ from standard functions in that the Gibbs free energies and enthalpies of formation of the elements are defined as zero only at 298.15 K and 1 bar (apparent functions), rather than being defined as zero at all temperatures and pressures (standard functions). The apparent Gibbs free energy and enthalpy of formation is defined by (Helgeson et al., 1978):

$$\Delta G°(T,P) \equiv \Delta G°_f + (G°(T,P) - G°(T_r,P_r)) \qquad 2.1$$

$$\Delta H°(T,P) \equiv \Delta H°_f + (H°(T,P) - H°(T_r,P_r)) \qquad 2.2$$

where

$$G°(T,P) - G°(T_r,P_r) = -S°(T_r,P_r) \times (T-T_r)$$

$$+ \int_{T_r}^{T} C°_p \, dT - T \int_{T_r}^{T} C°_p \, d\ln T + \int_{P_r}^{P} V°(T) \, dP \qquad 2.3$$

and

$$H°(T,P) - H°(T_r,P_r) = \int_{T_r}^{T} C°_p \, dT + \int_{P_r}^{P} (V°(T) - T(\partial V°/\partial T)_p) \, dP \qquad 2.4$$

where T is the temperature in K and P is the pressure in bars, $\Delta H^\circ_f$ and $\Delta G^\circ_f$ are the standard molal Gibbs free energy and enthalpy of formation from the elements at $T_r$ (298.15 K) and $P_r$ (1 bar), $G^\circ(T,P)$, $G^\circ(T_r,P_r)$, $H^\circ(T_r,P_r)$, $S^\circ(T_r,P_r)$, $C^\circ_p$ and $V^\circ(T)$ are the apparent molal Gibbs free energies, enthalpies, entropy, heat capacity and volume at the subscripted temperature and pressure. The corresponding equation for standard molal entropy at a given pressure and temperature is:

$$S^\circ(T,P) - S^\circ(T_r,P_r) = \int_{T_r}^{T} C^\circ_p \, d\ln T - T\int_{P_r}^{P}((\partial V^\circ/\partial T)_p)_T \, dP \quad 2.5$$

## MINERALS AND SOLIDS

### HEAT CAPACITY

The standard molal heat capacities of minerals or gases at one bar total pressure and temperatures greater than 298.15 K can be represented by the Maier-Kelley (Kelley, 1960) power function:

$$C^\circ_p = a + bT + cT^{-2} \quad 2.6$$

where a, b and c are temperature independent fit coefficients derived by regression of experimental heat capacities. Although higher order power functions have been employed by some investigators (Haas and Fisher, 1976 and Robie et al., 1978) to represent heat capacity measurements, equation 2.6 yields fits of experimental heat capacities to within 0.1 cal mole$^{-1}$ K$^{-1}$ or less for most minerals (Helgeson et al., 1978). The error resulting from fits of equation 2.6 to heat capacities of minerals with high Debye temperatures may exceed 1 cal mole$^{-1}$ K$^{-1}$. However, such large discrepancies are rare (Helgeson et al., 1978).

VOLUME

The data of Skinner (1966) indicates that, with the exception of alkali metal halides, the thermal expansion of minerals is five percent or less at 600°C. Most silicates have thermal expansions of about one percent at 600°C. Since temperature and pressure are typically related in geologic processes, and thermal expansion and compressibility have opposite effects on volume, assuming the volume of a solid to be independent of temperature and pressure will not introduce significant error into the calculated apparent molal Gibbs free energies.

INTEGRATED EQUATIONS

Integration of equations 2.3 to 2.5 using equation 2.6, and the assumption that standard molal volumes are temperature and pressure independent, yields:

$$G°(T,P) - G°(T_r,P_r) = -S°(T_r,P_r) \times (T-T_r) + a(T-T_r-T\ln(T/T_r))$$
$$- [(bTT_r^2+c)(T-T_r)^2]/(2TT_r^2) + V° \times (P-P_r) \qquad 2.7$$

$$H°(T,P) - H°(T_r,P_r) = a(T-T_r) + b(T^2-T_r^2)/2$$
$$- c(T^{-1}-T_r^{-1}) + V° \times (P-P_r) \qquad 2.8$$

and

$$S°(T,P) - S°(T_r,P_r) = a\ln T/T_r + b(T-T_r) - c(T^{-2}-T_r^{-2})/2 \quad 2.9$$

Using equations 2.1, 2.2, and 2.7 through 2.9, the thermodynamic properties of minerals at any temperature and pressure may be calculated from room temperature Gibbs free energies and enthalpies of formation, entropies and volumes using appropriate heat capacities.

GASES

Equations 2.1 and 2.3 are general equations, and are independent of the state of matter for a substances. As was mentioned earlier, the Maier-Kelley power function (equation 2.6) may be used to represent the heat capacity of gases. Evaluation of the last integral in equation 2.3 for real gases yields (Klotz and Rosenburg, 1972):

$$RT\ln[f(T,P)/f(T,P_r)] \quad = \quad \int_{P_r}^{P} V° dP \qquad\qquad 2.10$$

where R is the gas constant and $f(T,P)$ and $f(T,P_r)$ are the fugacities at the subscripted pressures and temperature. The fugacity of a gas is given by:

$$f(T,P) \quad = \quad \varphi(T,P) \times P \qquad\qquad 2.11$$

where $\varphi(T,P)$ is the fugacity coefficient. If the standard state for a gas is defined as unit fugacity at any temperature at the reference pressure, and the standard state partial pressure of a gas is equal to the reference pressure, then equation 2.10 becomes:

$$RT\ln \varphi(T,P) \quad = \quad \int_{P_r}^{P} V° \; dP \qquad\qquad 2.12$$

Integration of equation 2.3 using equations 2.6 and 2.12 yields:

$$G°(T,P) - G°(T_r,P_r) = -S°(T_r,P_r) \times (T-T_r) + a(T-T_r-T\ln(T/T_r))$$
$$- [(bTT_r^2+c)(T-T_r)^2]/(2TT_r^2) + RT\ln\varphi(T,P) \qquad\qquad 2.13$$

Equation 2.13 may be used to evaluate the change in the apparent Gibbs free energy of formation for gases resulting from a change in temperature and pressure.

Evaluation of fugacity coefficients ($\varphi(T,P)$) is dependent on the choice of an appropriate equation of state. The ideal gas law, while commonly used, is not adequate to describe the P-T-V° properties of real gases except over a limited range of pressures (less than 100 bars for most gases) at temperatures greater than 298.15 K. For this reason, Redlich and Kwong's (1948) modification of the ideal gas equation was used in this study to calculate the P-T-V° relationships for gases. The utility of the Redlich-Kwong equation in evaluating geologic problems is evident by the number of investigators who have used this equation in recent investigations (Holloway, 1977; Flower, 1979; and Jacob and Kerrick, 1981).

The Redlich-Kwong equation can be stated as:

$$P = RT/(V°-b) - a/(V°^2+bV°)T^{\frac{1}{2}} \qquad 2.14$$

where a is a measure of attractive force between the gas molecules, and b is a measure of the volume of the molecules of the gas. It is more convenient to cast the equation in terms of compressibility (Z). Compressibility for a gas is defined as:

$$Z = PV°/RT \qquad 2.15$$

The value of Z for an ideal gas is one, and Z for real gases is an indication of the extent of departure from ideal behavior. Rearrangement of equation 2.14 yields:

$$Z = 1/(1-h) - (A^2/B)h/(1+h) \qquad 2.16a$$

$$A^2 = a/R^2T^{2.5} = 0.4287T_c^{2.5}/P_cT^{2.5} \qquad 2.16b$$

$$B = b/RT = 0.0867T_c/P_cT \qquad 2.16c$$

$$h = BP/Z = b/V° \qquad 2.16d$$

where $T_c$ and $P_c$ are the critical temperatures and pressures of the gas

of interest. Critical constants for a wide variety of gases have been summarized by Matthews (1972).

The fugacity coefficient for a gas may be calculated from Redlich and Kwong (1948):

$$\ln\varphi = \int_0^P (Z-1)\, d\ln P = Z - 1 - \ln(Z-BP) - (A^2/B) \times \ln(1+h) \qquad 2.17$$

In practice geologic calculations are done at some fixed temperature and pressure. This requires evaluation of equation 2.14 for $V°$. This may be readily accomplished by the use of Newton's method. Once $V°$ is known, Z can be calculated from equation 2.15 and the integral in equation 2.12 can be evaluated using equations 2.17 and 2.16a through 2.16d.

## AQUEOUS IONS

Work by Helgeson and others (Helgeson and Kirkham, 1976, Walther and Helgeson, 1978 and Helgeson et al., 1981) has led to equations of state describing the volumes and heat capacities of aqueous electrolytes, individual ions and polar neutral species. These equations are based on the separation of volume and heat capacity into electrostatic and nonelectrostatic terms.

The equation of state developed by Helgeson and Kirkham (1976) to represent the partial molal volume of an aqueous species at infinite dilution is:

$$V°(T,P) = \sigma(P) + \xi(P)T/(T-\theta) - \omega Q(T,P) \qquad 2.18$$

where $\sigma(P)$ and $\xi(P)$ are temperature independent coefficients, $\omega$ is an electrostatic coefficient and $\theta$ is a temperature and pressure independent coefficient. The Born function, $Q(T,P)$, is defined by:

$$Q(T,P) \equiv \varepsilon(T,P)^{-1} \times (\partial \ln \varepsilon / \partial P)_T \qquad 2.19$$

where $\varepsilon(T,P)$ is the dielectric constant for water at the subscripted temperature and pressure.

The pressure dependence of $\sigma(P)$ and $\xi(P)$ are represented by:

$$\sigma(P) = a_1 + a_2 P \qquad 2.20a$$
$$\xi(P) = a_3 + a_4 P \qquad 2.20b$$

where $a_1$, $a_2$, $a_3$ and $a_4$ are pressure and temperature independent coefficients describing the nonelectrostatic volume of an ion or electrolyte.

The analogous equation for heat capacity is (Walther and Helgeson, 1978 and Helgeson et al., 1981):

$$C°_p(T,P_r) = c_1 + c_2 T/(T-\theta) + \omega T X(T,P_r) \qquad 2.21$$

where $c_1$ and $c_2$ are temperature and pressure independent coefficients

analogous to $\sigma(P)$ and $\xi(P)$ in equation 2.18. The Born function, $X(T,P)$, is defined by:

$$X(T,P) \equiv \varepsilon(T,P)^{-1} \times [(\partial^2 \ln /\partial T^2)_p - (\partial \ln \varepsilon /\partial T)_p{}^2] \qquad 2.22$$

Integration of equation 2.3 using equations 2.18 and 2.21 yields:

$$\text{(see facing page)} \qquad 2.23$$

where

$$Y(T,P) \equiv \varepsilon(T,P)^{-1} \times (\partial \ln \varepsilon /\partial T)_p \qquad 2.24$$

and

$$Z(T,P) \equiv -\varepsilon(T,P)^{-1} \qquad 2.25$$

Integration of equations 2.4 and 2.5 yields:

$$\text{(see facing page)} \qquad 2.26$$

and

$$\text{(see facing page)} \qquad 2.27$$

In addition, the standard molal heat capacity may be expressed as:

$$C^\circ{}_p(T,P) = c_1 + c_2 T/(T-\theta)$$
$$- T(2a_3(P-P_r)+a_4(P^2-P_r{}^2))/(T-\theta)^3 + \omega T X(T,P) \qquad 2.28$$

EQUATION 2.23

$$G^o(T,P) - G^o(T_r,P_r) = -S^o(T_r,P_r) \times (T-T_r) + c_1(T-T_r-T\ln(T/T_r))$$

$$-c_2\left[T-T_r-(T-\theta)\ln\left(\frac{T-\theta}{T_r-\theta}\right)\right] +$$

$$\frac{2(a_1(T-\theta) + a_3T)(P-P_r) + (a_2(T-\theta) + a_4T)(P^2-P_r^2)}{2(T-\theta)}$$

$$-\omega(Z(T,P) - Z(T_r,P_r) - Y(T_r,P_r) \times (T-T_r))$$

EQUATION 2.26

$$H^o(T,P) - H^o(T_r,P_r) = (c_1 + c_2)(T-T_r) + c_2\theta\ln\left(\frac{T-\theta}{T_r-\theta}\right) +$$

$$a_1(P-P_r) + a_2(P^2-P_r^2)/2 +$$

$$\frac{2a_3T(P-P_r) + a_4T(P^2-P_r^2)}{2(T-\theta)} +$$

$$\frac{2\theta a_3T(P-P_r) + \theta a_4T(P^2-P_r^2)}{2(T-\theta)^2} +$$

$$\omega(TY(T,P) - T_rY(T_r,P_r) - Z(T,P) + Z(T_r,P_r))$$

EQUATION 2.27

$$S^o(T,P) - S^o(T_r,P_r) = c_1\ln(T/T_r) + c_2\ln\left(\frac{T-\theta}{T_r-\theta}\right) +$$

$$\frac{\theta(2a_3(P-P_r) + a_4(P^2-P_r^2))}{2(T-\theta)^2} +$$

$$\omega(Y(T,P) - Y(T_r,P_r))$$

## EQUILIBRIUM CONSTANTS

The equations presented in this chapter, along with the thermodynamic properties of ions, gases and minerals at 298.15 K (Helgeson et al., 1978; Walther and Helgeson, 1978 and Helgeson et al., 1981) and equations describing the electrostatic properties of water (Helgeson and Kirkham, 1974a), can be used to calculate the apparent molal properties of ions, minerals and gases at elevated temperatures and pressures.

The Gibbs free energy of reaction, $\Delta G°_r(T,P)$, may be calculated from:

$$\Delta G°_r(T,P) = \sum \hat{n}_i \Delta G°_i(T,P)$$  2.29

where $\hat{n}_i$ is the stoichiometric reaction coefficient (positive for products and negative for reactants) for the ith species in a chemical reaction, and $\Delta G°_i(T,P)$ is the apparent Gibbs free energy of formation for the ith species. Calculation of other thermodynamic properties of reaction (entropy, enthalpy, etc.) are accomplished using expressions analogous to equation 2.29.

Finally, equilibrium constants may be calculated from:

$$\Delta G°_r(T,P) = -2.303RT\log K(T,P)$$  2.30

A computer code, SUPCRT (Helgeson et al., 1978), incorporating the above equations, was used extensively in this study to calculate equilibrium constants for reactions involving minerals, gases and aqueous ions at temperatures and pressures of up to 600°C and 5000 bars.

CHAPTER 3

THERMODYNAMIC PROPERTIES OF MOLYBDENUM MINERALS AND THE MOLYBDATE ION

MOLYBDENUM MINERALS

Table 3.1 contains the standard Gibbs free energies and enthalpies of formation, the third law entropies and the molal volumes at 298.15 K for the five molybdenum minerals considered in this study. In addition, the coefficients for the Maier-Kelley heat capacity power function for these minerals are included in this table.

MOLYBDENITE

The enthalpy of formation for molybdenite is listed in NBS 270-4 (Wagman et al., 1968) as -56.2 kcal mole$^{-1}$. However, fluorine-bomb calorimetry by O'Hare et al. (1970) has yielded a value of -65.8 ± 1.5 kcal mole$^{-1}$ for $\Delta H^{\circ}_{f}$. These authors evaluated several high temperature investigations of molybdenite using estimated Gibbs free energy functions and found reasonable agreement between their work and previous investigations. Figure 3.1 indicates that there is excellent agreement among the enthalpies of formation determined by different investigators. A value of -66.469 kcal mole$^{-1}$ (Schaefer and Goken, 1980) was selected as the enthalpy of formation for molybdenite used in this study.

WULFENITE

The heat capacity of wulfenite at high temperatures has not been measured. As a result, it was necessary to estimate the temperature dependence of the heat capacity of wulfenite. The estimates were based on the assumption proposed by Helgeson et al. (1978):

$$C^{\circ}_{p}(PbMoO_4) = C^{\circ}_{p}(CaMoO_4) - C^{\circ}_{p}(CaO) + C^{\circ}_{p}(PbO) \qquad 3.1$$

Table 3.1

Summary of thermodynamic data for molybdenum minerals at 298.15 K and 1 atmosphere (1.013 bars) pressure.

| Name | Formula | $V^{o,a}$ | $S^{o,b}$ | $\Delta H^o_f$ [c] | $\Delta G^o_f$ [c] | $C^o_p$ Coefficients[d] $a$ | $b \times 10^3$ | $c \times 10^{-5}$ | $T_t^e$ |
|---|---|---|---|---|---|---|---|---|---|
| Powellite | $CaMoO_4$ | 47.0 | 29.3 | -369.50 | -344.01 | 33.52 | 5.80 | -6.91 | 1300 |
| Wulfenite | $PbMoO_4$ | 53.86 | 39.7 | -247.96 | -223.93 | 37.79 | 7.13 | -6.71 | 762 |
| | | | | | | 32.03 | 8.15 | -5.24 | 1170 |
| Molybdite | $MoO_3$ | 30.56 | 18.58 | -178.10 | -159.69 | 17.97 | 7.80 | -2.10 | 1074 |
| Molybdenum Dioxide | $MoO_2$ | 19.58 | 11.95 | -140.50 | -127.42 | 14.11 | 5.82 | -2.18 | 1800 |
| Molybdenite | $MoS_2$ | 32.02 | 14.95 | -66.47 | -64.36 | 17.14 | 1.78 | -2.20 | 1200 |

[a] $cm^3$ mole$^{-1}$. [b] cal mole$^{-1}$ K$^{-1}$. [c] Kcal mole$^{-1}$. [d] Maier-Kelly power function coefficients for equation 2.6. [e] Upper temperature limit in K for the heat capacity power function coefficients. Lower limit is 298.15 K except where more than one set of heat capacity coefficients are given. In the latter case, the lower limit of the first set is 298.15 K, but the subsequent sets correspond to $T_t$ for the preceding set.

SOURCES OF DATA

POWELLITE: $V^o$-Robie et al. (1978); $S^o$ and $\Delta H^o_f$-Dellien et al. (1976); $C^o_p$-Zhidikova and Kuskov (1971).

WULFENITE: $V^o$ Robie et al. (1978); $S^o$-Dellien et al. (1976); $\Delta G^o_f$-from log K(298.15) = -12.98 for the reaction: $PbMoO_4 = Pb^{2+} + MoO_4^{2-}$ (Vlek and Lindsay, 1977); $C^o_p$-estimated, see text.

MOLYBDITE: $V^o$-Robie et al. (1978); $S^o$, $\Delta H^o_f$ and $\Delta G^o_f$-Stull and Prophet (1971); $C^o_p$-King et al. (1960).

Table 3.1 (cont.)

MOLYBDENUM DIOXIDE: $V^O$-Robie et al. (1978); $S^O$, $\Delta H^O_f$ and $\Delta G^O_f$-Stull and Prophet (1971); $C^O_p$-King et al. (1960).

MOLYBDENITE: $V^O$-Robie et al. (1978); $S^O$, $\Delta H^O$ and $\Delta G^O_f$-Schaefer and Goken (1980); $C^O_p$-Fredrickson and Chasanov (1970).

Fig. 3.1

Comparison of experimentally derived standard enthalpies of
formation for molybdenite.

$\Delta H_f^\circ$ MoS$_2$ at 25°C
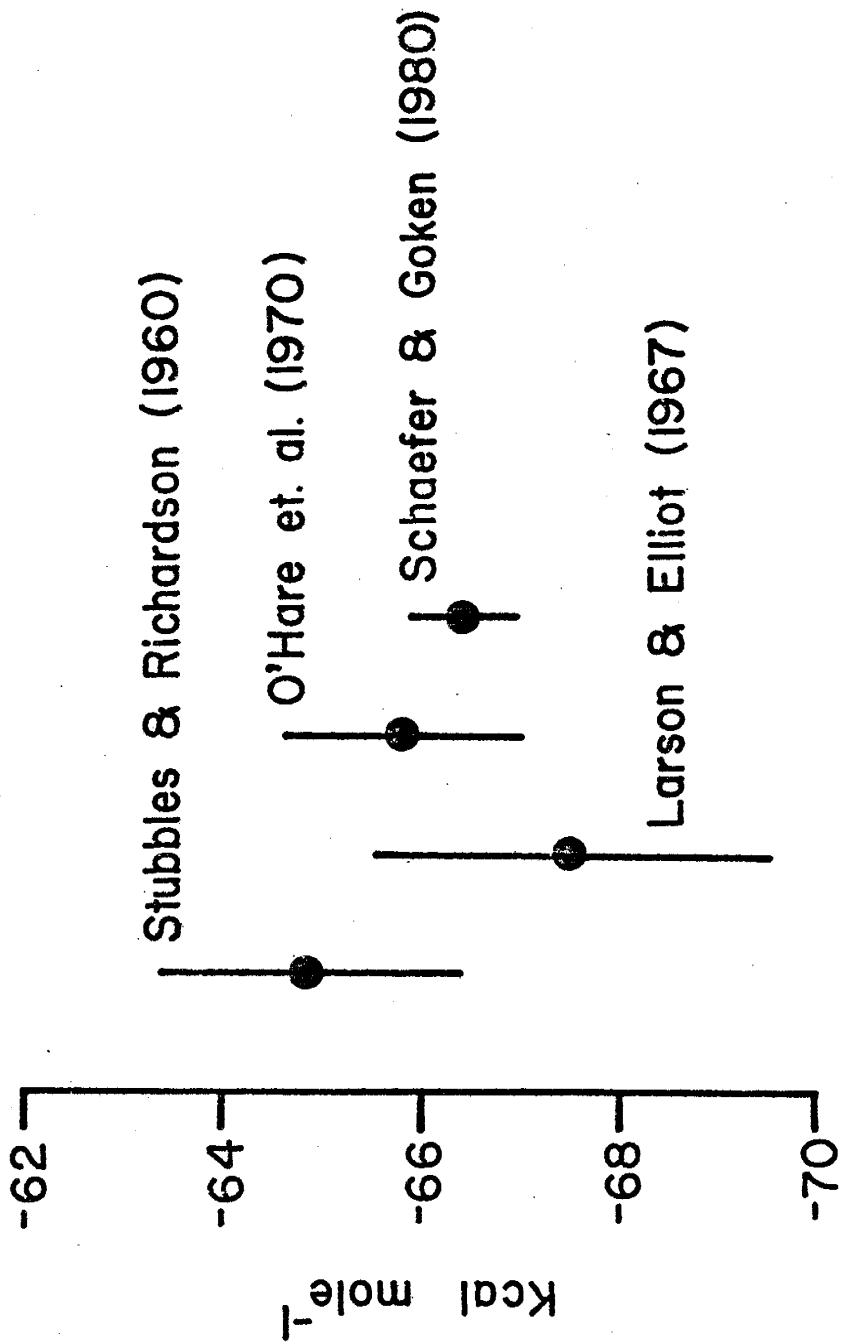
Calculations of heat capacities for wulfenite at elevated temperatures were carried out at 100 K intervals using the heat capacity of powellite and the heat capacities of lime and the stable form of lead oxide (litharge to 762 K and massicot from 762 K to the melting point, 1170 K) from Robie et al. (1978).

MOLYBDATE ION

ROOM TEMPERATURE

Zhidikova and Khodakovskiy (1971) reported the log of the solubility product for powellite as $-8.36 \pm 0.22$. This corresponds to a Gibbs free energy of $11.40 \pm 0.30$ Kcal for the following reaction:

$$CaMoO_4 = Ca^{2+} + MoO_4^{2-} \qquad 3.2$$

The Gibbs free energy of formation for the molybdate ion was calculated from the Gibbs free energy of reaction 3.2 and the Gibbs free energies of formation for powellite (Table 3.1) and the calcium ion (Helgeson et al., 1981) using equation 2.30. The value of the Gibbs free energy determined by this calculation is:

$$\Delta G^\circ_f(T_r,P_r,MoO_4^{2-}) = -200.45 \text{ Kcal mole}^{-1}$$

This value is in good agreement with the values of $-200.4$ Kcal mole$^{-1}$ reported by Dellien et al. (1976) and Ivanova et al. (1975).

Two determinations of the partial molal enthalpy of formation for the molybdate ion are reported in the literature (Graham and Helper, 1956 and O'Hare and Hoeksta, 1974). The agreement between these two studies was excellent. The value of $-238.3 \pm 0.2$ Kcal mole$^{-1}$ reported by O'Hare and Hoeksha (1974) was the value recommended in the review article by Dellien et al. (1976), and was selected for this study. From the Gibbs free energy and enthalpy of formation, the entropy of formation for the molybdate ion was determined using:

$$\Delta G^\circ_f(T_r,P_r) = \Delta H^\circ_f(T_r,P_r) - T\Delta S^\circ_f(T_r,P_r) \qquad 3.3$$

$$\Delta S^\circ_f(T_r,P_r,MoO_4^{2-}) = -126.95 \text{ cal mole}^{-1} \text{ K}^{-1}$$

The partial molal entropy of the molybdate ion was calculated from the entropy of formation and the entropies of the elements (Stull and Prophet, 1971):

$$S°(T_r,P_r,MoO_4^{2-}) = 9.1 \text{ cal mole}^{-1} K^{-1}$$

Olofsson et al. (1978) measured the relative partial molal heat capacities of aqueous solutions of sodium molybdate at 25°C. The partial molal heat capacity for the molybdate ion determined by Olofsson et al. (1978) is:

$$C°_p(T_r,P_r,MoO_4^{2-}) = -49.4 \text{ cal mole}^{-1} K^{-1}$$

The above value is in good agreement with the value of -47 cal mole$^{-1}$ K$^{-1}$ estimated using the method of Criss and Cobble (1964a,b).

Millero (1971) reports the partial molal volume of the molybdate ion as:

$$V°(T_r,P_r,MoO_4^{2-}) = 28.9 \text{ cm}^3 \text{ mole}^{-1}$$

The partial molal compressibility of the molybdate ion has not been measured. However, the compressibility of sodium molybdate was estimated to be 14.3 x 10$^{-3}$ cm$^3$ mole$^{-1}$ bar$^{-1}$ from a compressibility versus molal volume plot for 2:1 electrolytes (Fig. 3.2). The partial molal compressibility of the molybdate ion was calculated from;

$$-\kappa°(MoO_4^{2-}) = -\kappa°(Na_2MoO_4) - 2-\kappa°(Na^+) \qquad 3.4$$

and the partial molal compressibility of the sodium ion (Helgeson and Kirkham, 1976). The value for the partial molal compressibility for the molybdate ion is:

$$-\kappa°(T_r,P_r,MoO_4^{2-}) = 6.5 \text{ x } 10^{-3} \text{ cm}^3 \text{ mole}^{-1} \text{ bar}^{-1}$$

The thermodynamic properties of the molybdate ion at 25°C are summarized in Table 3.2.

Fig. 3.2

Correlation between the standard partial molal compressibility and the standard partial molal volume for 2:1 electrolytes at 25° C and 1 atmosphere pressure. The molal volume data are from Millero (1971) and the compressibility data are from Franks (1973). Compressibility data for $Na_2CO_3$ is calculated from the compressibilities of $K_2CO_3$, NaCl and HCl (Franks, 1973).
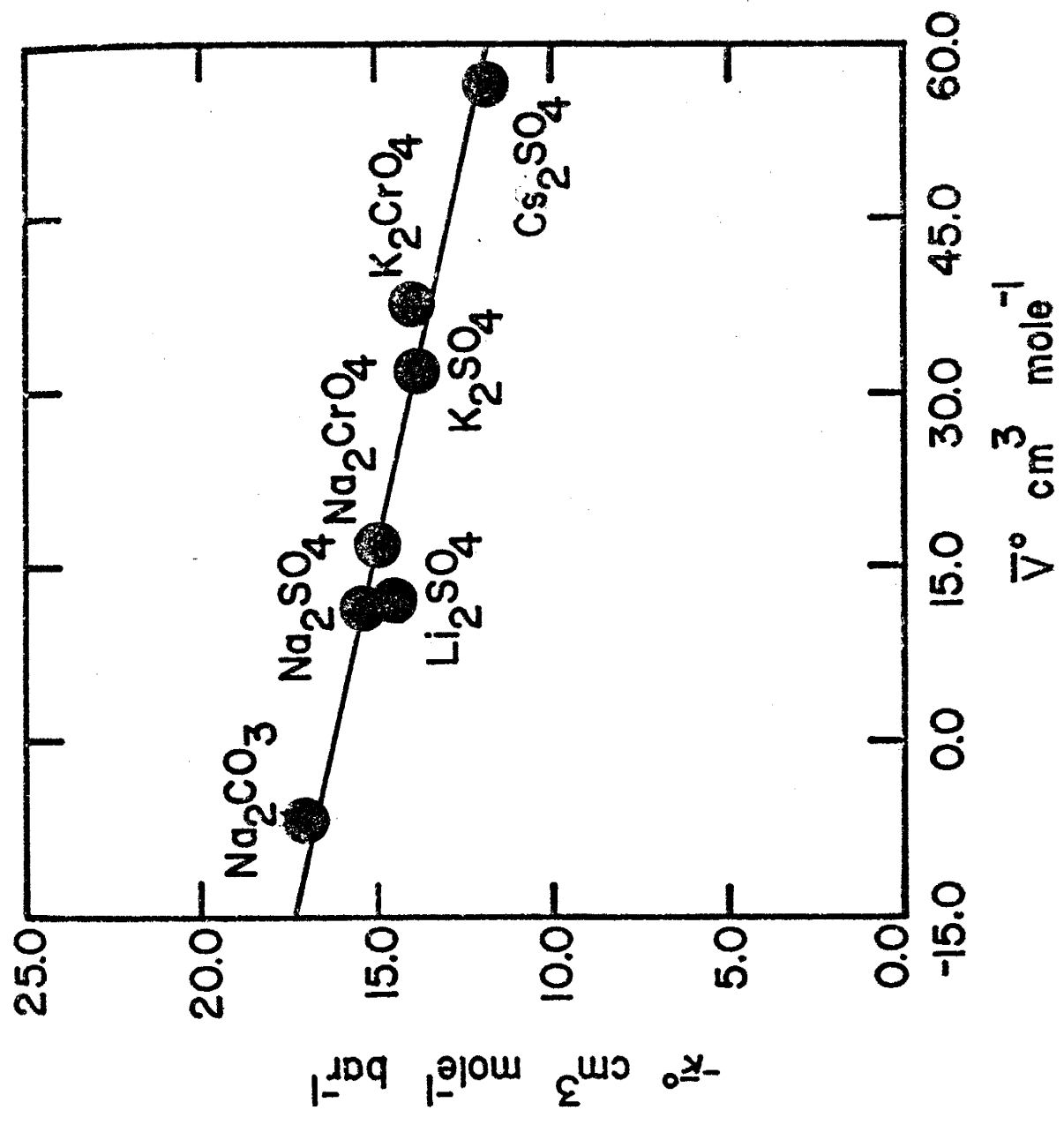
Table 3.2

Summary of the thermodynamic properties of the molybdate ion
at 298.15 K and 1 atmosphere (1.013 bars) pressure.  See
text for sources of data.

$$\Delta G^{O}_{f} = -200.45 \qquad \text{Kcal mole}^{-1}$$

$$\Delta H^{O}_{f} = -238.3 \qquad \text{Kcal mole}^{-1}$$

$$S^{O} = 9.1 \qquad \text{cal mole}^{-1} \text{K}^{-1}$$

$$C^{O}_{p} = -49.4 \qquad \text{cal mole}^{-1} \text{K}^{-1}$$

$$V^{O} = 28.9 \qquad \text{cm}^{3} \text{mole}^{-1}$$

$$-\kappa^{O} = 6.5 \times 10^{-3} \qquad \text{cm}^{3} \text{mole}^{-1} \text{bar}^{-1}$$

PROPERTIES AT ELEVATED TEMPERATURES

The Gibbs free energy of formation for the molybdate ion has been estimated to temperatures of 200°C by Naumov et al. (1974) and Ivanova et al. (1975). In both these studies the method proposed by Khodakovskiy et al. (1968) for estimating the temperature dependence of partial molal heat capacities was used. This method, which assumes that heat capacity is linearly related to temperature, allows the estimation of Gibbs free energies of formation for ions up to temperatures of 300°C that are in agreement with experimental determinations. However, the heat capacity for the molybdate ion at 25°C used by Naumov et al. (1974) and Ivanova et al. (1976) differs from the heat capacity measured by Olofsson et al. (1978) by 30 cal mole$^{-1}$ K$^{-1}$. In addition, work by Cobble and others (Ahluwalia and Cobble, 1964; Gardner et al., 1969) and more recently be Rogers and Pitzer (1981), leaves no doubt that the heat capacity of aqueous electrolytes passes through a maximum at about 60°C and then plummets to large negative values at high temperatures (cf., Fig. 3.7).

Zhidikova and Malinin (1972) measured the solubility of powellite over the temperature range 50-300°C. In their study, the effects of hydrolysis on solubility were ignored. Careful "second-law" calculations using the solubility data corrected for the effects of hydrolysis indicates that the measured solubilities are inconsistent with the enthalpies and heat capacities for the molybdate ion and powellite at 25°C reported in Tables 3.1 and 3.2. For these reasons, the solubility data of Zhidikova and Malinin (1972) were not used to determine the temperature dependence of the thermodynamic properties of the molybdate ion.

Zhidikova et al. (1973) determined the Gibbs free energy of formation for the molybdate ion at 300°C by measuring the solubility and mean ionic activity coefficient for sodium molybdate. Their reported value for the Gibbs free energy of formation for the molybdate ion at 300°C was $-154.0 \pm 3.9$ Kcal mole$^{-1}$. The large error associated with Zhidikova's measurements precluded their use for the accurate determination of the temperature dependence of thermodynamic properties.

After careful evaluation of the available high temperature data for the molybdate ion, it was concluded that these data would not allow accurate determination of the pressure and temperature independent coefficients of equations 2.20a, 2.20b, 2.21, 2.23 and 2.26 through 2.28. In order to determine the temperature dependences of the thermodynamic properties of the molybdate ion, the partial molal volume and heat capacity were estimated at several discrete temperatures.

### Estimation of the Born Constant

The equations of state selected for this study are those developed by Helgeson and co-workers (Helgeson and Kirkham, 1976 and Helgeson et al., 1981) and are presented in Chapter 2.

The correct Bjertran (1929) or Born (1920) equation for the absolute partial molal Gibbs free energy of solvation may be written as (Helgeson and Kirkham, 1976):

(see facing page)                                          3.5

where N° is Avrogado's number ($6.02252 \times 10^{23}$ mole$^{-1}$), e is the electrostatic charge ($4.80298 \times 10^{-10}$ esu), and $r_e$ is the effective electrostatic radius.

EQUATION 3.5

$$\Delta G^o_s{}^{abs} = \frac{N^o Z^2 e^2}{2r_e}\left(\frac{1}{\varepsilon} - 1\right) = \frac{\eta Z^2}{r_e}\left(\frac{1}{\varepsilon} - 1\right) = \omega^{abs}\left(\frac{1}{\varepsilon} - 1\right) \qquad 3.5a$$

$$\eta = \frac{N^o e^2}{2} = 1.66027 \times 10^5 \ \overset{o}{A} \ cal \ mole^{-1} \qquad 3.5b$$

$$\omega^{abs} = \frac{\eta Z^2}{r_e} \qquad 3.5c$$

Application of the Born Theory in solution chemistry has been criticized because of the difficulty in choosing an electrostatic radius, and the near impossibility of determining the microscopic dielectric constant of the solvent in the vicinity of an ion. Nevertheless, electrostatic radii consistent with the bulk dielectric constant of water can be determined by regression analysis. Helgeson and Kirkham (1976) have determined the electrostatic radius of several ions and found the electrostatic radii to be related to the partial molal entropy of the ion by:

$$\text{(see facing page)} \hspace{3cm} 3.6$$

where $a^*_1$ and $a^*_2$ are constants characteristic of the ion type. For divalent oxy-anions the values of $a^*_1$ and $a^*_2$ are 160 and -450 respectively. $Y(T_r, P_r)$ is defined in equation 2.24 and has a value of $-5.802 \times 10^{-5}$ at 25°C and one bar pressure.

The value of $\omega(abs)$ for the molybdate ion was estimated from equations 3.6 and 3.7. The calculations resulted in a value 3.16 A for $r_e$ and $2.053 \times 10^5$ cal mole$^{-1}$ for $\omega(abs)$. Conversion from the absolute to the conventional scale was accomplished by:

$$\omega = \omega(abs) - Z \times \omega(abs, H^+) \hspace{2cm} 3.7$$

where Z is the integer change. A value of $3.1301 \times 10^5$ cal mole$^{-1}$ was calculated for $\omega(MoO_4^{2-})$ using a value of $0.5387 \times 10^5$ cal mole$^{-1}$ (Helgeson and Kirkham, 1976) for $\omega(abs, H^+)$.

## Partial Molal Volumes at Elevated Temperatures

Several models have been proposed to estimate the partial molal volumes of aqueous electrolytes at 25°C from electrostatic, crystallographic and other considerations (Millero, 1972 and Matteoli, 1980). Attempts to accurately predict the partial molal volume of

EQUATION 3.6

$$r_e = \frac{Z^2 Y(T_r, P_r) + a^*_2}{S^0(T_r, P_r) - a^*_1}$$

aqueous electrolytes at elevated temperatues are limited by the fact that these models are only semi-quantitative at 25°C. Ellis (1966, 1967, 1968) has determined the partial molal volumes of over sixteen aqueous electrolytes at temperatures up to 200°C. From these partial molal volume data, Ellis (1968) has used the correspondence principle to correlate the partial molal volume of individual ions at high temperatures with their volumes at 25°C. This was similar to the technique developed by Criss and Cobble (1964a,b) for individual ionic entropies. Ellis (1968) attempted to fit all ion types to a single line by adjusting the value of the partial molal volume of the chloride ion. However, the partial molal volumes for the chloride ion chosen by Ellis (1968) differ substantially from the volumes later measured by Ellis and McFadden (1968). This indicates that a substantial correction is necessary to obtain standard partial molal volumes for individual ions from Ellis's (1968) curves. In addition, it is not likely that a single line should fit both anions and cations.

The temperature dependence of the partial molal volume for sodium sulfate is shown in Fig. 3.3. The partial molal volume passes through a maximum at about 60°C, and becomes increasingly more negative at elevated temperatures. This type of temperature dependence for partial molal volume is typical for both aqueous ions and electrolyte solutions. The temperature dependence of the partial molal volume of aqueous electrolytes may be interpreted in light of models proposed by Millero (1972) and Helgeson and Kirkham (1976). In these models the partial molal volume is represented by:

$$V° = V°(int) + \Delta V°(col) + \Delta V°(sol) \qquad 3.8$$

where $V°(int)$, $\Delta V°(col)$ and $\Delta V°(sol)$ are respectively the intrinsic

Fig. 3.3

The standard partial molal volume of sodium sulfate as a function

of temperature at 20 bars pressure (Helgeson and Kirkham, 1976

and Millero, 1972). Curve represents the volumes calculated

using equations 2.18 and the coefficients of Helgeson and

Kirkham (1976).
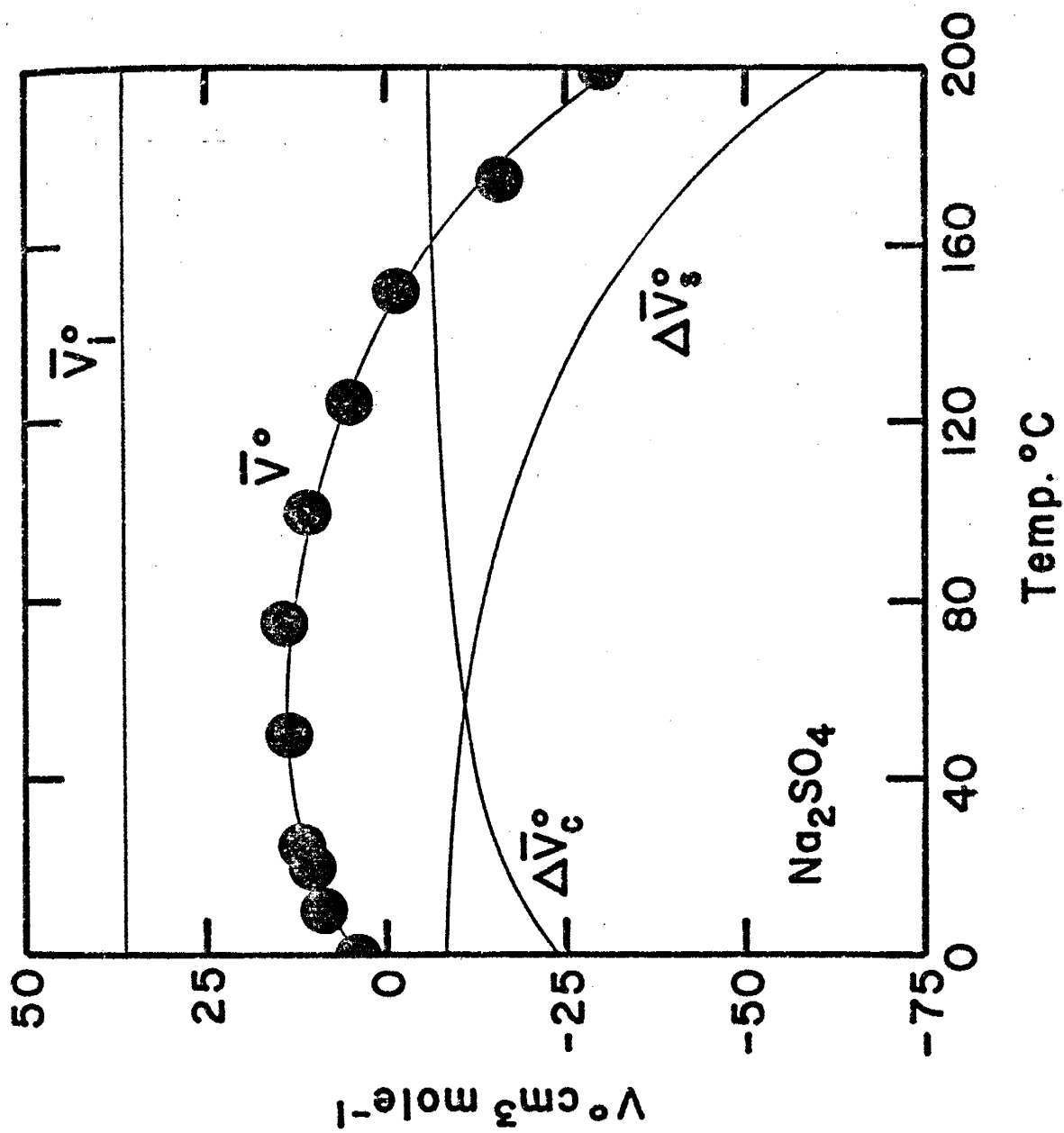
volume, the volume of solvent collapse and the solvation volume of the electrolyte. Equation 3.8 allows interpretation of the terms in equation 2.18:

$$V° = \sigma(P) + \xi(P)T/(T-\theta) + \omega Q(T,P) \qquad 2.18$$

The intrinsic volume, $V°(int)$, is assumed to be independent of temperature and is represented by the first term in equation 2.18 (Fig. 3.3). The collapse volume, $\Delta V°(col)$, is the volume which results from the loss of solvent structure in the immediate vicinity of an ion. This effect is most pronounced at low temperatures where the solvent is most ordered (Fig. 3.3). As temperature increases, $\Delta V°(col)$ approaches a constant value and is represented by the second term in equation 2.18. The solvation volume, $\Delta V°(sol)$, is the volume resulting from the transfer of the ion from a vacuum into the solvent. The volume of solvation becomes increasingly important at elevated temperatures were the dielectric permeability of water is decreased (Fig. 3.3). The solvation volume is represented by the last term in equation 2.18. At low temperatures the partial molal volume is dominated by $\Delta V°(col)$. As the temperature increases the absolute magnitude of $\Delta V°(col)$ decreases, resulting in an increase in the partial molal volume. At higher temperatures the solvation volume becomes increasingly negative. The summation of these three volumes results in the configuration of the curve in Fig. 3.3.

Separation of partial molal volume into electrostatic and nonelectrostatic terms results in:

$$V° = V°_n + V°_e \qquad 3.9a$$

$$V°_e = \omega Q(T,P) \qquad 3.9b$$

$$V°_n = V° - \omega Q(T,P) = \sigma(P) + \xi(P)T/(T-\theta) \qquad 3.9c$$

where $V^{\circ}_e$ and $V^{\circ}_n$ are the electrostatic and nonelectrostatic partial molal volumes respectively. In this study it was found that a linear relationship, analogous to the entropy correspondence principle, exists between $V^{\circ}_n$ at 25°C and $V^{\circ}_n$ at elevated temperatures. This relationship can be expressed as:

$$V^{\circ}_n(T,20) = a' \times V^{\circ}_n(T_r,20) + b' \qquad\qquad 3.10$$

where $V^{\circ}_n(T,20)$ and $V^{\circ}_n(T_r,20)$ are the nonelectrostatic volumes at the temperature of interest and the reference temperature respectively at a constant pressure of 20 bars (the only pressure at which experimental data is available over a wide range of temperatures). The correlation between $V^{\circ}_n$ at 25°C and $V^{\circ}_n$ at 100°C for anions is displayed in Fig. 3.4. The coefficients for equation 3.10 for anions at eight discrete temperatures between 0 and 200°C are given in Table 3.3.

The standard partial molal volumes of the molybdate ion at nine descrete temperatures and 20 bars pressure were estimated using equations 3.9a-c, 3.10 and the coefficients in Table 3.3. The results of these estimates are presented in Table 3.4.

The estimated partial molal volumes for the molybdate ion from Table 3.4 were regressed as a function of temperature using equation 2.18, the value of $\omega$ calculated earlier and the electrostatic properties of water reported by Helgeson and Kirkham (1974a). Evaluation of the sensitivity of the fit coefficients to small errors in the standard partial molal volume data indicated that acceptable fits could be obtained with values of $\theta$ which range over 70 K. As a result, $\theta$ was set to 185 K during the regression. This value was chosen because of similarity of the nonelectrostatic volume of the molybdate ion to the nitrate ( $\theta$ = 185.3 K) and iodide ($\theta$ = 186.5 K) ion (Helgeson and

Fig. 3.4

Correlation between the nonelectrostatic partial molal volume for anions at 25° and 100° C and 20 bars pressure. Data points are calculated from the data of Helgeson and Kirkham (1976) and equation 3.9c. The curve is determined from equation 3.10 and the coefficients given in Table 3.3. Units for volume are $cm^3 mole^{-1}$.
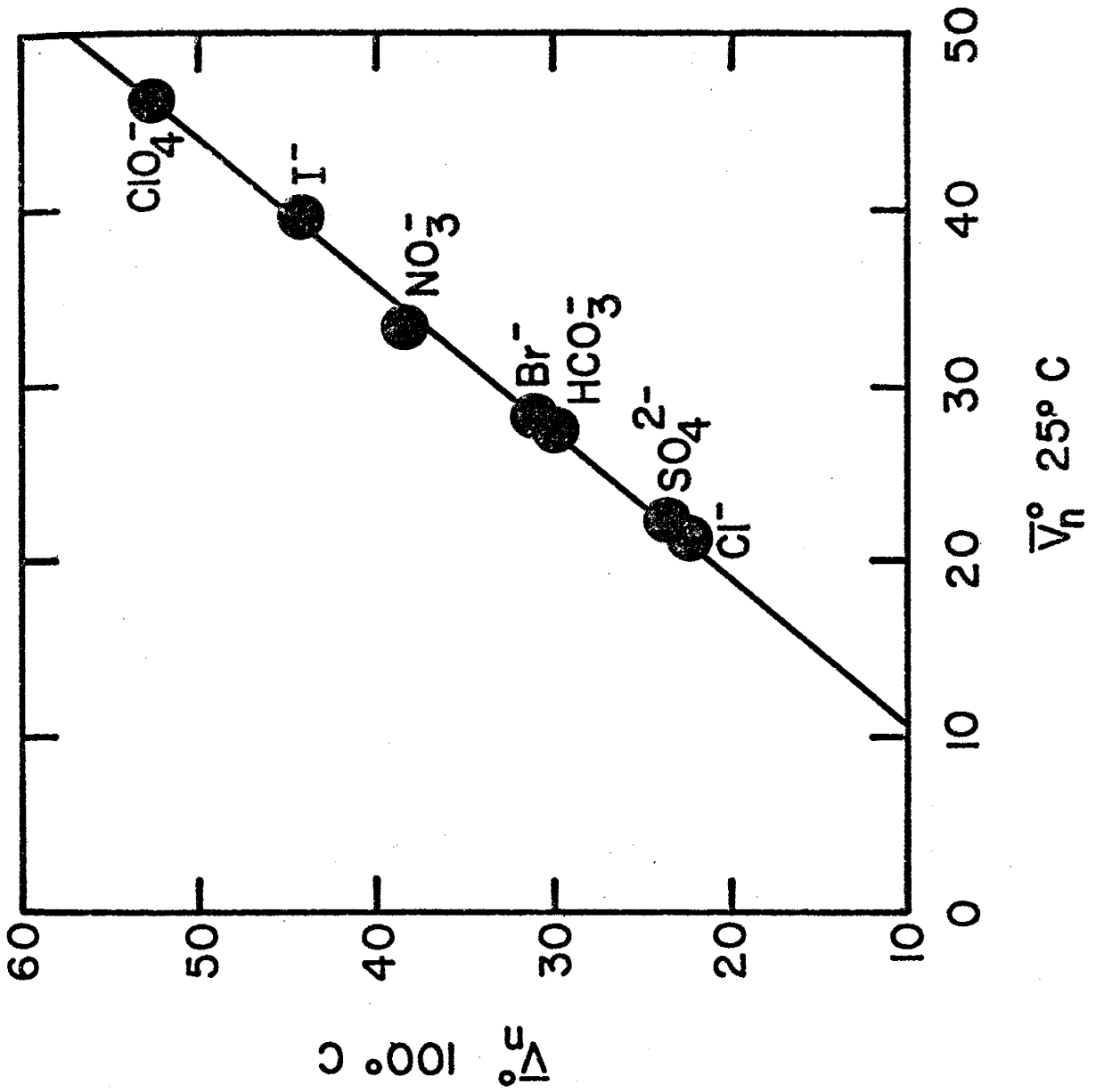
Table 3.3

Coefficients for equation 3.10 used to estimate $V^o_n$ for anions at elevated temperatures and 20 bars pressure.

| Temp $^oC$ | b´ | a´ |
|---|---|---|
| 0 | -3.57 | 1.013 |
| 50 | -0.43 | 1.062 |
| 75 | -1.86 | 1.142 |
| 100 | -3.02 | 1.204 |
| 125 | -4.12 | 1.259 |
| 150 | -5.11 | 1.306 |
| 175 | -6.02 | 1.349 |
| 200 | -6.86 | 1.385 |

Table 3.4

partial molal volumes and heat capacities for the molybdate
ion at elevated temperatures.  Volumes are at 20 bars
pressure.  Heat capacities are at 1 bar pressure below 100°C
and at pressures corresponding to steam saturated water at
higher temperatures.  Values at temperatures other than 25°C
are estimated (see text).

| Temp °C | $V^{o,a}$ | $C_p^{o,b}$ |
|---|---|---|
| 0 | 26.6 | |
| 25 | 29.0 | -49.4 |
| 50 | 29.4 | -43.9 |
| 75 | 28.7 | -44.9 |
| 100 | 26.4 | -50.2 |
| 125 | 22.5 | -59.6 |
| 150 | 16.3 | -73.3 |
| 175 | 6.6 | |
| 200 | -8.7 | |

[a] $cm^3$ mole$^{-1}$.  [b] cal mole$^{-1}$ K$^{-1}$.

Fig. 3.5

The conventional standard partial molal volume of the molybdate ion at 20 bars and temperatures to 200° C. The data points are from Table 3.4. The curve is calculated from equation 2.18 and the coefficients given in the text.
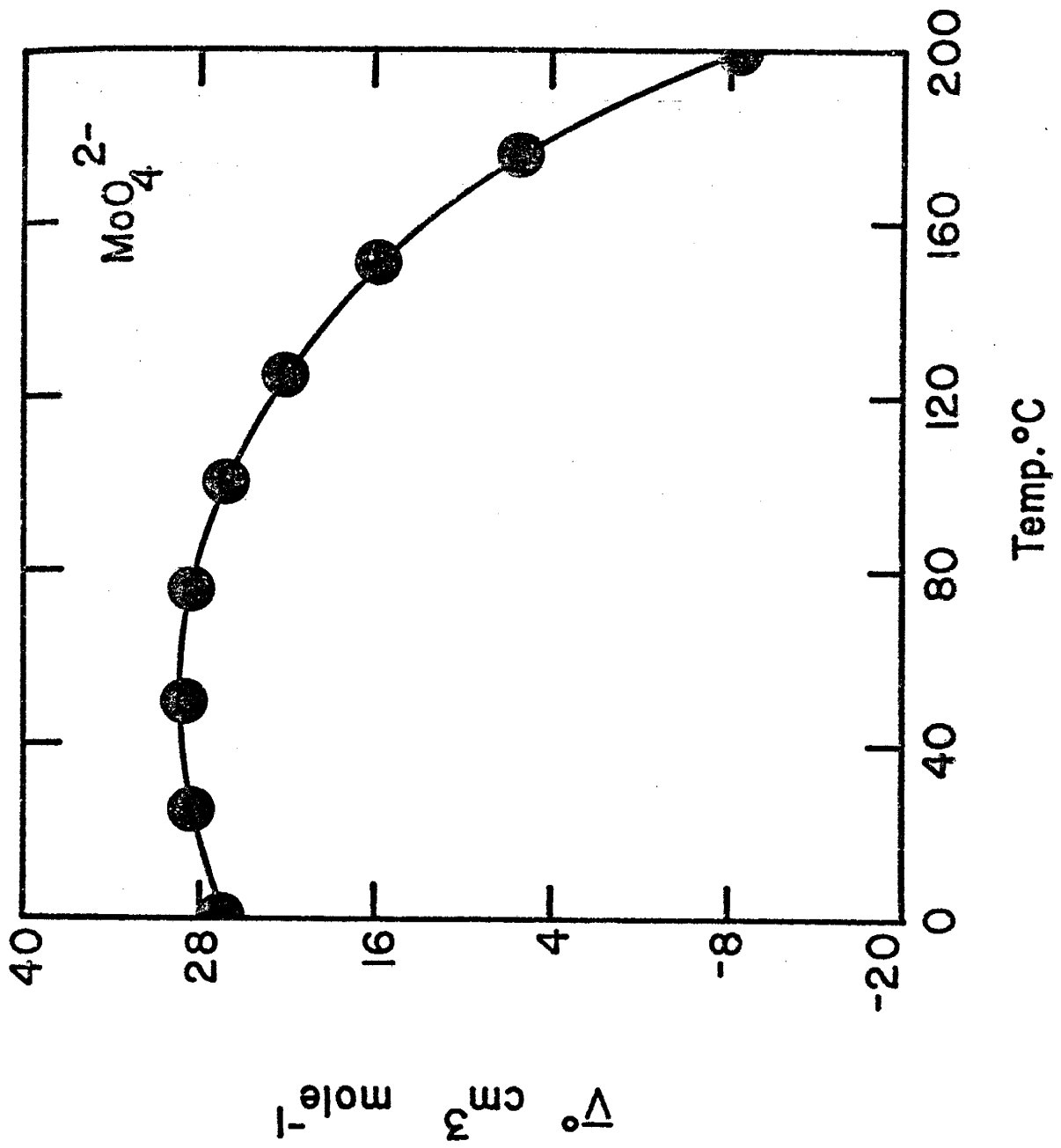
Kirkham, 1976). The regression analyses resulted in values of 1.327 cal mole$^{-1}$ bar$^{-1}$ and -0.1703 cal mole$^{-1}$ bar$^{-1}$ for $\sigma(20)$ and $\xi(20)$ respectively. The temperature dependence of the partial molal volume of the molybdate ion at 20 bars pressure is displayed graphically in Fig. 3.5.

The partial molal compressibility of an ion is defined by the partial derivative of volume (equations 2.18, 2.20a and b) with respect to pressure at constant temperature:

$$-\kappa^\circ = a_2 + a_4 T/(T-\theta) - \omega N(T,P) \qquad 3.11$$

where

$$N(T,P) \equiv \varepsilon(T,P)^{-1} \times [(\partial^2 \ln\varepsilon/\partial P^2)_T - (\partial \ln\varepsilon/\partial P)_T^2] \qquad 3.12$$

Using equations 2.18, 2.20a and b, and 3.11 the value of $a_1$, $a_2$, $a_3$ and $a_4$ can be determined by separate or combined regressions of experimental values of $V^\circ$ and $-\kappa^\circ$ as a function of temperature at constant pressure. However, in the case of the molybdate ion, the partial molal compressibility is known only at room temperature.

In the development of the equation of state for aqueous electrolytes, Helgeson and Kirkham (1976) found that a linear relationship exists between $a_3$ and $a_4$:

$$a_4 = 2 \times 10^{-6} - 6.16 \times 10^{-4} a_3 \qquad 3.13$$

Furthermore, they found that $a_3$ differed only slightly from $\xi(P)$ at 20 bars. These relationships allowed the estimation of $a_3$ and $a_4$ for the molybdate ion.

Using equations 2.20a, 2.20b, 3.11, 3.13 and the values of $\sigma(P)$, $\xi(P)$, $\theta$, $\omega$ and $-\kappa^\circ$ determined in this chapter, the values of $a_1$, $a_2$, $a_3$ and $a_4$ for the molybdate ion were calculated. These values are listed below:

$$a_1 = 1.331 \text{ cal mole}^{-1} \text{ bar}^{-1}$$

$$a_2 = -20.45 \times 10^{-5} \text{ cal mole}^{-1} \text{ bar}^{-2}$$

$$a_3 = -17.25 \times 10^{-2} \text{ cal mole}^{-1} \text{ bar}^{-1}$$

$$a_4 = 10.82 \times 10^{-5} \text{ cal mole}^{-1} \text{ bar}^{-2}$$

## Partial Molal Heat Capacities at Elevated Temperatures

In this study a correlation between nonelectrostatic partial molal heat capacities at room and elevated temperature, similar to that reported for volumes, was observed (Fig. 3.6). In this case, if the nonelectrostatic heat capacity of an ion was normalized by its absolute charge, $|Z|$, a gross linear relationship for all ions was found. The relationship between the nonelectrostatic heat capacity at room temperature and at elevated temperatures is given by:

$$C^{\circ}_{p,n}(T)/|Z| = a' \times C^{\circ}_{p,n}(T_r)/|Z| + b' \qquad 3.14$$

where $C^{\circ}_{p,n}(T)$ and $C^{\circ}_{p,n}(T_r)$ are the nonelectrostatic partial molal heat capacity for an ion at the indicated temperature. Values of $a'$ and $b'$ at five discrete temperatures are given in Table 3.5. Estimated values of the partial molal heat capacity for the molybdate ion to 150°C are given in Table 3.4.

The values of $c_1$ and $c_2$ in equation 2.21 for the molybdates were determined using the correlation between $a_4$ and $c_2$ reported by Helgeson et al. (1981):

$$c_2 = -2.90 - 2.30 \times 10^5 a_4 \qquad 3.15$$

Using equations 2.21 and 3.15, values of 53.34 and -27.80 cal mole$^{-1}$ K$^{-1}$ were calculated for $c_1$ and $c_2$ respectively. Heat capacities calculated using these values and equation 2.21 are in reasonable agreement with those estimated above (Fig. 3.7).

Fig. 3.6

Correlation between the nonelectrostatic heat capacities for ions at 25 and 100° C.  Data are calculated from Helgeson et al. (1981). The curve is calculated from equation 3.14 and the coefficients given in Table 3.5.
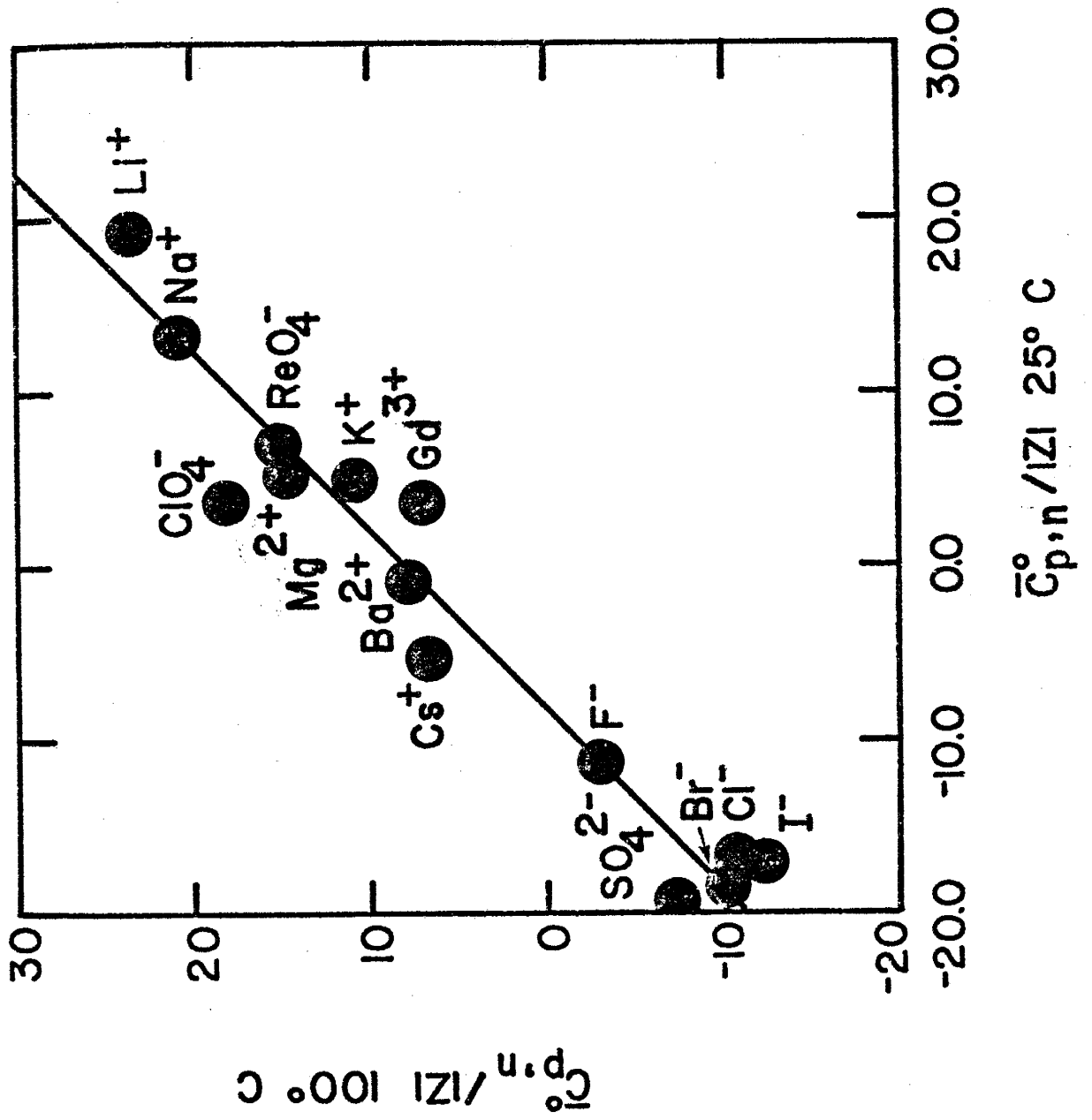
## Table 3.5

Coefficients for equation 3.14 used to estimate $C^O_{p,n}$ for ions at elevated temperatures.

| Temp $^OC$ | b´ | a´ |
|---|---|---|
| 50 | 4.41 | 0.982 |
| 75 | 6.61 | 0.974 |
| 100 | 7.98 | 0.968 |
| 125 | 8.80 | 0.966 |
| 150 | 9.47 | 0.956 |

Fig. 3.7

The conventional standard partial molal heat capacity for the
molybdate ion at temperatures up to 200° C in steam saturated water.
The symbols are from Table 3.4 and the curve is calculated from
equation 2.21 and the coefficients given in Table 3.6.
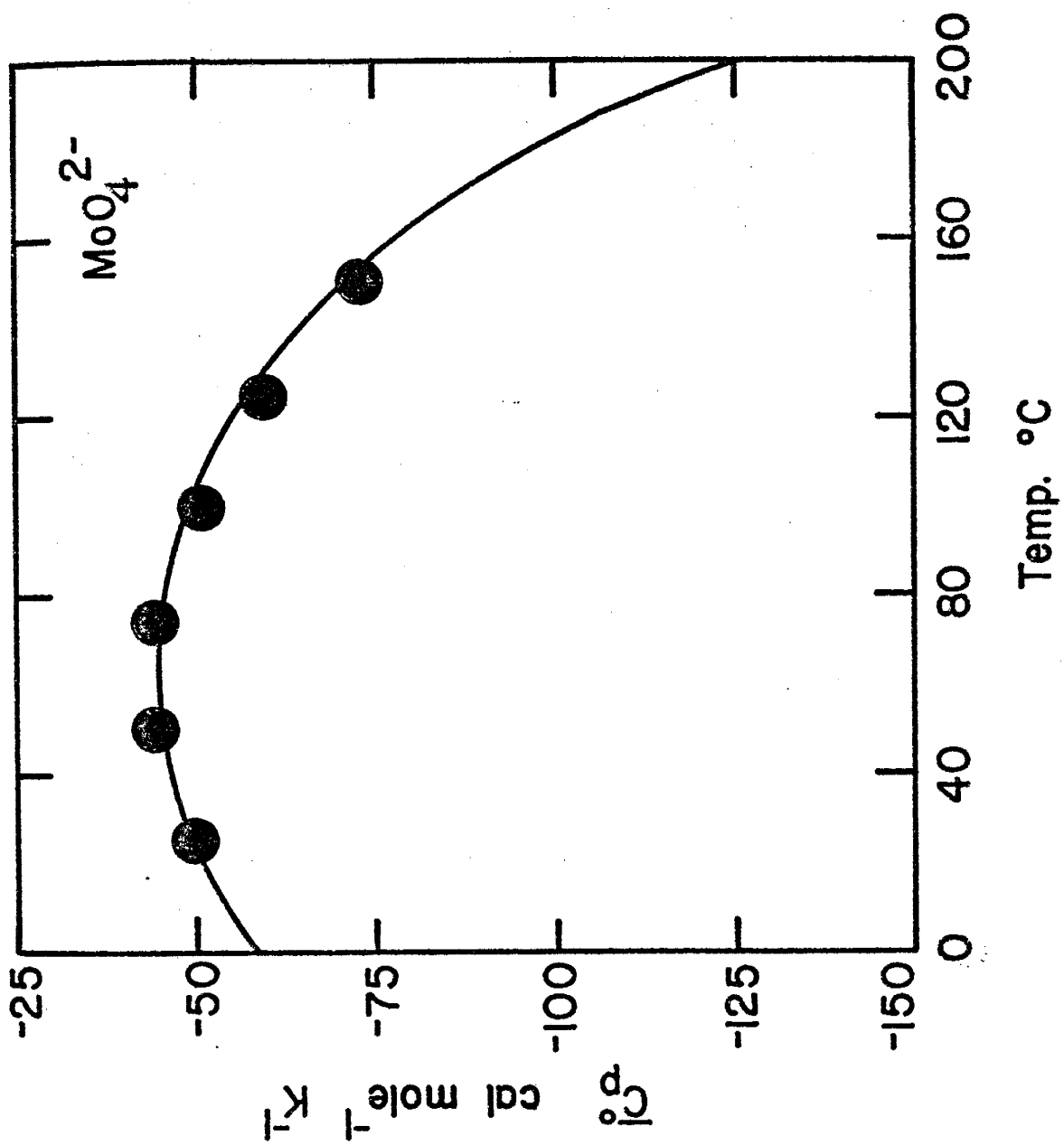
The shape of the partial molal heat capacity curve (Fig. 3.7) is similar to the partial molal volume curve (Fig. 3.5). The temperature dependence of partial molal heat capacity reflects the calorimetric consequence of solvent collapse at low temperatures and ion solvation at high temperatures.

The equation of state parameters for the molybdate ion derived in this chapter are presented in Table 3.6.

Table 3.6

Equation of state coefficients for the molybdate ion derived in this study.

$$a_1 = 1.331 \quad \text{cal mole}^{-1} \text{ bar}^{-1}$$

$$a_2 = -20.45 \times 10^{-5} \quad \text{cal mole}^{-1} \text{ bar}^{-2}$$

$$a_3 = -17.25 \times 10^{-2} \quad \text{cal mole}^{-1} \text{ bar}^{-1}$$

$$a_4 = 10.82 \times 10^{-5} \quad \text{cal mole}^{-1} \text{ bar}^{-2}$$

$$c_1 = 53.34 \quad \text{cal mole}^{-1} \text{ K}^{-1}$$

$$c_2 = -27.80 \quad \text{cal mole}^{-1} \text{ K}^{-1}$$

$$\theta = 185.0 \quad \text{K}$$

$$\omega = 3.1301 \times 10^5 \quad \text{cal mole}^{-1}$$

## EQUILIBRIUM CONSTANTS

Equilibrium constants for reactions involving molybdenum minerals and the molybdate ion were calculated from data presented in Tables 3.1, 3.2, and 3.6 using SUPCRT (Helgeson et al., 1978). The results of these calculations in the temperature and pressure range of 25° to 600°C and 1 to 5000 bars are presented in Tables 3.7 through 3.11.

Table 3.7

Log K(T,P) for the reaction:
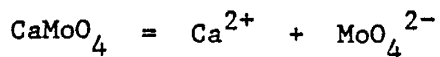
$$CaMoO_4 = Ca^{2+} + MoO_4^{2-}$$

Calculated from the data in Tables 3.1, 3.2 and 3.6 using SUPCRT (Helgeson et al., 1978). SAT refers to steam saturated water.

| | | | | Pressure (Kb) | | | | |
|------|--------|--------|--------|--------|--------|--------|--------|--------|
| Temp | SAT | 0.5 | 1.0 | 1.5 | 2.0 | 3.0 | 4.0 | 5.0 |
| 25 | -8.36 | -8.04 | -7.77 | -7.57 | -7.41 | -7.24 | -7.27 | -7.49 |
| 50 | -8.34 | -8.04 | -7.80 | -7.61 | -7.45 | -7.25 | -7.22 | -7.34 |
| 75 | -8.40 | -8.12 | -7.88 | -7.69 | -7.53 | -7.32 | -7.25 | -7.31 |
| 100 | -8.53 | -8.25 | -8.01 | -7.81 | -7.65 | -7.43 | -7.33 | -7.34 |
| 125 | -8.71 | -8.41 | -8.17 | -7.97 | -7.79 | -7.55 | -7.43 | -7.40 |
| 150 | -8.94 | -8.62 | -8.35 | -8.14 | -7.96 | -7.69 | -7.54 | -7.49 |
| 175 | -9.21 | -8.85 | -8.56 | -8.34 | -8.14 | -7.84 | -7.67 | -7.59 |
| 200 | -9.54 | -9.12 | -8.79 | -8.54 | -8.33 | -8.00 | -7.80 | -7.70 |
| 250 | -10.42 | -9.77 | -9.31 | -9.00 | -8.74 | -8.34 | -8.08 | -7.94 |
| 300 | -11.89 | -10.67 | -9.95 | -9.51 | -9.19 | -8.70 | -8.39 | -8.20 |
| 350 | -15.36 | -12.13 | -10.79 | -10.13 | -9.70 | -9.10 | -8.72 | -8.50 |
| 400 | | -15.04 | -12.00 | -10.94 | -10.33 | -9.56 | -9.11 | -8.84 |
| 450 | | | -13.82 | -12.00 | -11.11 | -10.11 | -9.55 | -9.23 |
| 500 | | | -16.48 | -13.40 | -12.06 | -10.71 | -10.02 | -9.63 |
| 550 | | | | -14.96 | -13.03 | -11.23 | -10.37 | -9.89 |
| 600 | | | | -16.11 | -13.57 | -11.32 | -10.31 | -9.76 |

Table 3.8

Log K(T,P) for the reaction:
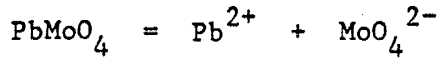
$$PbMoO_4 = Pb^{2+} + MoO_4^{2-}$$

Calculated from the data in Tables 3.1, 3.2 and 3.6 using SUPCRT (Helgeson et al., 1978). SAT refers to steam saturated water.

Pressure (Kb)

| Temp | SAT | 0.5 | 1.0 | 1.5 | 2.0 | 3.0 | 4.0 | 5.0 |
|------|-----|-----|-----|-----|-----|-----|-----|-----|
| 25 | -12.98 | -12.64 | -12.33 | -12.09 | -11.87 | -11.60 | -11.50 | -11.57 |
| 50 | -12.49 | -12.16 | -11.87 | -11.64 | -11.43 | -11.13 | -10.97 | -10.93 |
| 75 | -12.11 | -11.80 | -11.52 | -11.29 | -11.09 | -10.77 | -10.58 | -10.49 |
| 100 | -11.83 | -11.52 | -11.25 | -11.02 | -10.81 | -10.49 | -10.27 | -10.15 |
| 125 | -11.64 | -11.32 | -11.04 | -10.17 | -10.60 | -10.26 | -10.03 | -9.87 |
| 150 | -11.52 | -11.18 | -10.89 | -10.65 | -10.43 | -10.07 | -9.82 | -9.65 |
| 175 | -11.47 | -11.09 | -10.78 | -10.53 | -10.30 | -9.92 | -9.65 | -9.46 |
| 200 | -11.50 | -11.06 | -10.72 | -10.45 | -10.20 | -9.80 | -9.51 | -9.30 |
| 250 | -11.82 | -11.17 | -10.70 | -10.37 | -10.08 | -9.62 | -9.28 | -9.04 |
| 300 | -12.76 | -11.58 | -10.86 | -10.41 | -10.06 | -9.52 | -9.13 | -8.86 |
| 350 | -15.70 | -12.57 | -11.25 | -10.59 | -10.14 | -9.50 | -9.06 | -8.75 |
| 400 | | -14.99 | -12.04 | -10.99 | -10.37 | -9.58 | -9.07 | -8.73 |
| 450 | | | -13.45 | -11.68 | -10.79 | -9.77 | -9.17 | -8.78 |
| 500 | | | -15.69 | -12.70 | -11.39 | -10.04 | -9.31 | -8.86 |
| 550 | | | | -13.91 | -12.03 | -10.24 | -9.36 | -8.83 |
| 600 | | | | -14.75 | -12.28 | -10.06 | -9.03 | -8.44 |

Table 3.9

Log K(T,P) for the reaction:
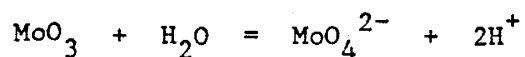
$$MoO_3 + H_2O = MoO_4^{2-} + 2H^+$$

Calculated from the data in Tables 3.1, 3.2 and 3.6 using SUPCRT (Helgeson et al., 1978). SAT refers to steam saturated water.

Pressure (Kb)

| Temp | SAT | 0.5 | 1.0 | 1.5 | 2.0 | 3.0 | 4.0 | 5.0 |
|------|-----|-----|-----|-----|-----|-----|-----|-----|
| 25 | -11.63 | -11.49 | -11.33 | -11.21 | -11.12 | -11.01 | -11.00 | -11.09 |
| 50 | -11.27 | -11.11 | -10.96 | -10.85 | -10.76 | -10.63 | -10.57 | -10.59 |
| 75 | -11.03 | -10.87 | -10.73 | -10.62 | -10.52 | -10.37 | -10.29 | -10.25 |
| 100 | -10.90 | -10.74 | -10.60 | -10.49 | -10.37 | -10.21 | -10.10 | -10.03 |
| 125 | -10.87 | -10.69 | -10.54 | -10.42 | -10.31 | -10.13 | -10.00 | -9.90 |
| 150 | -10.92 | -10.72 | -10.55 | -10.42 | -10.30 | -10.10 | -9.95 | -9.83 |
| 175 | -11.03 | -10.80 | -10.62 | -10.47 | -10.34 | -10.13 | -9.94 | -9.81 |
| 200 | -11.23 | -10.95 | -10.73 | -10.57 | -10.41 | -10.16 | -9.97 | -9.82 |
| 250 | -11.83 | -11.38 | -11.06 | -10.85 | -10.66 | -10.62 | -10.34 | -10.13 |
| 300 | -12.92 | -12.06 | -11.55 | -11.23 | -11.00 | -10.37 | -10.10 | -9.88 |
| 350 | -15.52 | -13.19 | -12.23 | -11.75 | -11.43 | -10.96 | -10.64 | -10.40 |
| 400 | | -15.39 | -13.20 | -12.42 | -11.97 | -11.39 | -11.00 | -10.73 |
| 450 | | | -14.64 | -13.32 | -12.66 | -11.89 | -11.43 | -11.12 |
| 500 | | | -16.70 | -14.46 | -13.47 | -12.45 | -11.89 | -11.53 |
| 550 | | | | -15.73 | -14.31 | -12.96 | -12.28 | -11.85 |
| 600 | | | | -16.71 | -14.86 | -13.18 | -12.38 | -11.91 |

Table 3.10

Log K(T,P) for the reaction:
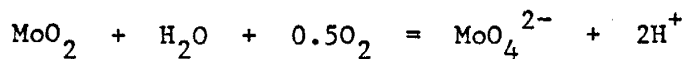
$$MoO_2 + H_2O + 0.5O_2 = MoO_4^{2-} + 2H^+$$

Calculated from the data in Tables 3.1, 3.2 and 3.6 using SUPCRT
(Helgeson et al., 1978). SAT refers to steam saturated water.

Pressure (Kb)

| Temp | SAT | 0.5 | 1.0 | 1.5 | 2.0 | 3.0 | 4.0 | 5.0 |
|------|-----|-----|-----|-----|-----|-----|-----|-----|
| 25 | 11.98 | 12.07 | 12.13 | 12.15 | 12.15 | 12.07 | 11.88 | 11.61 |
| 50 | 10.25 | 10.33 | 10.38 | 10.40 | 10.41 | 10.36 | 10.24 | 10.05 |
| 75 | 8.67 | 8.75 | 8.81 | 8.83 | 8.85 | 8.83 | 8.75 | 8.62 |
| 100 | 7.22 | 7.31 | 7.37 | 7.41 | 7.44 | 7.46 | 7.40 | 7.32 |
| 125 | 5.87 | 5.98 | 6.05 | 6.11 | 6.15 | 6.18 | 6.17 | 6.12 |
| 150 | 4.61 | 4.74 | 4.83 | 4.90 | 4.96 | 5.02 | 5.03 | 5.02 |
| 175 | 3.41 | 3.58 | 3.70 | 3.78 | 3.85 | 3.95 | 3.99 | 4.00 |
| 200 | 2.25 | 2.48 | 2.63 | 2.73 | 2.83 | 2.95 | 3.02 | 3.05 |
| 250 | -0.00 | 0.40 | 0.66 | 0.82 | 0.95 | 1.15 | 1.27 | 1.35 |
| 300 | -2.46 | -1.64 | -1.18 | -0.92 | -0.73 | -0.45 | -0.27 | -0.16 |
| 350 | -6.20 | -3.91 | -2.99 | -2.56 | -2.28 | -1.91 | -1.68 | -1.53 |
| 400 | | -7.07 | -4.93 | -4.19 | -3.78 | -3.28 | -2.98 | -2.79 |
| 450 | | | -7.19 | -5.91 | -5.27 | -4.60 | -4.22 | -3.99 |
| 500 | | | -9.97 | -7.76 | -6.82 | -5.87 | -4.39 | -5.10 |
| 550 | | | | -9.67 | -8.28 | -7.00 | -6.39 | -6.04 |
| 600 | | | | -11.21 | -9.38 | -7.77 | -7.04 | -6.63 |

Table 3.11

Log K(T,P) for the reaction:
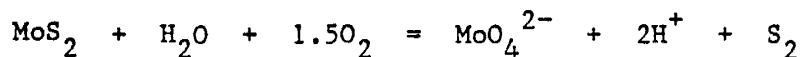
$$MoS_2 + H_2O + 1.5O_2 = MoO_4^{2-} + 2H^+ + S_2$$

Calculated from the data in Tables 3.1, 3.2 and 3.6 using SUPCRT
(Helgeson et al., 1978). SAT refers to steam saturated water.

Pressure (Kb)

| Temp | SAT | 0.5 | 1.0 | 1.5 | 2.0 | 3.0 | 4.0 | 5.0 |
|------|------|------|------|------|------|------|------|------|
| 25 | 44.30 | 44.49 | 44.63 | 44.75 | 44.84 | 44.95 | 44.94 | 44.85 |
| 50 | 40.11 | 40.27 | 40.42 | 40.52 | 40.62 | 40.74 | 40.78 | 40.76 |
| 75 | 36.43 | 36.58 | 36.72 | 36.83 | 36.92 | 37.06 | 37.14 | 37.17 |
| 100 | 33.15 | 33.31 | 33.45 | 33.56 | 33.67 | 33.82 | 33.92 | 33.98 |
| 125 | 30.21 | 30.38 | 30.53 | 30.65 | 30.76 | 30.93 | 31.05 | 31.14 |
| 150 | 27.54 | 27.73 | 27.89 | 28.02 | 28.14 | 28.34 | 28.48 | 28.59 |
| 175 | 25.09 | 25.32 | 25.50 | 25.64 | 25.77 | 25.99 | 26.15 | 26.28 |
| 200 | 22.81 | 23.09 | 23.31 | 23.46 | 23.61 | 23.86 | 24.04 | 24.19 |
| 250 | 18.64 | 19.09 | 19.40 | 19.61 | 19.80 | 20.11 | 20.32 | 20.51 |
| 300 | 14.60 | 15.45 | 15.97 | 16.28 | 16.52 | 16.89 | 17.16 | 17.37 |
| 350 | 9.54 | 11.86 | 12.82 | 13.30 | 13.62 | 14.08 | 14.40 | 14.64 |
| 400 | | 7.56 | 9.74 | 10.53 | 10.97 | 11.56 | 11.94 | 12.21 |
| 450 | | | 6.50 | 7.82 | 8.49 | 9.24 | 9.70 | 10.01 |
| 500 | | | 2.87 | 5.12 | 6.10 | 7.11 | 7.67 | 8.03 |
| 550 | | | | 2.46 | 3.88 | 5.23 | 5.91 | 6.32 |
| 600 | | | | 0.26 | 2.12 | 3.79 | 4.59 | 5.06 |

# CHAPTER 4

## COMPLEXING AND AQUEOUS SPECIATION

It has long been recognized that simple solubilities of metal sulfides are inadequate to account for the level of metals needed in solution to form ore deposits. In addition, it is not possible to account for observed metal concentrations in many hot springs and in deep basin oil field brines without calling upon complexing. Even so, the experimental coverage of complexing at temperatures, pressures and fluid compositions representative of ore deposits is woefully lacking. A great deal of work to correct this situation has been done in the last 15 years; most notably by Barnes and co-workers at Penn State (Crerar et al., 1978; Crerar and Barnes, 1976; Romberger and Barnes, 1970; and Barnes et al., 1967). In addition, work has been done on the complexing of non-ore solutions species by Quist, Marshall and others at Oak Ridge (Quist and Marshall, 1966, 1968a, 1968b, 1969, 1970; Quist et al., 1963, 1965; Yeatts and Marshall, 1969; Dunn and Marshall, 1969 and Marshall, 1967) and more recently by Frantz and others at the Geophysical Laboratory (Boctor et al., 1980; Frantz and Popp, 1979 and Popp and Frantz, 1979).

Evaluation of the distribution of aqueous species in a 'typical' hydrothermal fluid requires knowledge of 20 to 40 dissociation constants for aqueous species. This need, when coupled with the poor experimental coverage, requires that reasonable estimates of dissociation constants for many aqueous species must be made.

## EQUATION OF STATE FOR AQUEOUS DISSOCIATION REACTIONS

Helgeson (1967) has proposed a model to describe the temperature dependence of dissociation constants for aqueous reactions. This model, as the models proposed for individual ions (see Chapters 2 and 3), is based on the separation of thermodynamic properties for a dissociation reaction into electrostatic and nonelectrostatic terms. The temperature dependence of the electrostatic contributions can be evaluated from the Born theory, while the heat capacity of the nonelectrostatic contributions is linearly dependent on temperature. Equation 4.1 is a modification of equation 18 of Helgeson (1967):

$$\text{(see facing page)} \qquad \qquad 4.1$$

where $\Delta S^\circ_r(T_r)$ and $\Delta H^\circ_r(T_r)$ are the entropy and enthalpy of dissociation at the reference temperature, $\Delta S^\circ_e(T_r)$ is the electrostatic entropy at the reference temperature, $\alpha'$ and $\beta'$ are the nonelectrostatic heat capacity terms and $\hat{a}$, $\hat{b}$, $\hat{c}$, $\hat{\theta}$ and $\hat{\omega}$ are constants with values of 0.01875, - 12.741, 7.84 x $10^{-4}$, 219.0 and 1.00322 respectively. This equation adequately reproduces experimentally determined dissociation constants in steam saturated water to the critical point. The derivation of Equation 4.1 as well as the fit of this equation to several sets of high temperature data are given by Helgeson (1967).

The values of $\alpha'$, $\beta'$ and $\Delta S^\circ_e(T_r)$ for a particular aqueous dissociation reaction can be determined by regression of experimental dissociation constants as a function of temperature. However, adequate data at high temperatures are often not available for regression analyses. Helgeson (1967) has shown that if $\Delta S^\circ_e(T_r)$ is assumed to be proportional to $\Delta S^\circ_r(T_r)$ and $\alpha'$ and $\beta'$ are assigned values of zero, dissociation constants which are consistent with experimental work, in

EQUATION 4.1

$$\log K(T) = \frac{\Delta S^O_e(T_r)}{2.303RT} \left[ T_r - T - \frac{\theta}{\omega}(1 - \exp(\exp(\hat{b} + \hat{a}T) - \hat{c} + (T - T_r)/\theta)) \right]$$

$$- \frac{\Delta H^O_r(T_r)}{2.303RT} + \frac{\Delta S^O_r(T_r)}{2.303R}$$

$$+ \frac{\alpha'}{2.303R}(\ln T/T_r - 1 + T/T_r) + \frac{\beta'(T - T_r)^2}{4.606RT}$$

many cases to temperatures greater the 200°C, may be estimated. However, in some cases this approximation breaks down at temperatures of only 150°C. Above these temperatures large deviations between experimentally derived and calculated values may occur.

The occurrence of porphyry mineralization at temperatures greater than 300°C requires that better techniques be developed to estimate dissociation constants at elevated temperatures. The remainder of the chapter deals with development of these estimating techniques.

## ESTIMATION OF THERMODYNAMIC PROPERTIES FOR
## AQUEOUS DISSOCIATION REACTIONS

ENTROPY CORRELATION

Entropies of ions in aqueous solutions at 25°C can be estimated by the use of entropy correlation plots which are based on an empirical correlation between ionic entropy at 25°C and ion charge, size, mass and geometry (Powell and Latimer, 1951 and Cobble, 1953a,b). Helgeson (1969) has modified the method proposed by Cobble (1953b) and estimated the entropy of dissociation for chloride complexes at 25°C. This method was used to estimate the entropy of some chloride and fluoride complexes used in this study and is outlined below (Helgeson, 1969).

The sum of the entropies of an aqueous species and its coordinated water molecules may be defined as:

$$S^*[ML_y(H_2O)_x^{Z_c}] = S°[ML_y] + xS°[H_2O] \qquad 4.2$$

and

$$S^*[M(H_2O)_u^{Z_i}] = S°[M^{Z_i}] + uS°[H_2O] \qquad 4.3$$

where $S°$ is the conventional partial molal entropy, $ML_y$ is a mononuclear complex involving $y$ moles of ligand L, $x$ and $u$ are the number of water molecules coordinated to the complex and the cation respectively, and $z_c$ and $z_i$ represent the respective charges of the complex and the cation.

Subtraction of equation 4.2 from 4.3 yields:

$$S^*[ML_y(H_2O)_x^{Z_c}] - S^*[M(H_2O)_u^{Z_i}] = \Delta S^*_d \qquad 4.4a$$

$$\Delta S^*_d = S°[ML_y^{Z_c}] - S°[M^{Z_i}] + (x-u)S°[H_2O] \qquad 4.4b$$

where $\Delta S^*_d$ is the entropy change of the cation as a result of the inclusion of complexing ligands in the hydration sphere. Substitution of equation 4.4b into equation 2.30 results in:

$$\Delta S^\circ_r = yS^\circ[L^Z1] + (x-u)S^\circ[H_2O] - \Delta S^*_d \qquad 4.5$$

where $z_1$ is the charge on the ligand. As a first approximation, Helgeson (1969) suggested:

$$x = u - y \qquad 4.6$$

This assumption requires that a one to one exchange of a complexing ligand for a water molecule in the hydration shell occurs. Clearly this would not be an appropriate assumption for complexes which have more coordinating ligands than the cation has coordinating waters (i.e. $y > u$) or for reactions in which complexing is accomplished without the exchange of a ligand for a water molecule.

Substitution of equation 4.6 into 4.5 results in:

$$\Delta S^*_d = y(S^\circ[L^Z1] - S^\circ[H_2O]) - \Delta S^\circ_r \qquad 4.7$$

For complexes with a common ligand, Helgeson (1969) proposed:

$$\Delta S^*_d = a'_1 + a'_2/(r_i + r_1) \qquad 4.8$$

where $a'_1$ and $a'_2$ are coefficients characteristic of the ligand considered, and $r_i$ and $r_1$ are the ionic radii of the cation and the ligand respectively. The values for $a'_1$ and $a'_2$ for chloride complexes are -102.5 and 325 for a chloride radius ($r_1$) of 1.81 A (Helgeson, 1969).

Attempts to fit $\Delta S^*_d$ of fluoride complexes were unsuccessful. However, when equation 4.8 was modified to include the charge, Z, of the central metal ion, the fit was greatly improved. The modified form of equation 4.8 is given below:

$$\Delta S^*_d = a'_1 + a'_2 \times Z /(r_i + r_1) \qquad 4.9$$

Where $a'_1$ and $a'_2$ have values of -39.1 and 34.1 using a fluoride radius of 1.33 A. Figure 4.1 is an entropy correlation plot for fluoride complexes. The average deviation between entropies estimated using

Fig. 4.1

Entropy correlation plot for fluoride complexes at room temperature. Entropy data are from Sillen and Martel (1976). The solid line represents the values calculated from equation 4.9 and the coefficients given in the text.
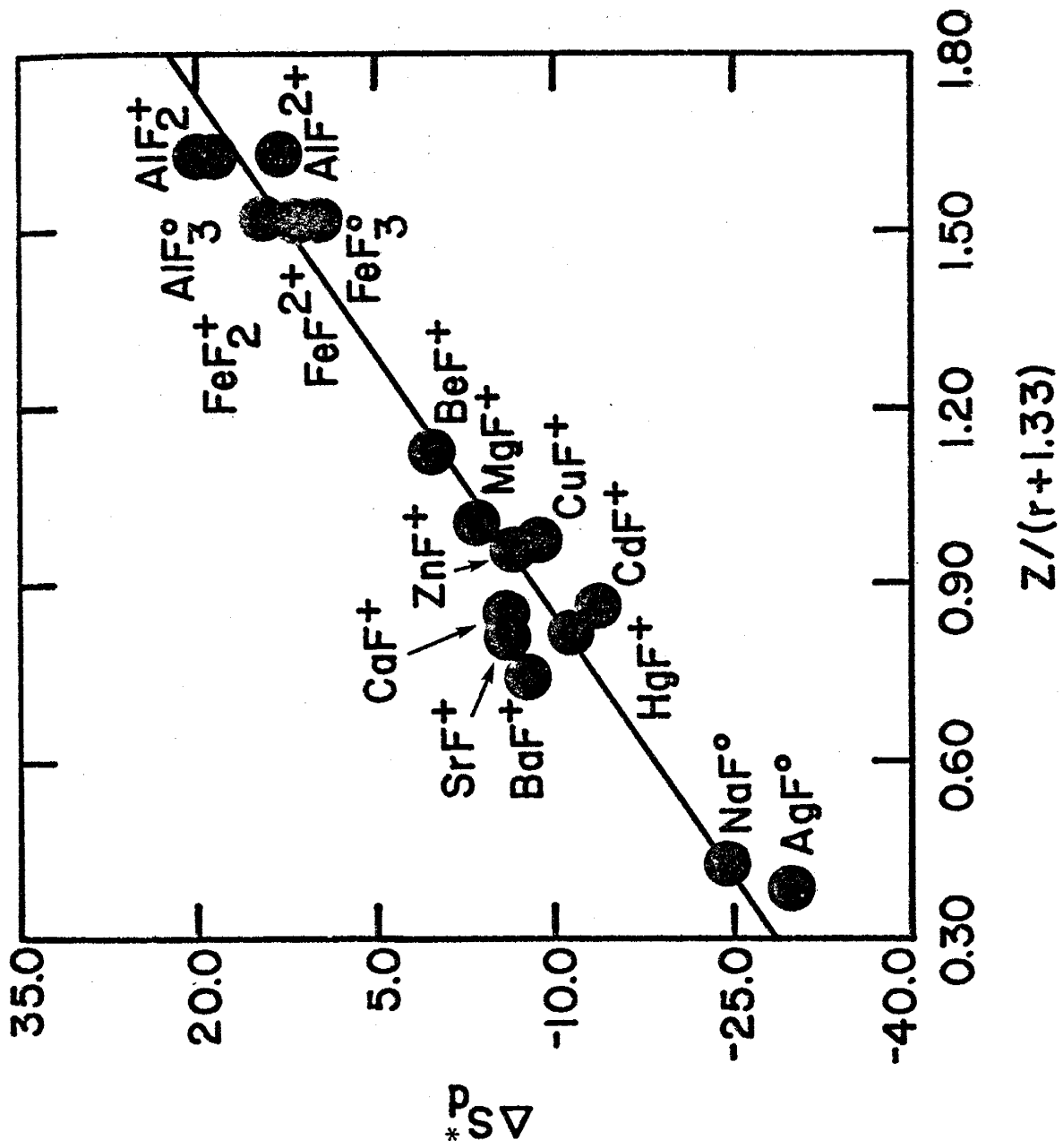
equation 4.9 and their experimental counterparts is 3 cal mole$^{-1}$ K$^{-1}$, with a maximum deviation of 6 cal mole$^{-1}$ K$^{-1}$ for BaF$^+$.


## ENTROPY CORRESPONDENCE PRINCIPLE

Criss and Cobble (1964a) found that empirical entropy correlations, such as the one described in the preceding section, exist for ions at elevated temperatures. This observation lead Criss and Cobble to conclude that a series of corresponding states for ionic entropy at elevated temperatures exist. They found that if the entropy of the hydrogen ion was fixed at each temperature, a linear relationship between ionic entropies at elevated temperatures and the corresponding ionic entropies at room temperature exists. This relationship, which is referred to as the entropy correspondence principle, may be stated as:

$$S°(T,abs) = a'' \times S°(T_r,abs) + b'' \qquad 4.10$$

where a" and b" are coefficients dependent on both ion type and temperature. The absolute entropy, $S°(T,abs)$, of an ion at the subscripted temperature is defined as:

$$S°(T,abs) = S°(T) + Z \times S°(T,H^+,abs) \qquad 4.11$$

where Z is the ionic charge, and $S°(T,H^+,abs)$ is the absolute entropy of the hydrogen ion at the subscripted temperature. Criss and Cobble determined the values of a", b" and $S°(T,H^+,abs)$ for several classes of ions by fitting experimental entropies at room and elevated temperatures to equation 4.10. In addition, these coefficients were estimated for temperatures of 200 to 300°C. The coefficients for equation 4.10, as well as the values of $S°(T,H^+,abs)$, at temperatures up to 300°C can be found in the literature (Criss and Cobble, 1964a and b). A description of the thermodynamic relationships for discretely spaced entropy data is given in Appendix A.

## Dissociation Reactions

In this study the entropy correspondence principle has been extended to include aqueous dissociation reactions. Helgeson (1967) proposed, based on limited data, that the entropy correspondence principle should apply to dissociation reactions as well as ions. The evaluation of aqueous dissociation reactions is easier than the ion counterparts because no consideration of the absolute entropy of the hydrogen ion needs be made (see Chapter 2). Hence, a linear correlation was found between entropies of dissociation at room and elevated temperatures.

### Fluoride and Hydroxide Complexes

Experimentally determined dissociation constants were taken from the literature (Table 4.1) and regressed as a function of temperature using equation 4.1. The results of these regressions are reported in Table 4.2. Smoothed equilibrium constants were used to evaluate the average heat capacity of reaction at 50° temperature interval in the range 25 to 250°C:

$$\Delta C^{\circ}_p \Big|_{T_r}^{T} = (\Delta G^{\circ}_r(T) - \Delta H^{\circ}_r(T_r) + \Delta S^{\circ}_r(T_r) \times T)/$$

$$(T - T_r - T\ln(T/T_r)) \qquad\qquad 4.12$$

The entropy of dissociation was then calculated from the average heat capacities:

$$\Delta S^{\circ}_r(T) = \Delta S^{\circ}_r(T_r) + \Delta C^{\circ}_p \Big|_{T_r}^{T} \times \ln(T/T_r) \qquad\qquad 4.13$$

Table 4.1

Experimental dissociation constants used to determine the coefficients in equation 4.1 for oxy-acids and fluoride and hydroxide complexes.
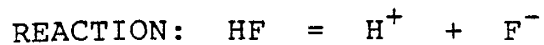
REACTION: HF = H$^+$ + F$^-$
SOURCE: Broene and DeVries (1947)

Log K(T) Temp $^\circ$C

| 15 | 25 | 35 |
|------|------|------|
| -3.10 | -3.18 | -3.25 |

REACTION: HF = H$^+$ + F$^-$
SOURCE: Ellis (1963)
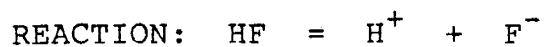
Log K(T) Temp $^\circ$C

| 25 | 50 | 75 | 100 | 125 | 150 | 175 | 200 |
|------|------|------|------|------|------|------|------|
| -3.18 | -3.40 | -3.63 | -3.84 | -4.09 | -4.34 | -4.58 | -4.89 |
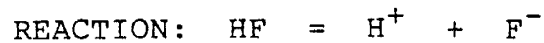
REACTION: HF = H$^+$ + F$^-$
SOURCE: Ryzhenko (1965)

Log K(T) Temp $^\circ$C

| 25 | 50 | 100 | 150 | 200 | 218 |
|------|------|------|------|------|------|
| -3.17 | -3.37 | -3.85 | -4.38 | -4.95 | -5.02 |
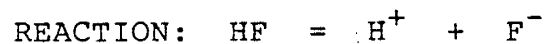
REACTION: HF = H$^+$ + F$^-$
SOURCE: Richardson and Holland (1979)

Log K(T) Temp $^\circ$C

| 100 | 200 | 260 |
|------|------|------|
| -4.00 | -4.85 | -5.40 |

REACTION: F$^-$ + HF = HF$_2^-$
SOURCE: Ellis (1963)
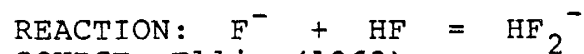
Log K(T) Temp $^\circ$C

| 25 | 50 | 75 | 100 | 125 | 150 | 175 | 200 |
|------|------|------|------|------|------|------|------|
| 0.53 | 0.60 | 0.67 | 0.68 | 0.69 | 0.76 | 0.76 | 0.9 |

Table 4.1 (cont.)

REACTION: NaF = Na$^+$ + F$^-$
SOURCE: Butler and Hudson (1970)

| Log K(T) | Temp $^oC$ |
|---|---|
| | 25 |
| | 0.80 |

REACTION: NaF = Na$^+$ + F$^-$
SOURCE: Miller and Kester (1976)

| Log K(T) | Temp $^oC$ | |
|---|---|---|
| 15 | 25 | 35 |
| 0.85 | 0.95 | 1.04 |

REACTION: NaF = Na$^+$ + F$^-$
SOURCE: Richardson and Holland (1979)

| Log K(T) | Temp $^oC$ |
|---|---|
| 200 | 260 |
| -0.04 | -0.54 |

REACTION: CaF$^+$ = Ca$^{2+}$ + F$^-$
SOURCE: Tanner et al. (1968)

| Log K(T) | Temp $^oC$ | |
|---|---|---|
| 2 | 25 | 39 |
| -1.04 | -1.19 | -1.41 |

REACTION: CaF$^+$ = Ca$^{2+}$ + F$^-$
SOURCE: Cadek et al. (1971)

| Log K(T) | Temp $^oC$ | | | |
|---|---|---|---|---|
| 15 | 25 | 35 | 45 | 60 |
| -1.14 | -1.26 | -1.25 | -1.27 | -1.42 |

REACTION: CaF$^+$ = Ca$^{2+}$ + F$^-$
SOURCE: Aziz and Lyle (1969)

| Log K(T) | Temp $^oC$ |
|---|---|
| | 25 |
| | -1.39 |

Table 4.1 (cont.)

REACTION: $CaF^+ = Ca^{2+} + F^-$
SOURCE: Richardson and Holland (1979)
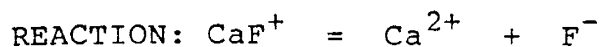
| Log K(T) | Temp $^\circ C$ |
|---|---|
| 200 | 260 |
| -2.51 | -2.98 |

REACTION: $MgF^+ = Mg^{2+} + F^-$
SOURCE: Tanner et al. (1968)

| | Log K(T) | Temp $^\circ C$ |
|---|---|---|
| 2 | 25 | 39 |
| -1.74 | -1.91 | -1.99 |
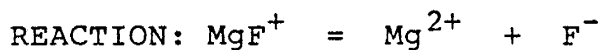
REACTION: $MgF^+ = Mg^{2+} + F^-$
SOURCE: Cadek et al. (1971)

| | | Log K(T) | Temp $^\circ C$ | |
|---|---|---|---|---|
| 15 | 25 | 35 | 45 | 60 |
| -1.86 | -1.92 | -1.94 | -2.00 | -2.08 |

REACTION: $MgF^+ = Mg^{2+} + F^-$
SOURCE: Richardson and Holland (1979)

| Log K(T) | Temp $^\circ C$ |
|---|---|
| 200 | 260 |
| -2.74 | -3.57 |

REACTION: $H_3PO_4 + OH^- = H_2PO_4^- + H_2O$
SOURCE: Mesmer and Baes (1974)
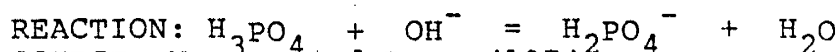
| | | log K(T) | Temp $^\circ C$ | | | |
|---|---|---|---|---|---|---|
| 0 | 25 | 50 | 75 | 100 | 125 | 150 |
| 12.88 | 11.85 | 10.98 | 10.26 | 9.65 | 9.13 | 8.68 |

| | | log K(T) | Temp $^\circ C$ | | |
|---|---|---|---|---|---|
| 175 | 200 | 225 | 250 | 275 | 300 |
| 8.29 | 7.954 | 7.65 | 7.38 | 7.13 | 6.90 |

Table 4.1 (cont.)

REACTION: $H_2PO_4^- + OH^- = HPO_4^{2-} + H_2O$
SOURCE: Mesmer and Baes (1974)
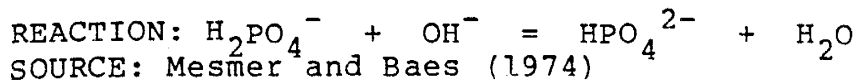
log K(T) Temp $^{\circ}C$

| 0 | 25 | 50 | 75 | 100 | 125 | 150 |
|------|------|------|------|------|------|------|
| 7.63 | 6.80 | 6.08 | 5.46 | 4.93 | 4.47 | 4.07 |

log K(T) Temp $^{\circ}C$

| 175 | 200 | 225 | 250 | 275 | 300 |
|------|------|------|------|------|------|
| 3.71 | 3.39 | 3.10 | 2.84 | 2.59 | 2.36 |

REACTION: $H_2CO_3 = H^+ + HCO_3^-$
SOURCE: Harned and Davis (1943)
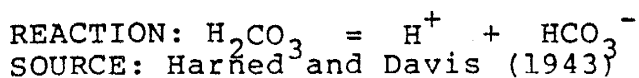
log K(T) Temp $^{\circ}C$

| 0 | 5 | 10 | 15 | 20 | 25 |
|-------|-------|-------|-------|-------|-------|
| -6.58 | -6.52 | -6.46 | -6.42 | -6.38 | -6.35 |

log K(T) Temp $^{\circ}C$

| 30 | 35 | 40 | 45 | 50 |
|-------|-------|-------|-------|-------|
| -6.33 | -6.31 | -6.30 | -6.29 | -6.29 |

REACTION: $H_2CO_3 = H^+ + HCO_3^-$
SOURCE: Ellis (1959)
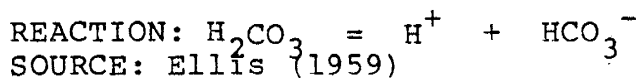
log K(T) Temp $^{\circ}C$

| 25 | 35 | 45 | 55 | 65 |
|-------|-------|-------|-------|-------|
| -6.38 | -6.32 | -6.31 | -6.30 | -6.31 |

REACTION: $H_2CO_3 = H^+ + HCO_3^-$
SOURCE: Ryzhenko (1963)
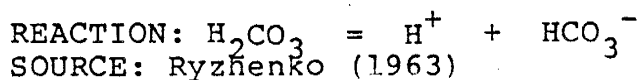
log K(T) Temp $^{\circ}C$

| 100 | 156 | 200 |
|-------|-------|-------|
| -6.46 | -6.81 | -7.14 |

REACTION: $H_2CO_3 = H^+ + HCO_3^-$
SOURCE: Reed (1975)
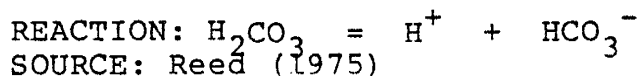
log K(T) Temp $^{\circ}C$

| 25 | 100 | 150 | 200 | 250 |
|-------|-------|-------|-------|-------|
| -6.36 | -6.42 | -6.76 | -7.25 | -7.79 |

Table 4.1 (cont.)

REACTION: $HCO_3^- = H^+ + CO_3^{2-}$
SOURCE: Harned and Scholes (1941)

log K(T) Temp $^O$C

| 0 | 5 | 10 | 15 | 20 | 25 | 30 |
|---|---|----|----|----|----|----|
| -10.66 | -10.56 | -10.49 | -10.43 | -10.38 | -10.33 | -10.29 |

log K(T) Temp $^O$C

| 35 | 40 | 45 | 50 |
|----|----|----|----|
| -10.25 | -10.22 | -10.20 | -10.18 |

REACTION: $HCO_3^- = H^+ + CO_3^{2-}$
SOURCE: Cuta and Stafelda (1954)

log K(T) Temp $^O$C

| 60 | 70 | 80 | 90 |
|----|----|----|----|
| -10.18 | -10.16 | -10.14 | -10.14 |

REACTION: $HCO_3^- = H^+ + CO_3^{2-}$
SOURCE: Ryzhenko (1963)

log K(T) Temp $^O$C

| 100 | 156 | 218 |
|-----|-----|-----|
| -10.14 | -10.41 | -10.96 |

REACTION: $HSO_4^- = H^+ + SO_4^{2-}$
SOURCE: Kerker (1957)

log K(T) Temp $^O$C

| 18 | 25 | 50 |
|----|----|----|
| -1.91 | -1.99 | -2.28 |

REACTION: $HSO_4^- = H^+ + SO_4^{2-}$
SOURCE: Nair and Nancollas (1958)

log K(T) Temp $^O$C

| 0 | 5 | 15 | 25 | 35 | 45 |
|---|---|----|----|----|----|
| -1.58 | -1.64 | -1.80 | -1.96 | -2.09 | -2.22 |

Table 4.1 (cont.)

REACTION: $HSO_4^- = H^+ + SO_4^{2-}$
SOURCE: Lietzke and Stoughton[4] (1961)

|  | | log K(T) Temp $^\circ$C | | |
| --- | --- | --- | --- | --- |
| 25 | 50 | 75 | 100 | 125 |
| -1.89 | -2.37 | -2.70 | -3.01 | -3.33 |

|  | log K(T) Temp $^\circ$C | | |
| --- | --- | --- | --- |
| 150 | 175 | 200 | 225 |
| -3.69 | -4.09 | -4.49 | -4.94 |

REACTION: $HSO_4^- = H^+ + SO_4^{2-}$
SOURCE: Ryzhenko (1964)

| log K(T) Temp $^\circ$C | | |
| --- | --- | --- |
| 100 | 156 | 218 |
| -3.04 | -3.90 | -4.87 |

REACTION: $HSO_4^- = H^+ + SO_4^{2-}$
SOURCE: Quist[4] and Marshall (1966)

| log K(T) Temp $^\circ$C | | |
| --- | --- | --- |
| 100 | 200 | 300 |
| -3.20 | -4.67 | -6.78 |

REACTION: $MgOH^+ = Mg^{2+} + OH^-$
SOURCE: McGee and Hostetler (1975)

|  |  | log K(T) Temp $^\circ$C | | | |
| --- | --- | --- | --- | --- | --- |
| 10 | 25 | 40 | 55 | 70 | 90 |
| -2.18 | -2.21 | -2.29 | -2.37 | -2.44 | -2.54 |

REACTION: $Al(OH)_4^- = Al^{3+} + 4OH^-$
SOURCE: Helgeson[4] (1969, 1971)

| log K(T) Temp $^\circ$C | | |
| --- | --- | --- |
| 25 | 100 | 150 |
| -33.73 | -32.3 | -32.8 |

Table 4.1 (cont.)

REACTION: $H_2O = H^+ + OH^-$
SOURCE: Ackermann (1958)

log K(T) Temp $^{O}C$

| 0 | 10 | 20 | 25 | 30 | 40 | 50 | 60 |
|---|---|---|---|---|---|---|---|
| -14.95 | -14.54 | -14.16 | -14.00 | -13.83 | -13.34 | -13.26 | -13.01 |

log K(T) Temp $^{O}C$

| 70 | 80 | 90 | 100 | 110 | 120 | 130 |
|---|---|---|---|---|---|---|
| -12.80 | -12.60 | -12.42 | -12.27 | -12.13 | -12.00 | -11.90 |

REACTION: $H_2O = H^+ + OH^-$
SOURCE: Noyes et al. (1910)

log K(T) Temp $^{O}C$

| 100 | 156 | 218 | 306 |
|---|---|---|---|
| -12.28 | -11.57 | -11.19 | -11.46 |

Table 4.2

Fit coefficients for oxy-acids and fluoride and hydroxide complexes
for use with equations 4.1 and 5.1. Sources of data are given in Table
4.1. Coefficient for acetic, formic and nitric acid are from Helgeson
(1967)

| Reaction | $\Delta S^o_r(T_r)^{\underline{a}}$ | $\Delta H^o_r(T_r)^{\underline{b}}$ | $\Delta S^o_e(T_r)^{\underline{a}}$ | $\alpha^{\underline{a}}$ | $\beta \times 10^2 \, ^{\underline{c}}$ |
|---|---|---|---|---|---|
| $H_2O = H^+ + OH^-$ | -19.3 | 13335 | -14.24 | -153.10 | 40.38 |
| $CaF^+ = Ca^{2+} + F^-$ | -13.8 | -2514 | 0.50 | -33.89 | |
| $MgF^+ = Mg^{2+} + F^-$ | -16.5 | -2336 | -3.49 | -19.52 | |
| $HF = H^+ + F^-$ | -25.5 | -3264 | 1.42 | -55.46 | 3.48 |
| $HF_2^- = H^+ + 2F^-$ | -32.2 | -4538 | -13.51 | -8.69 | |
| $NaF = Na^+ + F^-$ | 5.0 | 276 | -7.74 | -183.30 | 42.90 |
| $MgOH^+ = Mg^{2+} + OH^-$ | -15.7 | -1630 | -15.7 | | |
| $Al(OH)^+ = Al^{3+} + 4OH^-$ | -121.4 | 8460 | | | -33.77 |
| $CH_3COOH = CH_3COO^- + H^+$ | -22.1 | -112 | -3.95 | -30.20 | -0.88 |
| $HCOOH = HCOO^- + H^+$ | -17.2 | -12 | -20.59 | -135.09 | 41.48 |
| $H_2CO_3 = HCO_3^- + H^+$ | -22.9 | 1840 | -29.26 | -265.20 | 74.08 |
| $HCO_3^- = CO_3^{2-} + H^+$ | -35.2 | 3600 | -14.70 | -145.70 | 31.95 |
| $H_3PO_4 = H_2PO_4^- + H^+$ | -16.6 | -2033 | -15.98 | -149.90 | 44.52 |
| $H_2PO_4^- = HPO_4^{2-} + H^+$ | -30.4 | 759 | -15.98 | -173.50 | 47.40 |
| $HSO_4^- = SO_4^{2-} + H^+$ | -26.7 | -5246 | -17.87 | -74.20 | 17.48 |
| $HNO_3 = H^+ + NO_3^-$ | -7.2 | -4100 | 3.74 | 10.43 | -18.76 |

$\underline{a}$ cal mole$^{-1}$ K$^{-1}$. $\underline{b}$ cal mole$^{-1}$. $\underline{c}$ cal mole$^{-1}$ K$^{-2}$.

Fig. 4.2

Correlation of the entropy of reaction at 25° and 200° C for fluoride

and hydroxide dissociation reactions. Entropy data are calculated

from dissociation constants listed in Table 4.1 as described in the

text. The solid line represents the values calculated using equation

4.10 and the coefficients given in Table 4.3. Units of entropy are

cal mole$^{-1}$ K$^{-1}$.
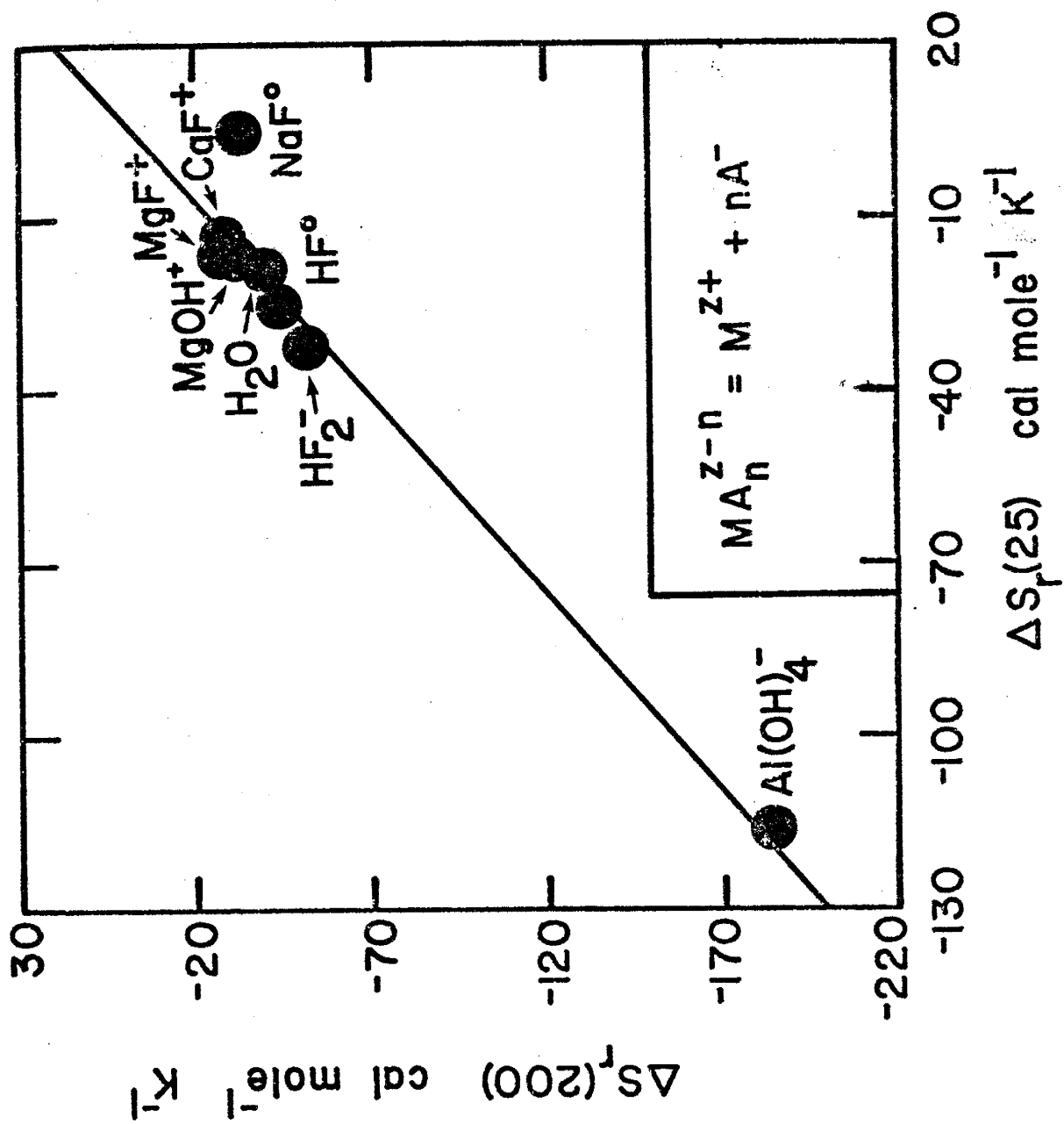
The entropies of dissociation for fluoride and hydroxide complexes were evaluated and it was found that they could be represented by equation 4.10. The coefficients a" and b" for fluoride and hydroxide complexes are given in Table 4.3. The agreement between the entropies estimated at 200°C using equation 4.10 and their experimentally derived counterparts is shown in Fig. 4.2. With the exception of NaF, the average deviation between the curve and the data points is 3 cal mole$^{-1}$ K$^{-1}$. Deviations of this magnitude are similar to the errors associated with the individual entropies (Richardson and Holland, 1979a).

Evaluation of the values of a" and b" indicated they are both linear functions of temperature. Equation 4.10 can be rewritten to describe the entropy of dissociation for fluoride and hydroxide complexes in the temperature range 25 to 300°C as:

$$\Delta S^\circ_r(T) = ((0.00249 + 0.258/T) \times \Delta S^\circ_r(T_r)$$
$$- 0.0602)T + 17.9 \qquad 4.14$$

Differentiation of equation 4.14 with respect to temperature yields the molal heat capacity of reaction:

$$\Delta C^\circ_{p,r}(T) = (0.00249 \times \Delta S^\circ_r(T_r) - 0.0602)T \qquad 4.15$$

Equations 4.14 and 4.15 can be used to evaluate the heat capacity and entropy of dissociation for both fluoride and hydroxide complexes at temperatures up to 300°C.

## Oxy-acids

The entropies of oxy-acids were determined in a matter analogous to fluoride and hydroxide complexes. The sources of the experimental data and the fit coefficients for equation 4.1 are given in Table 4.1 and 4.2 respectively.

## Table 4.3

Coefficients a" and b" for equation 4.10 used to estimate the entropy of dissociation of hydroxide and fluoride complexes at elevated temperatures.

| Temp $^O$C | b" | a" |
|---|---|---|
| 50 | -1.91 | 1.08 |
| 100 | -5.13 | 1.22 |
| 150 | -7.80 | 1.34 |
| 200 | -10.53 | 1.46 |
| 250 | -13.89 | 1.56 |
| 300 | -16.81 | 1.70 |

Modification of equation 4.10 was required in order to develop linear relationships between room temperature entropies of dissociation and entropies at elevated temperature. Techniques which have been proposed to estimate the entropy of gases, aqueous ions and solids contain a term related to the formula weight of the substances (Powell and Latimer, 1951, Latimer, 1952 and Cobble 1953a). Making this consideration, equation 4.10 can be rewritten as:

$$[\Delta S°_r(T) - (3/2)R\ln M] = a'' \times [\Delta S°_r(T_r) - 3/2R\ln M] + b'' \qquad 4.16$$

rearranging:

$$\Delta S°_r(T) = a'' \times \Delta S°_r(T_r) + b'' + (1-a'') \times (3/2)R\ln M \qquad 4.17$$

where M is the formula weight of the undissociated species and R is the gas constant. The coefficients a'' and b'' determined by regression analyses for oxy-acids are given in Table 4.4. A graphical comparison between equation 4.16 and the experimental entropies of dissociation at 200°C indicates, that with the exception of $H_2CO_3$ and $HNO_3$, the fit is very good (Fig. 4.3). The average deviation between the calculated entropies and their estimated counterparts was less than 2 cal mole$^{-1}$ K$^{-1}$.

The first dissociation of carbonic acid and the dissociation of nitric acid do not fall on the curve in Fig. 4.3. Dissociation reactions for carbonic acid are based on the convention that all dissolve carbon dioxide is treated as $H_2CO_3$. Wissburn et al. (1954) have demonstrated that, at room temperature, greater than 99% of the carbon dioxide in solution is present as molecular $CO_2$. As a consequence, $H_2CO_3$ is not an oxy-acid, and the dissociation reaction should be rewritten as:

$$H_2O + CO_2(aq) = H^+ + HCO_3^- \qquad 4.18$$
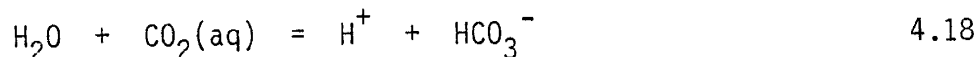
Table 4.4

Coefficients a" and b" for equations 4.16 and 4.17 used to estimate the entropy of dissociation of oxy-acids at elevated temperatures.

| Temp $^{\circ}$C | b" | a" |
|---|---|---|
| 50 | 2.66 | 1.18 |
| 100 | 4.26 | 1.41 |
| 150 | 4.74 | 1.57 |
| 200 | 4.25 | 1.70 |
| 250 | 2.74 | 1.84 |
| 300 | 0.50 | 2.06 |

Fig. 4.3

Correlation of the entropy of reaction at 25° and 200° C for oxy-acid

dissociation reactions. Entropy data are calculated from dissocia-

tion constants listed in Table 4.1 and Helgeson (1967) as described

in the text. The solid line represents the values calculated using

equation 4.16 and the coefficients given in Table 4.4. Units of

entropy are cal mole$^{-1}$ K$^{-1}$.
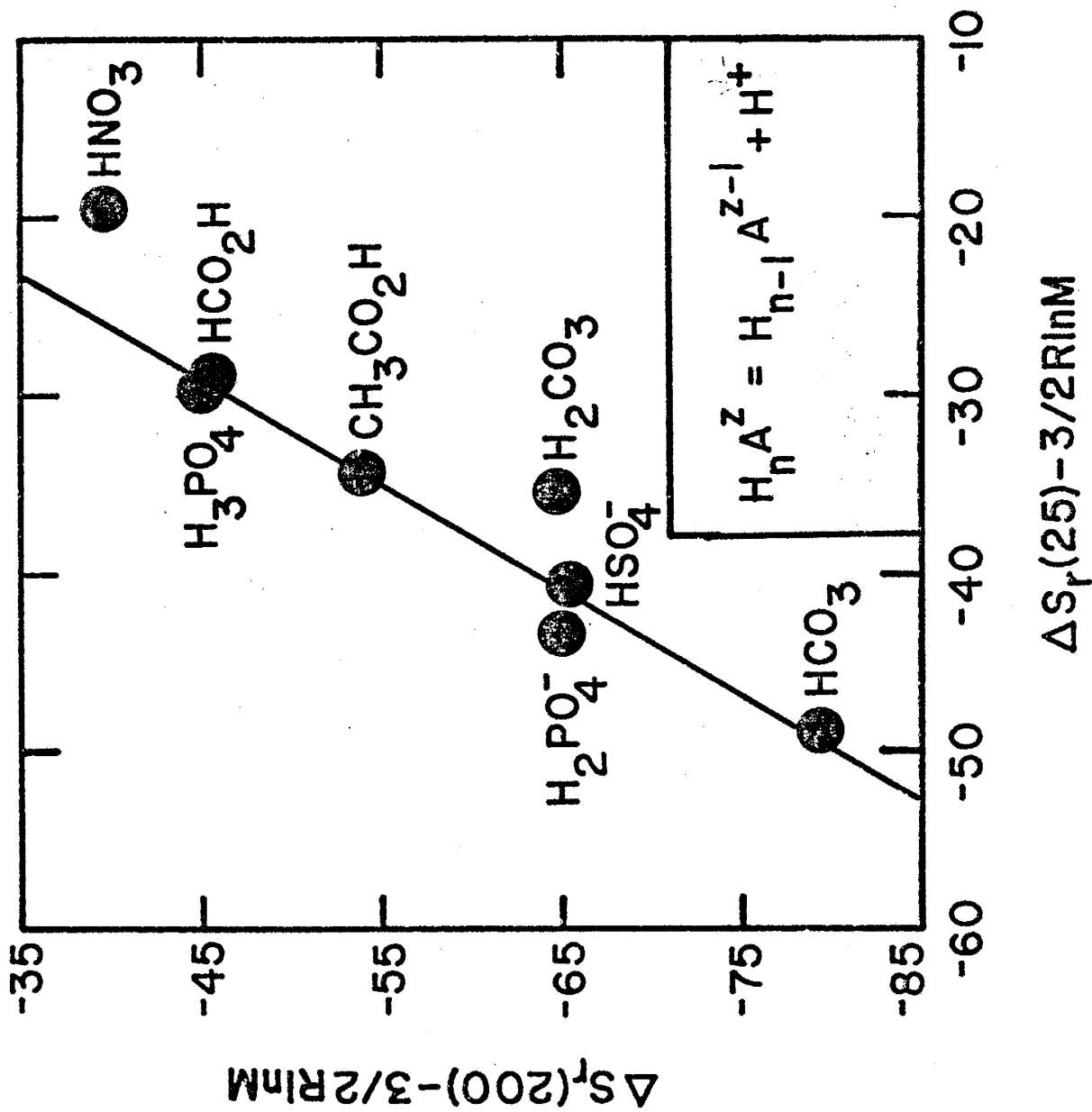
Dissociation constants for nitric acid have been determined at only three temperatures above 50°C (70, 218 and 306°C). Helgeson (1967) rejected the values at 70 and 306°C in his regression analyses. Consequently, the high temperature portion of the dissociation curve for nitric acid is poorly constrained and the deviation found in this study for the entropy of dissociation of nitric acid may be due to experimental uncertainties.

# CHAPTER 5

## STABILITY OF FLUORIDE COMPLEXES AT ELEVATED TEMPERATURES

Chloride complexes are the most important mechanism for the transport of base and precious metals in ore forming solutions (Helgeson, 1969). However, mineral assemblages associated with many ore deposits indicate that fluoride was a significant component of the mineralizing solutions (Gunow et al., 1980, Richardson and Holland 1979b, Putnam, 1980). The stabilities of fluoride complexes of potential geologic interest are evaluated in this chapter.

The dissociation constants for hydrofluoric acid have been measured by conductivity methods to temperatures of 200°C by Ellis (1963) and Ryzhenko (1965). Dissociation constants have also been determined at temperatures of 450 to 650°C and water densities of 0.3 to 0.8 g cm$^{-3}$ by conductivity methods (Franck, 1961). Richardson and Holland (1979a) have determined the dissociation constants of HF, CaF$^+$, MgF$^+$ and NaF at 100, 200 and 260°C by weight loss solubility experiments using fluorite. Dissociation constants for NaF at a temperature of 550°C and water densities of 0.3 to 0.7 g cm$^{-3}$ have also been reported (Franck, 1961).

Table 5.1 contains the dissociation constants for 26 fluoride complexes to temperatures of 300°C. These dissociation constants, except where noted, were calculated using the entropy correspondence principle. The dissociation constants for HF, NaF, HF$_2^-$, CaF$^+$ and MgF$^+$ were calculated from equation 4.1 and the coefficients given in Table 4.1. There is good agreement between the dissociation constants calculated from equation 4.1 and their experimentally determined counterparts (Fig. 5.1).

Table 5.1

Dissociation constants for fluoride complexes.

| Reaction | $\Delta S^\circ_r(T_r)$ [a] | $\Delta H^\circ_r(T_r)$ [b] | 25 | 50 | 100 | 150 | 200 | 250 | 300 |
|---|---|---|---|---|---|---|---|---|---|
| | | | | | | log K(T)°C | | | |
| $HF = H^+ + F^-$ [c] | -25.5 | -3264 | -3.18 | -3.40 | -3.88 | -4.38 | -4.87 | -5.33 | -5.72 |
| $NaF = Na^+ + F^-$ [c] | 5.0 | 276 | 0.89 | 0.86 | 0.63 | 0.31 | -0.05 | -0.43 | -0.92 |
| $MgF^+ = Mg^{2+} + F^-$ [c] | -16.5 | -2336 | -1.89 | -2.05 | -2.39 | -2.77 | -3.16 | -3.57 | -4.00 |
| $CaF^+ = Ca^{2+} + F^-$ [c] | -13.8 | -2514 | -1.17 | -1.34 | -1.69 | -2.07 | -2.45 | -2.84 | -3.27 |
| $SrF^+ = Sr^{2+} + F^-$ | -14.0 [d] | -3342 | -0.61 [e] | -0.82 | -1.25 | -1.68 | -2.12 | -2.55 | -3.00 |
| $BaF^+ = Ba^{2+} + F^-$ | -12.0 [d] | -3291 | -0.21 [e] | -0.42 | -0.84 | -1.26 | -1.67 | -2.09 | -2.53 |
| $MnF^+ = Mn^{2+} + F^-$ | -13.7 [f] | -2284 | -1.32 [e] | -1.47 | -1.80 | -2.16 | -2.53 | -2.92 | -3.33 |
| $FeF^+ = Fe^{2+} + F^-$ | -15.0 [f] | -2549 | -1.41 [e] | -1.57 | -1.94 | -2.32 | -2.71 | -3.12 | -3.55 |
| $CoF^+ = Co^{2+} + F^-$ | -15.3 [f] | -3170 | -1.02 [e] | -1.22 | -1.64 | -2.07 | -2.50 | -2.93 | -3.39 |
| $NiF^+ = Ni^{2+} + F^-$ | -15.8 [f] | -3182 | -1.12 [e] | -1.32 | -1.74 | -2.18 | -2.61 | -3.05 | -3.51 |
| $CuF^+ = Cu^{2+} + F^-$ | -11.0 [g] | -1206 | -1.52 [e] | -1.61 | -1.83 | -2.10 | -2.40 | -2.72 | -3.08 |
| $ZnF^+ = Zn^{2+} + F^-$ | -18.0 [d] | -3798 | -1.15 [d] | -1.39 | -1.87 | -2.36 | -2.84 | -3.32 | -3.81 |
| $SnF^+ = Sn^{2+} + F^-$ | -11.6 [f] | 2954 | -4.70 [e] | -4.55 | -4.40 | -4.39 | -4.46 | -4.60 | -4.81 |
| $SnF_2^\circ = Sn^{2+} + 2F^-$ | -31.0 [f] | 1058 | -7.55 [e] | -7.52 | -7.63 | -7.91 | -8.31 | -8.81 | -9.37 |
| $SnF_3^- = Sn^{2+} + 3F^-$ | -51.0 [f] | -1071 | -10.36 [e] | -10.46 | -10.84 | -11.39 | -12.08 | -12.86 | -13.73 |
| $PbF^+ = Pb^{2+} + F^-$ | -7.7 [f] | 514 | -2.06 [e] | -2.05 | -2.11 | -2.24 | -2.43 | -2.65 | -2.92 |
| $PBF_2^\circ = Pb^{2+} + 2F^-$ | -27.6 [f] | -3563 | -3.42 [e] | -3.65 | -4.17 | -4.74 | -5.37 | -6.03 | -6.73 |
| $AlF^{2+} = Al^{3+} + F^-$ | -33.0 [d] | -275 | -7.01 [i] | -7.06 | -7.30 | -7.68 | -8.17 | -8.74 | -9.38 |
| $AlF_2^+ = Al^{3+} + 2F^-$ | -60.0 [d] | -495 | -12.75 [i] | -12.82 | -13.18 | -13.75 | -14.48 | -15.33 | -16.28 |
| $AlF_3^\circ = Al^{3+} + 3F^-$ | -78.0 [a] | -34 | -17.02 [i] | -17.08 | -17.46 | -18.12 | -18.97 | -19.98 | -21.10 |
| $AlF_4^- = Al^{3+} + 4F^-$ | -91.0 [d] | -227 | -19.72 [i] | -19.80 | -20.25 | -21.00 | -21.97 | -23.11 | -24.39 |
| $AlF_5^{2-} = Al^{3+} + 5F^-$ | -97.0 [d] | -392 | -20.91 [i] | -21.00 | -21.49 | -22.29 | -23.32 | -24.53 | -25.87 |
| $AlF_6^{3-} = Al^{3+} + 6F^-$ | -94.0 [h] | -435 | -20.86 [i] | -20.90 | -21.30 | -22.03 | -22.99 | -24.13 | -25.41 |
| $FeF^{2+} = Fe^{3+} + F^-$ | -31.0 [d] | -784 | -6.20 [j] | -6.27 | -6.55 | -6.96 | -7.46 | -8.04 | -8.67 |
| $FeF_2^+ = Fe^{3+} + 2F^-$ | -54.0 [d] | -1368 | -11.80 [j] | -11.84 | -12.13 | -12.63 | -13.28 | -14.05 | -14.91 |
| $FeF_3^\circ = Fe^{3+} + 3F^-$ | -69.0 [d] | -1471 | -14.00 [j] | -14.14 | -14.62 | -15.31 | -16.17 | -17.15 | -18.23 |

[a] cal mole$^{-1}$ K$^{-1}$.  [b] cal mole$^{-1}$.  [c] calculated using equation 4.1 and coefficient in Table 4.2.  [d] Smith and Martell (1976).  [e] Smith and Martell (1976) extrapolated to zero ionic strength.  [f] estimated using equation 4.9.  [g] Connick and Paul (1957).  [h] Latimer and Jolly (1952).  [i] Hem (1968).  [j] Nordstrom and Jenne (1977).

Fig. 5.1

Comparison between experimental dissociation constants for fluoride complexes (symbols) and those calculated using equation 4.1 and the coefficients given in Table 4.2. Sources of data are given in Table 4.1.

Plot of $\log K(T)$ versus Temp. °C for the dissociation reaction $MF^{z-1} = M^{z+} + F^-$, showing curves labeled $NaF°$, $CaF^+$, $MgF^+$, and $HF°$.
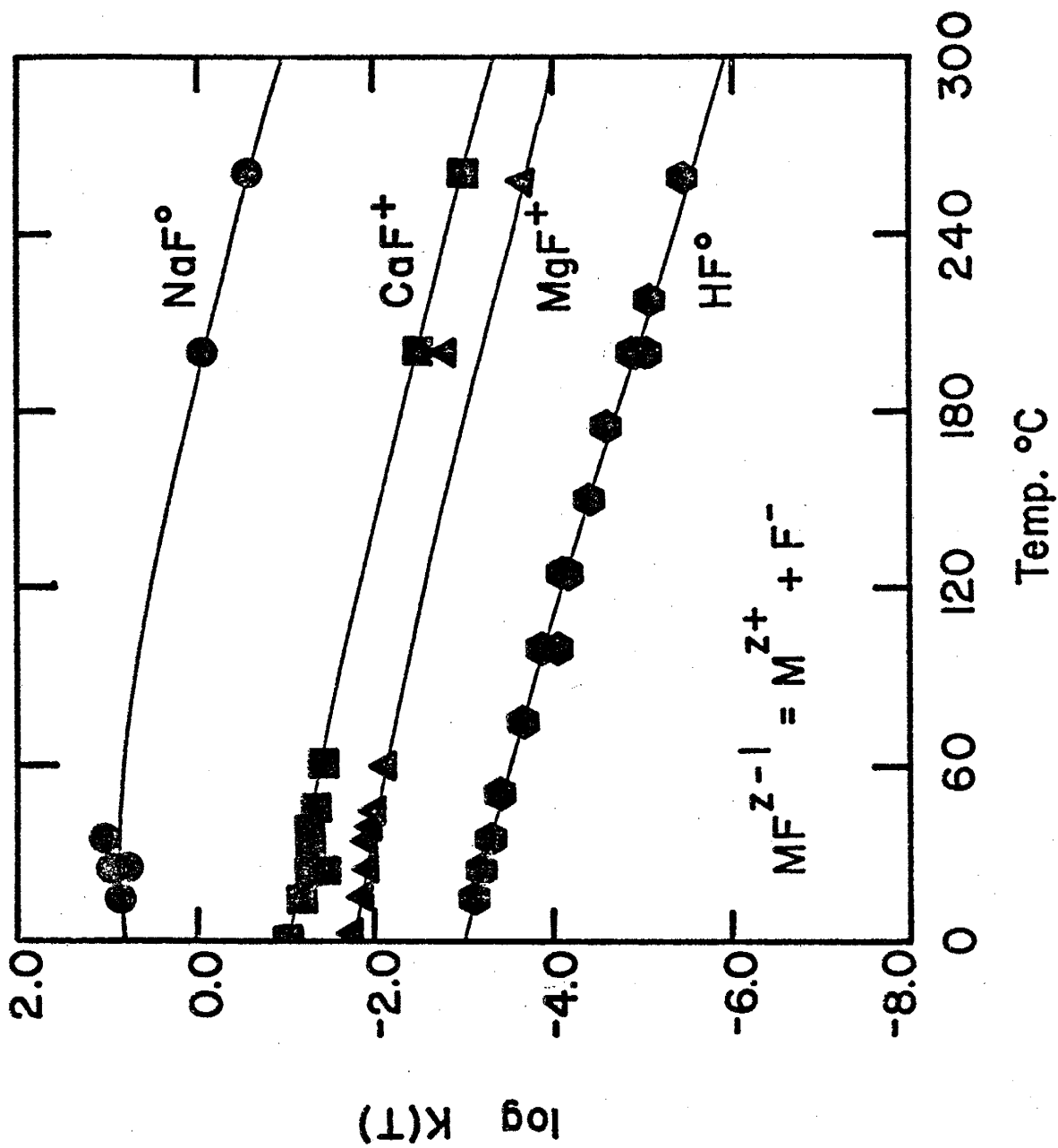
Examination of $\Delta S^{\circ}_r(T_r)$ reveals that both $MgF^+$ and $CaF^+$ have values close to zero. Furthermore, only one nonelectrostatic heat capacity term, $\alpha'$, is needed to fit the data. This observation suggests that the fitted coefficients in equation 4.1 can be determined from heat capacity data. The heat capacity of reaction for equation 4.1 is given by:

$$\text{(see facing page)} \qquad\qquad 5.1$$

where the terms in the equation have values described elsewhere (see Chapter 4). Acceptable fits of the experimental data for $MgF^+$ and $CaF^+$ were obtained by using an average value of -1.5 cal mole$^{-1}$ K$^{-1}$ for $\Delta S^{\circ}_r(T_r)$ and solving equation 5.1 for $\alpha'$ at 25°C using heat capacities of reaction estimated from equation 4.15. This same technique was used to estimate the dissociation of all one-to-one divalent fluoride complexes in Table 5.1.

All complexes exhibit typical behavior in that complexing becomes more significant at elevated temperatures (Figs. 5.2a-d). The existence of a maximum in the dissociation constant curve for a particular reaction depends on the sign and magnitude of the enthalpy of dissociation, with positive enthalpies producing maxima. Tabulations of the dissociation constants, Gibbs free energies, entropies and heat capacities at 25°C intervals for the complexes listed in Table 5.1 are given in Appendix B.


HYDROFLUORIC ACID

The temperature dependence of the dissociation of hydrofluoric acid exhibits characteristics worth special note. The electrostatic entropy, $\Delta S^{\circ}_e(T_r)$ of hydrofluoric acid is positive (see Table 4.2). Consequently, the electrostatic heat capacity is also positive, which results in large positive heat capacities at elevated temperatures.

## EQUATION 5.1

$$\Delta C^O_{p,r}(T) = \frac{T\Delta S^O_e(T_r)\exp(\exp(b+aT) - c + (T-T_r)/\theta)}{\hat{\omega}\theta} \times$$

$$\{(1 + \hat{a}\theta\exp(b+aT))^2 + \hat{a}^2\theta^2\exp(b+aT)\} +$$

$$\alpha' + \beta'T$$

Fig. 5.2

Temperature dependence of dissociation constants for fluoride

complexes in steam saturated water.  Dissociation constants are

from Table 5.1 and appendix B.


Fig. 5.2a

Alkaline earth element fluoride complexes


Fig. 5.2b

First row transition element fluoride complexes


Fig. 5.2c

Trivalent fluoride complexes


Fig. 5.2d

Lead and tin fluoride complexes

a)

b)

c)

d)
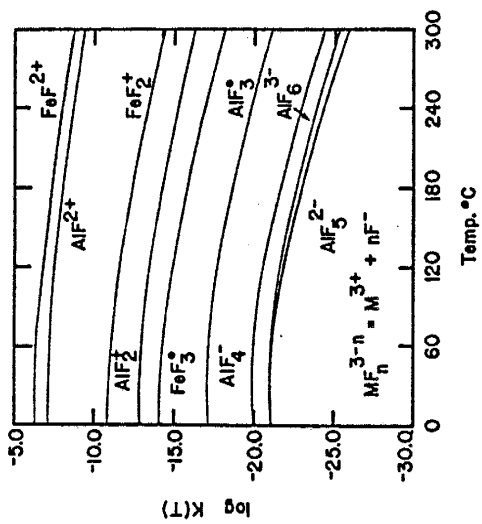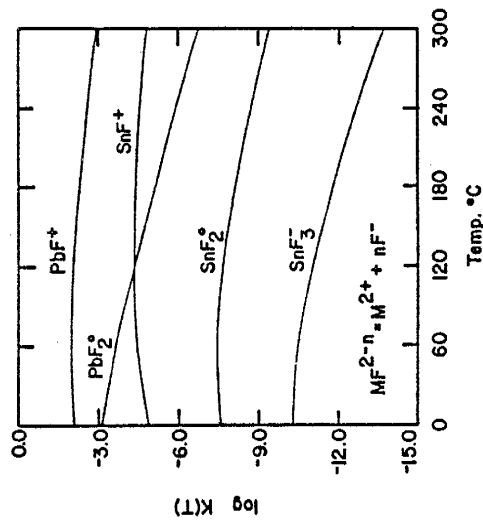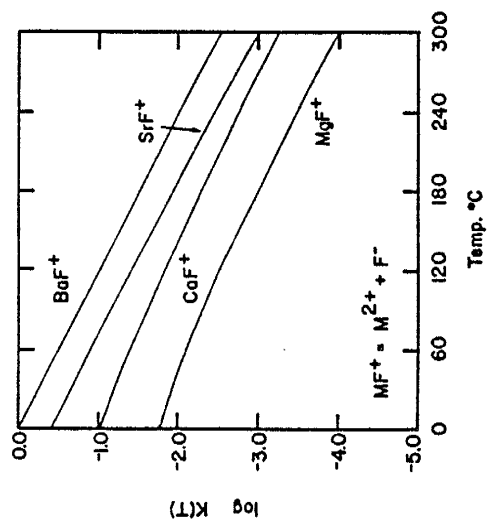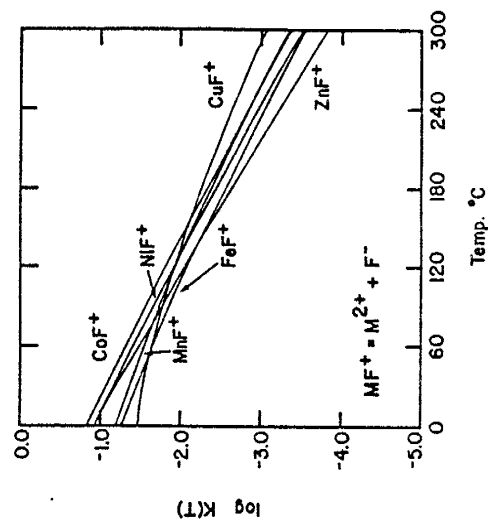
This behavior is highly unusual for dissociation reactions. In addition, the supercritical dissociation constants for hydrofluoric acid reported by Franck (1961) are inconsistent with positive heat capacities at elevated temperatures.

The possibility that one or both of the data sets are in error seems unlikely because of the good agreement between experimental work reported by different investigators. However, it is possible that the heat capacity reaches a maximum value at temperatures greater than 260°C (upper limit of experimental data) and then decreases at higher temperatures. This type of behavior is similar to that reported for HCl by Helgeson (1967). However, in the case of HCl, the maximum in the heat capacity occurs at approximately 200°C. This indicates that the sign of $\Delta S^\circ_e(T_r)$ must be negative. As a consequence, great care must be exercised when using the coefficients in Table 4.2 to calculate the dissociation constants of HF at temperatures greater than 300°C.

ALUMINUM FLUORIDE COMPLEXES

Hydroxide complexes of aluminum predominate in alkaline solutions at low temperatures (Baes and Messmer, 1976). At elevated temperatures these complexes are important in acid solutions (Helgeson, 1969 and Sokolava et at., 1977). Fig. 5.3 shows the relative importance of fluoride and hydroxide complexes at 300°C. Ellis and Mahon (1964), in an attempt to experimentally evaluate the composition of geothermal waters, found up to $10^{-2.6}$ molal fluoride in their leaching experiments at 300°C. This corresponds to a fluoride activity of $10^{-2.9}$ to $10^{-3.4}$ at pH's of 5 to 6. Comparison of this result to Fig. 5.3 reveals that aluminum fluoride complexes play an important role in the transport of aluminum in geothermal systems.

Fig. 5.3

Activity-activity diagram for hydroxide and fluoride complexes of aluminum at 300° C in steam saturated water in terms of pH and log $a_{F^-}$. Thermodynamic data are from Helgeson (1969, 1971) and Table 5.1.
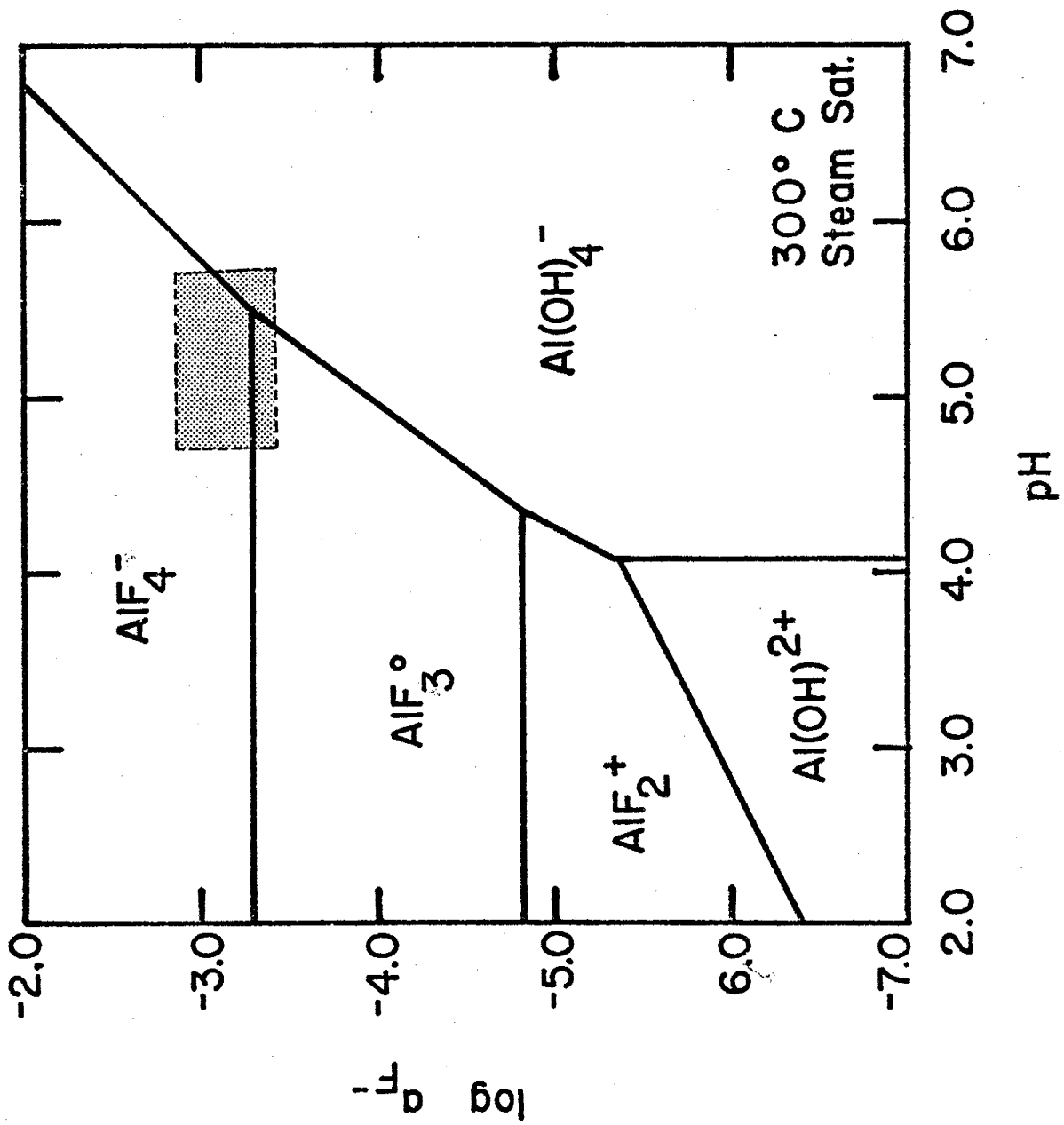
TIN FLUORIDE COMPLEXES

The high concentrations of fluorine found in tin granites has given rise to speculation that tin transport occurs by fluoride complexes. Zhu and Barnes (1981) estimated the dissociation constants of several complexes of tin and concluded that chloride complexes are more important than fluoride complexes in the transport of tin. Extremely high fluoride activities (greater than $10^{-2}$, Fig. 5.4) are required for tin fluoride complexes to predominate over chloride complexes at geologically reasonable chloride activities of about unity. Fluids similar to those reported by Ellis and Mahon (1964) plot in the region of the diagram in which chloride complexes predominate. This indicates fluoride complexes are probably not important in the transport of the stannous ion.


LEAD FLUORIDE COMPLEXES

The presence of fluoride minerals associated with some Mississippi Valley type lead-zinc deposits suggest a link between fluoride and lead in the hydrothermal solutions. Putnam (1980) analyzed fluid inclusions from the Hansonburg mining district in New Mexico and found fluoride concentrations of hundreds of ppm associated with the galena. These analyses correspond to fluoride activities of approximately $10^{-2.5}$ at 150°C. Even at these unusually high fluoride activities (cf., Nordstrom and Jenne, 1977) the contribution of fluoride complexes to the transport of lead in 3 molal sodium chloride solutions is insignificant (Fig. 5.5, Smith and Putnam, 1981).

Fig. 5.4

Activity-activity diagram for chloride and fluoride complexes of tin(II) at 300° C in steam saturated water in terms of log $a_{Cl^-}$ and log $a_{F^-}$. Thermodynamic data are from Helgeson (1969), Smith and Martell (1976) and Table 5.1.
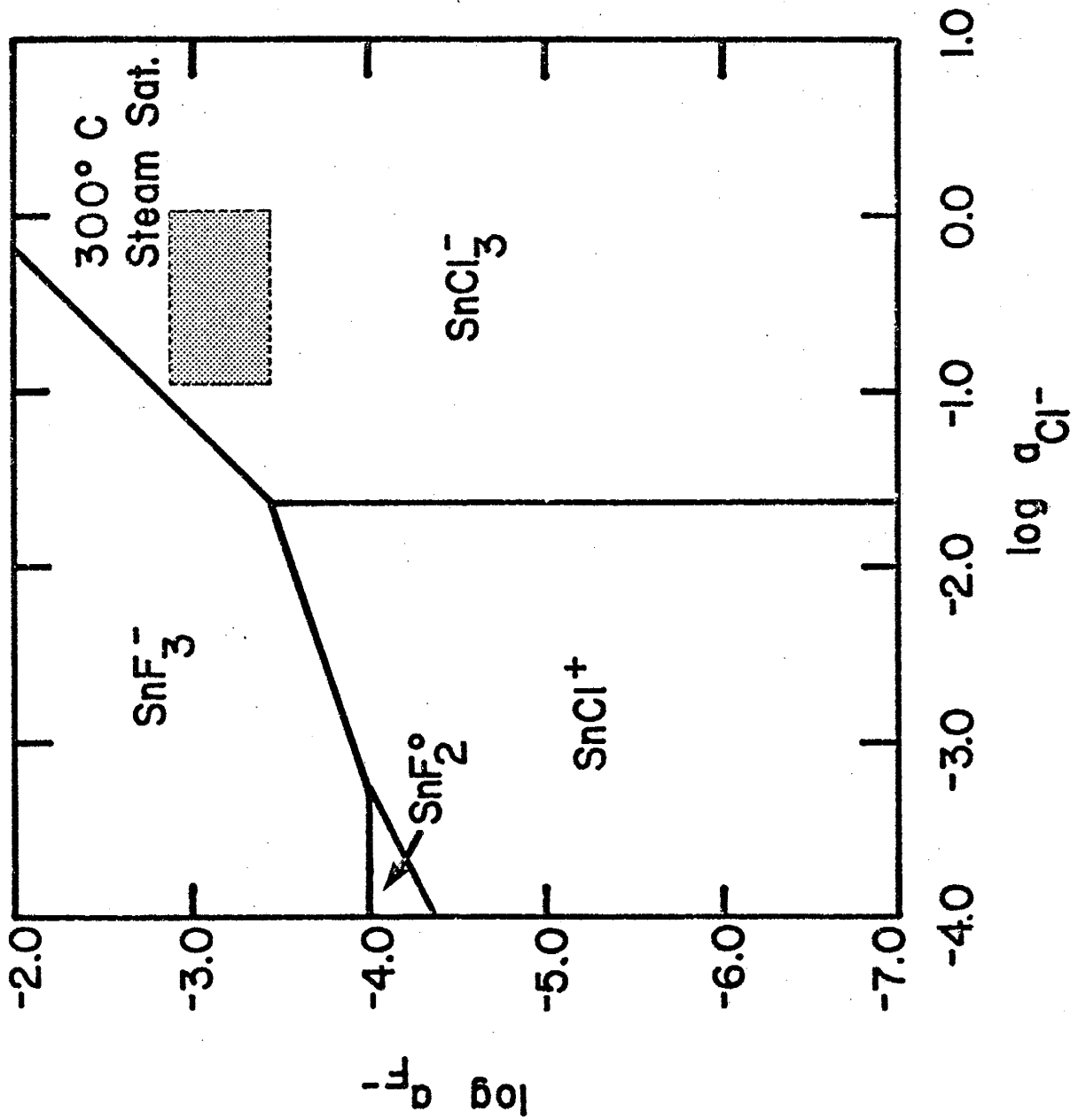
Fig. 5.5

Activity-activity diagram for chloride and fluoride complexes of lead at 150° C in steam saturated water in terms of $\log a_{Cl^-}$ and $\log a_{F^-}$. Thermodynamic data are from Helgeson (1969) and Table 5.1.
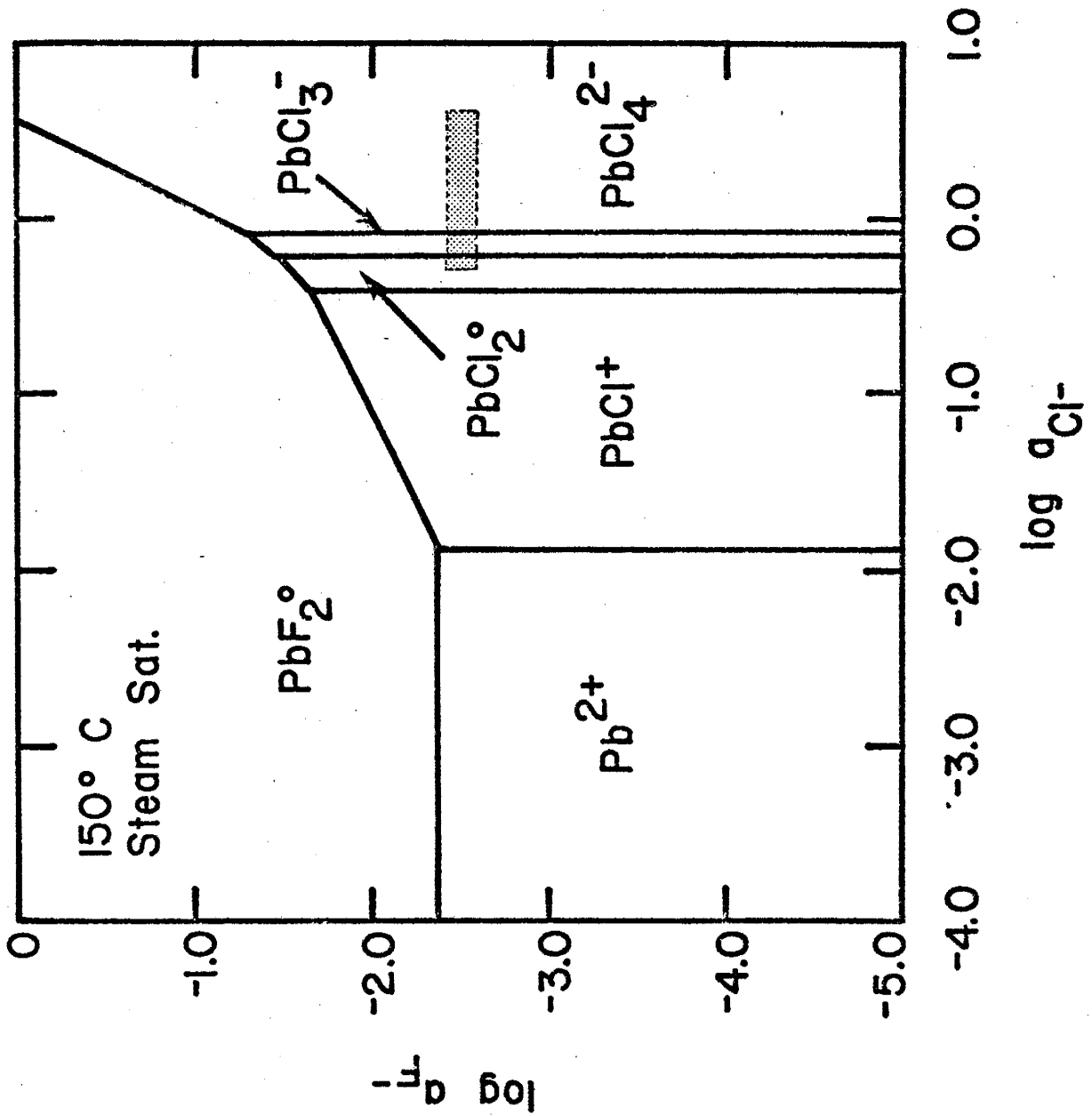
CONCLUSIONS REGARDING FLUORIDE COMPLEXING

The transport of significant amounts of divalent metals by fluoride complexes is not likely. Although fluoride complexes are more stable than chloride complexes (cf., Table 5.1 and Helgeson, 1969), chloride complexes predominate because of the high chloride-to-fluoride ratios (20-100) associated with hydrothermal systems. Since fluoride activity in hydrothermal systems is typically limited by mineral solubility, (Nordstrom and Jenne, 1977) the chloride to fluoride ration is determined in large part by the chloride concentrations. As a consequence, fluoride complexing is likely only in solutions with unusually low chloride concentrations. However, fluoride transport of trivalent aluminum in slightly acid solutions may be important as aluminum fluoride complexes are very stable and aluminum does not complex with the chloride ion (Helgeson, 1969).

CHAPTER 6

SOLUTION CHEMISTRY OF MOLYBDENUM

THERMODYNAMIC PROPERTIES OF MOLYBDENUM SOLUTION SPECIES

ROOM TEMPERATURE

Several studies during the past 15 years have been made on the properties of molybdenum solution species at room temperature (Baes and Messmer, 1976). Although most studies dealt with the hydrolysis of hexavalent molybdenum, work using other ligands and other oxidation states has been carried out. Table 6.1 contains the thermodynamic properties of twelve mononuclear molybdenum species. The standard partial molal Gibbs free energies of formation were determined from equilibrium constants. With the exception of $MoO_4^{2-}$ and $MoO_2^{2+}$, the partial molal entropies of the ions listed in Table 6.1 were estimated or determined from the temperature dependence of equilibrium constants.

Auxiliary data used to calculate the thermodynamic properties of molybdenum solution species at 25°C are listed in Table 6.2. These data are consistent with the thermodynamic properties for water and ions reported by Helgeson and others (Helgeson and Kirkham, 1974a and Helgeson et al., 1981).

ELEVATED TEMPERATURES

The thermodynamic properties of the molybdenum species listed in Table 6.1 have not been measured at elevated temperatures. The entropies at elevated temperatures of three of these species can be estimated using the entropy correspondence principle (Criss and Cobble, 1964a,b) outlined in Chapter 4. Table 6.3 contains the estimated

Table 6.1

The standard partial molal thermodynamic properties for
molybdenum solution species at 298.15 K and 1 atmosphere
(1.013 bars) pressure in a hypothetical 1 molal solution,
with properties at infinite dilution.

| SPECIES | $S^{o,a}$ | $\Delta H^o_f{}^b$ | $\Delta G^o_f{}^b$ |
|---------|-----------|-----------|-----------|
| $MoO_4^{2-}$ | 9.1 | -238.30 | -200.45 |
| $HMoO_4^-$ | 41.3 | -234.40 | -206.15 |
| $H_2MoO_4$ | 58.8 | -231.93 | -208.88 |
| $MoO_2(OH)^+$ | 19.7 | -171.70 | -153.61 |
| $MoO_2^{2+}$ | -18.5 | -110.40 | -97.54 |
| $MoO_3F^-$ | 38.0 | -252.39 | -227.89 |
| $MoO_2S_2^{2-}$ | 27.9 | -132.34 | -111.60 |
| $MoO_2Cl^-$ | 1.0 | -148.15 | -128.51 |
| $MoO_2Cl_2$ | 17.8 | -186.46 | -159.21 |
| $MoO_2Cl_3^-$ | 34.6 | -222.86 | -188.01 |
| $MoO_2^+$ | -1.4 | -126.91 | -114.50 |
| $MoOCl_3$ | 44.0 | -178.40 | -147.58 |

$^a$cal mole$^{-1}$ K$^{-1}$.  $^b$Kcal mole$^{-1}$.

## Table 6.1 (cont.)

### SOURCES OF DATA

$MoO_4^{2-}$: This study, see Chapter 3.

$HMoO_4^-$: $\Delta G^\circ_f$ from log K = -4.18 for the reaction: $HMoO_4^- = H^+ + MoO_4^{2-}$ calculated from the hydrolysis data for $Na_2MoO_4$ of Maksinova et al. (1976). $S^\circ$ calculated from the temperature dependences of of log K(T) for the reaction above (Maksinova et al., 1976)

$H_2MoO_4$: $\Delta G^\circ_f$ from log K = -2.00 for the reaction: $H_2MoO_4 = H^+ + HMoO_4^-$ (Ivanova et al., 1975). $S^\circ$ from Ivanova et al. (1975)

$MoO_2(OH)^+$: $\Delta G^\circ_f$ from log K = -1.04 for the reaction: $MoO_2(OH)^+ + H_2O = H_2MoO_4 + H^+$ (Naumov et al., 1974). $S^\circ$ from $\Delta S^\circ_r$ = 22.4 for the reaction above (Ivanova et al., 1975).

$MoO_2^{2+}$: $\Delta G^\circ_f$ from log K = -.45 for the reaction: $MoO_2^{2+} + H_2O = MoO_2(OH)^+ + H^+$ (Nazarenko and Shelikhina, 1971). $\Delta H^\circ_f$ from Naumov et al. (1974).

$MoO_3F^-$: $\Delta G^\circ_f$ from log K = -12.32 for the reaction: $MoO_3F^- + H_2O = MoO_4^{2-} + 2H^+ + F^-$, calculated from the data of Karyakin and Kryahko (1967). $S^\circ$ estimated by the method of Cobble (1953a) using ion size estimated by the method of Pauling (1952).

## Table 6.1 (cont.)

$MoO_2S_2^{2-}$: $\Delta G^{O}_{f}$ from log K = -7.2 for the reaction: $MoO_2S_2^{2-}$ + $2H_2O$ = $MoO_4^{2-}$ + $2H_2S$ (Tugarinov et al., 1973). $S^{O}$ estimated by the method of Cobble (1953a) using ion size estimated by the method of Pauling (1952).

$MoO_2Cl_n^{2-n}$: $\Delta G^{O}_{f}$ and $S^{O}$ from log K = .30 (n=1); .80 (n=2) and 2.69 (n=3) (Sillen and Martell, 1964) and $\Delta S^{O}_{r}$ = -6.0 (n=1); -9.2 (n=2) and -12.4 (n=3) (estimated by the method of Helgeson, 1969) for the reaction: $MoO_2Cl_n^{2-n}$ = $MoO_4^{2-}$ + $nCl^{-}$.

$MoO_2^{+}$: $\Delta G^{O}_{f}$ from log K = 15.96 for the reaction: $HMoO_4^{-}$ + $3H^{+}$ = $MoO_2+$ + $2H_2O$ + $e^{-}$ (Titley, 1963). $S^{O}$ estimated by the method of Powell and Latimer (1951).

$MoOCl_3$: $\Delta G^{O}_{f}$ from log K = 3.20 for the reaction: $MoOCl_3$ + $H_2O$ = $MoO_2+$ + $2H^{+}$ + $3Cl^{-}$ (Sillen and Martell, 1964). $S^{O}$ estimated by the method of Cobble (1953b).

Table 6.2

Auxiliary thermodynamic data at 298.15 K and 1 atmosphere
(1.013 bars) pressure used to calculate the thermodynamic
properties of aqueous molybdenum species.

| SPECIES | $S^{o,a}$ | $\Delta H^o_f{}^b$ | $\Delta G^o_f{}^b$ |
|---|---|---|---|
| $H^+$ | 0 | 0 | 0 |
| $H_2O$ | 16.71 | -68.315 | -56.687 |
| $Cl^-$ | 13.6 | -39.933 | -31.380 |
| $F^-$ | -3.2 | -80.151 | -67.232 |
| $H_2S$ (aq) | 29. | -9.5 | -6.66 |

$^a$cal mole$^{-1}$ K$^{-1}$.  $^b$Kcal mole$^{-1}$.

SOURCES OF DATA

$H^+$:  By definition

$H_2O$:  Helgeson and Kirkham (1974a)

$Cl^-$:  Helgeson et al. (1981)

$F^-$:  Helgeson et al. (1981)

$H_2S$ (aq):  Wagman et al. (1968)

Table 6.3

Average ionic heat capacities for molybdenum cations.
Calculated by the method of Criss and Cobble (1964b). Heat
capacity for $H^+$ is 0.0 at all temperatures.

Average heat capacity[a]

| Temp °C | $MoO_2(OH)^+$ | $MoO_2^{2+}$ | $MoO_2^+$ |
|---------|---------------|--------------|-----------|
| 60      | 6             | 1            | 15        |
| 100     | 7             | 0            | 18        |
| 150     | 4             | -3           | 17        |
| 200     | 6             | -2           | 19        |
| 250     | 6             | -3           | 20        |
| 300     | 7             | -2           | 21        |

[a] cal mole$^{-1}$ K$^{-1}$.

average ionic heat capacities of three oxy-cations. Although the entropy correspondence relationships for cations were developed for monatomic species, Cobble (1964) suggests these relationships should also hold for the oxy-cations. The apparent partial molal Gibbs free energies of the species listed in Table 6.3 were calculated from the equations summarized in Appendix A and the thermodynamic data presented in Tables 6.1 and 6.3. The results of these calculations are presented in Table 6.4. Also included in Table 6.4 are the apparent Gibbs free energies for the molybdate ion (Chapter 3), water (Helgeson and Kirkham, 1974a) and oxygen gas (Helgeson et al., 1978). Equilibrium constants involving $MoO_2^{2+}$, $MoO_2^+$, $MoO_2(OH)^+$, and $MoO_4^{2-}$ were calculated from the apparent molal Gibbs free energies and regressed as a function of temperature using equation 4.1 to define values of $\Delta S°_e(T_r)$ and $\alpha'$. These fit coefficients are presented in Table 6.5.

Dissociation constants for the reactions:

$$H_2MoO_4 = 2H^+ + MoO_4^{2-} \qquad\qquad 6.1$$

and

$$HMoO_4^- = H^+ + MoO_4^{2-} \qquad\qquad 6.2$$

were estimated at temperatures up to 300°C using equation 4.17 and the thermodynamic relationships outlined in Appendix A. The estimated dissociation constants were used in conjunction with equation 4.1 to determine the values of $\Delta S°_e(T_r)$ and $\alpha'$ (Table 6.5) for the dissociation of molybdic acid. In addition, dissociation constants of $H_2MoO_4$ via the reaction:

$$H_2MoO_4 = MoO_2^{2+} + 2OH^- \qquad\qquad 6.3$$
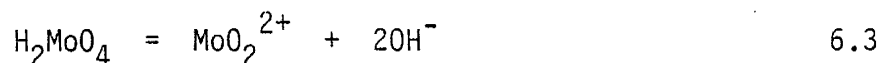
were determined from equation 4.10 and the thermodynamic relationships outlined in Appendix A. There was less than 0.05 log units difference

## Table 6.4

Apparent standard molal Gibbs free energies in Kcal mole$^{-1}$. Water, oxygen gas and the molybdate ion were calculated using SUPCRT (Helgeson et al., 1978). All others were calculated from the average ionic heat capacities presented in Table 6.3.

| Temp | $MoO_2(OH)^+$ | $MoO_2^{2+}$ | $MoO_2^+$ | Water | $MoO_4^{2-}$ | Oxygen |
|------|------|------|------|------|------|------|
| 25 | -153.61 | -97.54 | -114.50 | -56.69 | -200.45 | 0 |
| 60 | -154.33 | -96.90 | -114.49 | -57.31 | -200.69 | -1.73 |
| 100 | -155.18 | -96.17 | -114.58 | -58.10 | -200.79 | -3.74 |
| 150 | -156.21 | -95.19 | -114.76 | -59.19 | -200.65 | -6.29 |
| 200 | -157.38 | -94.25 | -115.13 | -60.33 | -200.14 | -8.89 |
| 250 | -158.53 | -93.22 | -115.64 | -61.69 | -199.02 | -11.52 |
| 300 | -159.81 | -92.31 | -116.29 | -63.07 | -196.54 | -14.20 |

## Table 6.5

Coefficients for calculating log K(T) for molybdenum solution species at elevated temperatures and pressures from equation 4.1 and 6.5. Two set of coefficients are reported for $H_2MoO_4$ see text for discussion.

| Reaction | a | b | c | d |
|---|---|---|---|---|
| $MoO_2^{2+} + 2H_2O = MoO_4^{2-} + 4H^+$ | -5.8 | 8735. | -14.98 | -40.12 |
| $MoO_2(OH)^+ + H_2O = MoO_4^{2-} + 3H^+$ | -27.3 | 1712. | -15.00 | -31.62 |
| $H_2MoO_4 = 2H^+ + MoO_4^{2-}$ (I) | -49.7 | -6386. | -12.94 | -52.20 |
| $H_2MoO_4 = 2H^+ + MoO_4^{2-}$ (II) | -49.7 | -6386. | -11.62 | -26.91 |
| $HMoO_4^- = H^+ + MoO_4^{2-}$ | -32.2 | -3897. | -10.43 | -38.81 |
| $MoO_3F^- + H_2O = MoO_4^{2-}$ $+ 2H^+ + F^-$ | -48.8 | 2256. | -26.21 | -39.41 |
| $MoO_2S_2^{2-} + 2H_2O =$ $MoO_4^{2-} + 2H^+ + 2HS^-$ | -22.2 | 22273. | -16.80 | -107.73 |
| $MoO_2Cl^+ + 2H_2O =$ $MoO_4^{2-} + 4H^+ + Cl^-$ | -11.7 | 6564. | -21.20 | -40.10 |
| $MoO_2Cl_2 + 2H_2O =$ $MoO_4^{2-} + 4H^+ + 2Cl^-$ | -14.9 | 4928. | -24.40 | -40.10 |
| $MoO_2Cl_3^- + 2H_2O =$ $MoO_4^{2-} + 4H^+ + 3Cl^-$ | -18.1 | 1395. | -27.60 | -40.10 |
| $MoO_2^+ + 1.5H_2O + 0.25O_2 =$ $MoO_4^{2-} + 3H^+$ | -26.8 | -8916. | -15.82 | -53.57 |
| $MoOCl_3 + H_2O = MoO_2^+$ $+ 2H^+ + 3Cl^-$ | -21.0 | -10627. | -21.00 | 0.00 |

[a] $\Delta S^{\circ}_r(T_r)$ (cal mole$^{-1}$ K$^{-1}$).  [b] $\Delta H^{\circ}_r(T_r)$ (cal mole$^{-1}$).
[c] $\Delta S^{\circ}_e(T_r)$ (cal mole$^{-1}$ K$^{-1}$).  [d] $\alpha'$ (cal mole$^{-1}$ K$^{-1}$).

between the log K(T)'s calculated for the first dissociation of molybdic acid by the two methods in the temperature range of 25 to 300°C. Although this agreement does not require the estimated values to be correct, it does demonstrate that the methods are self-consistent, as the hydroxide-fluoride data base and the oxy-acid data base are independent of each other. Furthermore, no attempt has been made to force the observed consistency.

The heat capacity for $MoO_3F^-$ was assumed to be the same as $HMoO_4^-$. The heat capacity of $MoO_2S_2^{2-}$ at 25°C was estimated using the method of Criss and Cobble (1964b). The temperature dependences of the heat capacity for $MoO_2S_2^{2-}$ was estimated from equation 5.1 and the value of $\Delta S^\circ_e(T_r)$ estimated by the method outlined by Helgeson and Kirkham (1976).

Evaluation of the temperature dependence of the dissociation of chloride complexes with charges of -1 or more positive (i.e., $MCl^+$, $MCl^\circ$, etc.) for silver (Stweard, 1976), copper (I) (Crerar and Barnes, 1976) and zinc (Sillen and Martell, 1964) using equation 4.1 indicates that the nonelectrostatic heat capacity for these chloride complexes is very close to zero at temperatures up to the critical point of water [1].

In addition, $\Delta S^\circ_e(T_r)$ is essentially the same as $\Delta S^\circ_r(T_r)$. The above observation suggests, the dissociation constants for chloride complexes at elevated temperatures may be estimated using equation 4.1 by setting $\alpha'$ and $\beta'$ equal to zero, and assuming $\Delta S^\circ_e(T_r) = \Delta S^\circ_r(T_r)$ (Helgeson, 1967). The dissociation constants for molybdenum chloride complexes were estimated using these assumptions.

---

[1] Evaluation of the dissociation constants for $AgCl_3^{2-}$, $AgCl_4^{3-}$ and $ZnCl_4^{2-}$ (Bourcier and Barnes, 1981 and Bourcier, persn. comm.) indicates the nonelectrostatic heat capacities for these complexes is not zero.

The estimated dissociation constants for molybdenum solution species calculated using equation 4.1 and the coefficients in Table 6.5 are presented in Table 6.6 and Figs. 6.1a and b. In addition, more complete tables including entropies and heat capacities of reaction are presented in Appendix C.

## EFFECTS OF PRESSURE ON EQUILIBRIUM

Evaluation of the effects of pressure on the attainment of equilibrium, and the numerical value of the equilibrium constant requires knowledge of the change in volume accompanying a chemical reaction (see Chapter 2). The assumption that the volume of a reaction is independent of temperature and pressure is adequate to describe reactions in which all species are solids. In fact, in these reactions the effects of pressure does not become significant until pressures of several kilobars are reached. However, the several studies done, evaluating the partial molal volumes of aqueous electrolytes at elevated temperatures, leave no doubt that large changes in partial molal volume accompany increases in temperature (Ellis, 1966, 1967, and 1968).

Helgeson and Kirkham (1976) indicate that, at elevated temperatures, the volume resulting from ion solvation ($\Delta V°(sol)$, equation 3.18) makes the largest contribution to the total volume of an ion, with the intrinsic volume ($V°(int)$) and volume of solvent collapse ($\Delta V°(col)$) making less significant contributions. The Born equation (3.5) relates the Gibbs free energy of solvation to a temperature and pressure independent constant characteristic of the ion and the reciprocal of the dielectric constant ($\varepsilon(T,P)^{-1}$) of water. This implies that no explicit considerations of volume change are needed in order to

Fig. 6.1

Temperature dependence of the dissociation of molybdenum solution species in steam saturated water. Calculated from equation 4.1 and the coefficients given in Table 6.6.

Fig. 6.1a

$$MoO_2^+ + 0.25O_2 + 1.5H_2O = 3H^+ + MoO_4^{2-}$$

$$MoO_2(OH)^+ + H_2O = 3H^+ + MoO_4^{2-}$$

$$MoO_2^{2+} + 2H_2O = 4H^+ + MoO_4^{2-}$$

$$H_2MoO_4 = 2H^+ + MoO_4^{2-}$$

$$HMoO_4^- = H^+ + MoO_4^{2-}$$

Fig. 6.1b

$$MoO_2Cl_n^{2-n} + 2H_2O = 4H^+ + nCl^- + MoO_4^{2-}$$

$$MoO_2S_2^{2-} + 2H_2O = 2H^+ + 2HS^- + MoO_4^{2-}$$

$$MoOCl_3 + H_2O = 2H^+ + 3Cl^- + MoO_2^+$$

$$MoO_3F^- + H_2O = 2H^+ + F^- + MoO_4^{2-}$$
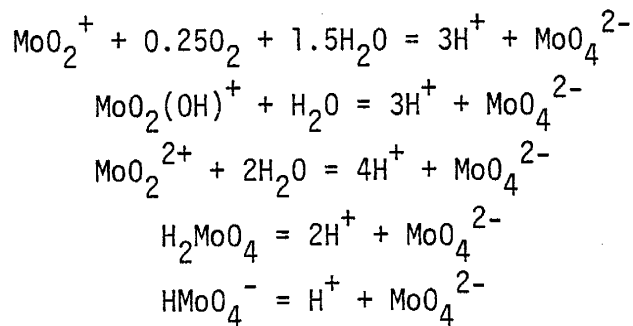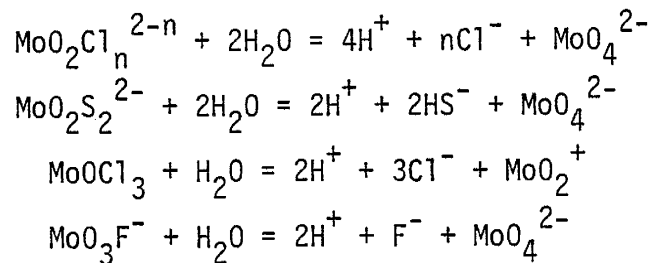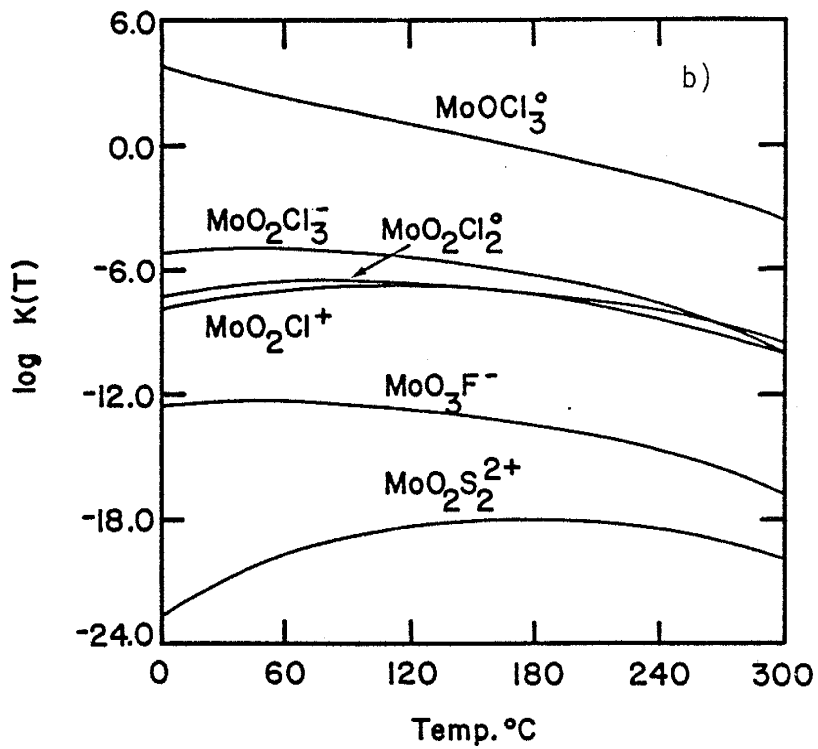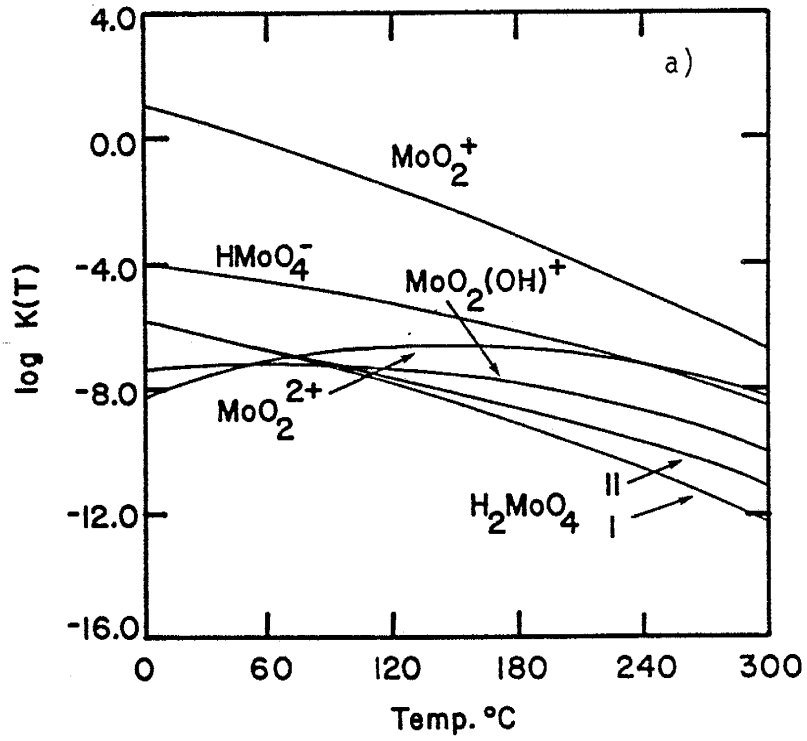
Table 6.6

Calculated log K(T)'s for molybdenum solution species at elevated temperatures and pressures. Calculations were carried out using equation 4.1 and the coefficients given in Table 6.5. Two sets of coefficents are reported for $H_2MoO_4$, see text for discussion.

| Reaction | log K(T) °C | | | | | | |
|---|---|---|---|---|---|---|---|
| | 25 | 50 | 100 | 150 | 200 | 250 | 300 |
| $MoO_2^{2+} + 2H_2O = MoO_4^{2-} + 4H^+$ | -7.67 | -7.22 | -6.72 | -6.61 | -6.81 | -7.32 | -9.17 |
| $MoO_2(OH)^+ = H_2O = MoO_4^{2-} + 3H^+$ | -7.22 | -7.16 | -7.26 | -7.58 | -8.10 | -8.85 | -10.02 |
| $H_2MoO_4 = 2H^+ + MoO_4^{2-}$ (I) | -6.18 | -6.59 | -7.50 | -8.50 | -9.57 | -10.78 | -12.30 |
| $H_2MoO_4 = 2H^+ + MoO_4^{2-}$ (II) | -6.18 | -6.57 | -7.36 | -8.16 | -9.00 | -9.94 | -11.15 |
| $HMoO_4^- = H^+ + MoO_4^{2-}$ | -4.18 | -4.44 | -5.40 | -5.74 | -6.51 | -7.40 | -8.55 |
| $MoO_3F^- + H_2O = MoO_4^{2-} + 2H^+ + F^-$ | -12.32 | -12.25 | -12.42 | -12.92 | -13.73 | -14.93 | -16.86 |
| $MoO_2S_2^{2-} + 2H_2O = MoO_4^{2-} + 2H^+ + 2HS^-$ | -21.18 | -20.01 | -18.60 | -18.04 | -18.10 | -18.67 | -19.90 |
| $MoO_2Cl^+ + 2H_2O = MoO_4^{2-} + 4H^+ + Cl^-$ | -7.37 | -7.05 | -6.79 | -6.93 | -7.39 | -8.22 | -9.69 |
| $MoO_2Cl_2 + 2H_2O = MoO_4^{2-} + 4H^+ + 2Cl^-$ | -6.87 | -6.64 | -6.56 | -6.86 | -7.49 | -8.51 | -10.23 |
| $MoO_2Cl_3^- + 2H_2O = MoO_4^{2-} + 4H^+ + 3Cl^-$ | -4.98 | -4.96 | -5.22 | -5.81 | -6.71 | -8.00 | -10.05 |
| $MoO_2^+ + 1.5H_2O + 0.25O_2 = MoO_4^{2-} + 3H^+$ | 0.68 | 0.12 | -1.05 | -2.27 | -3.56 | -5.00 | -6.81 |
| $MoOCl_3 + H_2O = MoO_2^+ + 2H^+ + 3Cl^-$ | 3.20 | 2.58 | 1.45 | 0.40 | -0.67 | -1.90 | -3.61 |

evaluate the effect of pressure on the Gibbs free energy of solvation for an aqueous species. All that is required is a knowledge of the dielectric constant and the appropriate partial derivatives which have been tabulated by Helgeson and Kirkham (1974a).

The success of schemes to estimate dissociation constants at high pressure based on isochoric and isoentropic extrapolation are due, in large part, to the similarity of these curves to iso-dielectric curves. The models proposed by Marshall (1972) based on the "absolute" dissociation constant and molar concentration scale are successful because of the strong dependence of the compressibility of water ($\beta°$) on $(\partial \ln\varepsilon/\partial P)_T$ (Helgeson and Kirkham, 1976).

The approximation proposed by Helgeson (1969) for evaluating the effect of pressure on dissociation reations does not account for the electrostatic and nonelectrostatic contributions at elevated pressures. However, equation 4.1 may be used, along with an "electrostatic temperature", to explicitly account for the electrostatic and nonelectrostatic consequences of ion dissociation. The "electrostatic temperature" is a derived temperature which, when used in conjunction with equation 4.1, yields appropriate electrostatic properties of the solvent at the pressure and temperature of interest. Values of the "electrostatic temperature" for pressures and temperatures of 500 to 2000 bars and 250 to 600°C are presented in Table 6.7. In this model nonelectrostatic volume changes are considered negligible. Consequently, the use of this model should be limited to the pressure temperature regime in which electrostatic volume contributions predominate (T greater than 250°C). Rewriting equation 4.1, using the "electrostatic temperature", $T_e$, results in:

Table 6.7

Electrostatic temperatures ($T_e$) for equation 6.4.

| Temp °C | Pressure (Kbars) | | | |
|---|---|---|---|---|
| | 0.5 | 1.0 | 1.5 | 2.0 |
| 250 | 506.16 | 493.15 | 484.83 | 477.39 |
| 300 | 546.93 | 530.84 | 520.38 | 511.94 |
| 350 | 586.95 | 565.23 | 552.33 | 542.78 |
| 400 | 626.16 | 596.35 | 580.80 | 570.27 |
| 450 | | 623.79 | 605.87 | 594.25 |
| 500 | | 646.86 | 627.87 | 614.51 |
| 550 | | | 643.43 | 630.51 |
| 600 | | | | 639.12 |

(see facing page)                                    6.4

where the terms have the same values as given in Chapter 4.  Estimated

dissociation constants for the reactions given in Table 6.6 at

temperatures and pressures up to 600°C and 2000 bars are presented in

Appendix D.


## SOLUTION CHEMISTRY OF MOLYBDENUM

When basic solutions of the molybdate ion are acidified at room

temperature, hexavalent molybdenum polymerizes.  This behavior is

similar to other group VIA elements (Cotton and Wilkinson, 1980).

However, whereas the dichromate ion is relativity stable, such stability

is not observed for the dimolybdate ion (Cotton and Wilkinson, 1980).

In fact, heptamolybdates (paramolybdic acid) are the most important

polynuclear molybdenum species in acid aqueous solutions.  These species

have been identified on the basis of emf titrations (Sasaki and Sillen,

1964) and by spectroscopic and other techniques (Aveston et al., 1968).

Work by Ivonava et al. (1976) at 200°C suggest that polynuclear species

predominate when molybdite is dissolved.  However, the stoichiometry of

the polynuclear species is unlike any found at low temperatures.

Polymerization appears to be important only at low pH's, high

molybdenum concentrations and low temperatures.  Enthalpy titrations of

paramolybdic acid resulted in large negative enthalpies of formation for

these species from the molybdate ion (Arnek and Szilard, 1968).  Using

these entalpies, thermodynamic calculations were done which indicate

that the formation constants for paramolybdate species decrease by about

ten orders of magnitude between 25 and 150°C.  This indicates that it is

unlikely that polynuclear species make a significant contribution to the

EQUATION 6.4

$$\log K(T,P) \simeq$$

$$\frac{\Delta S^O_e(T_r)}{2.303RT}\left[T_r - T_e - \frac{\theta}{\omega}(1 - \exp(\exp(\hat{b}+\hat{a}T) - \hat{c} + (T_e-T_r)/\theta))\right]$$

$$- \frac{\Delta H^O_r(T_r)}{2.303RT} + \frac{\Delta S^O_r(T_r)}{2.303R} + \frac{\alpha'}{2.303R}(\ln T/T_r - 1 + T_r/T)$$

$$+ \frac{\beta'(T-T_r)^2}{4.606RT}$$

transport of molybdenum in near neutral solutions at elevated temperatures, and for this reason they will not be considered further.

## HYDROXYL AND CHLORIDE COMPLEXES

The role of cationic molybdenum (VI) species diminishes at elevated temperatures (Figs. 6.2a-e). In addition, at increased temperatures, the predominant molybdenum species at neutral pH changes from the molybdate to the bimolybdate ion. Furthermore, at elevated temperatures and geologically reasonable oxygen fugacities, molybdenum (V) species become important in acid solutions. Work by Westrich (1974) indicated a slight increase in molybdenite solubility by the addition of both acid (HCl) and chloride (added as NaCl or KCl) to solutions buffered by nickel-nickel oxide, pyrite-pyrrhotite and granodiorite rock. These results are consistent with the formation of a chloride complex such as $MoOCl_3$ (Fig. 6.2e).

## FLUORIDE AND SULFIDE COMPLEXES

The complex $MoO_3F^-$ (Fig. 6.3) was used to evaluate the role of fluoride in the transport of molybdenum. At 400°C and 500 bars pressure, the fluoride complex is the predominant solution species at log $f_{HF}$ values greater than -2.0. Fugacities calculated from mica analyses at Henderson, CO indicate that log $f_{HF}$ values for this deposit were greater than -1.5 (Gunow et al., 1980). At pH's of 5 to 6 (see Chapter 8), fluoride complexes are important in the transport of molybdenum.

The effects of temperature on the stability of $MoO_3F^-$ may be evaluated from the reation:

Fig. 6.2

Activity-activity diagram depicting the predominate aqueous molybdenum species as a function of pH and log $f_{O_2}$ at five discrete temperatures and pressures.  Calculated from the data in Table 6.6 and Appendixes C and D.
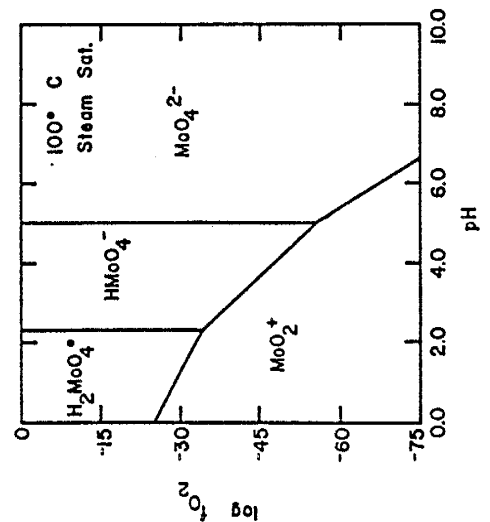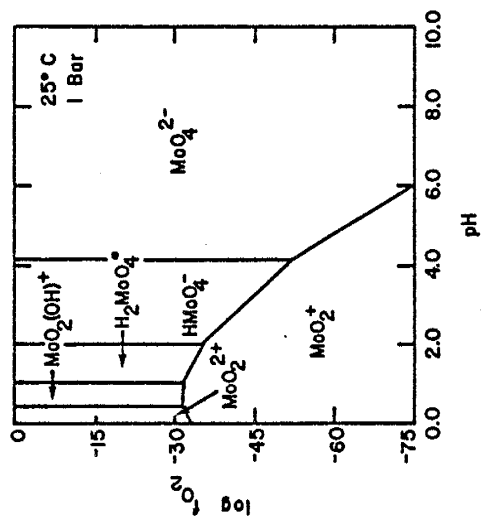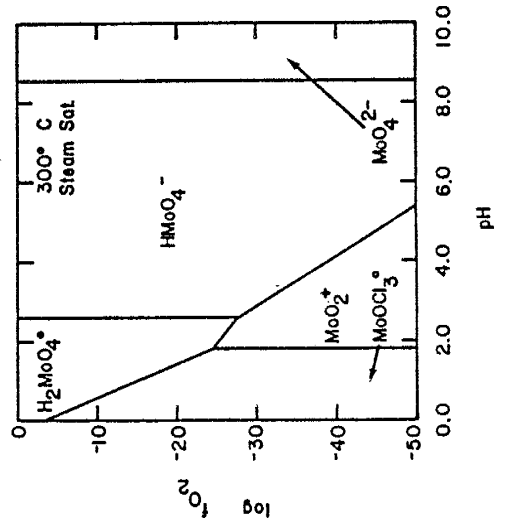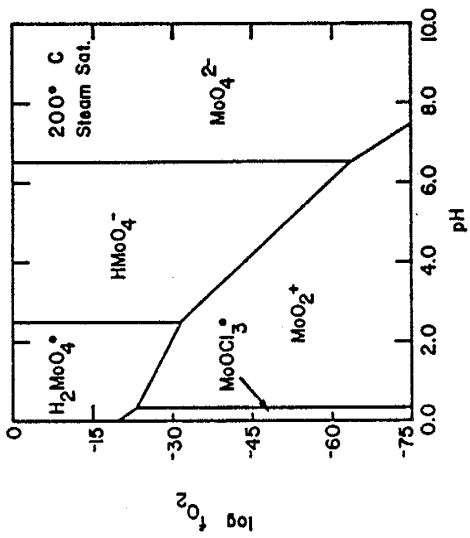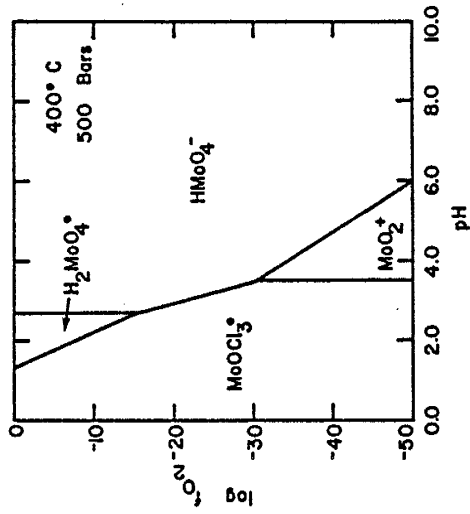
Fig. 6.3

Activity-activity diagram depicting the predominate aqueous species as a function of pH and log $a_{F^-}$. The oxygen fugacity is set at the nickel-nickel oxide buffer and the chloride activity is set at unity. Calculated from the data in Appendix D.

$$MoO_3F^- + H_2O = HMoO_4^- + H^+ + F^- \qquad\qquad 6.5$$
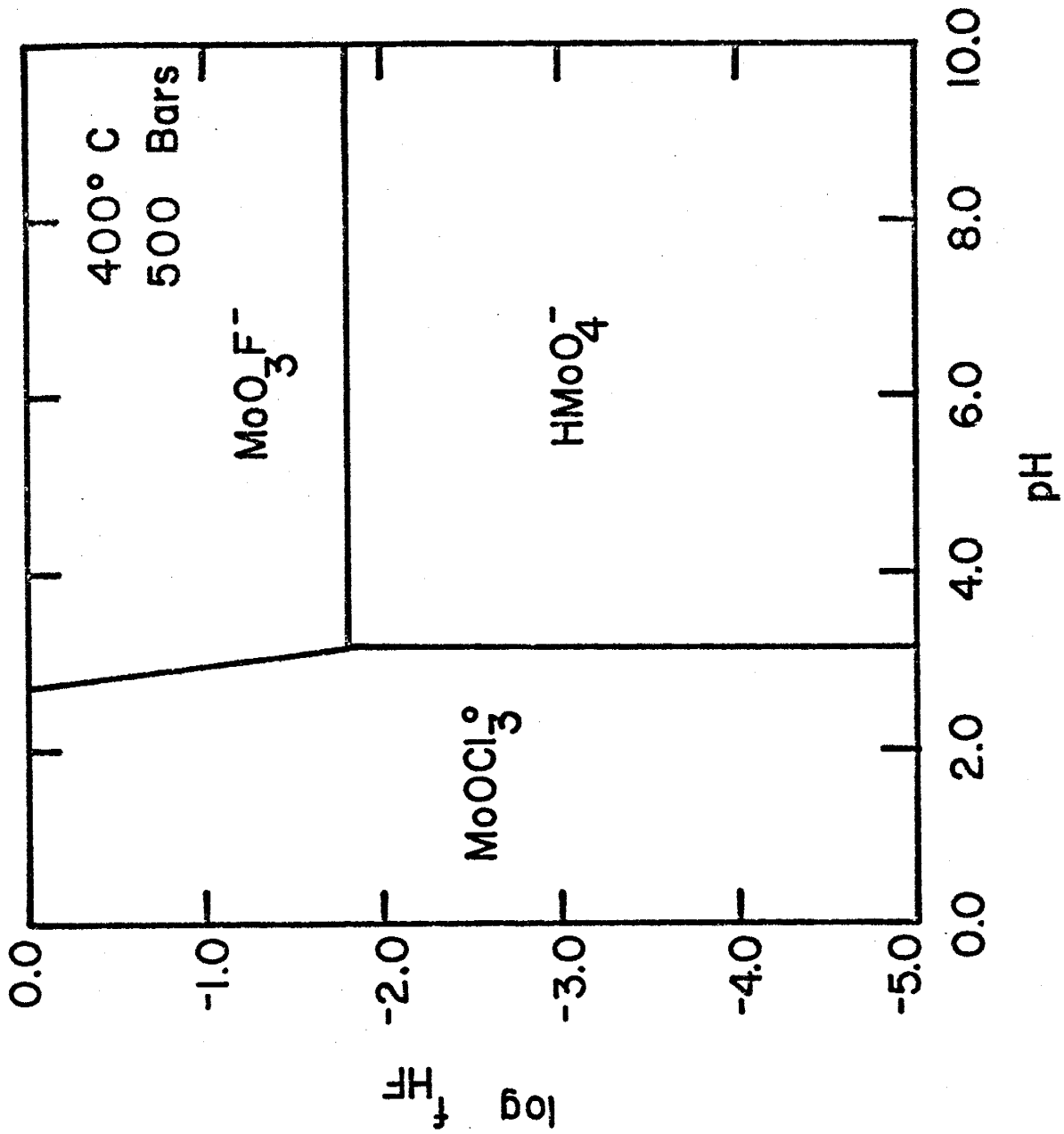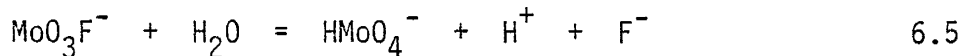
An evaluation of the stability relationships for the above reation (Fig. 6.4) indicates that at increased temperature $MoO_3F^-$ becomes stable at lower fluoride activities. Thus, fluoride complexes will be important only at high temperatures.

The sulfide complex evaluated in this study was $MoO_2S_2^{2-}$. Because this is a divalent complex it becomes increasingly less stable at elevated temperatures. Undoubtedly, the $MoO_2S_2^{2-}$ ion will react with water in a manner analogous to $MoO_4^{2-}$ to form $HMoO_2S_2^-$ and $H_2MoO_2S_2$. The relative stability of sulfide complexes can be determined by assuming that the dissociation constants for acid sulfide complexes ($H_2MoO_2S_2$ and $HMoO_2^-$) are similar to $H_2MoO_4$ and $HMoO_4^-$. These stability relationships suggest that molybdenum sulfide complexes may be important in solutions with $H_2S$ activities greater than $10^{-1.5}$ (Fig. 6.5). However, the results are tentative and an experimental investigation of the role of sulfide complexes on molybdenum transport at elevated temperatures is warranted.

## SOLUBILITY OF POWELLITE AND MOLYBDITE

Calculated solubility of powellite as a function of temperature at infinite dilution, accounting for both hydrolysis and charge balance, are in close agreement with reported measured solubilities (Fig. 6.6). This observation indicates that the estimated values for the heat capacity of the molybdate ion as well as the second dissociation constant of molybdic acid are correct.

Calculations of the solubility of molybdite at elevated temperatures are more difficult because of the formation of polynuclear

Fig. 6.4

The stability of $MoO_3F^-$ and $HMoO_4^-$ at 500 bars pressure as a function of temperature and log $f_{HF}$. The pH is set at 5. Calculated from the data in Appendix D and Naumov et al. (1974).
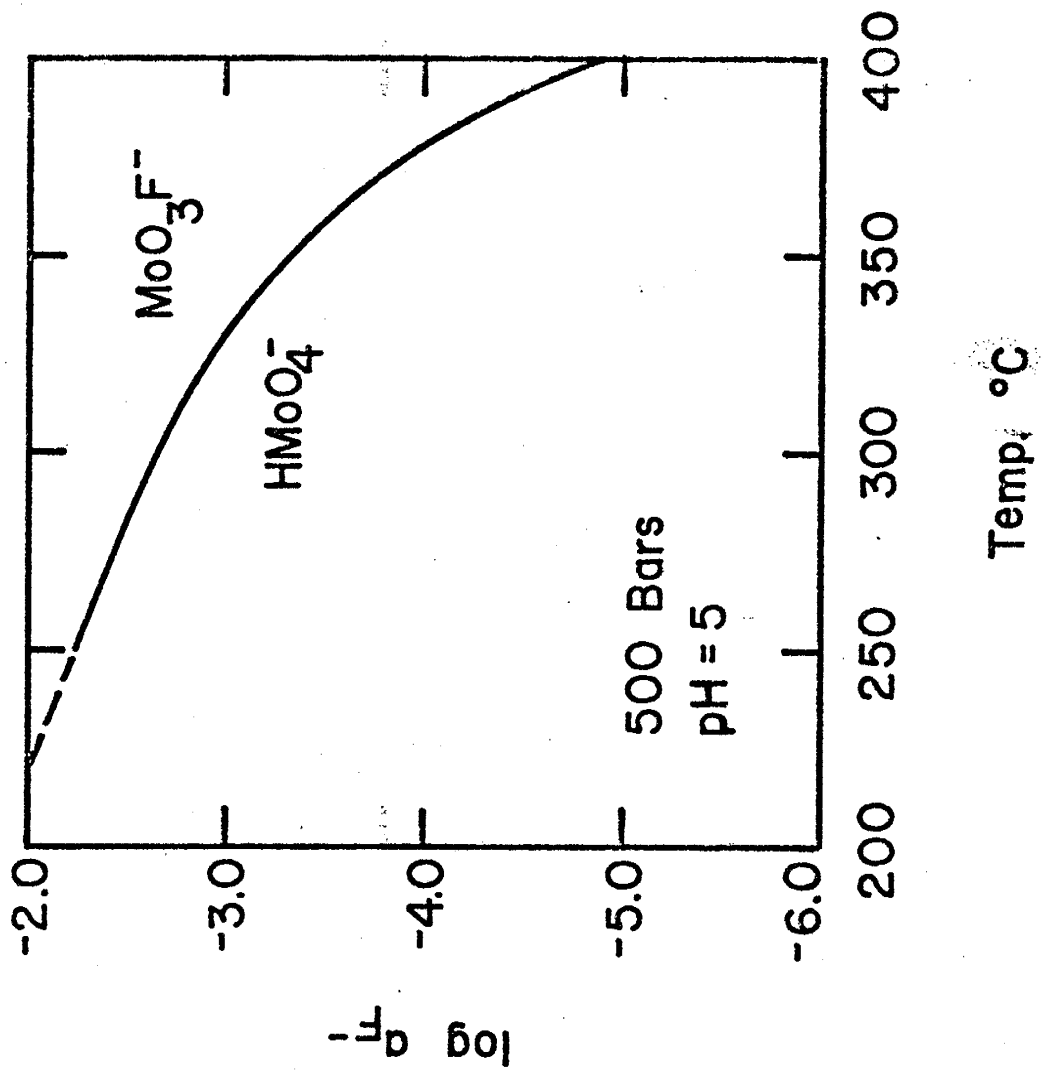
Fig. 6.5

The stability of $MoO_2S_2{}^{2-}$ and $MoO_4{}^{2-}$ at 500 bars pressure as a function of temperature and log $a_{H_2S}$. Calculated from the data in Appendix D, SUPCRT (Helgeson et al., 1978) and Naumov et al. (1974).
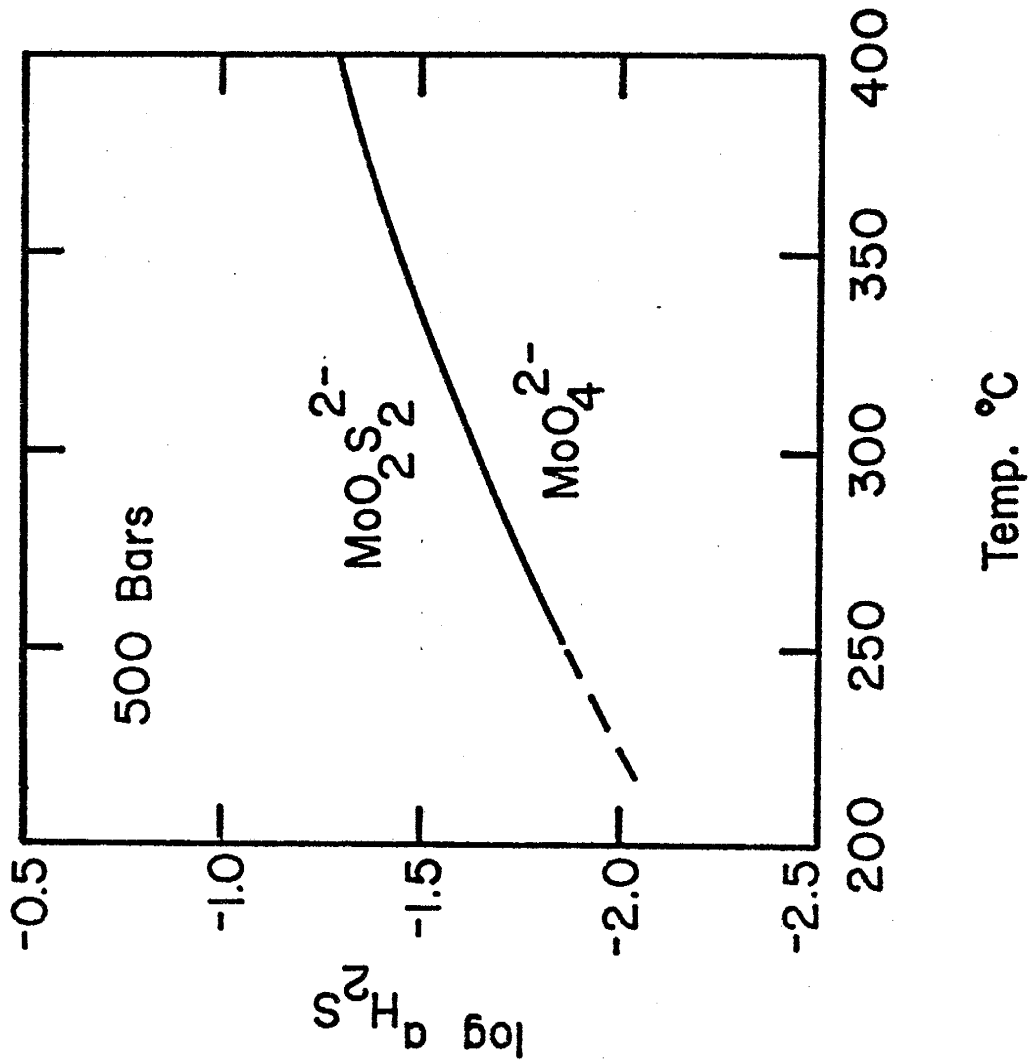
Fig. 6.6

Comparison between calculated solubilities of powellite and molybdite and experimentally measured solubilities. Solubility data are from Zhidikova and Malinin (1972, powellite) and Ivanova et al. (1975, molybdite).
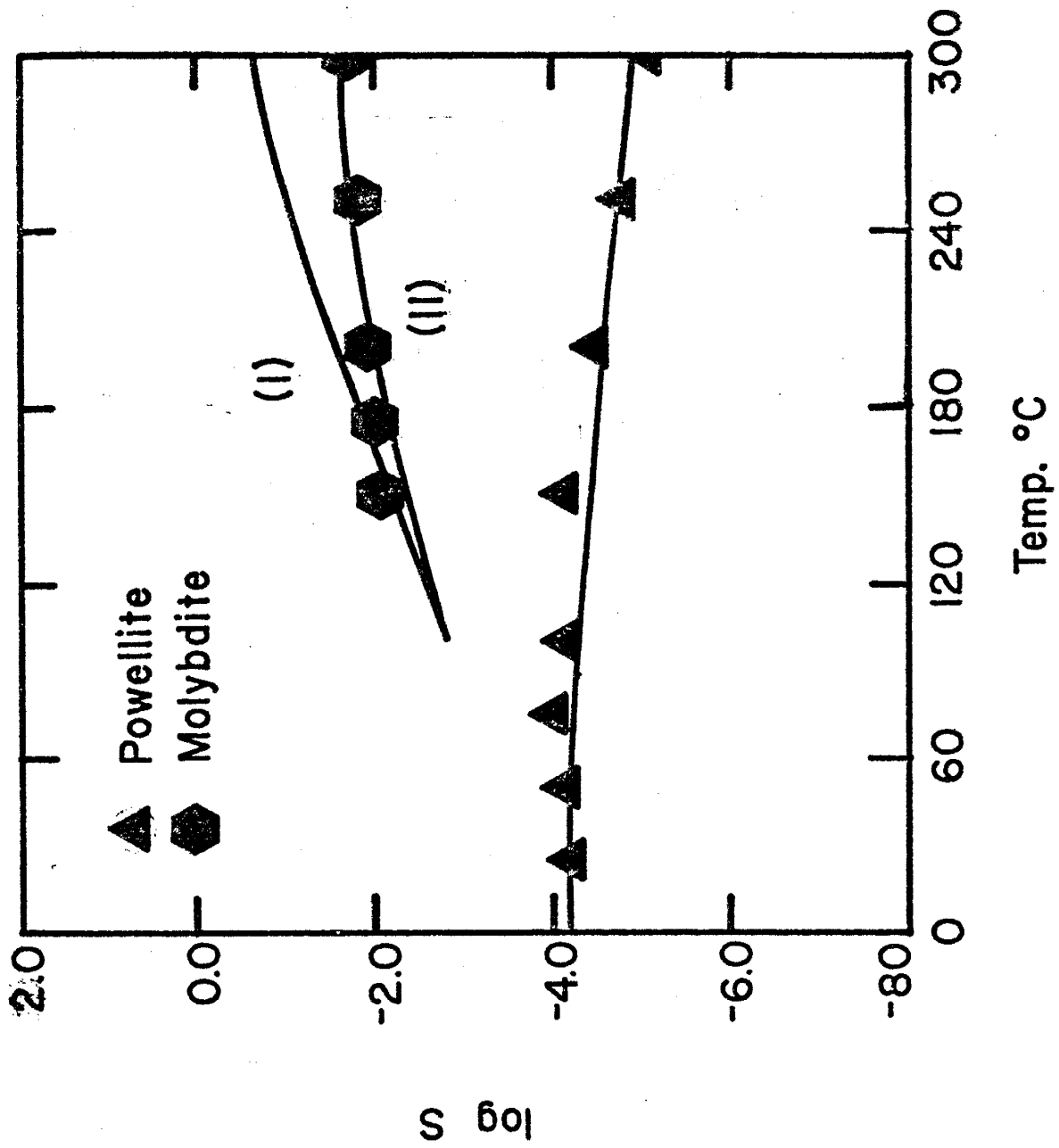
molybdenum species. However, calculated solubilities of molybdite at elevated temperatures assuming only mononuclear species form are presented graphically on Fig. 6.6. Curve I represents solubilities calculated using the dissociation constants for $H_2MoO_4$ calculated above. At temperatures greater than 150°C the calculated solubility of molybdite due to mononuclear species is greater than the total measured solubility. This discrepancy may be the result of errors in the solubility measurements reported by Ivanova et al. (1975), errors in the estimated dissociation constants for $H_2MoO_4$, or both. Alternate heat capacity coefficients of -11.6, and -26.91 for $\Delta S°_e(T_r)$ and $\alpha'$ respectively were calculated, assuming that the 300°C data reported by Ivanova et al. (1975) represents dissolution of molybdite to mononuclear species. Calculated solubilities based on this second set of heat capacity coefficients are also shown on Fig. 6.6 (curve II). The results of these calculations are consistent with the assumption that molybdenum depolymerizes at elevated temperatures. Since the second set of coefficients yields estimates of molybdite solubility which are more reasonable in light of the experimental work, this set has been chosen for subsequent calculations.

Although the estimated log K's for the dissociation of molybdic acid are highly uncertain, values for dissociation constants derived in this study are consistent with experimental work (cf., Fig. 6.6). These preliminary calculations suggest that molybdic acid species are important in the transport of molybdenum (VI) at elevated temperatures. In order to better define the role of these acid species, a study of the effect of acidity on the solubility of a sparingly soluble molybdate salt, such as powellite, should be carried out.

## ACTIVITY COEFFICIENTS

### AQUEOUS ELECTROLYTES

Because the defined standard state for aqueous ions and electrolytes is based on the hypothetical one molal solution with properties at infinite dilution, it is necessary to correct solution concentrations for departure from ideal behavior. These corrections are typically accomplished by the use of activity coefficients, which allow the determination of the relative partial molal Gibbs free energy for ions, aqueous electrolytes and neutral species in real solutions. In dilute solutions where the probability of ion-ion interactions is low, activity coefficients, $\gamma_{\pm,k}$ of the kth electrolyte can be estimated from the Debeye-Huckel equation:

$$\log \gamma_{\pm,k} = - \frac{A_\gamma |Z_+ Z_-| I^{\frac{1}{2}}}{1 + \overset{o}{a} B I^{\frac{1}{2}}}$$

where the ionic strength, I, is given by:

$$I = \tfrac{1}{2} \times \sum_j z_j^2 m_j \qquad\qquad 6.7$$

$A_\gamma$ and $B_\gamma$ are constants dependent on solvent properties (summarized by Helgeson and Kirkham, 1974b), $Z_+$ and $Z_-$ are the integer charges on the cation and anion, $z_j$ and $m_j$ are the molality and the charge of the jth ion and $\overset{o}{a}$ is the "distance of closest approach" for the positively and negatively charged ion in the solution. The use of the above equation is adequate to represent the long range effects in aqueous solutions. However, at ionic strengths greater than about 0.1, equation 6.6 is not adequate to describe activity coefficients.

Several modifications of the Debye-Huckel equation have been proposed. These are based on a variety of theoretical or empirical considerations and assume complete or partial dissociation of electrolytes. However, as Helgeson (1982) has pointed out, "different theoretical equations commonly yield regression results that satisfy the same experimental data, which neither supports nor denies the validity of any one of the theoretical models."

The model chosen in this study to estimate activity coefficients of aqueous electrolytes is the one proposed by Helgeson et al. (1981) and Helgeson (1982). This model incorporates explicit provisions for solvation and long- and short-range interactions. Evaluation of experimentally determined activity coefficients indicates that the effects of solvation and short-range interactions are linear functions of the ionic strength if the "true" or effective ionic strength (i.e., corrected for complexing) is used. The equation for mean ionic activity coefficients is given below (Helgeson et al., 1981):

$$\log\gamma_{\pm,k} = -\frac{A_\gamma|Z_+Z_-|I^{\frac{1}{2}}}{\Lambda} + \Gamma_\gamma + b_{\gamma,k}I \qquad 6.8$$

where:

$$\Gamma_\gamma = -\log(1 + 0.0180153m^*) \qquad 6.9a$$

$$m^* = \sum m_i \qquad 6.9b$$

$$\Lambda = 1 + \overset{0}{a}_k B_\gamma I^{\frac{1}{2}} \qquad 6.9c$$

$$a_k = 2\ \Sigma\Sigma\upsilon_{j,k}r_{e,j}/\Sigma\upsilon_{j,k} \qquad 6.9d$$

where $r_{e,j}$ is the electrostatic radius of the jth ion, $\upsilon_{j,k}$ is the stoichiometric number of the jth ion in the kth electrolyte, and $b_{\gamma,k}$ is the extended term parameter characteristic of the kth electrolyte and is dependent on temperature and pressure. The use of equation 6.9c

insures that equation 6.8 meets the requirements of an exact differential for mixed electrolyte solutions (Helgeson et al., 1981).

Values of $b_{\gamma,k}$ for sodium molybdate at 25 and 295°C have been determined by plotting the differences between the measured activity coefficients (Zhidikova et al., 1973) and the summation of the first two terms of equation 6.8. As may be seen from Fig. 6.7, equation 6.8 adequately represents the mean ionic activity coefficient to an ionic strength of ten at 25°C. However, at 295°C there is a systematic departure from linear behavior at high ionic strengths. This behavior is probably due to the formation of ion pairs at high concentration. The values of $b_{\gamma,k}$ for sodium molybdate are equivalent to the slope of the curves in Fig. 6.7. At 295°C, $b_{\gamma,k}$ was determined by calculating the tangent of the curve at zero ionic strength. The numerical values of $b_{\gamma,k}$ are 0.032 and -0.096 kg mole$^{-1}$ at 25 and 295°C respectively.

INDIVIDUAL IONS

The activity coefficients for individual ions in sodium chloride solutions may be approximated by (Helgeson et al., 1981):

$$\log \gamma_j = \frac{-A\ Z_j^2 I^{\frac{1}{2}}}{\Lambda} + \Gamma_\gamma$$

$$+ (\omega(abs)b_{NaCl} + b_{Na^+Cl^-} - 0.19(|Z_j| - 1))I \qquad 6.10$$

where $b_{NaCl}$ is a slope parameter relating the dielectric constant of the solution to the molality of sodium chloride and $b_{Na^+Cl^-}$ is a short range ion interaction parameter for sodium chloride. The electrostatic coefficient, $\omega(abs)$, is characteristic of each ion and is described in Chapters 2 and 3. Values of $b_{NaCl}$ and $b_{Na^+Cl}$ are summarized by Helgeson et al. (1981). Evaluation of the form of equation 6.11 indicates that

Fig. 6.7

Evaluation of the extended term, b, for sodium molybdate at 25° and 295°C.  Experimental data are from Zhidikova et al. (1973).

$$\rho^* = \log\gamma_{\pm,k} + \frac{A_\gamma |Z_+ Z_-| \sqrt{I}}{\Lambda} - \Gamma_\gamma$$

Na$_2$MoO$_4$
▲ 25°C
● 295°C

$\rho$*

I mole Kg$^{-1}$
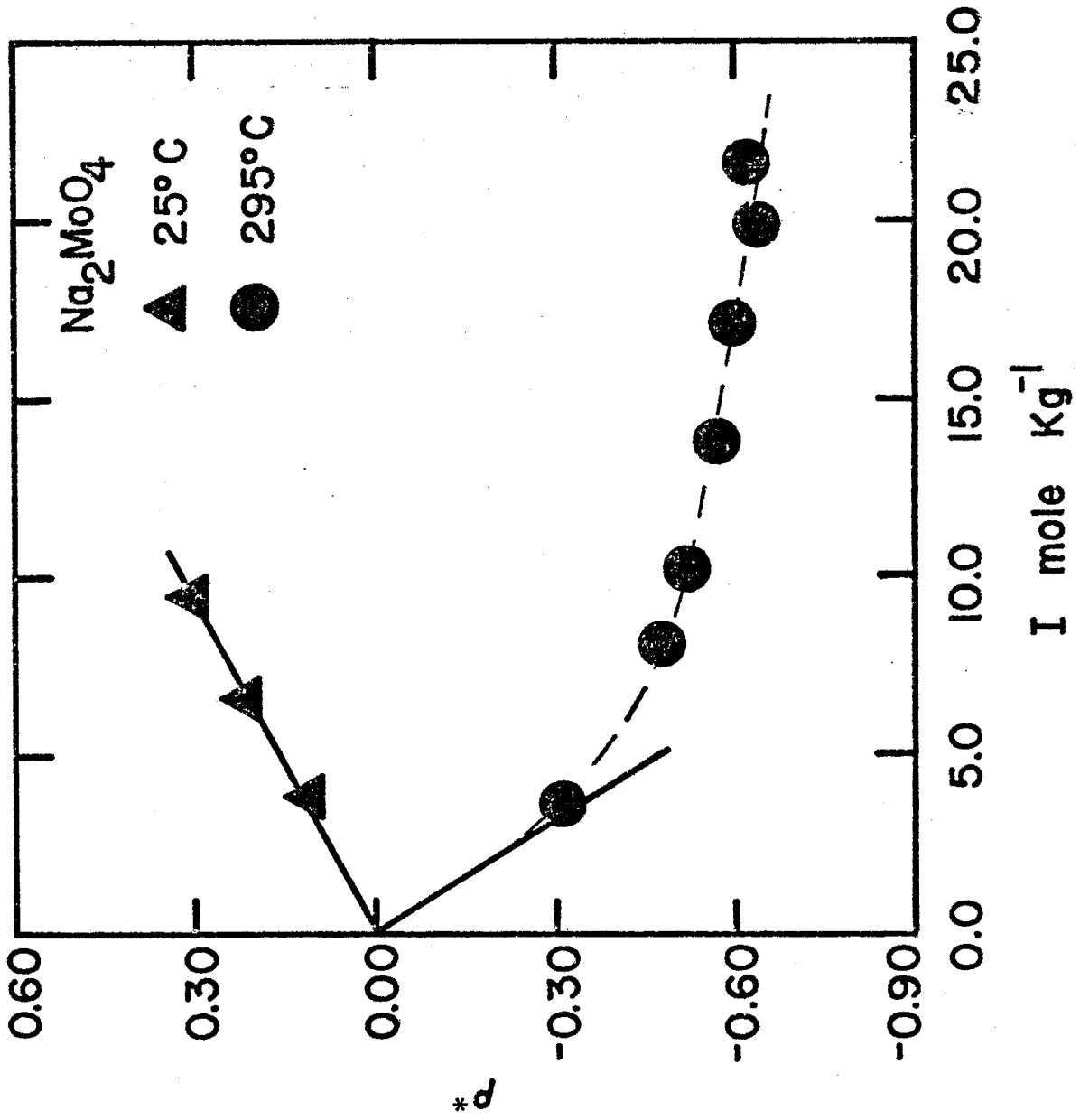
the quantity in parentheses is a constant ($b_{\gamma,j}$) and depends only on the value of $\omega(abs)$ and the charge of the ion. Values of the extended term parameter for molybdenum ions in aqueous sodium chloride solutions at four discrete temperatures are presented in Table 6.8. The values of $b_{\gamma,j}$ become increasingly more negative with increasing temperature as a consequence of the dramatic effects of sodium chloride on the properties of low density water.

## STOICHIOMETRIC INDIVIDUAL ION ACTIVITY COEFFICIENTS

The calculations of mineral solubilities in solutions of a concentrated supporting electrolyte may be simplified by the use of stoichiometric individual ion activity coefficients (Helgeson, 1969). The stoichiometric individual ion activity coefficient, $\dot{\gamma}_j$, is defined as:

$$\dot{\gamma}_j = a_j/m_{j,tot} \qquad 6.11$$

where $a_j$ and $m_{j,tot}$ are the actual activity and total molality of the jth ion present in small quantities in the solution.

Methods to calculate $\dot{\gamma}_j$ for aqueous sodium chloride solutions are reviewed by Helgeson (1969). The details and the equations used to calculate $\dot{\gamma}_j$ for the molybdate ion are presented in Appendix E. Table 6.9 summarizes the stoichiometric individual ion activity coefficients for molybdenum ion at elevated temperatures and pressures as functions of both pH and ionic strength. It is interesting to note that at high temperatures and low pH's the activity of the molybdate ion may be only a billionth of its concentration, suggesting, that while the solubility products of molybdate minerals may be low, the molality of molybdenum in solution is not necessarily low.

Table 6.8

Calculated extended term for Debeye-Huckel equation for the calculation of activity coefficients. At $400^\circ C$ the pressure used in the calculation was 500 bars. At all other temperatures the pressure of steam saturated water was used. Calculation were done as described in text and Helgeson et al. (1981).

| | Temp $^\circ C$ | | | |
|---|---|---|---|---|
| ION | 250 | 300 | 350 | 400 |
| $MoO_4^{2-}$ | -0.298 | -0.455 | -0.767 | -0.799 |
| $HMoO_4^-$ | 0.060 | 0.044 | -0.015 | -0.003 |
| $MoO_2(OH)^+$ | 0.024 | -0.021 | -0.133 | -0.130 |
| $MoO_2^{2+}$ | -0.338 | -0.529 | -0.903 | -0.944 |
| $MoO_3F^-$ | 0.054 | 0.034 | -0.033 | -0.022 |
| $MoO_2S_2^{2-}$ | -0.270 | -0.404 | -0.675 | -0.699 |
| $MoO_2Cl+$ | -0.003 | -0.072 | -0.226 | -0.230 |
| $MoO_2Cl_3^-$ | 0.049 | 0.024 | -0.052 | -0.043 |
| $MoO_2^+$ | -0.010 | -0.085 | -0.250 | -0.256 |

## Table 6.9

Calculated stoichiometric individual ion activity coefficients for the molybdate ion at elevated temperatures and pressures in NaCl solutions. Activity coefficients included consideration for hydrolysis and chloride complexes. At $400^{\circ}C$ a pressure of 500 bars was used in the calculations. At all other temperatures calculations were carried out for steam saturated water.

$\log \dot{\gamma}$ in 2 molal NaCl

|  | | | pH | | | |
|---|---|---|---|---|---|---|
| Temp $^{\circ}C$ | 3.0 | 4.0 | 5.0 | 6.0 | 7.0 | 8.0 |
| 250 | -4.76 | -3.70 | -2.77 | -2.19 | -2.05 | -2.03 |
| 300 | -6.01 | -4.95 | -3.96 | -3.10 | -2.67 | -2.59 |
| 350 | -8.23 | -7.19 | -6.19 | -5.21 | -4.40 | -4.06 |
| 400 | -8.57 | -7.53 | -6.53 | -5.54 | -4.62 | -4.06 |

$\log \dot{\gamma}$ in 4 molal NaCl

|  | | | pH | | | |
|---|---|---|---|---|---|---|
| Temp $^{\circ}C$ | 3.0 | 4.0 | 5.0 | 6.0 | 7.0 | 8.0 |
| 250 | -4.73 | -3.70 | -2.92 | -2.62 | -2.58 | -2.57 |
| 300 | -6.01 | -4.96 | -4.06 | -3.55 | -3.44 | -3.42 |
| 350 | -8.35 | -7.33 | -6.48 | -6.06 | -5.98 | -5.98 |
| 400 | -8.67 | -7.64 | -6.71 | -6.12 | -5.96 | -5.95 |

Table 6.9 (cont.)

log $\dot{\gamma}$ in 4 molal NaCl at 400°C and 500 bars, molybdenum(V) species considered.

pH

| 3.0 | 4.0 | 5.0 | 6.0 | 7.0 | 8.0 |
|------|------|------|------|------|------|
| -9.91 | -7.71 | -6.71 | -6.12 | -5.96 | -5.95 |

log $\dot{\gamma}$ in 4 molal NaCl at 400°C and 500 bars, molybdenum(V) species considered, log $f_{HF} = 10^{-1}$.

pH

| 3.0 | 4.0 | 5.0 | 6.0 | 7.0 | 8.0 |
|------|------|------|------|------|------|
| -10.05 | -8.56 | -7.56 | -6.65 | -6.09 | -5.96 |

log $\dot{\gamma}$ in 4 molal NaCl at a pH of 5 and 500 bars, molybdenum(V) species considered.

Temperature °C

| 250 | 300 | 350 | 400 |
|------|------|------|------|
| -2.80 | -3.57 | -5.20 | -6.71 |

# CHAPTER 7

## CALCULATED SOLUBILITY OF MOLYBDENITE AT ELEVATED TEMPERATURES

The solubility of molybdenite is a function of $f_{O_2}$, $a_{H_2S}$, pH temperature, pressure and solution composition. In this discussion, attempts will be made to evaluate the effects of the six variables on molybdenite solubility.

The solubility of molybdenite at constant temperature and pressure may be represented by the reaction:

$$MoS_2 + \tfrac{1}{2}O_2 + 3H_2O = 2H^+ + MoO_4^{2-} + 2H_2S(aq) \qquad 7.1$$

If the oxygen fugacity is fixed by external buffers, the molal solubility of molybdenite as a function of pH can be calculated from:

$$\log S = [(\log K(T,P,f_{O_2}) - \log\gamma_{MoO_4^{2-}} - 2\log\gamma_{H_2S}$$

$$- \log 4.0 + 2pH)]/3 \qquad\qquad 7.2$$

where S is the molal solubility of molybdenite, $\dot{\gamma}_j$ is the stoichiometric ion activity coefficient for the subscripted species. Stoichiometric ion activity coefficients for the molybdate ion are given in Chapter 6. The predominant form of reduced sulfur in acidic or mildly alkaline solutions is $H_2S$ (Barnes, 1979). A predictive theory, such as the Debeye-Huckel theory, does not exist for neutral solution species. As a consequence, there is little alternative but to assign a value of unity for the activity coefficient for $H_2S$ (Helgeson et al., 1981).

The oxygen fugacities for fluids associated with geological processes at elevated temperatures are often bounded by the mineral buffers: hematite-magnetite and nickel-nickel oxide. Equilibrium constants for the dissolution of molybdenite in aqueous solution buffer by hematite and magnetite or nickel and nickel oxide are presented in

Table 7.1. The equilibrium constants and equation 7.2 were used to calculate the solubility of molybdenite at elevated temperatures.

The numerical experiments presented in this Chapter represent an attempt to quantify the amount of molybdenum in hydrothermal solutions. Although the calculations can be carried out to a high degree of precision, the accuracy of the results depends on the coverage and accuracy of the dissociation constants presented in Chapter 6 and Appendix D. As has been pointed out earlier, good agreement between calculated solubilities and their experimental counterparts has been found. However, such comparisons are not possible for molybdenite solubility because of the lack of appropriate experimental work. Nevertheless, the calculations presented in the following pages represent reasonable first approximations. Although the magnitude of the calculated solubilities may be in error, the conclusions regarding the effects of temperature, pressure, etc. are insensitive to these errors.

## Table 7.1

Equilibrium constants for the dissolution of molybdenite at elevated temperatures and pressures. Calculated from the data presented in Chapter 3, SUPCRT (Helgeson et al., 1978) and Naumov et al. (1974). SAT refers to steam saturated water.

$$MoS_2 + 3H_2O + NiO = 2H^+ + MoO_4^{2-} + 2H_2S \text{ (aq)} + Ni$$
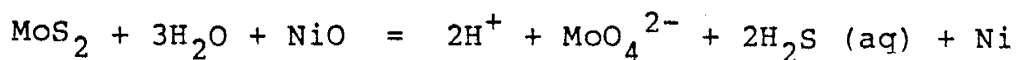
| P (bars) | log K(T,P) °C | | | |
| | 250 | 300 | 350 | 400 |
|---|---|---|---|---|
| SAT | -31.24 | -29.58 | -29.64 | |
| 500 | -30.58 | -28.53 | -27.16 | -27.19 |

$$MoS_2 + 3H_2O + 3Fe_2O_3 = 2H^+ + MoO_4^{2-} + 2H_2S \text{ (aq)} + 2Fe_3O_4$$
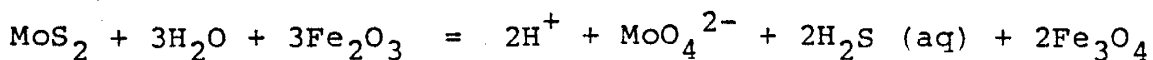
| P (bars) | log K(T,P) °C | | | |
| | 250 | 300 | 350 | 400 |
|---|---|---|---|---|
| SAT | -29.84 | -28.11 | -28.10 | |
| 500 | -29.19 | -27.07 | -25.62 | -25.58 |

# FACTORS AFFECTING MOLYBDENITE SOLUBILITY

## PRESSURE AND TEMPERATURE

The results of numerical experiments to evaluate the effects of temperature and pressure on molybdenite solubility are presented in Fig. 7.1. These results indicate that increasing the temperature at constant pressure results in a substantial increase in molybdenite solubility. Molybdenite solubility exhibits pro-grade solubility behavior in the temperature range considered. However, at higher temperatures (above 450°C) this may not be the case (cf., Isuk and Carnan, 1981) because of the decreased density of water at high temperatures.

An increase in the total pressure also resulted in an increase in molybdenite solubility (Fig. 7.1). The effect of pressure on solubility is a function of the volume of reaction. Since ions at elevated temperatures have large negative partial molal volumes, an increase in solubility at elevated temperatures is expected. The effects of pressure on solubility increase with temperature because the volume of reaction becomes more negative.

## CONCENTRATION OF A SUPPORTING ELECTROLYTE

Calculated molal solubilities of molybdenite in 2 and 4 molal sodium chloride solutions at temperatures of 250 to 350°C in steam saturated water are presented in Fig. 7.2. There is a marked decrease in molybdenite solubility with a decrease in the oxygen fugacity or the concentration of sodium chloride. Molybdenite solubility decreases because a decrease in the solium chloride concentration results in an increase in the activity coefficient of the molybdate ion.

Fig. 7.1

Calculated solubility of molybdenite as a function of temperature
at 500 bars pressure and in steam saturated water.  The pH is fixed
at 5 and the oxygen fugacity is fixed by the hematite-magnetite
mineral buffer.  Calculated using equation 7.1 and the data in
Tables 7.1 and 6.9.
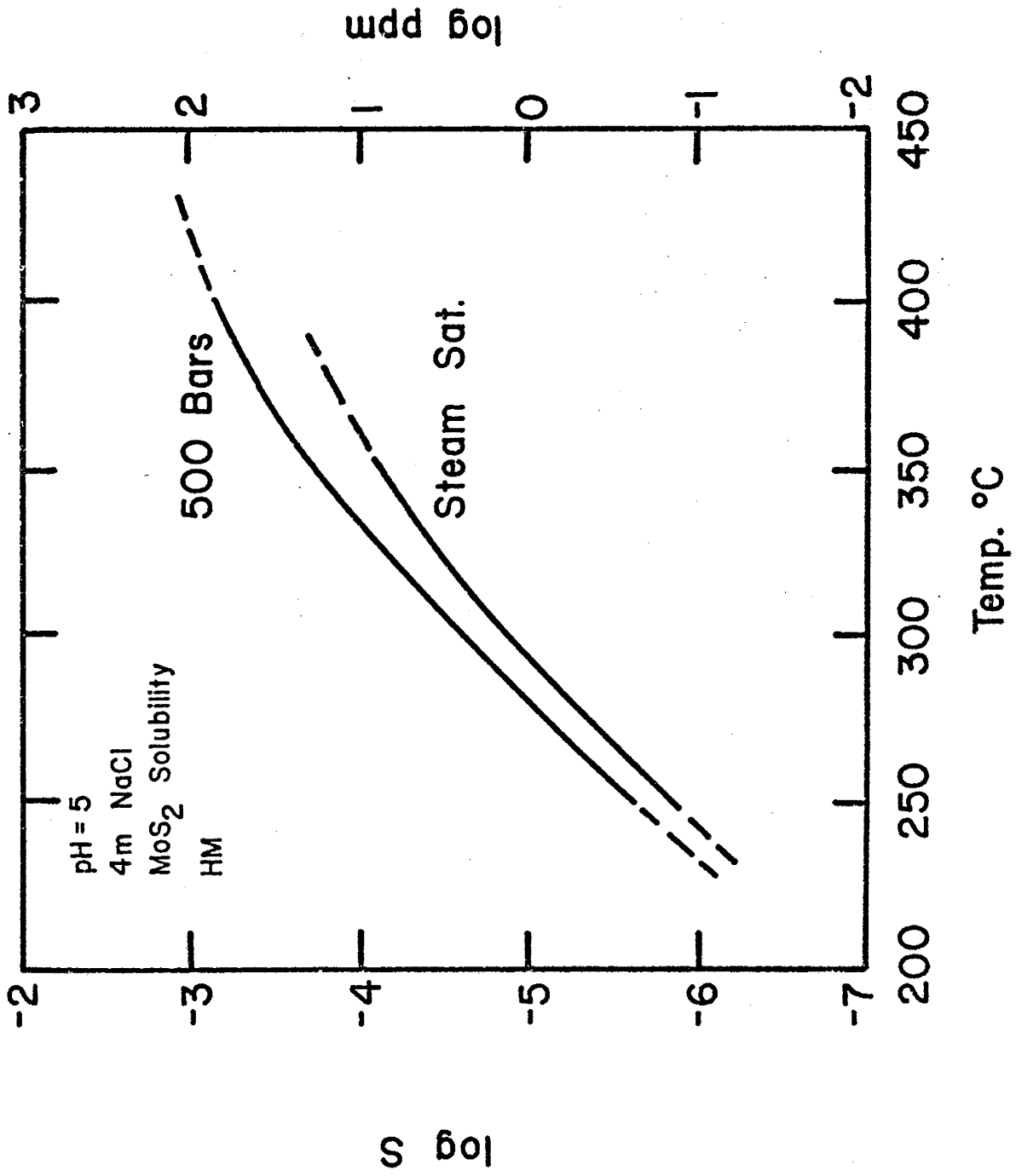
Fig. 7.2

Calculated solubility of molybdenite as a function of temperature in steam saturated water in 2 and 4 molal sodium chloride solutions buffered by nickel-nickel oxide (NNO) and hematite-magnetite (HM). Calculated using equation 7.1 and the data in Tables 7.1 and 6.9.
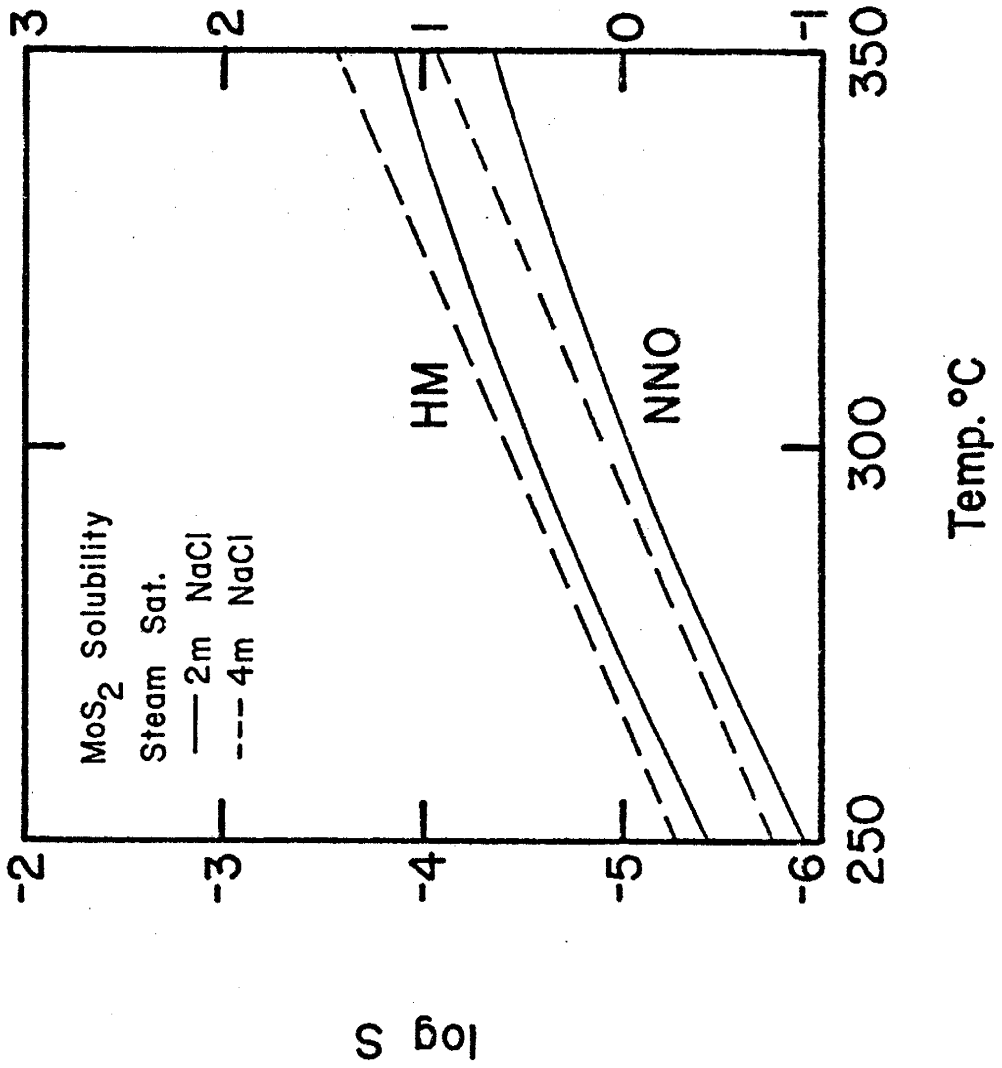
FLUORINE AND pH

Several numerical experiments at 400°C and 500 bars pressure were carried out to evaluate the effects of pH on solubility. The results of the first of these experiments are presented in Fig. 7.3. A minimum solubility of molybdenite occurs at a pH of about four. Westrich (1974) observed an increase in molybdenite solubility with decreasing pH, which is consistent with the acid portion of the curves presented here (Fig. 7.3). The numerical experiments indicate that solubilities of over 100 ppm Molybdenum are possible in near neutral solutions (Fig. 7.3).

Numerical experiments to evaluate the role of fluorine on the solubility of molybdenite were conducted. A value of $10^{-1}$ was selected for the HF fugacity, which is consistent with the HF values estimated by Gunow et al. (1980) for the ore zone at Henderson, CO (see Chapter 8). The results of these calculations are presented in Fig. 7.4. Comparison of this figure with Fig. 7.3 indicates that in the pH range of 4 to 6, molybdenite solubility is increased by a factor of two in fluorine-rich fluids. This results in molybdenum concentrations of up to 300 ppm at near neutral pH's. In fluorine-rich solutions molybdenite solubility increases with increasing pH except in very acid solutions (pH's less than 3).


DISTRIBUTION OF SOLUTION SPECIES

The distribution of molybdenum solution species at 400°C and 500 bars pressure for a 4 molal NaCl, HF rich fluid and a 2 molal NaCl solution are presented in Fig. 7.5a and b respectively. In both these figures molybdenum (V) solution species ($MoO_2^+$ and $MoOCl_3$) predominate at low pH's. Less acid solutions (3.5 to 6) favor the formation of

Fig. 7.3

Calculated solubility of molybdenite at 400°C and 500 bars as a function of pH in 4 molal sodium chloride solution buffered by nickel-nickel oxide (NNO) and hematite-magnetite (HM). Calculated using equation 7.1 and the data in Tables 7.1 and 6.9.

Figure: MoS₂ Solubility, 400° C, 500 Bars, 4m NaCl, low $f_{HF}$. Curves labeled HM and NNO, plotted as log S (and log ppm) versus pH.
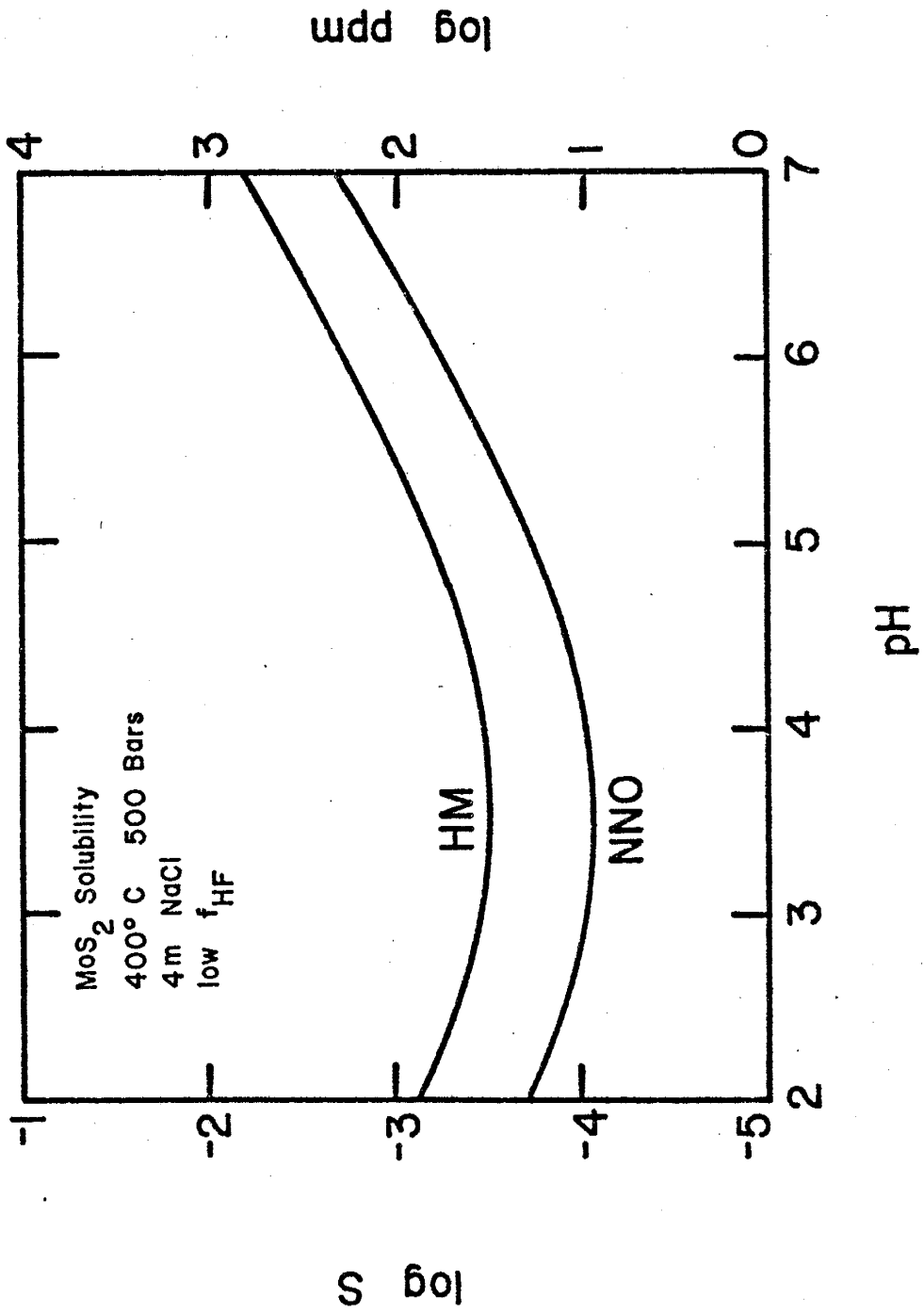
Fig. 7.4

Calculated solubility of molybdenite at 400°C and 500 bars as a function of pH in 4 molal sodium chloride solution with a HF fugacity of $10^{-1}$ buffered by nickel-nickel oxide (NNO) and hematite-magnetite (HM). Calculated using equation 7.1 and the data in Tables 7.1 and 6.9.

MoS$_2$ Solubility
400° C  500 Bars
4m NaCl
$f_{HF} = 10^{-1}$
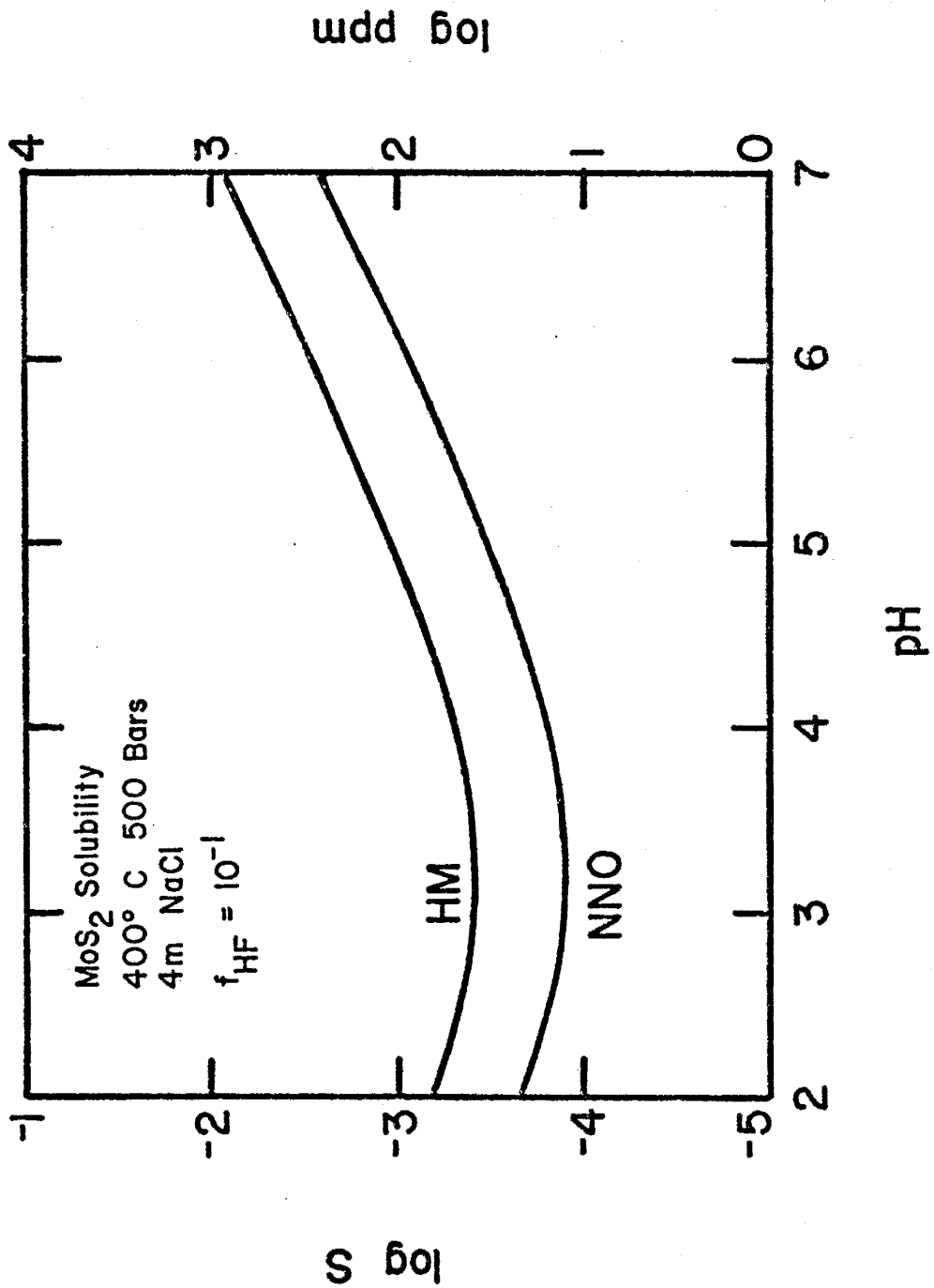
Fig. 7.5

Distribution of molybdenum solution species at 400°C and 500 bars

pressure as a function of pH.

Fig. 7.5a

4 m NaCl    log $f_{HF}$ = $10^{-1}$

Fig. 7.5b

2 m NaCl

a)
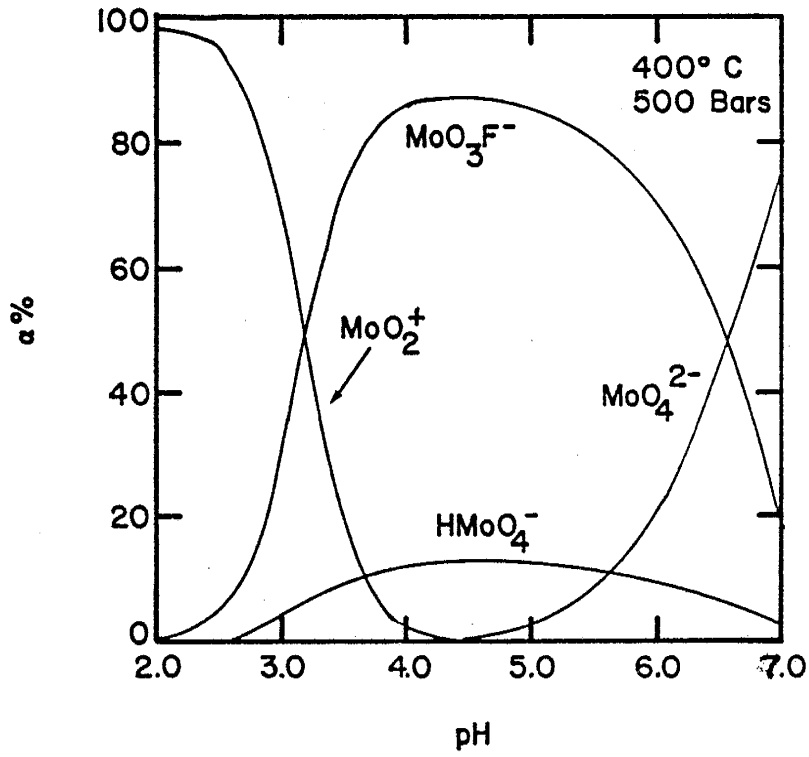


b)
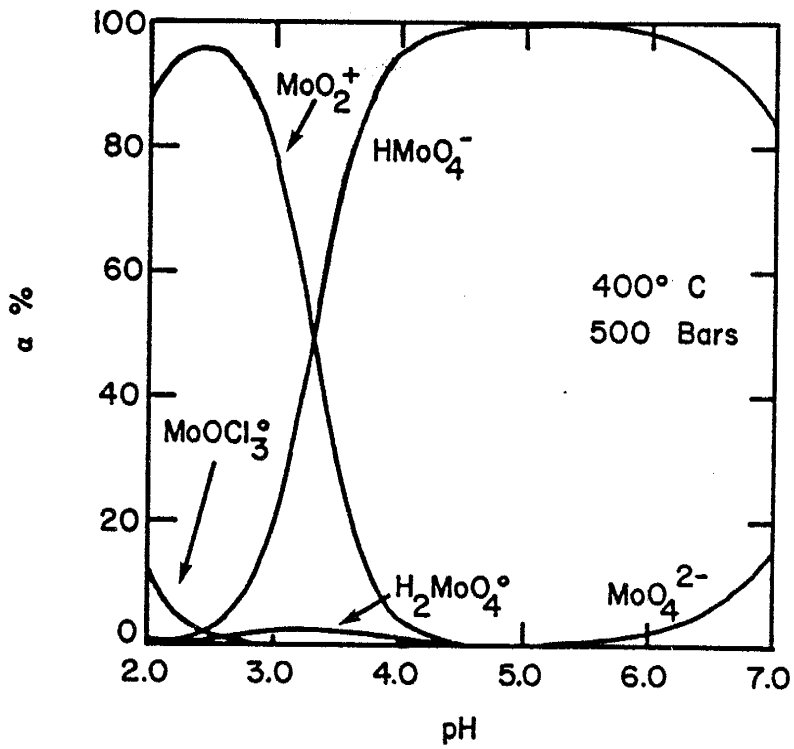
molybdenum (VI) species. The relative abundance of $HMoO_4^-$ $(MoO_3(OH)^-)$ and $MoO_3F^-$ is dependent on the HF fugacity. These results indicate that in near neutral solutions, molybdenum transport is by oxy-acid or fluoro-oxy-acid solution species.

The relative distribution of molybdenum solution species as a function of ionic strength is strongly influenced by the bulk dielectric constant of the sodium chloride solution. At low temperatures an increase in the molality of sodium chloride results in a decrease of the dielectric constant of the solvent (Helgeson et al., 1981). However, at higher temperatures sodium chloride molality has an opposite effect on the dielectric constant. An increase in the dielectric constant favors the dissociation of complexes. This dissociation results in a greater fraction of the total molybdenum being present as the molybdate ion at increased ionic strengths and temperatures.

## FACTORS AFFECTING THE DEPOSITION OF MOLYBDENITE

The formation of an ore deposit requires the transport and the deposition of metals from an aqueous solution. Barnes (1979) has indicated that 1 to 10 ppm represents the minimum concentrations of base metals necessary to produce an ore deposit. Examination of Figs. 7.1 through 7.4 indicates that, at temperatures greater than 300°C, molybdenum concentrations exceed this requirement. Deposition of molybdenite is affected by the same factors that affect the solubility. Barnes (1979) discusses various mechanisms which would result in ore deposition. Among these mechanisms are temperature change, dilution, wall rock reactions and changes in oxygen fugacity. Results of numerical experiments designed to evaluate these effects are presented below.

## TEMPERATURE

Decreasing the temperature from 350 to 250°C results in a 98% decrease in molybdenite solubility. A larger decrease in solubility (+99.99%) is expected for a fluid which is externally buffered for both $H_2S$ and log $f_{O_2}$ (Smith et al., 1980).

## PRESSURE

Decreasing the pressure from 500 bars to 165 bars at 350°C results in a 60% decrease in molybdenite solubility. The decrease in solubility becomes more pronounced at higher temperatures.

## DILUTION

A one-to-one dilution with pure water of a near neutral 4 molal NaCl ore solution at 400°C and 500 bars results in a 35% decrease in the solubility of molybdenite. Acid solutions do not show a significant change in solubility with dilution.

## OXYGEN FUGACITY

Decreasing the oxygen fugacity from the hematite-magnetite buffer to the nickel-nickel oxide buffer results in a 70% decrease in molybdenite solubility.

## WALL ROCK REACTIONS

The effects of wall rock reactions on the deposition of molybdenum could not be numerically evaluated. Typically wall rock reactions involve fluids which never equilibrate with the original rock, but convert the rock to a stable hydrothermal mineral assemblage (i.e., pervasive alteration). However, the effects of wall rock reactions on mineralization can be evaluated in a general way. At Questa, NM for example, molybdenite mineralization occurs as veins associated with potassic alteration in andesite volcanics (see Chapter 8). A generalized reaction of a solution rich in potassium, molybdenum, sulfur and fluoride reacting with plagioclase and pyroxene would be:

$$3Mg_2Si_2O_6 + CaAl_2Si_2O_8 + 9H_2S + 2K^+ + 2H^+ + 4MoO_3F^-$$
$$= 4MoS_2 + 2KMg_3AlSi_3O_{10}F_2 + 2SiO_2 + CaSO_4 + 10H_2O \qquad 7.3$$
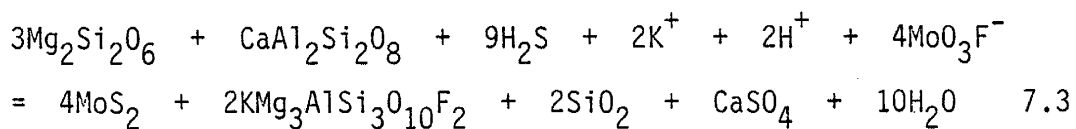
Examination of the above reaction indicates that molybdenite deposition would occur in response to the formation of fluorine rich micas. Another reaction involving the wall rocks during potassic alteration would be the alteration of igneous biotite to magnesium rich hydrothermal biotite:

$$3KFeMg_2AlSiO_{10}(OH)_2 + 2H_2S + H^+ + HMoO_4^- = KAlSi_3O_8$$
$$+ 2KMg_3AlSiO_{10}(OH)_2 + Fe_3O_4 + MoS_2 + 4H_2O \qquad 7.4$$
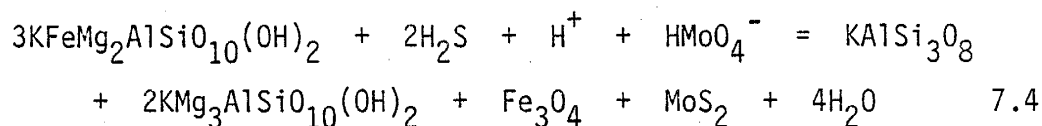
Examination of reaction 7.4 again indicates that the wall rock reactions which attend potassic alteration would result in molybdenite deposition.

## CONCLUSIONS

The results presented in this chapter indicate that substantial concentrations of molybdenum may be transported in saline hydrothermal fluids at elevated temperatures. These results show that molybdenum transport may be accomplished by molybdenum (V) oxy-cations and chloride complexes in acid solutions. In near neutral solutions, molybdenum is transported as hexavalent oxy-acid species. High fluoride activities enhance the transport of molybdenum, but are not essential. Deposition of molybdenite occurs from decreases in pressure and temperature and wall rock reactions. Dilution and decreases in oxygen fugacity have lesser effects on solubility.

The results presented are limited in that it has not been possible to consider molybdenum (IV) species. However, in spite of this limitation, the models for hydrothermal transport presented in this chapter allow for the transport of molybdenum in both high-fluoride (Climax-type deposits) and low-fluoride (quartz-monzonite type) solutions.

## SUMMARY OF PART I

The principle of corresponding states has been demonstrated for aqueous eletrolytes and dissociation reactions. The partial molal volume and heat capacity of ions at elevated temperatures are related by a simple linear function to the corresponding property at room temperature. If the effects of ion solvation are considered, the partial molal volume and heat capacity of aqueous ions may be estimated to a high degree of accuracy from room temperature properties. This allows evaluation of the apparent molal Gibbs free energies at elevated temperatures which, when coupled with similar data for minerals, allows calculation of equilibrium constants for solubility and hydrolysis reactions of geologic interest.

The entropy of dissociation at elevated temperatures for fluoride and hydroxide complexes, as well as oxy-acids also exhibit a linear relationship with the room temperature entropy of dissociation. When coupled with proposed schemes which allow the estimation of the entropy of dissociation for fluoride complexes at 25°C, dissociation constants for fluoride complexes can be estimated to temperatures of 300°C if the dissociation constant at room temperature is known.

Application of the correspondence principle to 26 fluoride complexes indicates that fluoride complexes of divalent metals are not important in the transport of metals because of the high $Cl^-/F^-$ ratios associated with most hydrothermal solutions. However, fluoride complexes can be important in the transport of aluminum at elevated temperatures in slightly acid solutions.

Application of the correspondence principle to twelve molybdenum complexes and ions indicates that at elevated temperatures in neutral solutions, bimolybate ($HMoO_4^-$) is the predominate solution species. In acid solutions (pH less than 3), molybdenum (V) ($MoO_2^+$, $MoOCl_3$) species predominate. Fluoride and sulfide complexes are important at high temperatures (greater than 350°C) and high activities of $H_2S$ (approximately $10^{-1.5}$) and high HF fugacities (approximately $10^{-2}$).

At 400°C and 500 bars calculated solubilities of molybdenite are several hundred ppm (as Mo) in both fluoride-rich and fluoride-poor solutions. Deposition of molybdenite occurs in response to the following physico-chemical changes: decrease in temperature, decrease in pressure, decrease in the oxygen fugacity and an increase in pH. Wall rock reactions attending potassic alteration also result in molybdenite deposition.

PART II

CHAPTER 8

MINERALIZATION TEMPERATURES AND SOURCES OF HYDROTHERMAL FLUIDS AT THE
QUESTA, NM MOLYBDENITE DEPOSIT


INTRODUCTION

The use of fluid inclusion and isotopic data allows  evaluation of
the roles and sources of fluids in hydrothermal systems associated with
porphyry metal deposits.  For example, fluid inclusions may provide
samples of mineralizing fluids.  This, coupled with field observations
and an understanding of the thermodynamic and spatial relationships
among various alteration assemblages, allows interpretations of ore
forming processes which are consistent with both geologic and chemical
constraints.  Results of a reconnaissance fluid inclusion and stable
isotope study of the Questa molybdenite deposits will be presented.  In
addition, results of analyses of fluid inclusion volatiles by mass
spectrometry are presented.

Numerous studies of fluid inclusions and stable isotopes have been
carried out on porphyry copper systems.  However, this literature review
will be limited to studies of porphyry molybdenum mineralization.  Fluid
inclusion measurements have been made on material from Questa (Bloom,
1981), Climax, Colorado (Roedder, 1971; Hall et al., 1976), Henderson,
Colorado (White et al., 1981), Boss Mountain, British Columbia
(Macdonald and Spooner, 1981) and Endako and Hudson Bay Mountain,
British Columbia (Bloom, 1981).  A summary of fluid inclusion
homogenization temperatures from these works is presented in Table 8.1.

Table 8.1

Summary of fluid inclusion homogenization temperatures from porphyry molybdenum deposits of western North America.

| Deposit | Temperature $^{o}C$ | Source |
|---|---|---|
| Boss Mountain, British Columbia | 250-370 | 2 |
| Climax, Colorado | 360±25 | 3,4 |
| Endako, British Columbia | 340-380 | 1 |
| Henderson, Colorado | 325-450 | 5 |
| Hudson Bay Mountain, British Columbia | 340-400 | 1 |
| Questa, New Mexico | 360-420 | 1 |

1 - Bloom (1981)

2 - Macdonald and Spooner (1981b)

3 - Hall et al. (1974)

4 - Roedder (1971)

5 - White et al. (1981)

Although a large range of temperatures is reported by the different investigators, a generalized temperature of mineralization may be placed as 350 to 450°C. The salinities of inclusions measured in these studies fall into two groups. The first group is saline, typically having a halite daughter mineral at room temperature and is prevalent at Questa, Climax, and Henderson. The second group is more dilute, typically less than 10 eq. wt. % NaCl, and is prevalent at the British Columbia deposits. In addition, low salinity inclusions also occur in deposits which have high salinity inclusions. Distribution of fluid inclusion filling temperatures and salinities for porphyry molybdenum deposits is similar to the distributions found in porphyry copper deposits (Nash, 1976).

Light stable isotope studies on porphyry molybdenum deposits have been limited to the Climax deposit (Sheppard et al., 1971 and Hall et al., 1974). These studies suggest that mineralization at Climax was associated with at least some magmatic water. In addition, Hall et al. (1974) demonstrated that potassium feldspars were drastically depleted in $\delta^{18}O$ by exchange with heated, surface-derived waters.

## LOCATION AND HISTORY

The Questa molybdenite deposits are located in north central New Mexico between the communities of Questa and Red River along State Highway 38 in the Sangre de Cristo Mountains (Fig. 8.1). Molybdenite has been produced from the region since the mid-'20s. Early production was from Sulfur Gulch, and these old workings are currently referred to as the "Old Vein Deposits". Production continued until 1958. The most comprehensive publication dealing with this early underground activity is by Schilling (1956), although the first investigations were made by Larsen and Ross (1920) and Vanderwilt (1938).

Fig. 8.1

Index map showing location of the Questa molybdenite mine
(courtesy New Mexico Bureau of Mines).
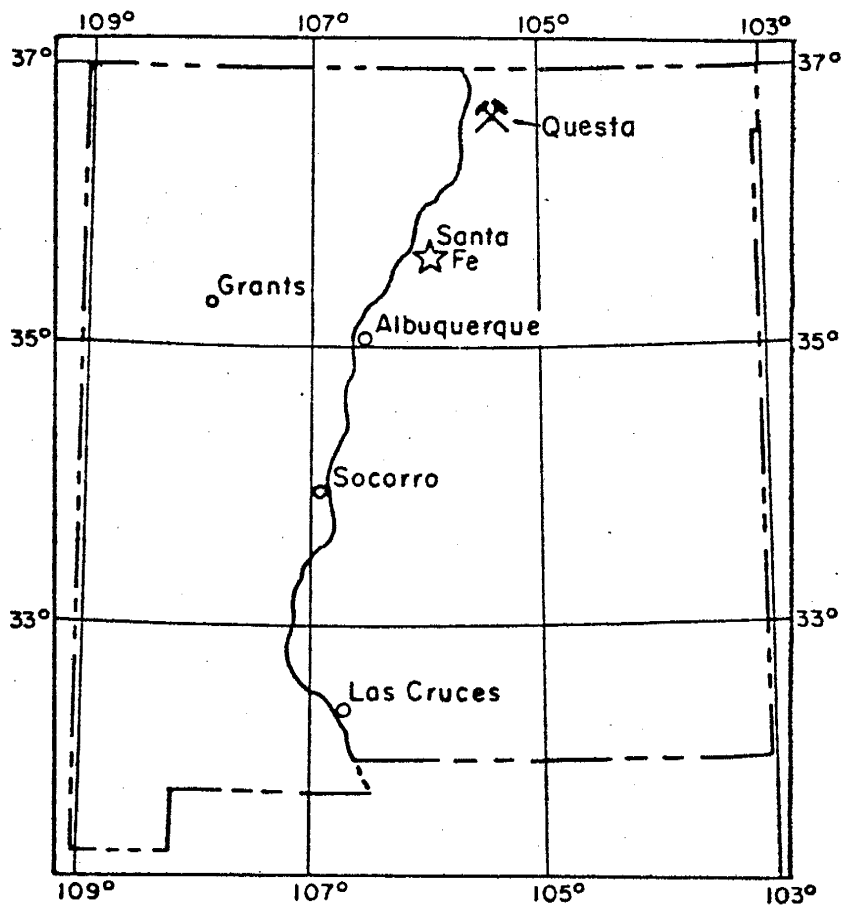
By the mid-'50s renewed exploration for ore had begun. By 1964, sufficient ore reserves had been outlined to justify production by open-pit methods and the first ore was delivered to the mill in late 1965. In 1977, following heavy rains, the west wall of the pit collapsed, filling the pit with approximately five million tons of waste which curtailed normal production.

Joint exploration by Molycorp and Kennecott lead to the definition of several mineable ore reserves. In 1977, Kennecott sold its interest in Molycorp to Union Oil Company of California. Development of a large underground mine in the Goat Hill Gulch (Southwest Zone) has continued to the present time.

GENERAL GEOLOGY

Geologic studies of the Questa-Red River area have been conducted by Schilling (1956), McKinley (1956, 1957), Clark (1968), Carpenter (1968) and Clark (1972). At the present time, studies of the area are being conducted by the U.S. Geological Survey (Lipman, 1981). The discussion that follows is a summary of this previous work (especially, Carpenter, 1968 and Clark, 1968). In addition, an unpublished geological report on the Questa area was used (Martineau et al., 1977).

Precambrian metamorphic rocks and granites form the basement complex in the Sangre de Cristo Mountains of northern New Mexico. The Precambrian rock of the Questa area (Fig. 8.2) consists predominately of amphibolities, schists, gneisses, metaquartzites and foliated granites.

The Precambrian rocks are overlain in places by remnants of the Pennsylvanian-age Sangre de Cristo Formation (Shilling, 1956 and McKinley, 1957). Carpenter (1968) reports the occurrence of

Fig. 8.2

Generalized map of the "Red River Trench" (compiled by Molycorp, 1977).

EXPLANATION

granite to monzonite intrusives

rhyolite volcanics

andesite volcanics

Precambrian

0 1 2 3 4 5 km
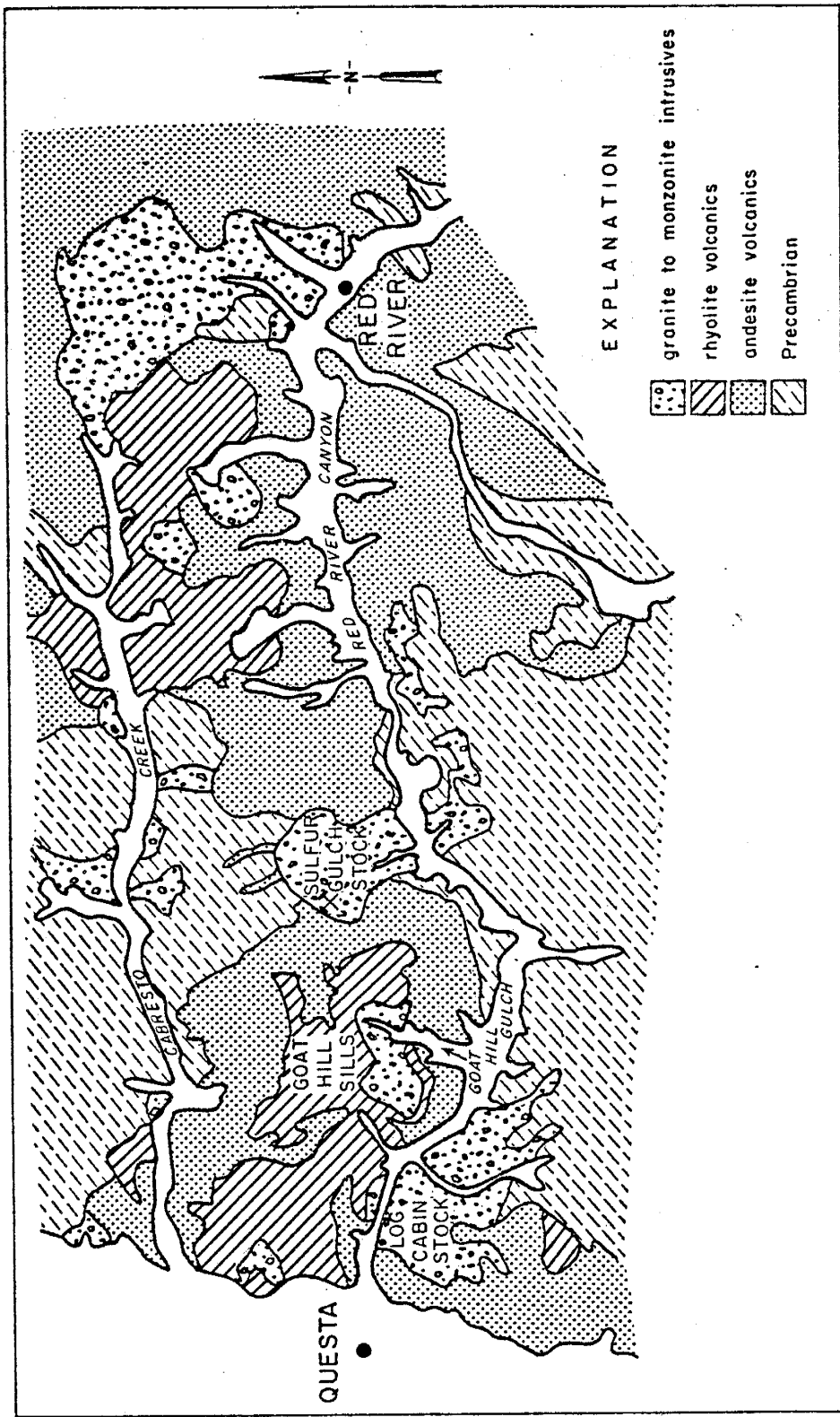
Cretaceous-age, fine grained clastic sediment resting on Precambrian rocks, while Clark (1968) concludes that the sediments are in part tuffaceous and included them with and considers them as part of the Tertiary volcanic units.

Up to 2000 meters of Tertiary volcanic rocks have accumulated in the Questa area. These rocks consist of Oligocene to lower Miocene andesites, latites and rhyolite tuffs. The basal unit is a fine-grained, hornblende andesite flow which occurs immediately above the Precambrian. Toward the top of the fine-grained andesite in the area of the mine are fine-grained andesite tuffs which have been extensively altered by hydrothermal fluids. These are overlain disconformably by porphyritic, quartz-bearing, hornblende-biotite latites. The rhyolites unconformably overlie the andesites and the latites. The lower unit of the rhyolite series is a course grained welded rhyolite tuff. The coarse grained tuff grades upward into a fine-grained, welded rhyolite tuff. The volcanic rocks in the area yield potassium-argon ages of 36 to 22 million years b.p. (Pillmore et al., 1973).

Late plutonic to hypabyssal intrusives, ranging from monzonite to granite in composition, cross-cut the volcanic sequence. These intrusive rocks exhibit a wide variety of textural types, including aplites, porphyries and crowded porphyries, and equigranular biotite and hornblende granites and quartz monzonites. The porphyries are commonly characterized by potassium feldspar, quartz and biotite in aphanitic to aplitic ground mass. The bulk composition of these rocks is near the "granite-minimum" in the quartz-albite-orthoclase ternary.

Potassium-argon ages for mineralized intrusives are 23 million years b.p. (Isahara, 1967 and Laughlin et al., 1969). Ages of vein biotites associated with mineralization are indistinguishable from the intrusive ages (Isahara, 1967 and Laughlin et al., 1969). A generalized stratigraphic section for the area is presented in Fig. 8.3.

The major mineralization in the area of Questa is confined to an east-northeast structure referred to in the literature as the "Red River Trench". This feature has been interpreted by Lipman (1981) as being the southern edge of the Questa Caldera (Fig. 8.4). The geometry of the caldera has been inferred from the distribution of granitic intrusives and the presence of thick welded tuffs and massive megabreccias, interpreted as caldera fill and caldera collapse breccias. The core of the caldera has been resurgently domed. The age of the silicic intrusives and volcanics define the age of the caldera as 23 million years b.p. The western margin of the caldera has been normally faulted into the Rio Grande rift and covered by younger sediments.


## ALTERATION AND MINERALIZATION

Mineralization and alteration of the Red River Trench was controlled to a large extent by the overlap in time and space of intrusion and fracturing of the rock in the area (Clark, 1968). As a result, molybdenum mineralization occurs in two styles. The first is "disseminated" mineralization in host intrusives. The second is vein and fissure filling in the country rock. Mineralization in the Goat Hill Gulch (Southwest Zone) area is primarily of the second type, with extensive mineralization and alteration in the andesite volcanics.

Fig. 8.3

Generalized stratigraphic section of the Questa area (after Carpenter, 1968).
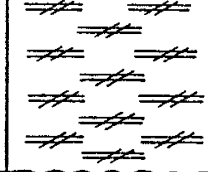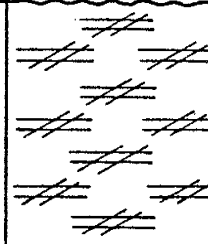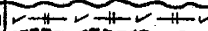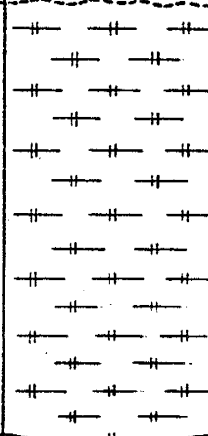
| SERIES | MEMBER | COLUMNAR SECTION | DESCRIPTION | THICKNESS IN METERS |
|---|---|---|---|---|
| PLIO. | Rhyolite | | Banded, spherulitic, highly contorted, glassy rhyolite | 60 |
| | | | Light gray, banded, porphyro-aphanitic rhyolite | 30 |
| EARLY MIOCENE | Upper Rhyolite Tuff | | Fine grained, light to dark gray, banded, glassy and pumaceous, welded rhyolitic tuff. Somewhat fragmental towards top | 400 |
| | Lower Rhyolite Tuff | | Coarse grained, welded tuff with alternating dark gray glassy and light gray pumaceous bands up to an inch in thickness | 500 |
| | Latite | | Porphyritic, quartz-bearing, hornblende-biotite latite tuffs and flows with agglomerate lenses toward top | 200 |
| | PORPH | | Medium to coarse grained, tuffaceous andesite porphyry | 0-60 |
| | Andesite | | Dark green to gray, fine grained, featureless, hornblende andesite with infrequent, finely crystalline tuffaceous lenses | 160-900 |
| CRET. | SANDS | | Sandstones, siltstones and grits | 0-30 |
| PENN. | GRITS | | Arkosic shales, sandstones and conglomerates | 0-90 |
| PRECAMBRIAN | | | Biotite gneiss and schists, amphibolite gneisses and schists, feldspar gneisses, acidic granite gneisses, quartzite and granite | |

Fig. 8.4

Generalized geologic map of the Questa Caldera (after Lipman, 1981).
Ti, Tertiary intrusive rocks; Tv, Tertiary volcanic rocks; pT, pre-
Tertiary rocks.

Geologic map showing the Questa Caldera area, Rio Grande Rift, with locations including Costilla, Costilla Mountains, Latir Mesa, Questa, Red River, Wheeler Peak, and Arroyo Hondo. Coordinates range from 105°15' to 105°45' longitude and 36°30' to 37°00' latitude. Scale bar: 5 0 5 10 km.
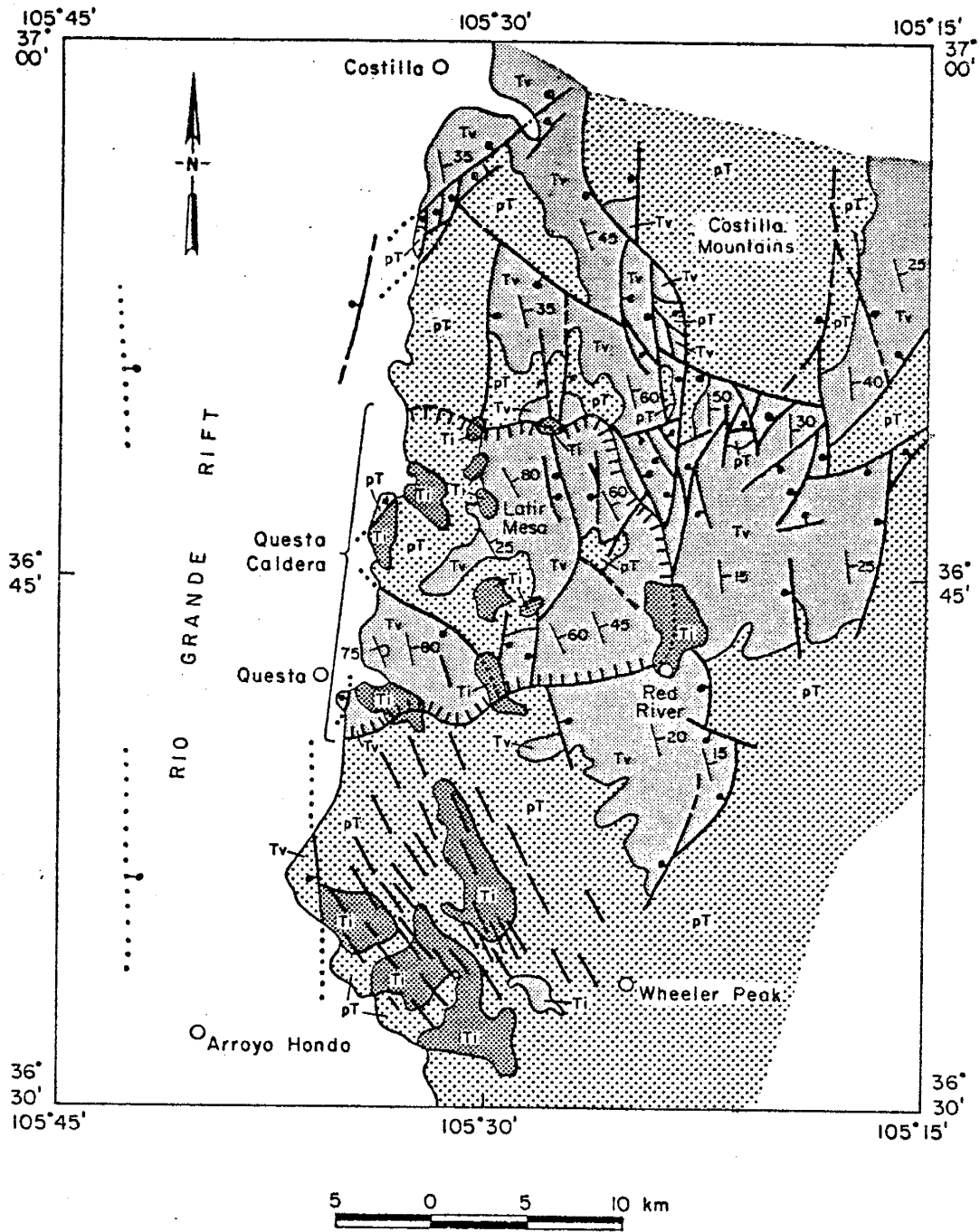
As with most Climax type molybdenum deposits, interpretation of paragenesis and alteration mineralogies is complicated by superimposed intrusive and mineralizing events. At Questa, three mineralizing events have been recognized (Martineau et al., 1977). The relative ages of these three events are: the early aplite system associated with mineralization in the open pit area, followed by the Goat Hill Granite associated with Southwest Zone system, and finally the deep granite system. Although the alteration systems overlapped, a generalized vein paragenesis based on cross cutting relationships for a single mineralizing event at Questa was determined (Martineau et al., 1977 and Bloom, 1981). The paragenesis is:

1) barren quartz and quartz-biotite veins;

2) quartz-biotite-K-feldspar±molybdenite veins;

3) quartz-molybdenite veins;

4) quartz-pyrite±molybdenite veins;

5) quartz-base metal sulfide veins;

6) fluorite-carbonate veins.

Potassic alteration, sericization, propyllization and silicificaiton have all been recognized at Questa. Molybdenum mineralization, in the form of quartz-molybdenite veins is associated primarily with potassic, and to a lesser extent, sericitic alteration. The alteration is associated with the veining, however, locally in areas with high vein densities pervasive alteration is developed. Although mineralization and alteration were controlled by the fracturing in the volcanics, and clear zoning is not developed, there is a tendency for silicification and potassic alteration to occur towards the center of the deposit and sericization with a pyrite halo to occur further out.

## EXPERIMENTAL

Materials used in this study were selected from drill cores provided by Molycorp. Cores from the Southwest Zone were selected because the mineralization and alteration occurs in the andesites and is well preserved. The alteration mineralogy of the Southwest Zone allows highly constrained reconstructions of the hydrothermal fluid chemistries.

## FLUID INCLUSIONS

Doubly polished plates of quartz were prepared (cf., Holland et al., 1978) for fluid inclusion studies. Heating and freezing measurements of fluid inclusions were accomplished using a Linkam TH600 (Linkam Scientific Instrument) Programmable heating and freezing stage (Shepherd, 1981). Calibration of the stage has been described by Macdonald and Spooner (1981). In this laboratory, calibration of the temperature range -90 to +7°C was done using the fusion point of six organic liquids. The fusion point of twelve solids were used to calibrate the stage in the temperature range +80 to 590°C. Daily measurements of the ice point varied less than 0.2°C. Reproducibilities of measurements were found to be 0.2°C for freezing and 2°C at 400°C. Homogenization temperatures were determined based on the last reversible phase change observed in the inclusion. Salinities, reported as eq. wt. % NaCl, were calculated from freezing point depression of the inclusions and the equations of Potter et al. (1978). Salinities of fluid inclusions containing halite were determined from a regression of halite solubility as a function of temperature (Int. Crit. Tables, 1928 and Keevil, 1942).

STABLE ISOTOPES

Vein minerals (Quartz, K-feldspar and biotite), phenocryst from samples of the intruvives (Quartz and K-feldspar) and whole rock samples from Questa were analyzed for stable isotopes of hydrogen and oxygen. All isotope analyses were carried out by Gary Landis at the Branch of Isotope Geology, U.S. Geological Survey, Denver, Colorado.

The isotopic data in this study are reported as $\delta D$ and $\delta^{18}O$ in the standard per mil notation. The $\delta$ value is the difference in the isotopic ratio between the standard and the sample normalized to the standard.

$$\delta = \frac{R(sample) - R(standard)}{R(standard)} \times 1000 \qquad 8.1$$

where R(sample) and R(standard) are the D/H or $^{18}O/^{16}O$ ratio of the sample and standard respectively. In this study, SMOW (Standard Mean Ocean Water) was used as the standard for both hydrogen and oxygen (Craig, 1957, 1961). The uncertainty associated with the isotopic ratios is 0.1 and 1 per mil for $\delta^{18}O$ and $\delta D$ respectively.

The temperature dependence for isotopic fractionation, $\Delta(a-b)$, is given by:

$$\Delta(a-b) = \delta a - \delta b = 1000\ln\alpha = (A/T) \times 10^6 + B \qquad 8.2$$

where $\alpha$ is the fractionation factor, $\delta a$ and $\delta b$ are the $\delta$ values for phases a and b, and A and B are coefficients describing the temperature dependence of the fractionation. The coefficients, A and B, for fractionations used in this study are summarized in Table 8.2.

Table 8.2

Coefficients for equation 8.2 describing the isotopic
fractionation between two phases in isotopic equilibrium.

| Phases | A | B | Source |
|--------|------|-------|--------|
| quartz-water | 3.57 | -2.73 | Taylor (1974) |
| feldspar-water | 2.91 | -3.41 | O'Neil and Taylor (1969) |
| quartz-biotite | 2.54 | 0.85 | Shieh and Schwarcz (1974) |

## VOLATILE ANALYSES

Fluid inclusion volatiles were analysed from selected quartz samples using an Inficon IQ 200 quadrupole mass spectrometer. Fluid inclusions were thermally decrepitated at temperatures of 550 or 600°C in a high-vacuum line (pressures less than $10^{-6}$ torr). The evolved gases were introduced into the mass spectrometer after separations based on the vapor pressure of the various gases. Water was collected in capillaries and weighed. The mass spectrum for each gas fraction was evaluated using linear least squares techniques and fractionation patterns for known gases previously determined in this laboratory. This allowed determination of the relative abundances of gases in the mixtures. From the relative abundances and measured pressures of the gas fractions, the mole fraction of each species was calculated. The estimated relative uncertainty associated with the gas analyses are 31% for hydrogen, 23% for hydrogen sulfide and sulfur dioxide and 16% for carbon dioxide. For a more complete description of the techniques used in this study to determine the composition of volatiles in fluid inclusions the reader is referred to Appendix F. In addition, a description of the estimated errors is also included in Appendix F.

The molalities of volatile species (other than water) were calculated from:

$$m_i = X_i \times 55.5 \qquad\qquad 8.3$$

where $m_i$ and $X_i$ are the molality and mole fraction respectively of the subscripted species. The moles of water per kilogram (55.5) is the conversion factor between the two concentration scales.

Fugacity coefficients for pure gases were calculated from equations 2.13 through 2.16 and the critical constants for the gases (Mathews, 1972) or the equations of Jacobs and Kerrick (1981). Fugacities of the gases were calculated from the mole fraction of the gases and the fugacity coefficients using equation 2.11 and Dalton's law of partial pressures.

RESULTS

FLUID INCLUSION

Doubly polished plates of quartz were examined in order to select inclusions suitable for microthermometry. Inclusion generations (i.e., primary, secondary, etc.) were determined using the criteria outlined by Roedder (1979, pp. 689-691). Four types of primary fluid inclusions were observed in quartz from Questa. These are:

1) Two phase inclusions which homogenize by vapor-bubble dissappearance;

2) Two phase inclusions which homogenize to a vapor;

3) Three phase inclusions which contained a halite daughter mineral. In addition, a molybdenite or hematite daughter mineral was sometimes present in these inclusions. This inclusion type homogenized by disappearance of the vapor bubble or by halite dissolution. This type of inclusion was the most common.

4) Multi-phase inclusions which contained both halite and sylvite daughter minerals. In addition, these inclusions often contained one or more of the following daughter minerals; hematite, molybdenite, anhydrite and another small opaque mineral. In one inclusion of this type, liquid carbon dioxide was observed.

Results of the fluid inclusion microthermometry are presented in Fig. 8.5. Also included in these temperature and salinity histograms are measurements made by Bloom (persn. comm. and 1981). The fluid inclusions exhibited a wide range of homogenization temperatures and a bimodal distribution of salinities. Temperatures and salinities

Fig. 8.5

Salinity and homogenization temperature histograms for primary fluid inclusions in quartz from the Questa molybdenite deposit.  Data from this study (shaded) and Bloom (1981).

Homogenization temperature
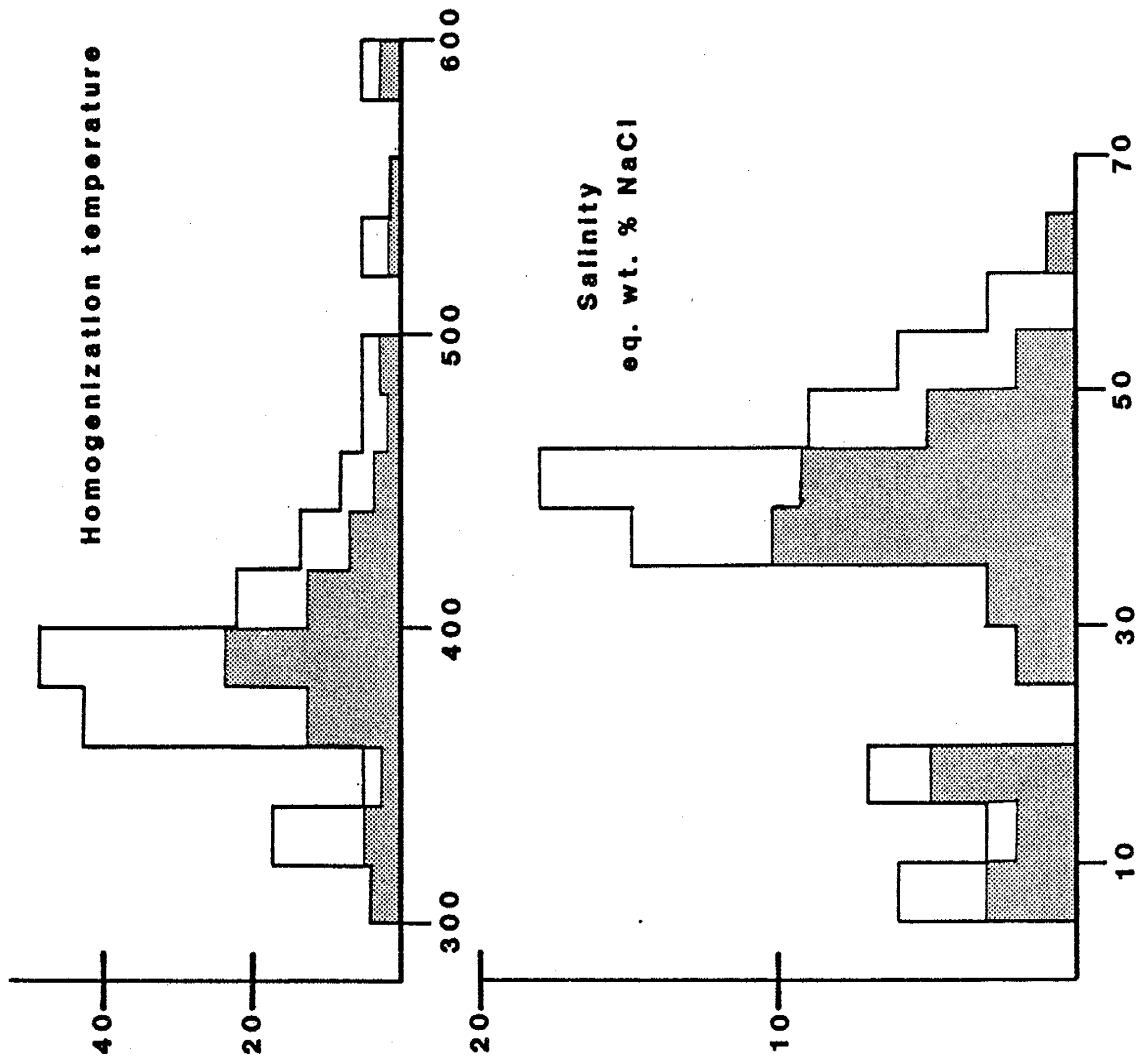
Salinity
eq. wt. % NaCl

observed in this study are similar to those for porphyry copper deposits (Fig. 8.6), and the observed primary inclusions may be classified as low-salinity, type I and high-salinity, type IIIb porphyry inclusions (Nash, 1976 as modified by Beane and Titley, 1981). The trend evident in the high-salinity inclusions (Fig. 8.6) resulted from inclusions which homogenized by halite dissolution. Inclusions above this trend contained both halite and sylvite daughter minerals at room temperature.

## STABLE ISOTOPES

The results of the determination of $\delta^{18}O$ values for eleven quartz samples, six potassium feldspar samples, five biotite samples and two whole rock samples are presented in Table 8.3. Also included in Table 8.3 are $\delta D$ values for five biotite samples. The samples are grouped according to rock type and alteration. Quartz associated with potassic alteration have a $\delta^{18}O$ range of from 6.8 to 12 per mil, potassium feldspar ranged from 1.8 to 8.5 per mil and biotite ranged from 1.2 to 5.4 per mil. Quartz samples associated with sericitic alteration have $\delta^{18}O$ values of 9.3 and 9.7 per mil. Potassium feldspar and quartz from granitic intrusives have $\delta^{18}O$ ranges of 0.5 to 1.9 and 7.0 to 7.7 per mil respectively. $\delta D$ for the biotites ranged from -110 to -117 per mil.

## VOLATILE ANALYSES

Results of the analyses of volatiles from fluid inclusions in vein quartz associated with both potassic and sericitic alteration, as well as quartz phenocrysts from the granitic intrusive are presented in Table 8.4 and Fig. 8.7. Two groups of data are prevalent, one associated with potassic alteration and one associated with sericitic alteration (Fig. 8.7).

Fig. 8.6

Relationships between homogenization temperatures and salinities for primary fluid inclusions from Questa. Type I and type IIIb classifications are from Nash (1976) as modified by Beane and Titley (1981). Data from this study and Bloom (1981).
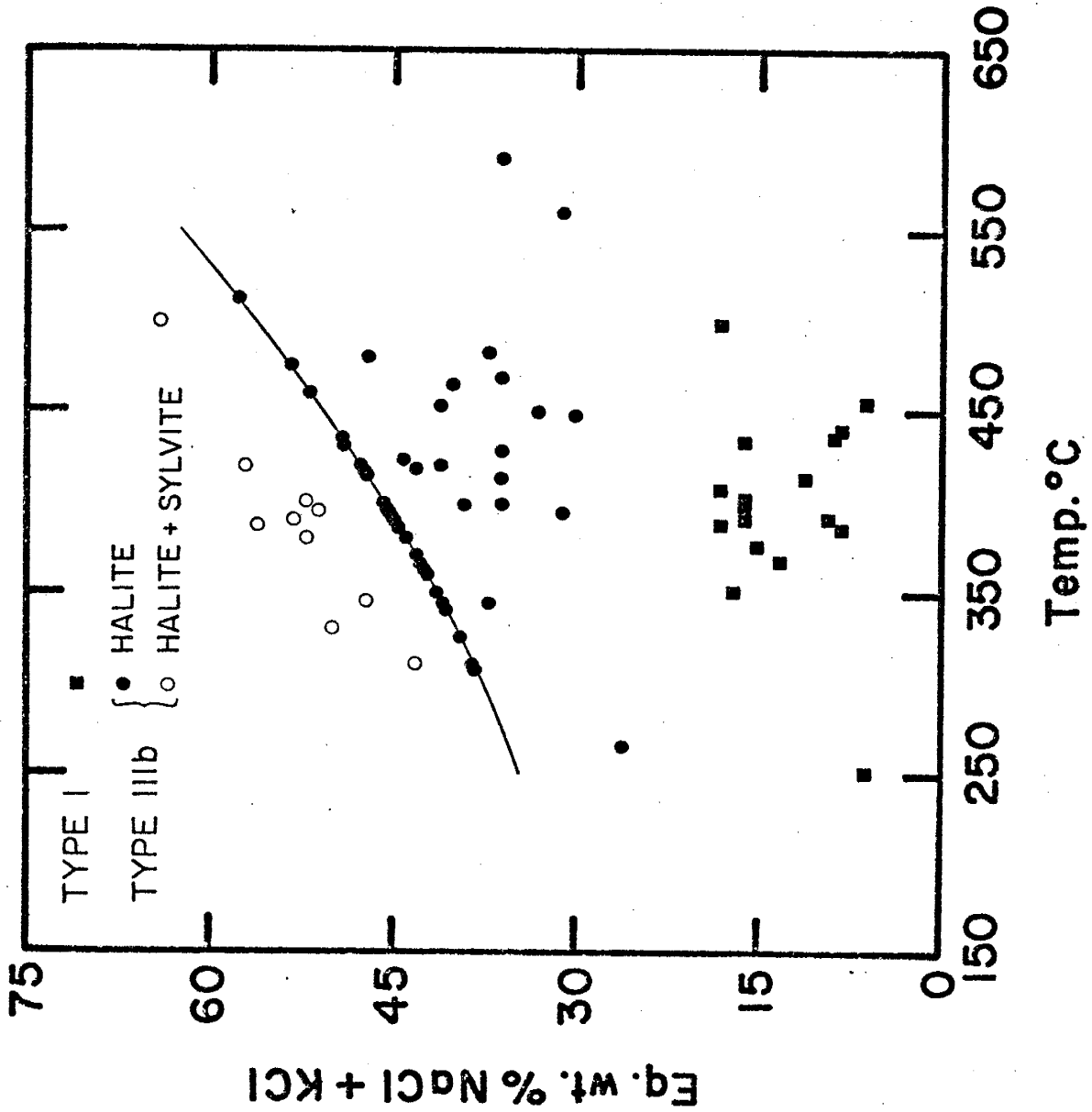
Table 8.3

Oxygen and hydrogen isotope composition of materials from the Southwest Zone ore body at Questa, NM. Values are reported as $\delta^{18}O$ and $\delta D$ in standard per mil notation (see text).

| Sample | Qtz $\delta^{18}O$ | Kspar $\delta^{18}O$ | Biotite $\delta^{18}O$ | $\delta D$ | Whole Rock $\delta^{18}O$ |
|---|---|---|---|---|---|
| Vein Samples Associated with Potassic Alteration | | | | | |
| B593 | 10.3 | 8.5 | 5.4 | -110 | |
| C857 | 6.8 | 2.6 | 2.8 | -112 | |
| C860 | 12.8 | | 1.2 | -111 | |
| E1638 | 7.8 | | 5.3 | -117 | |
| I1533 | 7.5 | 1.8 | 4.6 | -117 | |
| I1626 | 9.1 | | | | |
| Vein Samples Associated with Phyllic Alteration | | | | | |
| B259 | 9.7 | | | | |
| E1188 | 9.3 | | | | |
| Volcanics | | | | | |
| Andesite | | | | | 3.2 |
| Intrusives | | | | | |
| Aplite | | | | | 4.6 |
| Goat Hill Porphyry | | | | | |
| C1000 | 7.0 | 1.9 | | | |
| I1404 | 7.6 | 0.9 | | | |
| K2137 | 7.7 | 0.5 | | | |

Table 8.4

Analyses of fluid inclusion volatiles in vein quartz associated with potassic alteration (K.A) and sericitic alteration (S.A) or quartz phenocrysts from a granite intrusive.  Samples are from Southwest Zone ore body, Questa, NM.

| Sample | He | Mole Fraction ($\times 10^4$) | | | | | | Mole % Water | Amt. in Sample[c] | |
|---|---|---|---|---|---|---|---|---|---|---|
| | | $H_2$ | $CO_2$ | CO | $S_2O$ | $H_2S$ | $N_2$ | | Water mg | size g |
| | | | | | | K.A. | | | | |
| C857 | 0.003 | 3 | 83 | 0.6 | 5.5 | 7.2 | 0.7 | 99.0 | 5.7 | 5.62 |
| C860 | 0.01 | 0.6[a] | 95 | -[a] | 5.0 | 3.0 | -[a] | 99.0 | 4.1 | 4.55 |
| E1638 | nd | 7 | 57 | 2 | 1.6 | 3.2 | 5 | 99.2 | 2.6 | 3.29 |
| I1533[b] | nd | 20 | 220 | 6 | 14 | 21 | 20 | 97.0 | 0.7 | 4.65 |
| I1533[b] | nd | 6 | 59 | 2 | 3.7 | 5.5 | 4 | 99.2 | - | - |
| I1626 | nd | 4 | 28 | 0.2 | 0.6 | 1.4 | 0.9 | 99.6 | 5.9 | 10.13 |
| | | | | | | S.A. | | | | |
| B259 | nd | 4 | 49 | 2 | 30 | 48 | 9 | 98.6 | 1.9 | 6.15 |
| E1188 | nd | 6 | 130 | 10 | 73 | 120 | 9 | 96.5 | 1.4 | 5.11 |
| | | | | | | Intrusive | | | | |
| K2137 | nd | 2a | 57 | -a | 2. | 12 | -a | 99.4 | 3.5 | 4.36 |

[a]Air contamination in noncondensable fraction.  [b]Sample E1188 yielded an unusually low amount of $H_2O$ for K.A. samples.  This may be the result of the loss of water during the experimental procedure.  The second results were calculated assuming the sample was 99.2 % water.  [c]Recovered amount of water and size of sample analysed.

Fig. 8.7

Projection of the fluid inclusion volatile analyses from Questa quartz onto the anhydrous base of the $H_2O-H_2-CO_2-H_2S$ quaternary.

QUESTA, NM GASES

+ Intrusive
▲ Potassic Alt. Zone
○ Phyllic Alt. Zone

CARBON DIOXIDE

HYDROGEN SULFIDE

HYDROGEN
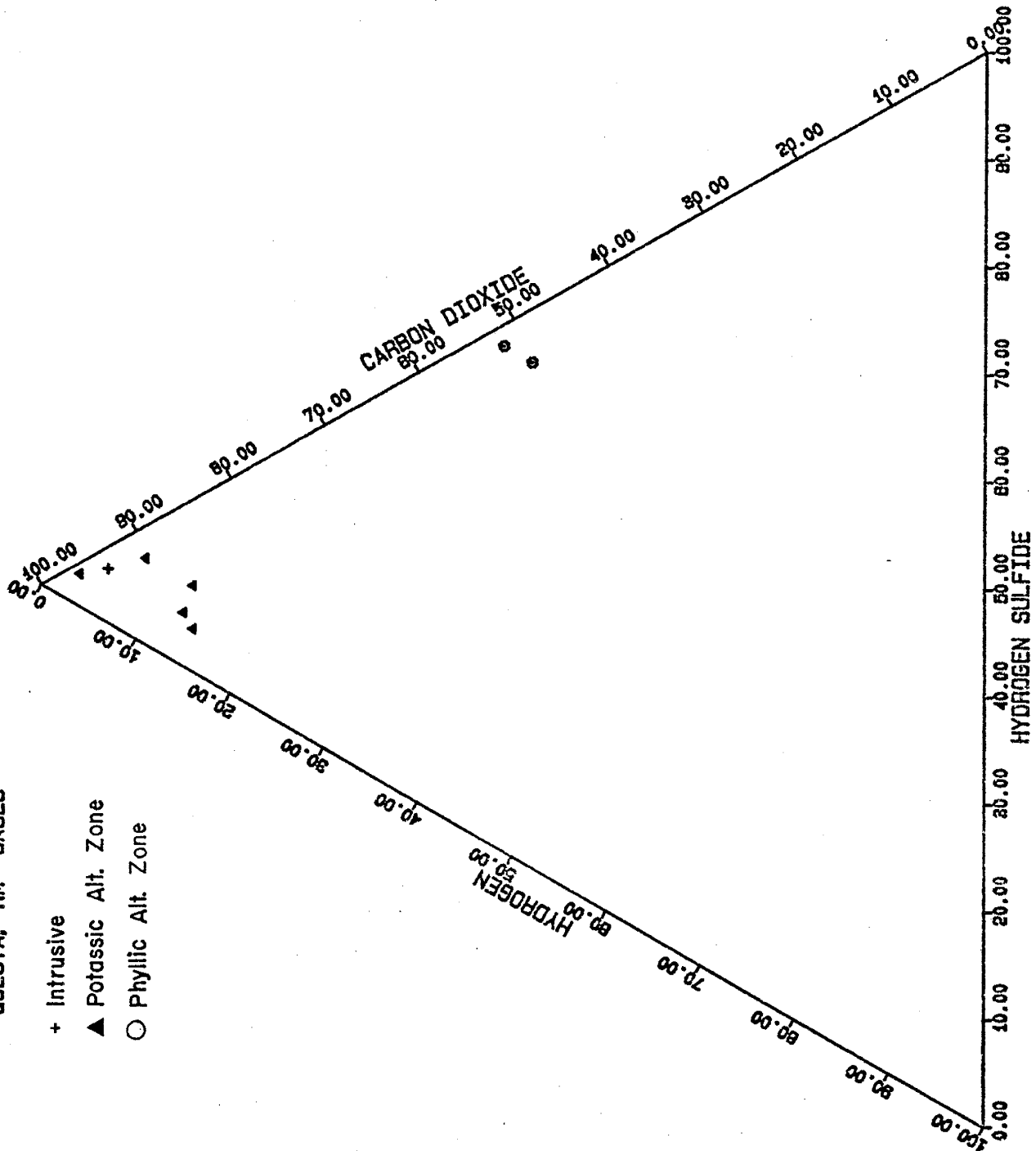
In order for the analyses of gases from fluid inclusions to have any relevance to the formation of an ore deposit, two very important criteria must be established:

1) The inclusions have not leaked since the fluids were trapped.

2) The composition of the volatile phase was not modified during the analytical procedures.

Norman (1977) has established, based on the presence of helium in fluid inclusions, that the first criterion can be satisfied. In this study helium was detected in some, but not all of the samples (Table 8.4). However, the similar concentration of hydrogen in all gas samples suggests the inclusions have remained closed.

It was not possible to remove all grains of sulfide minerals from samples B259 and E1188 because the sulfide minerals were fine grained and intergrown with the quartz. Both of these samples yielded very high amounts of sulfur gases (Table 8.4). In order to determine if sulfur gases could be made from sulfide minerals during the analytical procedures used in this study, a mixture of Georgia kaolinite and molybdenite was analysed. Kaolinite was chosen for two reasons: 1) Kaolinite dehydrates to give off water and carbon dioxide between 550 and 600°C; and 2) The kaolinite was formed under oxidizing ambient conditions and should not contain methane, carbon monoxide or reduced sulfur species.

The results of the kaolinite dehydration experiment are presented below.

<div align="center">

Moles x $10^7$

| $H_2S$ | $SO_2$ | $CO$ | $CO_2$ | $H_2$ | $H_2O$ |
|--------|--------|------|--------|-------|--------|
| 1.2    | 1.5    | 3.6  | 39     | 5.4   | 2600   |

</div>

The molar $H_2S/SO_2$ ratio for the above analysis is 0.8 as compared to greater than 1 for most fluid inclusion samples. In addition, the amount of $H_2S$ produced above ($2.5 \times 10^{-5}$ μmole/mg $H_2O$) is much lower than the amounts measured for samples B259 ($2.7 \times 10^{-4}$ μmole/mg $H_2O$) and E1188 ($6.7 \times 10^{-4}$ μmole/mg $H_2O$). These results are similar to work done by Norman and Palin (1982) in which they found that substantial amounts of sulfur gases (predominately $SO_2$) are not produced from sulfide minerals at temperatures less than 700°C. These results indicate that the $H_2S$ values reported in this study reflect the composition of the fluid inclusions.

Work by Norman (1977) indicates that the presence of sulfate results in unreliable values for $SO_2$. Since the cleaning procedures involve the use of an oxidizing acid, the possibility of creating sulfate minerals from sulfide minerals is real. Consequently, the validity of the $SO_2$ measurements is questionable.

The results of the kaolinite experiment indicate that substantial amounts of CO ($7.7 \times 10^{-5}$ μmole/mg $H_2O$) are produced during the heating processes. These high CO values cast serious doubt on the validity of the CO measurements reported in Table 8.4. As a result, CO was not used in thermodynamic calculations.

Hydrogen can be produced from water at temperatures greater than 500°C (Norman, 1977). However, large amounts of hydrogen are not produced at temperatures less than 600°C. In this study, the fluid inclusions were decrepitated at temperatures of 550 or 600°C. Since, a systematic variation between the amount of hydrogen and temperature was not observed, the amount of hydrogen produced was probably small

compared to the amount present in the inclusions. Nevertheless, the oxygen fugacities calculated from these data should be considered to represent minimum fugacities.

The evaluation of the gas data presented above indicates the values of $H_2$, $H_2S$ and $CO_2$ presented in Table 8.4 can be accepted as reasonable representations of the composition of the fluid inclusions from Questa. The values reported for $SO_2$ and CO are more uncertain.

# DISCUSSION

## FLUID INCLUSIONS

The determination of an unambiguous paragenesis of fluid inclusion types was very difficult because superimposed populations of inclusion types appeared in most plates.  Furthermore, repeated tectonic activity has resulted in most veins being multiply fractured and healed, often making the identification of primary inclusions impossible.  However, in spite of these limitations, some comments may be made on the relationships among fluid inclusion populations.

Hypersaline, type IIIb, fluid inclusions, containing both halite and sylvite daughter minerals, appear to represent the earliest fluids at Questa.  The presence of this inclusion type is limited to quartz-biotite veins which predate molybdenite mineralization or to isolated quartz grains which were protected from fracturing by being enclosed in biotite.

Type IIIb fluid inclusions containing halite daughter minerals are found in quartz veins associated with both potassic and sericitic alteration.  This type of inclusion may represent fluids which were generated from the hypersaline fluids by the exchange of potassium for sodium during potassic alteration.  Both halite bearing type IIIb and liquid rich type I fluid inclusions are associated with molybdenite mineralization.

Placement of vapor-rich inclusions in the paragenesis was not possible, as this inclusion type occurred with all other types and did not appear to predominate in any of the environments observed.

Observation of a limited number of secondary fluid inclusions in quartz phenocrysts from the intrusives showed only liquid-rich inclusions at temperatures of approximately 370 and 200°C. Populations of 200°C secondary inclusions were observed in essentially every plate. The fluid inclusion paragenesis observed in this study is very similar to the paragenesis reported by Bloom (1981) for this deposit.

The presence of fluid inclusions, which are interpreted as having formed from boiling solutions (Roedder, 1979), allows estimates to be made of the pressure of the fluids at the time of trapping. Assuming that the volumetric properties of the fluid inclusions may be represented by sodium chloride solution, the pressure of the boiling fluids was approximately 180 bars (Sourirajan and Kennedy, 1962).

Although evidence of sporadic boiling was observed, most inclusions were not trapped at P-T-V conditions which allowed boiling. However, using inclusion salinities and temperatures measured for Questa material, the minimum vapor pressure at the time of homogenization may be estimated from data reported by Sourirajan and Kennedy (1962). Estimates of minimum vapor pressures range from less than 100 bars for halite-saturated type IIIb inclusions (Fig. 8.6) to pressures of approximately 550 bars for high-temperature type I inclusions.

Many inclusions homogenized by halite dissolution (Fig. 8.6). This has been cited as evidence for high fluid pressure at the time the inclusions formed (Klevtson and Lemmlein, 1959 and Lyakhov, 1973). However, Roedder and Bodnar (1980) indicate that homogenization by halite dissolution does not indicate high pressures and attribute the high pressure estimates to the use of inaccurate density data for

concentrated sodium chloride solutions. Bodnar and Beane (1980, footnote 3) indicate that the isochores for saturated sodium chloride solutions between 300 and 400°C have slopes of about 5 bars °C$^{-1}$. In this study, fluid inclusions which homogenized by halite dissolution did so within 40° of the disappearance of the vapor bubble. This corresponds to pressures of about 330 bars.

Estimated cover at Questa during the time of mineralization was 1000 to 1600 meters (Isahara, 1967) and corresponds to lithostatic pressures of 290 to 460 bars or hydrostatic pressures of 100 to 160 bars. Thus, the pressure at Questa was probably less than 500 bars, although sporadic boiling indicates that the pressure fluctuated. From the data of Urusova (1975), the pressure correction for most inclusions is less than 40°C.


STABLE ISOTOPES

Taylor (1979) has presented convincing arguments that hydrothermal biotites associated with potassic alteration in porphyry copper deposits were derived from magmatic fluids. However, the biotite associated with potassic alteration at Questa has much lighter hydrogen than do the other porphyry biotites (Fig. 8.8). These results are similar to the results reported for Pre-Main-Stage potassic biotites at Butte, MT by Sheppard and Taylor (1974). The results from Butte are interpreted as representing biotites which underwent hydrogen exchange with low $\delta$D water during the Main-Stage alteration event (Sheppard and Taylor, 1974). A similar interpretation is proposed for the Questa biotites. Martineau et al. (1977), based on observations of overlapping and superimposed alteration assemblages, concluded that mineralization of

Fig. 8.8

Comparison of the isotopic composition of hydrothermal biotites from Questa and other porphyry deposits (Taylor, 1979).
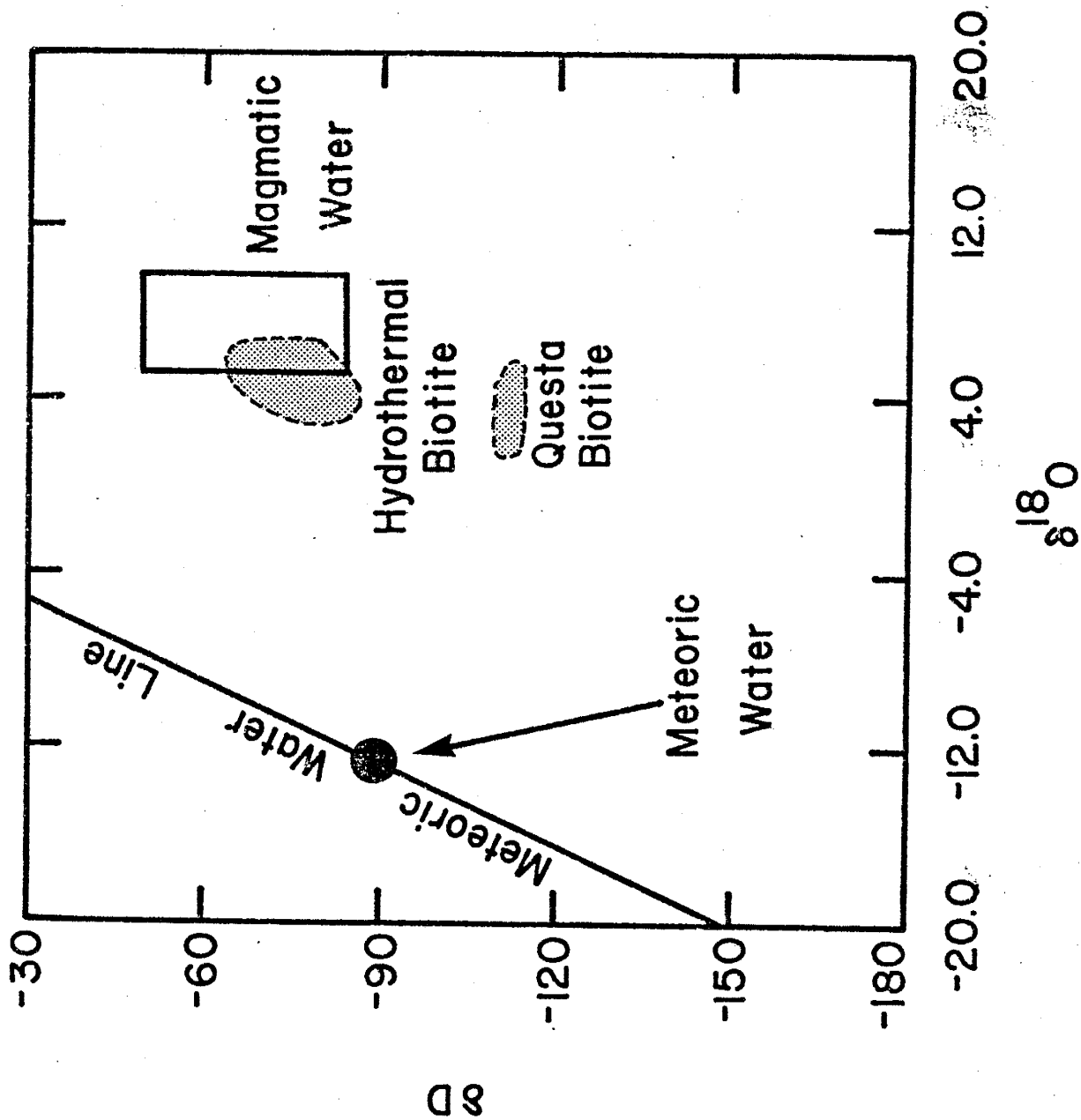
the Southwest Zone was the second of the three recognized mineralization events. The occurrence of later mineralization and alteration could have resulted in the exchange and re-equilibration of the biotite deuterium with surface derived water.

Most of the quartz and coexisting K-feldspar analysed in this study are not in isotopic equilibrium (Fig. 8.9). The isotopic temperatures calculated from quartz-feldspar pairs yield, in most cases, temperatures of less than 200°C. These results are similar to the observations of Hall et al. (1974) for the Climax, CO deposit. They concluded that the quartz was more resistant to isotopic exchange with late, light meteoric water than was feldspar. The same conclusion is drawn in this study for the Questa deposit. The widespread nature of the later, meteoric hydrothermal exchange is evident by the fact that the three samples of intrusive K-feldspar exhibited the same dis-equilibrium as the K-feldspar associated with potassic alteration.

Although most samples yield isotopic temperatures which indicate the mineral pairs are in gross disequilibrium, one sample (B593) yields temperatures of approximately 550°C from bio-qtz, bio-K-spar and K-spar-qtz pairs (Fig. 8.10). The temperature of 550°C is at the upper end of the fluid inclusion homogenization temperatures. Unfortunately, the quartz in this sample was not suitable for fluid inclusion measurements.

The oxygen isotope composition of water in equilibrium with sample B593 was calculated from the isotopic temperature and the temperature dependence of the isotopic fractionation between water and the minerals (Table 8.2). Water in equilibrium with sample B593 had a value for $\delta^{18}O$ of 7.7 per mil. This value is similar to that for magmatic waters (Taylor, 1979) and is interpreted as such.

Fig. 8.9

Diagram relating $\Delta$(qtz-K-feldspar) to $\delta^{18}$O(qtz).  Contours are

isotopic temperatures calculated from the fractionation equations
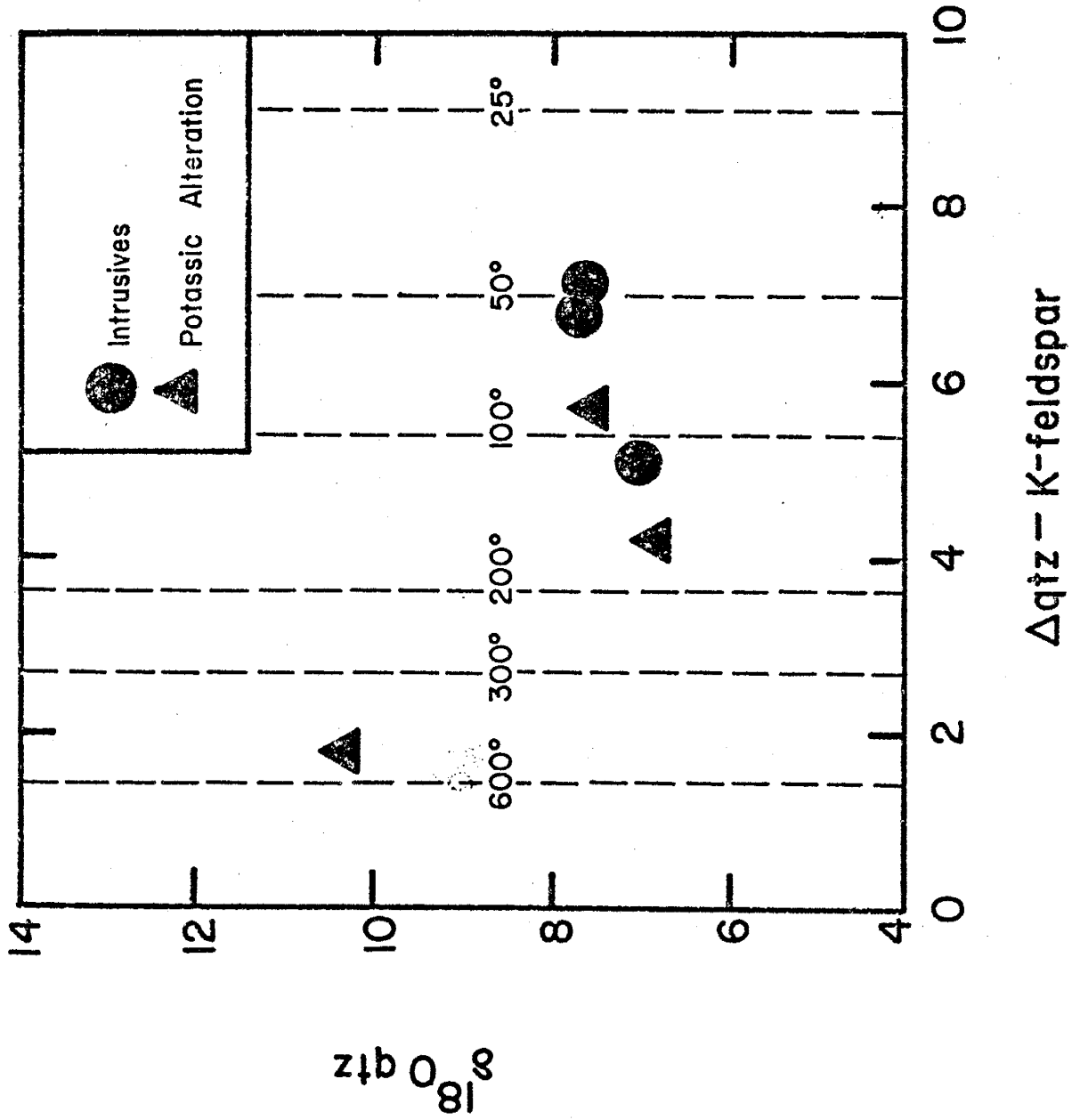
given in Table 8.2.

Fig. 8.10

Oxygen isotope temperatures for sample B593 calculated from the fraction-
ation equations given in Table 8.2.  Error bars corespond to an
uncertainty of 0.2 per mil in the $\Delta(a-b)$ values.

Isotopic Temperatures for Sample B593
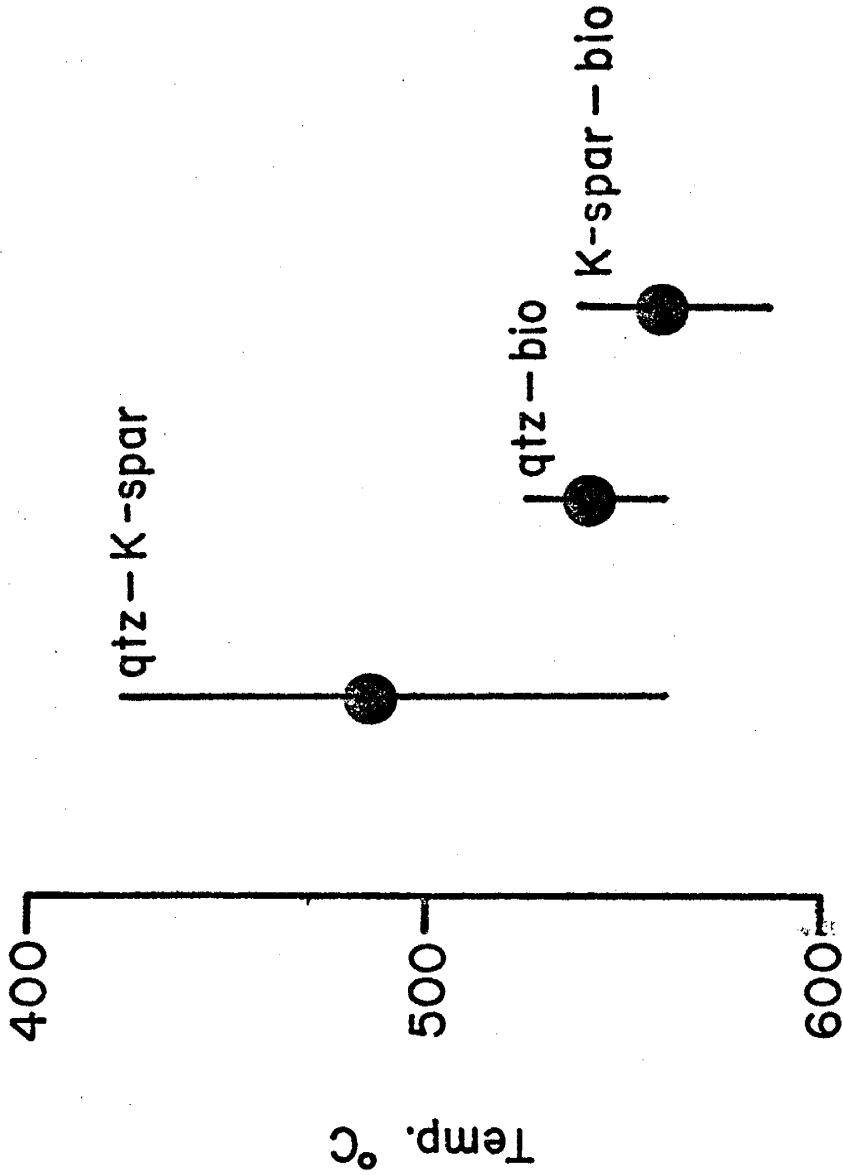
The isotopic composition of present day meteoric water in the Questa area was not determined. However, surface waters (interpreted as of meteoric origin) from the Jemez Mountains in north-central New Mexico had $\delta D$ values of -76 to -93 per mil, with an average of -88 per mil (Frieman et al., 1963). Using the meteoric water line of Craig (1961):

$$D = 8\delta^{18}O + 10 \qquad\qquad 8.4$$

results in a $\delta^{18}O$ range for these meteoric waters of -10.8 to -12.9 per mil with an average of -12.3 per mil. Taylor and Mararita (1978) state that the isotopic composition and distribution of meteoric water for western North America has been grossly similar for the last 100 million years. It has been assumed in this study that the meteoric component of the hydrothermal systems at Questa had values similar to those calculated above.

Values of $\delta^{18}O$ for hydrothermal fluids in equilibrium with vein quartz were calculated from the fluid inclusion temperatures using equation 8.2 and the coefficients in Table 8.2. The results of these calculations are presented in Table 8.5. These values are intermediate between the magmatic values and meteoric values, suggesting a mixing of the two fluids. The relative abundance of magmatic water may be calculated if the compositions of the two end members are known. If one assumes that the surface derived component had the same composition as meteoric water, the "maximum" magmatic contribution may be calculated. This calculation assumes that there was no exchange of oxygen with the volcanic pile before the mixing occurred. Alternately, the assumption that the meteoric water exchanged with the volcanic pile was made. Assuming that the water-rock fractionation for andesite is the same as andesine (Taylor, 1979), the composition of water equilibrated at 300°C

Table 8.5

Calculated values of $\delta^{18}O$ for hydrothermal fluids in
equilibrium with vein quartz from the Southwest Zone ore
body, Questa, NM.  Values are reported in standard per mil
notation.

| Sample | Temperature $^{o}C$ | $\delta^{18}O$ % (SMOW) |
|--------|------------------|------------------------|
| Vein Quartz Associated with Potassic Alteration | | |
| B593 | 550 | 7.8 |
| C857 | 400 | 1.6 |
| C860 | 400 | 7.6 |
| E1638 | 400 | 2.7 |
| I1533 | 400 | 2.4 |
| I1626 | 400 | 4.0 |
| Vein Quartz Associated with Sericitic Alteration | | |
| B259 | 320 | 2.3 |
| E1188 | 320 | 1.9 |

with the andesite in Table 8.3 was calculated. This resulted in a $\delta^{18}O$ value of -1.5 per mil for the exchanged meteoric water. Relative abundances of magmatic water calculated using both assumptions are presented in Table 8.6. The relative abundance of magmatic water was 40% to 70%, depending on the model used. The relative abundance of magmatic water is similar for most samples.

VOLATILE ANALYSES

There is good agreement between oxygen fugacities calculated from the gas data presented in this study and fugacities calculated from potassic mineral assemblages found at Questa (Fig. 8.11). In addition, examination of Fig. 8.11 indicates that the sulfur and carbon should be present as hydrogen sulfide and carbon dioxide, again consistent with the composition of the volatiles analysed in this study. The above observations suggest that the fluid inclusion volatiles analysed in this study are reasonable representations of the hydrothermal fluids which were associated with alteration and mineralization at Questa.

Consideration of the volatile analyses and the stability of iron minerals indicates that the iron minerals associated with potassic alteration should include biotite and magnetite, but not pyrite (Fig. 8.12). In contrast, the gas analyses indicate that pyrite is the stable iron bearing phase associated with sericitic alteration. In addition, these fluids (Fig. 8.12) were only slightly undersaturated with respect to pyrrhotite. Similar calculations for molybdenum minerals indicated that molybdenite is the stable molybdenum mineral in equilibrium with the fluids associated with both potassic and sericitic alteration.

Table 8.6

Calculated fractions of magmatic water in hydrothermal fluids
from the Southwest Zone ore body Questa, NM.  Calculations
are based on a two-component mixture of magmatic water ($\delta^{18}O$
= +7.7) and meteoric water ($\delta^{18}O$ = -12.3); or meteoric water
which exchanged with the andesite volcanics ($\delta^{18}O$ = -1.5).
The composition of the hydrothermal fluids are from Table
8.5.  See text for description of assumptions.

| | Fraction of Magmatic water (%) | |
| | | exchanged |
| Sample | meteoric water | meteoric water |
|---|---|---|
| Vein Quartz Associated with Potassic Alteration | | |
| B593 | 100 | 100 |
| C857 | 70 | 34 |
| C860 | 100 | 99 |
| E1638 | 75 | 46 |
| I1533 | 74 | 42 |
| I1623 | 82 | 60 |
| Vein Quartz Associated with Sericitic Alteration | | |
| B259 | 73 | 41 |
| E1188 | 71 | 37 |

Fig 8.11

Calculated oxygen fugacities for various reactions involving minerals and gases. The shaded region represents oxygen fugacities calculated from the gas analyses in Table 8.4, the equations in Chapter 2, and the equilibrium constants for the reaction:

$$H_2O = H_2 + \tfrac{1}{2}O_2$$
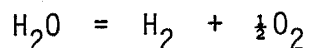
Thermodynamic data are from SUPCRT (Helgeson et al., 1978) and Robie et al. (1978).

ABBREVIATIONS

py - pyrite

po - pyrrhotite

H  - hematite

M  - magnetite

C  - graphite

B  - biotite

K  - K-feldspar
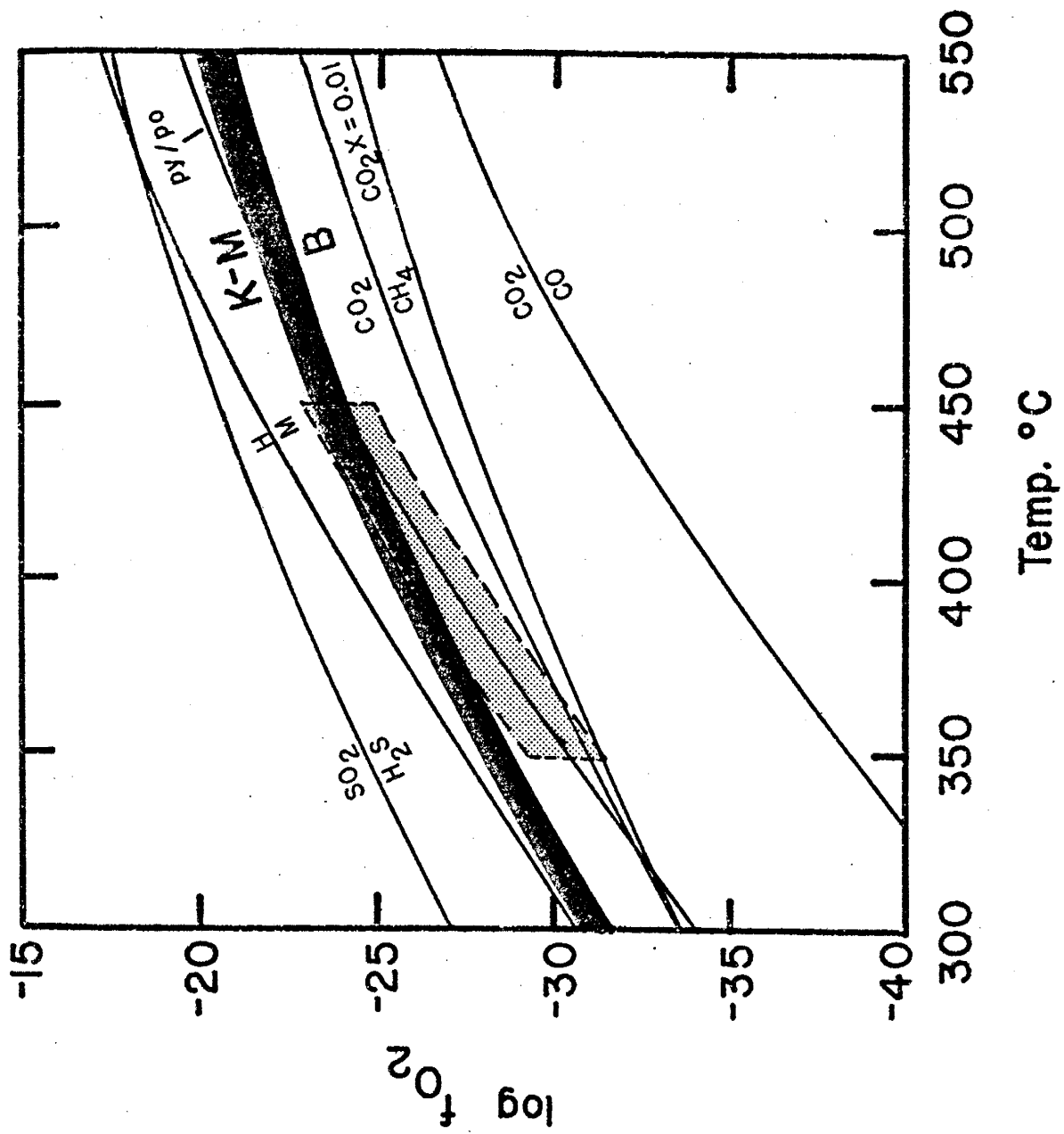
Fig. 8.12

The system $FeO-H_2S-O_2-H_2O$ at 400°C and 500 bars. KAZ and PAZ represent the conditions calculated from the volatile analyses reported in Table 8.4 for potassic and sericitic alteration assemblage respectively. Thermodynamic data are from SUPCRT (Helgeson et al., 1978) and Naumov et al. (1974).

ABBREVIATIONS

Py - pyrite

Po - pyrrhotite

Hem - hematite

Mag - magnetite

Bio - biotite

Micro - K-feldspar

Soln - solution
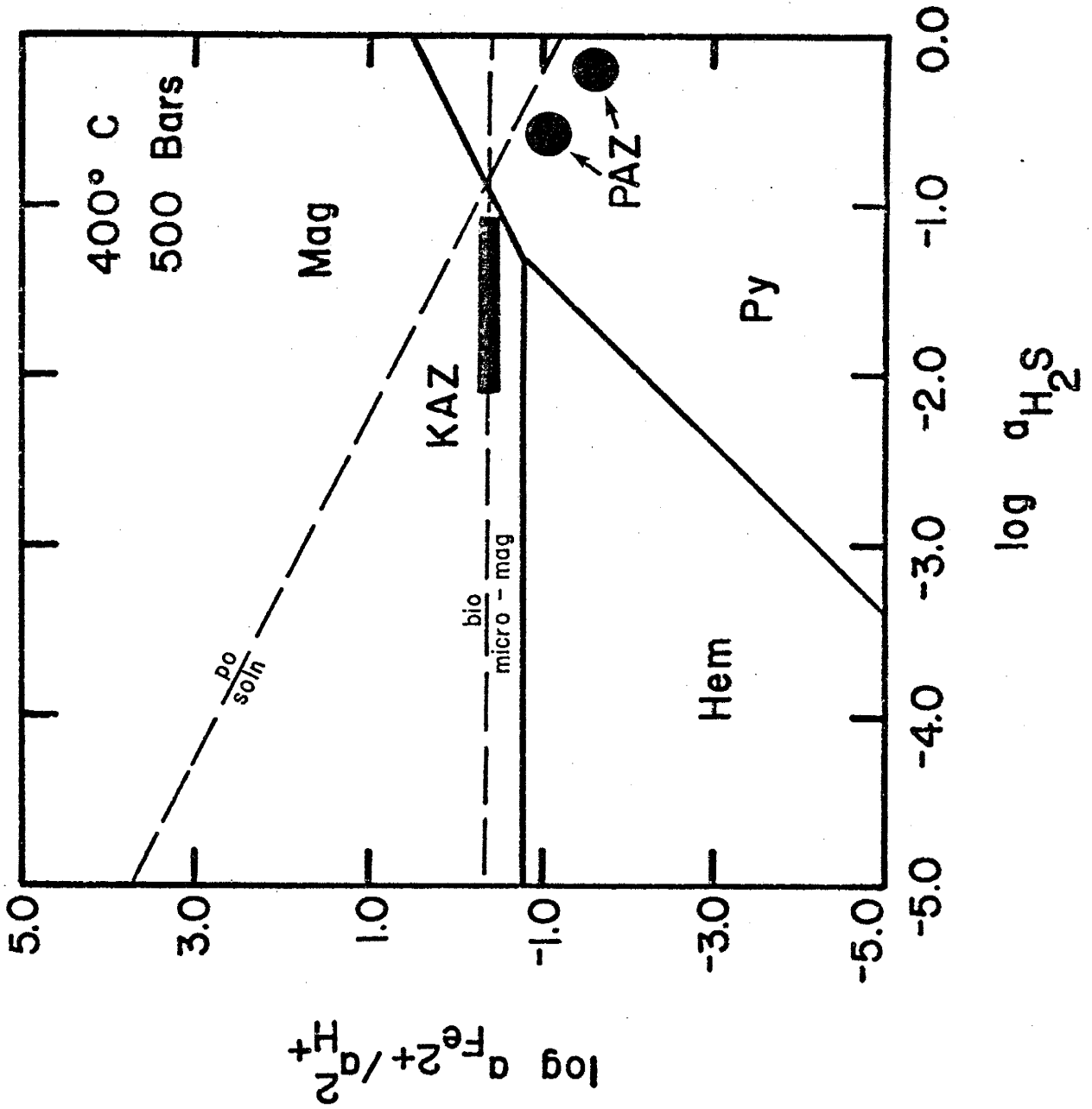
The most notable difference between the gas analyses from samples associated with potassic alteration and those associated with sericitic alteration is the concentration of hydrogen sulfide (Table 8.4 and Fig. 8.7). Fluid inclusion data and field evidence indicates that the mineralization (quartz-pyrite±molybdenite veins) associated with the sericitic alteration postdates the mineralization associated with potassic alteration. In addition, the oxygen isotope data indicate that the fluids responsible for both the potassic and sericitic alteration have the same oxygen isotopic composition, suggesting a similar source for both fluids. These data require that the hydrogen sulfide rich fluids associated with sericitic alteration were derived from the fluids associated with potassic alteration, or that both fluids were derived from the same source.

A simple single step model which would allow a hydrogen sulfide rich fluid to be produced from the earlier fluids would be boiling. Boiling would create a low density fluid rich in volatiles such as hydrogen sulfide and carbon dioxide. Since carbon dioxide is less soluble in water than hydrogen sulfide (Naumov et al., 1974), the steam phase would have a higher $CO_2/H_2S$ ratio than the early fluids. Conversely, the $CO_2/H_2S$ ratio in the remaining fluid would be decreased. Since the $CO_2/H_2S$ ratio for the early fluids (18, Table 8.4) is higher than the ratio for the fluids associated with sericitic alteration (1, Table 8.4), the later fluids may have been enriched in hydrogen sulfide and depleted in carbon dioxide by boiling.

Alternately, the two fluids could have been derived from a similar source (the stock) and subsequently underwent different chemical evolutions. For example, the composition of the fluids associated with

potassic alteration would have been modified by the precipitation of molybdenite. Therefore, the hydrogen sulfide concentration associated with these fluids does not reflect the concentration of original magmatic fluids, but rather magmatic fluids equilibrated with molybdenite. The hydrogen sulfide rich solutions may more realistically reflect the composition of the original magmatic fluids. For example, these fluids may have been explosively released and were not modified by earlier mineralization. The $H_2S/CO_2$ ratio (about 1) for these fluids compares favorably to the ratio of sulfur gases to carbon dioxide observed in some volcanic gases (MacDonald, 1972) and supports the hypothesis that the sulfur rich fluids reflect the gas composition of magmatic water.

More complicated, multistage models for the a low- and a high-$H_2S$ fluid are possible. For example, in a high temperature (greater than 550° C), magmatic fluid a significant portion of the total sulfur would be present as $SO_2$ (Ohmoto, 1979). If this fluid is boiled, two phases would form. Because $SO_2$ is much more soluble than $H_2S$ (Ohmoto, 1979), the steam phase would be enriched in $H_2S$ and depleted in $SO_2$ relative to the original fluid. Conversely the liquid phase would be depleted in $H_2S$ and enriched in $SO_2$. Cooling of the liquid would result in the loss of $SO_2$ by the reaction (Ohmoto, 1979):

$$4SO_2 + 4H_2O = 3HSO_4^- + 3H^+ + H_2S \qquad\qquad 8.5$$
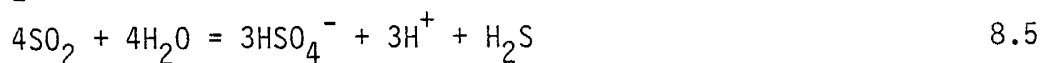
As a consequence, a hypersaline fluid depleted in $H_2S$ (represented by sylvite-saturated type 111b inclusions) and a low salinity, $H_2S$-rich (Type I) fluid would be produced from a common magmatic source.

Although it has not been possible in this study to conclusively determine how the hydrogen sulfide rich fluids were formed, the second model proposed above is favored. Further work on the composition of volatiles at Questa, with the goal of defining the gas composition of magmatic water is warranted. In addition, analyses of similar alteration at other porphyry deposits are recommended.

# MINERALIZATION

The fluid inclusion and isotopic data indicate that the earliest fluids at Questa were high temperature, (greater than 550°C) hypersaline, magmatic fluids with high concentrations of sodium and potassium chloride. Salinity measurements indicate that these fluids had molal KCl/NaCl ratios of 0.23 to 0.29 (Bloom, 1981 and Fig. 8.6). Work by Lagache and Weisbrod (1977) indicates that the molal KCl/NaCl ratio will exceed 0.20 only at temperatures in excess of 500°C for fluids equilibrated with two alkali feldspars. Assuming the KCl/NaCl ratio reflects a magmatic fluid equilibrated with granite, these fluids had equilibrium temperatures of 550 to 640°C (Lagache and Weisbrod, 1977). The upper end of the temperature range is near the temperature minimum in the granite ternary, while the lower end of the range corresponds to the oxygen isotope temperatures determined for potassic alteration. These results are consistent with an interpretation in which isotopically heavy fluids ($\delta^{18}O$ = +7.7 mil) were derived from a crystallizing granite at magmatic to sub-magmatic temperatures.

The early high temperature fluids also had high fluoride concentrations as evidenced by the high fluorine contents of the early hydrothermal biotites (up to 7 wt. %, Bloom, persn. comm., 1982). Potassic alteration of the volcanic rocks would result in the loss of fluoride from the fluids by the formation of fluorine-rich biotite (see, reaction 7.3). A consequence of the alteration would be to lower the KCl/NaCl ratio of the fluids, resulting in fluids similar to the halite saturated type IIIb fluids observed in this study. In addition, the loss of fluoride would destabilize molybdenum fluoride complexes and

result in the precipitation of molybdenite (AB, Fig. 8.13). Although the bulk of molybdenum mineralization occurs in quartz veins which are associated with lower temperature and salinity fluids, mineralization in the form of "clotty-moly" does occur as intergrowths of molybdenite and biotite.

Fluorine enhances the transport of molybdenum in hydrothermal fluids, but is not essential to molybdenum transport (see Chapter 7). As a consequence, fluids which have interacted with the volcanic rocks would have lesser amounts of fluoride and potassium, but would still contain substantial amounts of molybdenum in the form of bimolybdate. Preliminary calculations (Fig. 8.13) indicate that molybdenite solubility is retrograde at high temperatures. This behavior is similar to quartz solubility (Walthers and Helgeson, 1977). Retrograde solubility would mean that decreasing temperature, either as a result of conductive heat loss or adiabatic decompression (Bloom, 1981), would not result in deposition of molybdenite (BC, Fig. 8.13) until the solubility curve was again intersected (point C, Fig. 8.13). The strong prograde solubility of molybdenite at temperatures less than about 450°C would result in the deposition of molybdenite in a confined zone in response to a temperature decrease.

The quartz-molybdenite mineralization occurred from fluids represented by the halite saturated type IIIb fluid inclusions. The fluids were mixtures of magmatic and meteoric waters and had hydrogen sulfide concentrations of 0.03 molal. This mineralization is younger than the mineralization associated with biotite. The occurrence of this type of mineralization in fractures and as open space fillings indicates that mineralization resulted from temperature and pressure decreases (point C, Fig. 8.13) rather than resulting from wall rock reactions.

Fig. 8.13

A generalized representation of the effects of temperature and fluoride
on molybdenum transport and molybdenite mineralization at the Questa
molybdenite deposit.

Solubility in HF rich fluid

Solubility in HF poor fluid

AB   MoS$_2$ mineralization due
     to loss of HF during
     Potassic alteration

BC   Adiabatic decompression
     or conductive cooling, no
     mineralization

C    MoS$_2$ mineralization in
     response to a temperature
     decrease

A

B

C

Temp →

← MoS$_2$ Solubility
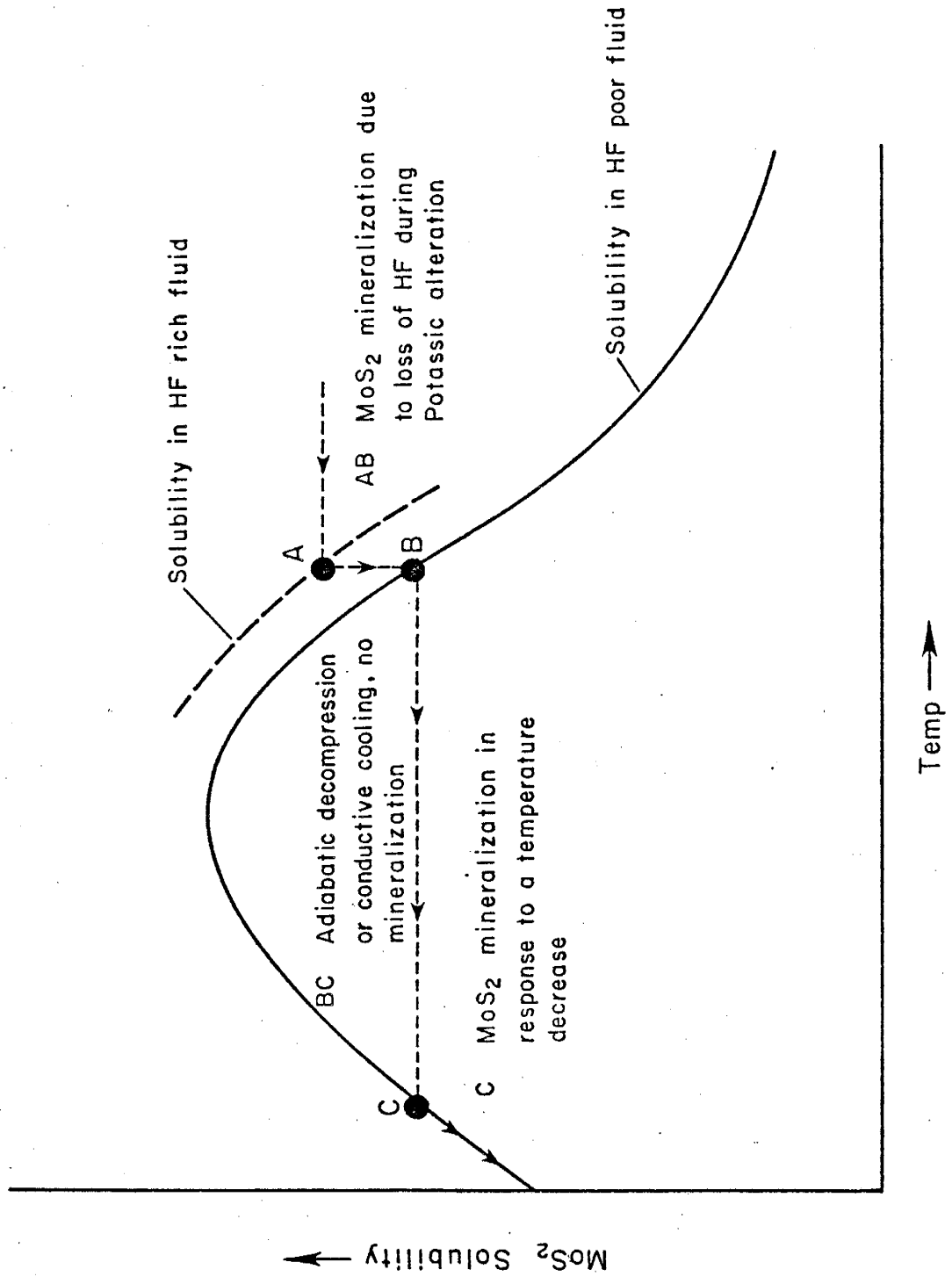
The fluid inclusion evidence indicates that pressure fluctuated from lithostatic to hydrostatic load conditions. These observations suggest that the system was closed to the surface and an accumulation of hydrothermal fluids occurred. As the fluids accumulated, the pressure increased until it exceeded the lithostatic load and resulted in the fracturing of the overlying volcanic rocks. The sudden release of pressure would result in an adiabatic decompression of the fluids. Mineralization in the form of quartz-molybdenite veins would occur in the newly opened fractures in response to the temperature decrease accompanying the decompression. Continued mineralization would choke-off the fractures and the system would again become closed to the surface. Multiple mineralization events at Questa may reflect a repeated cycle of fluid accumulation and fracturing.

Evidence for the accumulation of hydrothermal fluids at Questa has also been reported by Bloom (1981). In addition, Ganster (1976) reached similar conclusion regarding the accumulation of hydrothermal fluids at the Henderson, CO molybdenum deposit.

Later sulfide mineralization in the form of quartz-pyrite veins with minor molybdenum occurred in association with sericitic alteration. Although the fluids responsible for this mineralization had $\delta^{18}O$ values similar to the fluids associated with the quartz-molybdenite mineralization, the hydrogen sulfide concentration was much higher (0.4 molal). The quartz-pyrite mineralization occurred toward the outside of the deposit and at lower temperatures (less than 350°C). The association of this type of mineralization with sericitic alteration indicates that the solution chemistry was different (probably more acid,

Beane, 1982) than the fluids associated with earlier mineralization. In addition, the minor occurrence of molybdenite mineralization associated with sericitic alteration indicates that molybdenite solubility in these fluids was low.

The isotopic dis-equilibrium between quartz and coexisting K-feldspars, as well as the low $\delta D$ values measured in the biotites indicates that an influx of meteoric water into the hydrothermal system occurred after mineralization. This influx may have been the result of fracturing of the volcanic rocks and a collapse of the hydrothermal system. However, the unusually low $\delta D$ values of biotites (approximately -115 per mil) argues for a later meteoric hydrothermal event associated with the Deep Granite mineralization system.

## MOLYBDENUM TRANSPORT

The techniques used to calculate the solubility of molybdenum in hydrothermal solution are described in Chapter 7 and Appendix E.

### HYDROGEN FLUORIDE FAUACITY

In order to calculate the solubility of molybdenite it is necessary to know the hydrogen fluoride fugacity for the fluids. Gunow et al. (1980) have determined the value of $f_{H_2O}/f_{HF}$ for fluids which were associated with mineralization at Henderson, CO from mica analyses. Although similar data for Questa micas are not published, microprobe analyses indicate that some biotites at Questa have compositions approaching stoichiometric fluoro-phlogopite (Bloom, persn. comm., 1982). As a consequence, the HF fugacities calculated from micas at Henderson (Table 8.7) are reasonable first approximations for Questa fluids.

### pH

Based on mass transfer calculations, fluids associated with potassic alteration have pH's which are near neutral or slightly acidic (Helgeson et al., 1970, Helgeson, 1970 and Beane 1972). At 400°C and 500 bars pressure, neutral pH is 6.0. As a consequence, the pH of fluids associated with potassic alteration at Questa was probably between 5 and 6.

Similar calculations for phyllic alteration (sericite-quartz-pyrite) suggests that fluid pH's were less than 4. However, Beane (1982) indicates that the pH could not be less than about 3. Therefore, the probable pH of fluids associated with the sericitic alteration and the quartz-pyrite-molybdenite veins at Questa was between 3 and 4.

## ACTIVITY COEFFICIENTS

The stoichiometric activity coefficients, $\dot{\gamma}_j$, reported in Chapter 6, are not adequate to account for activity relationships in halite saturated solutions at elevated temperatures. As a result, new values of $b_{\gamma,j}$ (Table 6.8) which are consistent with estimated values of the dielectric constant at 400°C, 500 bars and halite saturation were estimated. The dielectric constant was estimated using halite solubility data (Sourirajan and Kennedy, 1962), the ion activity product for halite (SUPCRT), equation 6.10 and the theoretical considerations relating $b_{\gamma,j}$ to the dielectric constant (Helgeson et al., 1981). Using the new values of $b_{\gamma,j}$, stoichiometric individual ion activities were calculated for the fluids summarized in Table 8.7 and are given in the table.

## MOLYBDENUM

The calculated molybdenum concentrations for fluids in equilibrium with molybdenite associated with both potassic and sericitic alteration are presented in Table 8.7. The fugacities of oxygen and hydrogen fluoride as well as the activity coefficients, pH's and hydrogen sulfide concentration presented in Table 8.7 were employed in these calculations. The results of these calculations indicate that only low concentrations of molybdenum would occur in the hydrogen sulfide rich fluids associated with sericitic alteration. The fluids associated with potassic alteration would transport substantially more molybdenum. These results are consistent with the association of molybdenum mineralization at Questa with potassic minerals.

Table 8.7

Composition of fluids associated with alteration at Questa.

| Species | Sericitic Alteration | Potassic Alteration |
|---|---|---|
| NaCl | 14 m | 14 m |
| $\log f_{O_2}$ | -26.9 | $-26.9 \pm 0.9$ |
| $\log f_{CO_2}$ | 1.3 | $1.3 \pm 0.1$ |
| $\log m_{H_2S}$ | -0.4 | $-1.6 \pm 0.5$ |
| $\log f_{HF}$ | $-1.4 \pm 0.1$ | $-1.2 \pm 0.1$ |
| pH | 3 - 4 | 5 - 6 |
| $\log \dot{\gamma}(MoO_4^{2-})$ | -13.4 - -10.8 | -9.47 |
| $\log m_{Mo}$ | -6.2 - -6.8 | -4.1 - -2.1 |
| total Mo | 0.06 - 0.02 ppm | 8 - 800 ppm |

Sources of Data

NaCl:  fluid inclusion measurements (this study).

$\log f_{O_2}$:  fluid inclusion volatile analyses (this study).

$\log f_{CO_2}$:  fluid inclusion volatile analyses (this study).

$\log m_{H_2S}$:  fluid inclusion volatile analyses (this study).

$\log f_{HF}$:  Gunow et al. (1980) (see text).

pH:  estimated (see text).

$\log (MoO_4^{2-})$:  calculated as described in text.

$\log m_{Mo}$:  calculated as described in Chapter 7.

There is a high degree of uncertainty associated with the calculated activity coefficients used above. Hence the concentrations of molybdenum presented in Table 8.7 represent only first approximations. Nevertheless, the reasonable agreement between the theoretical models and calculation presents in this study, and the observed mineral associations at Questa and fluid inclusions data, indicates that in spite of the numerous assumptions made, the approaches used in this study represent a rapid and accurate technique to evaluate the role of complexing in hydrothermal mineralizaing systems.

## GENESIS OF THE QUESTA MOLYBDENITE DEPOSIT

The Questa molybdenite deposit is a rift related deposit, as are all Climax-type porphyry molybdenum deposits (Sillitoe, 1980). The formation of Climax-type deposits may have reflected the steepening of the subducting Farallon Plate (Cooney and Reynolds, 1977) as a consequence of the annihilation of portions of the East Pacific Rise 15 to 30 million years ago as the North American plate overrode the rise and the plate margin changed from a subduction zone to a transform fault zone (Atwater, 1970). This change was reflected in the southwestern United States by a change from compression-related calc-alkaline volcanic activity to bimodal volcanic activity related to rifting (Christiansen and Lipman, 1972). Christiansen and Lipman (1972) have suggested that the silicic volcanics at Questa were the consequence of bimodal volcanic activity.

About 23 million years ago, silicic magmatism gave rise to both rhyolitic tuffs and shallow (approximately 1600 meters) intrusives. The initial $^{87}Sr/^{86}Sr$ ratio for the mineralizing intrusive was 0.707 (Laughlin et al., 1969). This initial ratio precludes large-scale assimilation of materials from the surrounding Precambrian rocks, which have $^{87}Sr/^{86}Sr$ ratios of greater than about 0.74 (Condie, 1982, persn. comm.) and argue for a lower-crustal or upper-mantle source for the intrusives. The very low molybdenum content of island-arc porphyry copper systems argues against the source of molybdenum being the upper mantle, and indicates that some thickness of sialic crust is necessary to produce a molybdenite deposit (Westra and Keith, 1981). However, Westra and Keith (1981) point out that the high molybdenum contents of some carbonatites indicate that the mantle may be locally enriched in

molybdenum. They further suggest that the fluorine associated with Climax-type molybdenum deposits is derived from a mantle source. Sulfur isotope data (Laughlin et al., 1969 and Field, 1966) indicate a homogeneous igneous source similar to that of copper porphyry deposits. This source may be interpreted as upper-mantle, 0 per mil sulfur.

The rocks responsible for mineralization had compositions very near the granite system minimum. A hypersaline fluid with high concentrations of potassium, sodium and fluorine and a $\delta^{18}O$ of greater than 7 per mil exsolved from a rapidly crystallizing, shallow intrusive. This fluid, at temperatures of greater than 550°C, reacted irreversibly with the intermediate volcanic pile to produce early quartz and magnesium- and fluorine-rich biotite. As a result of this interaction, the KCl/NaCl ratio of the fluid decreased and gave rise to halite saturated type IIIb fluids. In addition, the loss of fluorine resulted in the precipitation of molybdenite because of decreased fluoride complexing of molybdenum.

Mineralization, in the form of quartz-molybdenite veins, occurred over the temperature range of 450 to 350°C from these saline fluids in response to a decrease in temperature. Oxygen isotope data indicate that this mineralization occurred from fluids which were a mixture of magmatic (40-70%) water and exchanged meteoric (60-30%) water. The mineralization was associated with potassic alteration and occurred from near neutral fluids with log $f_{O_2}$ between -28 and -24. The reduced-sulfur concentration of these fluids was approximately 0.03 molal. Theoretical calculations have shown that approximately 800 ppm molybdenum may have been transported by these fluids, predominately as

bimolybdate and fluoro-molybdate complexes. The low pH and high reduced sulfur content (0.4 m) of the phyllic alteration zone were not favorable for molybdenum transport, except perhaps as sulfide complexes or molybdenum (VI) species.

Subsequent intrusion and alteration associated with the Deep Granite system reinitiated hydrothermal flow of light, meteoric water through the potassic zone, which resulted in the re-equilibration of the deuterium in the hydrothermal biotites and oxygen-18 in the potassium feldspars.

# CONCLUDING STATEMENT

The use of theoretical calculations coupled with field and laboratory observations of the Questa, NM, molybdenite mine has allowed several conclusions to be reached regarding the genesis of the Questa deposit and the transport of molybdenum in high temperature ore forming fluids.

The molybdenite mineralization occurs in two stages: an early high-temperature (+550°C) stage characterized by the biotite-molybdenite assemblage and a later, lower-temperature (350 to 450°C) quartz-molybdenite vein stage.

The early stage mineralization is associated with high-fluorine biotites; these biotites are essentially fluoro-phlogopite and indicate a high fluoride concentration in the fluids that formed them.

The results of theoretical calculations indicate that molybdenum is transported in hypersaline, hydrothermal fluids as both a fluoride complex and the bimolybdate ion. The interaction of these fluids with the andesite volcanic rocks at Questa resulted in the formation of fluorine-rich biotites. Solubility calculations indicate that molybdenite mineralization should occur in response to this alteration because fluoride complexes will be destabilized by the loss of fluoride from the solution into the biotites. Futhermore, the retrograde solubility of molybdenite at temperatures of greater than approximately 450°C indicates that mineralization at these high temperature will not occur in response to a temperature decrease. These calculated results are consistent with the observed occurrence of early, high-temperature, molybdenite mineralization associated with high-fluorine biotites at Questa.

The quartz-molybdenum vein mineralization at Questa reflects the consequences of adiabatic decompression of hydrothermal fluids. Theoretical calculations have shown that substantial amounts of molybdenum may be transported in fluids with low fluoride concentrations at temperatures of 350 to 450°C. In addition, the calculations indicate that mineralization will occur over the temperature range observed in fluid inclusions (350 to 450°C) as a result of both decreases in temperature and pressure.

The calculations conducted in this study indicate that hydrothermal solutions associated with quartz-pyrite mineralization will transport only small amounts of molybdenum, chiefly as sulfide or chloride complexes. At Questa only minor amounts of molybdenite are found in veins associated with pyrite.

The results of this study demonstrate that theoretical calculations can be used with confidence in the evaluation of ore-forming processes associated with molybdenum mineralization. Although the calculated results will require modification as experimental results become available, the overall consistency between theoretical calculations and field and laboratory studies of the Questa molybdenite deposit demonstrates the validity of the approaches used in this study.

# APPENDIX A

## THERMODYNAMIC RELATIONSHIPS FROM DISCRETE ENTROPY DATA

Given the entropy of an ion, gas, mineral or reaction at two temperatures, the average heat capacity between those two temperatures may be calculated from:

$$C^o_p \Big|^T_{T_r} = (S^o(T) - S^o(T_r))/(\ln T/T_r) \qquad\qquad A.1$$

Evaluation of equations 2.3-2.5 yields:

$$G^o(T) - G^o(T_r) = -S^o(T_r)(T-T_r) +$$

$$C^o_p \Big|^T_{T_r} \cdot (T-T_r-T \ln T/T_r) \qquad\qquad A.2$$

$$H^o(T) - H^o(T_r) = C^o_p \Big|^T_{T_r} \cdot (T-T_r) \qquad\qquad A.3$$

$$S^o(T) - S^o(T_r) = C^o_p \Big|^T_{T_r} \cdot \ln T/T_r \qquad\qquad A.4$$

Although the effects of pressure are ignored in equations A.2-A.3, Helgeson (1969) suggests these effects are small in steam saturated water at temperatures of less than $300^o$C.

APPENDIX B

Thermodynamic properties of dissociation for fluoride complexes at elevated temperatures in steam saturated water. All units are consistent with cal mole$^{-1}$ or cal mole$^{-1}$ K$^{-1}$.

THERMODYNAMIC PROPERTIES FOR THE REATION:

HF (aq)  =  $H^+$  +  $F^-$
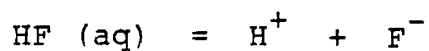
IN STEAM SATURATED WATER.

| TEMP | LOG K(T) | FREE ENERGY | ENTROPY | HEAT CAPACITY |
|------|----------|-------------|---------|---------------|
| 0    | -3.00    | 3748        | -21.67  | -44.36        |
| 25   | -3.18    | 4339        | -25.50  | -43.12        |
| 50   | -3.40    | 5020        | -28.92  | -41.79        |
| 75   | -3.63    | 5782        | -31.98  | -40.37        |
| 100  | -3.88    | 6616        | -34.73  | -38.79        |
| 125  | -4.13    | 7516        | -37.19  | -36.99        |
| 150  | -4.38    | 8474        | -39.38  | -34.84        |
| 175  | -4.62    | 9483        | -41.30  | -32.11        |
| 200  | -4.87    | 10536       | -42.95  | -28.35        |
| 225  | -5.10    | 11628       | -44.28  | -22.71        |
| 250  | -5.33    | 12747       | -45.19  | -13.47        |
| 275  | -5.54    | 13882       | -45.47  | 3.03          |
| 300  | -5.72    | 15012       | -44.71  | 34.98         |
| 325  | -5.88    | 16101       | -41.98  | 102.63        |
| 350  | -5.99    | 17077       | -35.02  | 262.11        |

THERMODYNAMIC PROPERTIES FOR THE REATION:

$NaF \ (aq) \ = \ Na^+ \ + \ F^-$
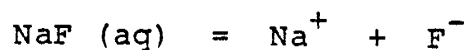
IN STEAM SATURATED WATER.

| TEMP | LOG K(T) | FREE ENERGY | ENTROPY | HEAT CAPACITY |
|------|----------|-------------|---------|---------------|
| 0 | 0.81 | −1015 | 11.18 | −74.84 |
| 25 | 0.89 | −1215 | 5.00 | −66.13 |
| 50 | 0.86 | −1275 | 0.01 | −57.87 |
| 75 | 0.77 | −1223 | −4.02 | −50.18 |
| 100 | 0.63 | −1081 | −7.26 | −43.30 |
| 125 | 0.48 | −865 | −9.88 | −37.63 |
| 150 | 0.31 | −591 | −12.04 | −33.85 |
| 175 | 0.13 | −266 | −13.95 | −33.26 |
| 200 | −0.05 | 107 | −15.85 | −38.24 |
| 225 | −0.23 | 530 | −18.15 | −53.45 |
| 250 | −0.43 | 1023 | −21.51 | −88.29 |
| 275 | −0.65 | 1624 | −27.13 | −162.53 |
| 300 | −0.92 | 2418 | −37.44 | −320.86 |
| 325 | −1.31 | 3576 | −57.58 | −673.36 |
| 350 | −1.92 | 5476 | −99.81 | −1525.27 |

THERMODYNAMIC PROPERTIES FOR THE REATION:

$$MgF^+ = Mg^{2+} + F^-$$
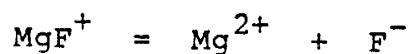
IN STEAM SATURATED WATER.

| TEMP | LOG K(T) | FREE ENERGY | ENTROPY | HEAT CAPACITY |
|------|----------|-------------|---------|---------------|
| 0    | -1.76    | 2203        | -13.88  | -29.78        |
| 25   | -1.89    | 2583        | -16.50  | -30.18        |
| 50   | -2.05    | 3027        | -18.95  | -30.65        |
| 75   | -2.22    | 3530        | -21.25  | -31.24        |
| 100  | -2.39    | 4089        | -23.44  | -31.99        |
| 125  | -2.58    | 4701        | -25.55  | -32.96        |
| 150  | -2.77    | 5366        | -27.59  | -34.31        |
| 175  | -2.97    | 6081        | -29.62  | -36.27        |
| 200  | -3.16    | 6846        | -31.66  | -39.32        |
| 225  | -3.36    | 7664        | -33.80  | -44.34        |
| 250  | -3.57    | 8538        | -36.17  | -53.17        |
| 275  | -3.78    | 9476        | -38.99  | -69.64        |
| 300  | -4.00    | 10495       | -42.73  | -102.40       |
| 325  | -4.25    | 11629       | -48.40  | -172.79       |
| 350  | -4.54    | 12950       | -58.35  | -339.96       |

THERMODYNAMIC PROPERTIES FOR THE REATION:

$CaF^+ = Ca^{2+} + F^-$
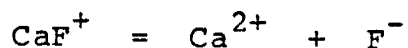
IN STEAM SATURATED WATER.

| TEMP | LOG K(T) | FREE ENERGY | ENTROPY | HEAT CAPACITY |
|------|----------|-------------|---------|---------------|
| 0 | -1.03 | 1286 | -11.35 | -27.78 |
| 25 | -1.17 | 1600 | -13.80 | -28.18 |
| 50 | -1.34 | 1974 | -16.09 | -28.65 |
| 75 | -1.51 | 2404 | -18.24 | -29.24 |
| 100 | -1.69 | 2886 | -20.30 | -29.99 |
| 125 | -1.88 | 3418 | -22.27 | -30.96 |
| 150 | -2.07 | 3999 | -24.19 | -32.31 |
| 175 | -2.26 | 4627 | -26.10 | -34.27 |
| 200 | -2.45 | 5304 | -28.04 | -37.32 |
| 225 | -2.65 | 6030 | -30.07 | -42.34 |
| 250 | -2.84 | 6810 | -32.34 | -51.17 |
| 275 | -3.05 | 7651 | -35.07 | -67.64 |
| 300 | -3.27 | 8571 | -38.72 | -100.40 |
| 325 | -3.51 | 9603 | -44.30 | -170.79 |
| 350 | -3.80 | 10821 | -54.18 | -337.96 |

THERMODYNAMIC PROPERTIES FOR THE REATION:

$$SrF^+ = Sr^{2+} + F^-$$
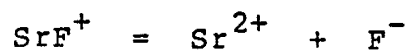
IN STEAM SATURATED WATER.

| TEMP | LOG K(T) | FREE ENERGY | ENTROPY | HEAT CAPACITY |
|------|----------|-------------|---------|---------------|
| 0 | -0.41 | 513 | -11.53 | -27.98 |
| 25 | -0.61 | 832 | -14.00 | -28.38 |
| 50 | -0.82 | 1211 | -16.30 | -28.85 |
| 75 | -1.03 | 1646 | -18.47 | -29.44 |
| 100 | -1.25 | 2134 | -20.54 | -30.19 |
| 125 | -1.47 | 2672 | -22.53 | -31.16 |
| 150 | -1.68 | 3260 | -24.46 | -32.51 |
| 175 | -1.90 | 3896 | -26.38 | -34.47 |
| 200 | -2.12 | 4579 | -28.33 | -37.52 |
| 225 | -2.33 | 5313 | -30.38 | -42.54 |
| 250 | -2.55 | 6100 | -32.65 | -51.37 |
| 275 | -2.77 | 6949 | -35.39 | -67.84 |
| 300 | -3.00 | 7877 | -39.06 | -100.60 |

THERMODYNAMIC PROPERTIES FOR THE REATION:

$$BaF^+ = Ba^{2+} + F^-$$
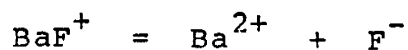
IN STEAM SATURATED WATER.

| TEMP | LOG K(T) | FREE ENERGY | ENTROPY | HEAT CAPACITY |
|------|----------|-------------|---------|---------------|
| 0 | -0.01 | 16 | -9.66 | -26.48 |
| 25 | -0.21 | 287 | -12.00 | -26.88 |
| 50 | -0.42 | 614 | -14.18 | -27.35 |
| 75 | -0.62 | 995 | -16.24 | -27.94 |
| 100 | -0.84 | 1426 | -18.20 | -28.69 |
| 125 | -1.05 | 1904 | -20.09 | -29.66 |
| 150 | -1.26 | 2430 | -21.94 | -31.01 |
| 175 | -1.46 | 3001 | -23.77 | -32.97 |
| 200 | -1.67 | 3619 | -25.64 | -36.02 |
| 225 | -1.88 | 4284 | -27.61 | -41.04 |
| 250 | -2.09 | 5001 | -29.81 | -49.87 |
| 275 | -2.30 | 5778 | -32.48 | -66.34 |
| 300 | -2.53 | 6632 | -36.08 | -99.10 |

THERMODYNAMIC PROPERTIES FOR THE REATION:

$MnF^+ = Mn^{2+} + F^-$
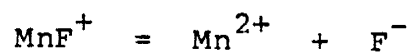
IN STEAM SATURATED WATER.

| TEMP | LOG K(T) | FREE ENERGY | ENTROPY | HEAT CAPACITY |
|------|----------|-------------|---------|---------------|
| 0    | -1.19    | 1488        | -11.26  | -27.68        |
| 25   | -1.32    | 1801        | -13.70  | -28.08        |
| 50   | -1.47    | 2172        | -15.98  | -28.55        |
| 75   | -1.63    | 2599        | -18.13  | -29.14        |
| 100  | -1.80    | 3077        | -20.17  | -29.89        |
| 125  | -1.98    | 3607        | -22.14  | -30.86        |
| 150  | -2.16    | 4184        | -24.06  | -32.21        |
| 175  | -2.35    | 4809        | -25.96  | -34.17        |
| 200  | -2.53    | 5482        | -27.89  | -37.22        |
| 225  | -2.72    | 6205        | -29.92  | -42.24        |
| 250  | -2.92    | 6980        | -32.18  | -51.07        |
| 275  | -3.12    | 7818        | -34.91  | -67.54        |
| 300  | -3.33    | 8733        | -38.56  | -100.30       |

THERMODYNAMIC PROPERTIES FOR THE REATION:

$$FeF^+ = Fe^{2+} + F^-$$
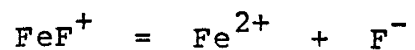
IN STEAM SATURATED WATER.

| TEMP | LOG K(T) | FREE ENERGY | ENTROPY | HEAT CAPACITY |
|------|----------|-------------|---------|---------------|
| 0 | -1.26 | 1579 | -12.47 | -28.68 |
| 25 | -1.41 | 1923 | -15.00 | -29.08 |
| 50 | -1.57 | 2328 | -17.36 | -29.55 |
| 75 | -1.75 | 2790 | -19.58 | -30.14 |
| 100 | -1.94 | 3306 | -21.70 | -30.89 |
| 125 | -2.13 | 3874 | -23.73 | -31.86 |
| 150 | -2.32 | 4492 | -25.71 | -33.21 |
| 175 | -2.52 | 5160 | -27.67 | -35.17 |
| 200 | -2.71 | 5876 | -29.65 | -38.22 |
| 225 | -2.91 | 6643 | -31.74 | -43.24 |
| 250 | -3.12 | 7465 | -34.05 | -52.07 |
| 275 | -3.33 | 8349 | -36.82 | -68.54 |
| 300 | -3.55 | 9313 | -40.51 | -101.30 |

THERMODYNAMIC PROPERTIES FOR THE REATION:

$$CoF^+ = Co^{2+} + F^-$$
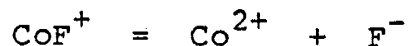
IN STEAM SATURATED WATER.

| TEMP | LOG K(T) | FREE ENERGY | ENTROPY | HEAT CAPACITY |
|------|----------|-------------|---------|---------------|
| 0 | -0.83 | 1041 | -12.75 | -28.88 |
| 25 | -1.02 | 1392 | -15.30 | -29.28 |
| 50 | -1.22 | 1804 | -17.68 | -29.75 |
| 75 | -1.43 | 2274 | -19.91 | -30.34 |
| 100 | -1.64 | 2799 | -22.04 | -31.09 |
| 125 | -1.85 | 3376 | -24.09 | -32.06 |
| 150 | -2.07 | 4003 | -26.08 | -33.41 |
| 175 | -2.28 | 4679 | -28.05 | -35.37 |
| 200 | -2.50 | 5406 | -30.04 | -38.42 |
| 225 | -2.71 | 6182 | -32.14 | -43.44 |
| 250 | -2.93 | 7014 | -34.46 | -52.27 |
| 275 | -3.15 | 7909 | -37.24 | -68.74 |
| 300 | -3.39 | 8884 | -40.94 | -101.50 |

THERMODYNAMIC PROPERTIES FOR THE REATION:

$NiF^+ = NiF^+ + F^-$
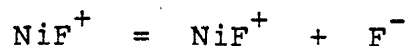
IN STEAM SATURATED WATER.

| TEMP | LOG K(T) | FREE ENERGY | ENTROPY | HEAT CAPACITY |
|------|----------|-------------|---------|---------------|
| 0 | -0.93 | 1166 | -13.22 | -29.28 |
| 25 | -1.12 | 1529 | -15.80 | -29.68 |
| 50 | -1.32 | 1954 | -18.21 | -30.15 |
| 75 | -1.53 | 2438 | -20.48 | -30.74 |
| 100 | -1.74 | 2977 | -22.63 | -31.49 |
| 125 | -1.96 | 3569 | -24.70 | -32.46 |
| 150 | -2.18 | 4212 | -26.72 | -33.81 |
| 175 | -2.39 | 4905 | -28.71 | -35.77 |
| 200 | -2.61 | 5647 | -30.73 | -38.82 |
| 225 | -2.83 | 6442 | -32.84 | -43.84 |
| 250 | -3.05 | 7292 | -35.18 | -52.67 |
| 275 | -3.27 | 8205 | -37.98 | -69.14 |
| 300 | -3.51 | 9198 | -41.71 | -101.90 |

THERMODYNAMIC PROPERTIES FOR THE REATION:

$CuF^+ = Cu^{2+} + F^-$
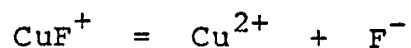
IN STEAM SATURATED WATER.

| TEMP | LOG K(T) | FREE ENERGY | ENTROPY | HEAT CAPACITY |
|------|----------|-------------|---------|---------------|
| 0 | -1.46 | 1827 | -8.73 | -25.68 |
| 25 | -1.52 | 2074 | -11.00 | -26.08 |
| 50 | -1.61 | 2375 | -13.12 | -26.55 |
| 75 | -1.71 | 2729 | -15.12 | -27.14 |
| 100 | -1.83 | 3130 | -17.02 | -27.89 |
| 125 | -1.96 | 3579 | -18.86 | -28.86 |
| 150 | -2.10 | 4073 | -20.66 | -30.21 |
| 175 | -2.25 | 4612 | -22.44 | -32.17 |
| 200 | -2.40 | 5196 | -24.27 | -35.22 |
| 225 | -2.56 | 5826 | -26.20 | -40.24 |
| 250 | -2.72 | 6507 | -28.36 | -49.07 |
| 275 | -2.89 | 7248 | -30.99 | -65.54 |
| 300 | -3.08 | 8065 | -34.55 | -98.30 |

THERMODYNAMIC PROPERTIES FOR THE REATION:

$$ZnF^+ = Zn^{2+} + F^-$$
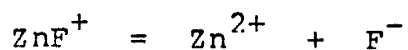
IN STEAM SATURATED WATER.

| TEMP | LOG K(T) | FREE ENERGY | ENTROPY | HEAT CAPACITY |
|------|----------|-------------|---------|---------------|
| 0 | -0.92 | 1152 | -15.28 | -30.88 |
| 25 | -1.15 | 1569 | -18.00 | -31.28 |
| 50 | -1.39 | 2051 | -20.54 | -31.75 |
| 75 | -1.63 | 2594 | -22.92 | -32.34 |
| 100 | -1.87 | 3196 | -25.19 | -33.09 |
| 125 | -2.12 | 3853 | -27.37 | -34.06 |
| 150 | -2.36 | 4564 | -29.48 | -35.41 |
| 175 | -2.60 | 5327 | -31.56 | -37.37 |
| 200 | -2.84 | 6142 | -33.67 | -40.42 |
| 225 | -3.08 | 7011 | -35.87 | -45.44 |
| 250 | -3.32 | 7937 | -38.28 | -54.27 |
| 275 | -3.56 | 8929 | -41.16 | -70.74 |
| 300 | -3.81 | 10003 | -44.95 | -103.50 |

THERMODYNAMIC PROPERTIES FOR THE REATION:

$PbF^+ + Pb^{2+} + F^-$
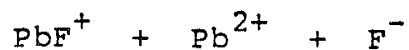
IN STEAM SATURATED WATER.

| TEMP | LOG K(T) | FREE ENERGY | ENTROPY | HEAT CAPACITY |
|------|----------|-------------|---------|---------------|
| 0 | -2.11 | 2643 | -5.64 | -23.28 |
| 25 | -2.06 | 2810 | -7.70 | -23.68 |
| 50 | -2.05 | 3027 | -9.62 | -24.15 |
| 75 | -2.07 | 3290 | -11.45 | -24.74 |
| 100 | -2.11 | 3598 | -13.19 | -25.49 |
| 125 | -2.17 | 3949 | -14.87 | -26.46 |
| 150 | -2.24 | 4341 | -16.52 | -27.81 |
| 175 | -2.33 | 4775 | -18.17 | -29.77 |
| 200 | -2.43 | 5250 | -19.86 | -32.82 |
| 225 | -2.53 | 5769 | -21.66 | -37.84 |
| 250 | -2.65 | 6335 | -23.71 | -46.67 |
| 275 | -2.77 | 6958 | -26.23 | -63.14 |
| 300 | -2.92 | 7654 | -29.68 | -95.90 |

THERMODYNAMIC PROPERTIES FOR THE REATION:

$PbF_2$ (aq) $=$ $Pb^{2+}$ $+$ $2F^-$
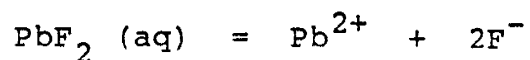
IN STEAM SATURATED WATER.

| TEMP | LOG K(T) | FREE ENERGY | ENTROPY | AVERAGE HEAT CAPACITY |
|---|---|---|---|---|
| 0 | -3.21 | 4015 | -24.39 | -36.67 |
| 25 | -3.42 | 4666 | -27.61 | 0.00 |
| 50 | -3.65 | 5397 | -30.83 | -40.14 |
| 75 | -3.90 | 6211 | -34.05 | -41.63 |
| 100 | -4.17 | 7112 | -37.28 | -43.12 |
| 125 | -4.45 | 8102 | -40.50 | -44.59 |
| 150 | -4.74 | 9182 | -43.72 | -46.04 |
| 175 | -5.05 | 10355 | -46.94 | -47.46 |
| 200 | -5.37 | 11622 | -50.16 | -48.86 |
| 225 | -5.70 | 12984 | -53.39 | -50.23 |
| 250 | -6.03 | 14443 | -56.61 | -51.59 |
| 275 | -6.38 | 16001 | -59.83 | -52.93 |
| 300 | -6.73 | 17658 | -63.05 | -54.24 |

THERMODYNAMIC PROPERTIES FOR THE REATION:

$$SnF^+ = Sn^{2+} + F^-$$
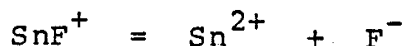
IN STEAM SATURATED WATER.

| TEMP | LOG K(T) | FREE ENERGY | ENTROPY | HEAT CAPACITY |
|------|----------|-------------|---------|---------------|
| 0 | -4.92 | 6151 | -9.29 | -26.18 |
| 25 | -4.70 | 6413 | -11.60 | -26.58 |
| 50 | -4.55 | 6730 | -13.76 | -27.05 |
| 75 | -4.46 | 7099 | -15.79 | -27.64 |
| 100 | -4.40 | 7519 | -17.74 | -28.39 |
| 125 | -4.38 | 7986 | -19.61 | -29.36 |
| 150 | -4.39 | 8499 | -21.43 | -30.71 |
| 175 | -4.42 | 9057 | -23.25 | -32.67 |
| 200 | -4.46 | 9661 | -25.10 | -35.72 |
| 225 | -4.52 | 10313 | -27.05 | -40.74 |
| 250 | -4.60 | 11016 | -29.24 | -49.57 |
| 275 | -4.70 | 11779 | -31.90 | -66.04 |
| 300 | -4.81 | 12618 | -35.48 | -98.80 |

THERMODYNAMIC PROPERTIES FOR THE REATION:

$$SnF_2 (aq) = Sn^{2+} + 2F^-$$
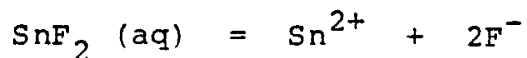
IN STEAM SATURATED WATER.

| TEMP | LOG K(T) | FREE ENERGY | ENTROPY | AVERAGE HEAT CAPACITY |
|------|----------|-------------|---------|-----------------------|
| 0 | -7.66 | 9568 | -27.58 | -39.07 |
| 25 | -7.55 | 10301 | -31.01 | 0.00 |
| 50 | -7.52 | 11119 | -34.45 | -42.79 |
| 75 | -7.55 | 12027 | -37.88 | -44.37 |
| 100 | -7.63 | 13027 | -41.31 | -45.96 |
| 125 | -7.75 | 14121 | -44.75 | -47.53 |
| 150 | -7.91 | 15312 | -48.18 | -49.07 |
| 175 | -8.10 | 16601 | -51.61 | -50.58 |
| 200 | -8.31 | 17991 | -55.05 | -52.07 |
| 225 | -8.55 | 19483 | -58.48 | -53.54 |
| 250 | -8.81 | 21078 | -61.91 | -54.98 |
| 275 | -9.08 | 22777 | -65.35 | -56.40 |
| 300 | -9.37 | 24582 | -68.78 | -57.81 |

THERMODYNAMIC PROPERTIES FOR THE REATION:

$$SnF_3^- = Sn^{2+} + 3F^-$$
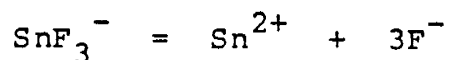
IN STEAM SATURATED WATER.

| TEMP | LOG·K(T) | FREE ENERGY | ENTROPY | AVERAGE HEAT CAPACITY |
|---|---|---|---|---|
| 0 | -10.34 | 12917 | -46.34 | -53.20 |
| 25 | -10.36 | 14135 | -51.02 | 0.00 |
| 50 | -10.46 | 15469 | -55.70 | -58.35 |
| 75 | -10.63 | 16925 | -60.38 | -60.48 |
| 100 | -10.84 | 18506 | -65.06 | -62.64 |
| 125 | -11.10 | 20216 | -69.73 | -64.77 |
| 150 | -11.39 | 22058 | -74.41 | -66.87 |
| 175 | -11.72 | 24034 | -79.09 | -68.93 |
| 200 | -12.08 | 26147 | -83.77 | -70.96 |
| 225 | -12.46 | 28398 | -88.45 | -72.95 |
| 250 | -12.86 | 30791 | -93.13 | -74.92 |
| 275 | -13.29 | 33325 | -97.80 | -76.86 |
| 300 | -13.73 | 36004 | -102.48 | -78.77 |

THERMODYNAMIC PROPERTIES FOR THE REATION:

$$AlF^{2+} = Al^{3+} + F^-$$
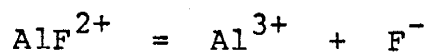
IN STEAM SATURATED WATER.

| TEMP | LOG K(T) | FREE ENERGY | ENTROPY | AVERAGE HEAT CAPACITY |
|------|----------|-------------|---------|-----------------------|
| 0 | -7.03 | 8783 | -29.45 | -40.48 |
| 25 | -7.01 | 9564 | -33.01 | 0.00 |
| 50 | -7.06 | 10434 | -36.57 | -44.35 |
| 75 | -7.15 | 11397 | -40.13 | -45.98 |
| 100 | -7.30 | 12455 | -43.69 | -47.63 |
| 125 | -7.47 | 13610 | -47.24 | -49.25 |
| 150 | -7.68 | 14866 | -50.80 | -50.85 |
| 175 | -7.91 | 16225 | -54.36 | -52.41 |
| 200 | -8.17 | 17687 | -57.92 | -53.96 |
| 225 | -8.45 | 19254 | -61.48 | -55.48 |
| 250 | -8.74 | 20929 | -65.03 | -56.97 |
| 275 | -9.06 | 22712 | -68.59 | -58.45 |
| 300 | -9.38 | 24604 | -72.15 | -59.90 |

THERMODYNAMIC PROPERTIES FOR THE REATION:

$$AlF_2^+ = Al^{3+} + 2F^-$$
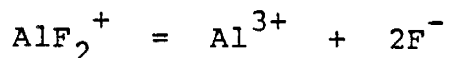
IN STEAM SATURATED WATER.

| TEMP | LOG K(T) | FREE ENERGY | ENTROPY | AVERAGE HEAT CAPACITY |
|---|---|---|---|---|
| 0 | -12.77 | 15958 | -54.78 | -59.55 |
| 25 | -12.75 | 17394 | -60.02 | 0.00 |
| 50 | -12.82 | 18961 | -65.26 | -65.35 |
| 75 | -12.97 | 20663 | -70.50 | -67.73 |
| 100 | -13.18 | 22506 | -75.74 | -70.15 |
| 125 | -13.45 | 24493 | -80.98 | -72.53 |
| 150 | -13.75 | 26628 | -86.22 | -74.88 |
| 175 | -14.10 | 28913 | -91.46 | -77.19 |
| 200 | -14.48 | 31351 | -96.69 | -79.46 |
| 225 | -14.89 | 33945 | -101.93 | -81.69 |
| 250 | -15.33 | 36696 | -107.17 | -83.90 |
| 275 | -15.79 | 39606 | -112.41 | -86.07 |
| 300 | -16.28 | 42678 | -117.65 | -88.21 |

THERMODYNAMIC PROPERTIES FOR THE REATION:

$AlF_3$ (aq) $=$ $Al^{3+}$ + $3F^-$
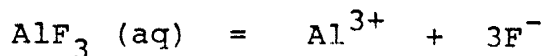
IN STEAM SATURATED WATER.

| TEMP | LOG K(T) | FREE ENERGY | ENTROPY | AVERAGE HEAT CAPACITY |
|------|----------|-------------|---------|-----------------------|
| 0 | -17.08 | 21350 | -71.67 | -72.27 |
| 25 | -17.02 | 23222 | -78.03 | 0.00 |
| 50 | -17.08 | 25253 | -84.39 | -79.36 |
| 75 | -17.23 | 27449 | -90.75 | -82.23 |
| 100 | -17.46 | 29815 | -97.11 | -85.16 |
| 125 | -17.76 | 32356 | -103.47 | -88.05 |
| 150 | -18.12 | 35077 | -109.83 | -90.90 |
| 175 | -18.52 | 37980 | -116.19 | -93.70 |
| 200 | -18.97 | 41068 | -122.55 | -96.46 |
| 225 | -19.46 | 44346 | -128.90 | -99.17 |
| 250 | -19.98 | 47814 | -135.26 | -101.84 |
| 275 | -20.53 | 51477 | -141.62 | -104.48 |
| 300 | -21.10 | 55335 | -147.98 | -107.08 |

THERMODYNAMIC PROPERTIES FOR THE REATION:

$$AlF_4^- = Al^{3+} + 4F^-$$
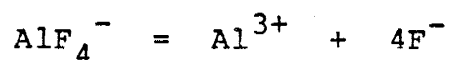
IN STEAM SATURATED WATER.

| TEMP | LOG K(T) | FREE ENERGY | ENTROPY | AVERAGE HEAT CAPACITY |
|---|---|---|---|---|
| 0 | -19.78 | 24718 | -83.87 | -81.45 |
| 25 | -19.72 | 26905 | -91.04 | 0.00 |
| 50 | -19.80 | 29271 | -98.20 | -89.47 |
| 75 | -19.98 | 31823 | -105.37 | -92.70 |
| 100 | -20.25 | 34568 | -112.54 | -96.00 |
| 125 | -20.59 | 37509 | -119.71 | -99.26 |
| 150 | -21.00 | 40653 | -126.88 | -102.47 |
| 175 | -21.46 | 44002 | -134.05 | -105.63 |
| 200 | -21.97 | 47560 | -141.22 | -108.73 |
| 225 | -22.52 | 51332 | -148.38 | -111.79 |
| 250 | -23.11 | 55319 | -155.55 | -114.81 |
| 275 | -23.73 | 59524 | -162.72 | -117.78 |
| 300 | -24.39 | 63950 | -169.89 | -120.71 |

THERMODYNAMIC PROPERTIES FOR THE REATION:

$$AlF_5^{2-} = Al^{3+} + 5F^-$$
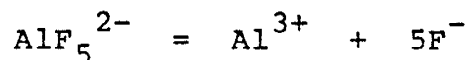
IN STEAM SATURATED WATER.

| TEMP | LOG K(T) | FREE ENERGY | ENTROPY | AVERAGE HEAT CAPACITY |
|------|----------|-------------|---------|------------------------|
| 0 | -20.96 | 26196 | -89.50 | -85.69 |
| 25 | -20.91 | 28529 | -97.04 | 0.00 |
| 50 | -21.00 | 31050 | -104.58 | -94.14 |
| 75 | -21.20 | 33766 | -112.12 | -97.54 |
| 100 | -21.49 | 36685 | -119.66 | -101.01 |
| 125 | -21.85 | 39812 | -127.21 | -104.43 |
| 150 | -22.29 | 43150 | -134.75 | -107.81 |
| 175 | -22.78 | 46705 | -142.29 | -111.13 |
| 200 | -23.32 | 50481 | -149.83 | -114.40 |
| 225 | -23.90 | 54480 | -157.37 | -117.62 |
| 250 | -24.53 | 58706 | -164.92 | -120.79 |
| 275 | -25.19 | 63162 | -172.46 | -123.91 |
| 300 | -25.87 | 67850 | -180.00 | -127.00 |

THERMODYNAMIC PROPERTIES FOR THE REATION:

$$AlF_6^{3-} = Al^{3+} + 6F^-$$
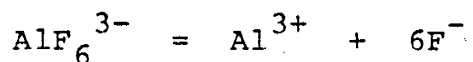
IN STEAM SATURATED WATER.

| TEMP | LOG K(T) | FREE ENERGY | ENTROPY | AVERAGE HEAT CAPACITY |
|------|----------|-------------|---------|-----------------------|
| 0 | -20.97 | 26201 | -86.68 | -83.57 |
| 25 | -20.86 | 28461 | -94.04 | 0.00 |
| 50 | -20.90 | 30905 | -101.39 | -91.80 |
| 75 | -21.06 | 33539 | -108.75 | -95.12 |
| 100 | -21.30 | 36371 | -116.10 | -98.50 |
| 125 | -21.63 | 39405 | -123.46 | -101.85 |
| 150 | -22.03 | 42646 | -130.81 | -105.14 |
| 175 | -22.48 | 46098 | -138.17 | -108.38 |
| 200 | -22.99 | 49765 | -145.52 | -111.57 |
| 225 | -23.54 | 53650 | -152.88 | -114.71 |
| 250 | -24.13 | 57757 | -160.23 | -117.80 |
| 275 | -24.76 | 62088 | -167.59 | -120.85 |
| 300 | -25.41 | 66645 | -174.94 | -123.85 |

THERMODYNAMIC PROPERTIES FOR THE REATION:

$$FeF^{2+} = Fe^{3+} + F^-$$
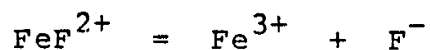
IN STEAM SATURATED WATER.

| TEMP | LOG K(T) | FREE ENERGY | ENTROPY | AVERAGE HEAT CAPACITY |
|------|----------|-------------|---------|-----------------------|
| 0 | -6.18 | 7726 | -27.58 | -39.07 |
| 25 | -6.20 | 8459 | -31.01 | 0.00 |
| 50 | -6.27 | 9277 | -34.45 | -42.79 |
| 75 | -6.39 | 10185 | -37.88 | -44.37 |
| 100 | -6.55 | 11185 | -41.31 | -45.96 |
| 125 | -6.74 | 12279 | -44.75 | -47.53 |
| 150 | -6.96 | 13470 | -48.18 | -49.07 |
| 175 | -7.20 | 14759 | -51.61 | -50.58 |
| 200 | -7.46 | 16149 | -55.05 | -52.07 |
| 225 | -7.74 | 17641 | -58.48 | -53.54 |
| 250 | -8.04 | 19236 | -61.91 | -54.98 |
| 275 | -8.35 | 20935 | -65.35 | -56.40 |
| 300 | -8.67 | 22740 | -68.78 | -57.81 |

THERMODYNAMIC PROPERTIES FOR THE REATION:

$$FeF_2^+ = Fe^{3+} + 2F^-$$
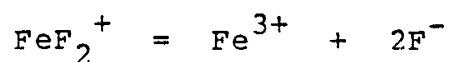
IN STEAM SATURATED WATER.

| TEMP | LOG K(T) | FREE ENERGY | ENTROPY | AVERAGE HEAT CAPACITY |
|------|----------|-------------|---------|-----------------------|
| 0    | -11.85   | 14807       | -49.16  | -55.32                |
| 25   | -11.80   | 16097       | -54.02  | 0.00                  |
| 50   | -11.84   | 17509       | -58.89  | -60.68                |
| 75   | -11.96   | 19047       | -63.75  | -62.90                |
| 100  | -12.13   | 20716       | -68.62  | -65.14                |
| 125  | -12.36   | 22518       | -73.48  | -67.36                |
| 150  | -12.63   | 24457       | -78.35  | -69.54                |
| 175  | -12.94   | 26536       | -83.21  | -71.68                |
| 200  | -13.28   | 28757       | -88.08  | -73.79                |
| 225  | -13.66   | 31123       | -92.94  | -75.87                |
| 250  | -14.05   | 33635       | -97.81  | -77.91                |
| 275  | -14.47   | 36295       | -102.67 | -79.93                |
| 300  | -14.91   | 39105       | -107.54 | -81.92                |

THERMODYNAMIC PROPERTIES FOR THE REATION:

$$FeF_3 \ (aq) \ = \ Fe^{3+} \ + \ 3F^-$$
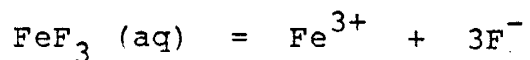
IN STEAM SATURATED WATER.

| TEMP | LOG K(T) | FREE ENERGY | ENTROPY | AVERAGE HEAT CAPACITY |
|------|----------|-------------|---------|-----------------------|
| 0 | -13.96 | 17447 | -63.23 | -65.91 |
| 25 | -14.00 | 19101 | -69.03 | 0.00 |
| 50 | -14.14 | 20900 | -74.83 | -72.35 |
| 75 | -14.34 | 22849 | -80.62 | -74.98 |
| 100 | -14.62 | 24954 | -86.42 | -77.65 |
| 125 | -14.94 | 27218 | -92.22 | -80.29 |
| 150 | -15.31 | 29646 | -98.02 | -82.89 |
| 175 | -15.72 | 32240 | -103.82 | -85.44 |
| 200 | -16.17 | 35003 | -109.62 | -87.96 |
| 225 | -16.65 | 37939 | -115.42 | -90.43 |
| 250 | -17.15 | 41048 | -121.22 | -92.87 |
| 275 | -17.68 | 44335 | -127.02 | -95.27 |
| 300 | -18.23 | 47800 | -132.82 | -97.64 |

APPENDIX C

Thermodynamic properties of dissociation for molybdenum complexes at elevated temperatures in steam saturated water. All units are consistent with cal mole$^{-1}$ or cal mole$^{-1}$ K$^{-1}$.

THERMODYNAMIC PROPERTIES FOR THE REATION:

$$MoO_2^{2+} + 2H_2O = MoO_4^{2-} + 4H^+$$

IN STEAM SATURATED WATER.

| TEMP | LOG K(T) | FREE ENERGY | ENTROPY | HEAT CAPACITY |
|------|----------|-------------|---------|---------------|
| 0 | -8.31 | 10383 | -0.65 | -56.93 |
| 25 | -7.67 | 10464 | -5.80 | -60.85 |
| 50 | -7.22 | 10673 | -10.88 | -65.60 |
| 75 | -6.91 | 11008 | -15.98 | -71.48 |
| 100 | -6.72 | 11473 | -21.18 | -78.93 |
| 125 | -6.63 | 12069 | -26.60 | -88.70 |
| 150 | -6.61 | 12806 | -32.38 | -102.15 |
| 175 | -6.68 | 13693 | -38.76 | -121.75 |
| 200 | -6.81 | 14752 | -46.13 | -152.15 |
| 225 | -7.03 | 16013 | -55.13 | -202.35 |
| 250 | -7.32 | 17531 | -66.97 | -290.53 |
| 275 | -7.74 | 19403 | -83.92 | -454.99 |
| 300 | -8.32 | 21807 | -110.59 | -782.18 |
| 325 | -9.17 | 25093 | -156.89 | -1485.20 |
| 350 | -10.52 | 30003 | -246.49 | -3154.78 |

THERMODYNAMIC PROPERTIES FOR THE REATION:

$MoO_2(OH)^+ + H_2O = MoO_4^{2-} + 3H^+$
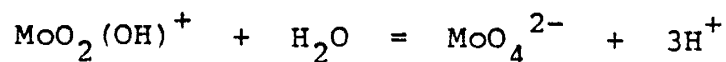
IN STEAM SATURATED WATER.

| TEMP | LOG K(T) | FREE ENERGY | ENTROPY | HEAT CAPACITY |
|------|----------|-------------|---------|---------------|
| 0 | -7.38 | 9224 | -22.89 | -48.45 |
| 25 | -7.22 | 9851 | -27.30 | -52.37 |
| 50 | -7.16 | 10589 | -31.70 | -57.14 |
| 75 | -7.18 | 11437 | -36.17 | -63.02 |
| 100 | -7.26 | 12398 | -40.78 | -70.48 |
| 125 | -7.40 | 13478 | -45.65 | -80.26 |
| 150 | -7.58 | 14684 | -50.92 | -93.73 |
| 175 | -7.82 | 16029 | -56.82 | -113.36 |
| 200 | -8.10 | 17534 | -63.73 | -143.79 |
| 225 | -8.44 | 19230 | -72.30 | -194.06 |
| 250 | -8.85 | 21172 | -83.74 | -282.35 |
| 275 | -9.35 | 23459 | -100.31 | -447.02 |
| 300 | -10.02 | 26268 | -126.63 | -774.62 |
| 325 | -10.94 | 29951 | -172.63 | -1478.53 |
| 350 | -12.36 | 35251 | -261.99 | -3150.23 |

THERMODYNAMIC PROPERTIES FOR THE REATION:

$$H_2MoO_4 = 2H^+ + MoO_4^{2-} \qquad (I)$$
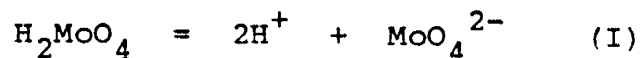
IN STEAM SATURATED WATER.

| TEMP | LOG K(T) | FREE ENERGY | ENTROPY | HEAT CAPACITY |
|------|----------|-------------|---------|---------------|
| 0 | -5.81 | 7264 | -43.72 | -66.72 |
| 25 | -6.18 | 8432 | -49.70 | -70.10 |
| 50 | -6.59 | 9747 | -55.50 | -74.21 |
| 75 | -7.04 | 11206 | -61.21 | -79.29 |
| 100 | -7.50 | 12808 | -66.92 | -85.72 |
| 125 | -7.99 | 14553 | -72.74 | -94.16 |
| 150 | -8.50 | 16447 | -78.80 | -105.78 |
| 175 | -9.02 | 18497 | -85.32 | -122.70 |
| 200 | -9.57 | 20720 | -92.63 | -148.95 |
| 225 | -10.15 | 23140 | -101.31 | -192.31 |
| 250 | -10.78 | 25805 | -112.39 | -268.45 |
| 275 | -11.48 | 28796 | -127.86 | -410.48 |
| 300 | -12.30 | 32266 | -151.67 | -693.03 |
| 325 | -13.34 | 36517 | -192.40 | -1300.15 |
| 350 | -14.80 | 42189 | -270.50 | -2741.98 |

THERMODYNAMIC PROPERTIES FOR THE REATION:

$$H_2MoO_4 \;=\; 2H^+ \;+\; MoO_4^{2-} \qquad (II)$$
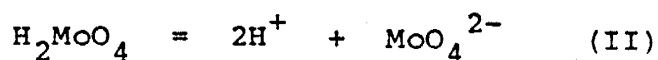
IN STEAM SATURATED WATER.

| TEMP | LOG K(T) | FREE ENERGY | ENTROPY | HEAT CAPACITY |
|------|----------|-------------|---------|---------------|
| 0 | -5.79 | 7235 | -46.08 | -39.94 |
| 25 | -6.18 | 8432 | -49.70 | -42.98 |
| 50 | -6.57 | 9720 | -53.30 | -46.67 |
| 75 | -6.97 | 11097 | -56.94 | -51.23 |
| 100 | -7.36 | 12567 | -60.68 | -57.00 |
| 125 | -7.76 | 14133 | -64.61 | -64.58 |
| 150 | -8.16 | 15801 | -68.84 | -75.01 |
| 175 | -8.57 | 17579 | -73.55 | -90.20 |
| 200 | -9.00 | 19484 | -79.03 | -113.77 |
| 225 | -9.45 | 21541 | -85.79 | -152.70 |
| 250 | -9.94 | 23792 | -94.77 | -221.07 |
| 275 | -10.49 | 26312 | -107.72 | -348.59 |
| 300 | -11.15 | 29240 | -128.21 | -602.28 |
| 325 | -12.00 | 32847 | -163.93 | -1147.39 |
| 350 | -13.23 | 37709 | -233.23 | -2441.96 |

THERMODYNAMIC PROPERTIES FOR THE REATION:

$$HMoO_4^- = H^+ + MoO_4^{2-}$$
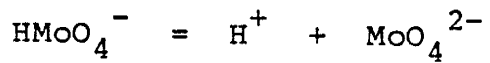
IN STEAM SATURATED WATER.

| TEMP | LOG K(T) | FREE ENERGY | ENTROPY | HEAT CAPACITY |
|------|----------|-------------|---------|---------------|
| 0    | -3.96    | 4955        | -27.66  | -50.52        |
| 25   | -4.18    | 5703        | -32.20  | -53.25        |
| 50   | -4.44    | 6564        | -36.61  | -56.56        |
| 75   | -4.73    | 7534        | -40.97  | -60.65        |
| 100  | -5.04    | 8613        | -45.35  | -65.84        |
| 125  | -5.38    | 9802        | -49.83  | -72.65        |
| 150  | -5.74    | 11106       | -54.52  | -82.01        |
| 175  | -6.11    | 12531       | -59.59  | -95.66        |
| 200  | -6.51    | 14090       | -65.30  | -116.83       |
| 225  | -6.93    | 15805       | -72.13  | -151.80       |
| 250  | -7.40    | 17713       | -80.91  | -213.20       |
| 275  | -7.93    | 19880       | -93.23  | -327.74       |
| 300  | -8.55    | 22430       | -112.28 | -555.60       |
| 325  | -9.36    | 25606       | -144.99 | -1045.20      |
| 350  | -10.50   | 29924       | -207.84 | -2207.95      |

THERMODYNAMIC PROPERTIES FOR THE REATION:

$$MoO_3F^- + H_2O = MoO_4^{2-} + 2H^+ + F^-$$

IN STEAM SATURATED WATER.

| TEMP | LOG K(T) | FREE ENERGY | ENTROPY | HEAT CAPACITY |
|------|----------|-------------|---------|---------------|
| 0 | -12.53 | 15665 | -42.49 | -68.83 |
| 25 | -12.32 | 16806 | -48.80 | -75.68 |
| 50 | -12.25 | 18106 | -55.21 | -84.00 |
| 75 | -12.28 | 19568 | -61.84 | -94.29 |
| 100 | -12.42 | 21200 | -68.80 | -107.31 |
| 125 | -12.63 | 23013 | -76.28 | -124.42 |
| 150 | -12.92 | 25021 | -84.53 | -147.95 |
| 175 | -13.29 | 27249 | -93.93 | -182.24 |
| 200 | -13.73 | 29732 | -105.14 | -235.42 |
| 225 | -14.27 | 32530 | -119.30 | -323.26 |
| 250 | -14.93 | 35739 | -138.51 | -477.53 |
| 275 | -15.76 | 39530 | -166.74 | -765.27 |
| 300 | -16.86 | 44216 | -212.02 | -1337.71 |
| 325 | -18.42 | 50412 | -291.72 | -2567.72 |
| 350 | -20.84 | 59417 | -447.22 | -5488.81 |

THERMODYNAMIC PROPERTIES FOR THE REATION:

$$MoO_2S_2^{2-} + 2H_2O = MoO_4^{2-} + 2H^+ + 2HS^-$$
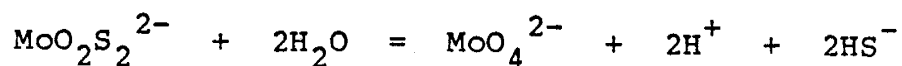
IN STEAM SATURATED WATER.

| TEMP | LOG K(T) | FREE ENERGY | ENTROPY | HEAT CAPACITY |
|------|----------|-------------|---------|---------------|
| 0 | -22.79 | 28477 | -10.93 | -126.58 |
| 25 | -21.18 | 28892 | -22.20 | -130.97 |
| 50 | -20.01 | 29582 | -32.95 | -136.30 |
| 75 | -19.17 | 30536 | -43.34 | -142.89 |
| 100 | -18.60 | 31748 | -53.52 | -151.24 |
| 125 | -18.23 | 33212 | -63.67 | -162.20 |
| 150 | -18.04 | 34932 | -73.97 | -177.28 |
| 175 | -18.00 | 36915 | -84.73 | -199.25 |
| 200 | -18.10 | 39176 | -96.39 | -233.33 |
| 225 | -18.32 | 41748 | -109.71 | -289.62 |
| 250 | -18.67 | 44686 | -126.06 | -388.48 |
| 275 | -19.18 | 48097 | -148.00 | -572.87 |
| 300 | -19.90 | 52175 | -180.69 | -939.70 |
| 325 | -20.94 | 57310 | -235.29 | -1727.90 |
| 350 | -22.56 | 64332 | -338.31 | -3599.79 |

THERMODYNAMIC PROPERTIES FOR THE REATION:

$$MoO_2Cl^+ \quad + \quad 2H_2O \quad = \quad MoO_4{}^{2-} \quad + \quad 4H^+ \quad + \quad Cl^-$$
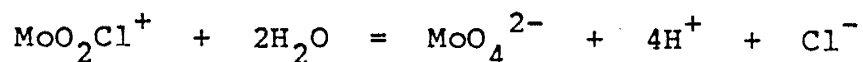
IN STEAM SATURATED WATER.

| TEMP | LOG K(T) | FREE ENERGY | ENTROPY | HEAT CAPACITY |
|------|----------|-------------|---------|---------------|
| 0 | -7.87 | 9833 | -5.87 | -63.90 |
| 25 | -7.37 | 10052 | -11.70 | -69.44 |
| 50 | -7.05 | 10418 | -17.55 | -76.17 |
| 75 | -6.86 | 10931 | -23.52 | -84.49 |
| 100 | -6.79 | 11596 | -29.72 | -95.02 |
| 125 | -6.82 | 12420 | -36.31 | -108.85 |
| 150 | -6.93 | 13416 | -43.48 | -127.89 |
| 175 | -7.12 | 14602 | -51.55 | -155.63 |
| 200 | -7.39 | 16006 | -61.07 | -198.64 |
| 225 | -7.75 | 17674 | -72.95 | -269.69 |
| 250 | -8.22 | 19686 | -88.88 | -394.47 |
| 275 | -8.84 | 22179 | -112.10 | -627.20 |
| 300 | -9.69 | 25404 | -149.09 | -1090.21 |
| 325 | -10.91 | 29860 | -213.91 | -2085.08 |
| 350 | -12.84 | 36597 | -340.02 | -4447.77 |

THERMODYNAMIC PROPERTIES FOR THE REATION:

$$MoO_2Cl_2 \; + \; 2H_2O \; = \; MoO_4^{2-} \; + \; 4H^+ \; + \; 2Cl^-$$
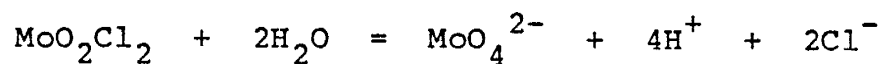
IN STEAM SATURATED WATER.

| TEMP | LOG K(T) | FREE ENERGY | ENTROPY | HEAT CAPACITY |
|------|----------|-------------|---------|---------------|
| 0 | -7.26 | 9075 | -8.72 | -67.49 |
| 25 | -6.87 | 9370 | -14.90 | -73.86 |
| 50 | -6.64 | 9821 | -21.14 | -81.61 |
| 75 | -6.55 | 10429 | -27.57 | -91.19 |
| 100 | -6.56 | 11202 | -34.29 | -103.31 |
| 125 | -6.67 | 12147 | -41.47 | -119.23 |
| 150 | -6.86 | 13281 | -49.36 | -141.14 |
| 175 | -7.13 | 14624 | -58.30 | -173.06 |
| 200 | -7.49 | 16210 | -68.92 | -222.57 |
| 225 | -7.94 | 18093 | -82.29 | -304.34 |
| 250 | -8.51 | 20363 | -100.33 | -447.96 |
| 275 | -9.24 | 23178 | -126.77 | -715.82 |
| 300 | -10.23 | 26831 | -169.08 | -1248.72 |
| 325 | -11.65 | 31894 | -243.41 | -2393.76 |
| 350 | -13.88 | 39575 | -388.32 | -5113.08 |

THERMODYNAMIC PROPERTIES FOR THE REATION:

$$MoO_2Cl_3^- + 2H_2O = MoO_4^{2-} + 4H^+ + 3Cl^-$$
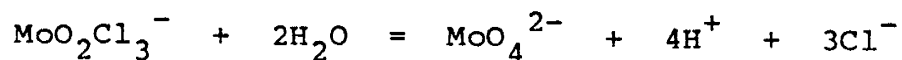
IN STEAM SATURATED WATER.

| TEMP | LOG K(T) | FREE ENERGY | ENTROPY | HEAT CAPACITY |
|------|----------|-------------|---------|---------------|
| 0 | −5.14 | 6421 | −11.57 | −71.08 |
| 25 | −4.98 | 6792 | −18.10 | −78.29 |
| 50 | −4.96 | 7327 | −24.74 | −87.06 |
| 75 | −5.04 | 8030 | −31.61 | −97.89 |
| 100 | −5.22 | 8910 | −38.85 | −111.60 |
| 125 | −5.48 | 9977 | −46.64 | −129.61 |
| 150 | −5.81 | 11249 | −55.23 | −154.39 |
| 175 | −6.22 | 12749 | −65.05 | −190.50 |
| 200 | −6.71 | 14517 | −76.78 | −246.50 |
| 225 | −7.29 | 16614 | −91.62 | −339.00 |
| 250 | −8.00 | 19142 | −111.78 | −501.45 |
| 275 | −8.88 | 22281 | −141.44 | −804.44 |
| 300 | −10.05 | 26361 | −189.06 | −1407.23 |
| 325 | −11.70 | 32030 | −272.92 | −2702.44 |
| 350 | −14.26 | 40655 | −436.61 | −5778.39 |

THERMODYNAMIC PROPERTIES FOR THE REATION:

$$MoO_2^+ + 1.5H_2O + 0.25O_2 = MoO_4^{2-} + 3H^+$$
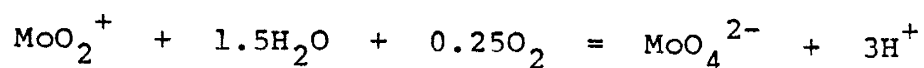
IN STEAM SATURATED WATER.

| TEMP | LOG K(T) | FREE ENERGY | ENTROPY | HEAT CAPACITY |
|------|----------|-------------|---------|---------------|
| 0 | 1.21 | -1516 | -20.38 | -71.33 |
| 25 | 0.68 | -926 | -26.80 | -75.46 |
| 50 | 0.12 | -177 | -33.07 | -80.49 |
| 75 | -0.46 | 727 | -39.29 | -86.69 |
| 100 | -1.05 | 1788 | -45.56 | -94.56 |
| 125 | -1.65 | 3007 | -52.00 | -104.88 |
| 150 | -2.27 | 4391 | -58.79 | -119.08 |
| 175 | -2.90 | 5951 | -66.18 | -139.78 |
| 200 | -3.56 | 7708 | -74.56 | -171.88 |
| 225 | -4.25 | 9693 | -84.64 | -224.90 |
| 250 | -5.00 | 11965 | -97.69 | -318.01 |
| 275 | -5.83 | 14622 | -116.12 | -491.69 |
| 300 | -6.81 | 17855 | -144.78 | -837.20 |
| 325 | -8.05 | 22031 | -194.16 | -1579.61 |
| 350 | -9.80 | 27933 | -289.24 | -3342.73 |

THERMODYNAMIC PROPERTIES FOR THE REATION:

$$MoOCl_3 + H_2O = MoO_2^+ + 2H^+ + 3Cl^-$$

IN STEAM SATURATED WATER.

| TEMP | LOG K(T) | FREE ENERGY | ENTROPY | HEAT CAPACITY |
|------|----------|-------------|---------|---------------|
| 0 | 3.89 | −4862 | −18.71 | −23.57 |
| 25 | 3.20 | −4366 | −21.00 | −29.06 |
| 50 | 2.58 | −3809 | −23.60 | −35.73 |
| 75 | 2.00 | −3183 | −26.55 | −43.97 |
| 100 | 1.45 | −2478 | −29.94 | −54.40 |
| 125 | 0.92 | −1681 | −33.89 | −68.11 |
| 150 | 0.40 | −777 | −38.57 | −86.96 |
| 175 | −0.12 | 256 | −44.29 | −114.44 |
| 200 | −0.67 | 1450 | −51.56 | −157.04 |
| 225 | −1.25 | 2854 | −61.28 | −227.42 |
| 250 | −1.90 | 4548 | −75.12 | −351.03 |
| 275 | −2.66 | 6670 | −96.27 | −581.57 |
| 300 | −3.61 | 9474 | −131.14 | −1040.21 |
| 325 | −4.92 | 13452 | −193.64 | −2025.69 |
| 350 | −6.89 | 19649 | −316.94 | −4366.09 |

APPENDIX D

Dissociation constants for molybdenum complexes in supercritical water.

LOG K(T,P) FOR THE REACTION:

$$MoO_2^{2+} + 2H_2O = MoO_4^{2-} + 4H^+$$

| TEMP | PRESSURE (KB) | | | |
|------|------|------|------|------|
|  | 0.5 | 1.0 | 1.5 | 2.0 |
| 250 | -7.08 | -6.92 | -6.83 | -6.75 |
| 300 | -7.67 | -7.38 | -7.22 | -7.11 |
| 350 | -8.67 | -8.04 | -7.75 | -7.57 |
| 400 | -10.56 | -8.96 | -8.44 | -8.16 |
| 450 |  | -10.27 | -9.32 | -8.87 |
| 500 |  | -12.11 | -10.41 | -9.70 |
| 550 |  |  | -11.64 | -10.58 |
| 600 |  |  |  | -11.23 |

LOG K(T,P) FOR THE REACTION:

$$MoO_2(OH)^+ + H_2O = MoO_4^{2-} + 3H^+$$
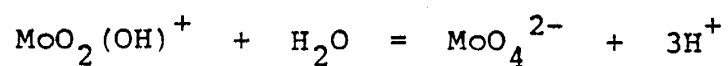
|  | PRESSURE (KB) | | | |
|------|-------|-------|--------|--------|
| TEMP | 0.5 | 1.0 | 1.5 | 2.0 |
| 250 | -8.60 | -8.44 | -8.35 | -8.27 |
| 300 | -9.37 | -9.08 | -8.92 | -8.81 |
| 350 | -10.51 | -9.87 | -9.59 | -9.41 |
| 400 | -12.50 | -10.90 | -10.38 | -10.10 |
| 450 | | -12.30 | -11.34 | -10.89 |
| 500 | | -14.20 | -12.50 | -11.79 |
| 550 | | | -13.78 | -12.72 |
| 600 | | | | -13.40 |

LOG K(T,P) FOR THE REACTION:

$$H_2MoO_4 = 2H^+ + MoO_4^{2-} \quad (II)$$
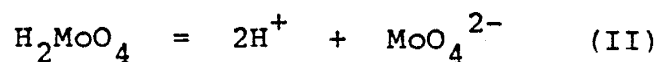
| TEMP | PRESSURE (KB) | | | |
| | 0.5 | 1.0 | 1.5 | 2.0 |
|---|---|---|---|---|
| 250 | -9.75 | -9.62 | -9.55 | -9.50 |
| 300 | -10.65 | -10.43 | -10.30 | -10.21 |
| 350 | -11.79 | -11.30 | -11.08 | -10.94 |
| 400 | -13.56 | -12.32 | -11.91 | -11.70 |
| 450 | | -13.59 | -12.85 | -12.50 |
| 500 | | -15.24 | -13.92 | -13.37 |
| 550 | | | -15.06 | -14.24 |
| 600 | | | | -14.91 |

LOG K(T,P) FOR THE REACTION:

$$HMoO_4^- = H^+ + MoO_4^{2-}$$
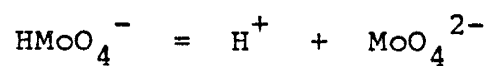
| TEMP | PRESSURE (KB) | | | |
|------|------|------|------|------|
| | 0.5 | 1.0 | 1.5 | 2.0 |
| 250 | -7.23 | -7.12 | -7.05 | -7.00 |
| 300 | -8.10 | -7.90 | -7.79 | -7.71 |
| 350 | -9.20 | -8.76 | -8.56 | -8.44 |
| 400 | -10.88 | -9.76 | -9.40 | -9.21 |
| 450 | | -11.00 | -10.34 | -10.02 |
| 500 | | -12.57 | -11.39 | -10.90 |
| 550 | | | -12.51 | -11.77 |
| 600 | | | | -12.46 |

LOG K(T,P) FOR THE REACTION:

$$MoO_3F^- + H_2O = MoO_4^{2-} + 2H^+ + F^-$$

| TEMP | PRESSURE (KB) | | | |
|------|------|------|------|------|
| | 0.5 | 1.0 | 1.5 | 2.0 |
| 250 | -14.50 | -14.22 | -14.06 | -13.93 |
| 300 | -15.73 | -15.22 | -14.95 | -14.75 |
| 350 | -17.60 | -16.49 | -15.99 | -15.68 |
| 400 | -20.96 | -18.16 | -17.25 | -16.76 |
| 450 | | -20.47 | -18.81 | -18.02 |
| 500 | | -23.68 | -20.71 | -19.47 |
| 550 | | | -22.81 | -20.96 |
| 600 | | | | -22.03 |

LOG K(T,P) FOR THE REACTION:

$$MoO_2S_2{}^{2-} + 2H_2O = MoO_4{}^{2-} + 2H^+ + 2HS^-$$

| TEMP | PRESSURE (KB) | | | |
|---|---|---|---|---|
| | 0.5 | 1.0 | 1.5 | 2.0 |
| 250 | -18.39 | -18.21 | -18.11 | -18.03 |
| 300 | -19.17 | -18.85 | -18.67 | -18.54 |
| 350 | -20.48 | -19.77 | -19.46 | -19.26 |
| 400 | -22.85 | -21.05 | -20.47 | -20.16 |
| 450 | | -22.81 | -21.74 | -21.24 |
| 500 | | -25.18 | -23.28 | -22.48 |
| 550 | | | -24.97 | -23.79 |
| 600 | | | | -24.85 |

LOG K(T,P) FOR THE REACTION:

$$MoO_2Cl^+ + 2H_2O = MoO_4^{2-} + 4H^+ + Cl^-$$
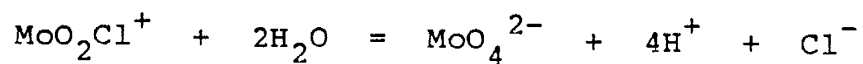
| TEMP | PRESSURE (KB) | | | |
|------|------|------|------|------|
|  | 0.5 | 1.0 | 1.5 | 2.0 |
| 250 | -7.87 | -7.65 | -7.52 | -7.42 |
| 300 | -8.78 | -8.36 | -8.14 | -7.98 |
| 350 | -10.21 | -9.32 | -8.91 | -8.66 |
| 400 | -12.88 | -10.62 | -9.88 | -9.49 |
| 450 | | -12.46 | -11.11 | -10.47 |
| 500 | | -15.03 | -12.63 | -11.62 |
| 550 | | | -14.32 | -12.82 |
| 600 | | | | -13.68 |

LOG K(T,P) FOR THE REACTION:

$$MoO_2Cl_2 + 2H_2O = MoO_4^{2-} + 4H^+ + 2Cl^-$$
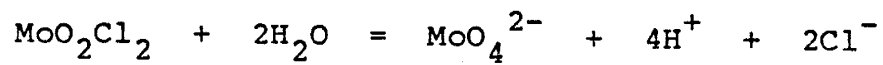
| TEMP | PRESSURE (KB) | | | |
|------|------|------|------|------|
| | 0.5 | 1.0 | 1.5 | 2.0 |
| 250 | -8.10 | -7.84 | -7.70 | -7.58 |
| 300 | -9.18 | -8.71 | -8.45 | -8.26 |
| 350 | -10.86 | -9.83 | -9.37 | -9.07 |
| 400 | -13.95 | -11.34 | -10.49 | -10.04 |
| 450 | | -13.46 | -11.91 | -11.18 |
| 500 | | -16.42 | -13.66 | -12.50 |
| 550 | | | -15.59 | -13.87 |
| 600 | | | | -14.85 |

LOG K(T,P) FOR THE REACTION:

$$MoO_2Cl_3^- + 2H_2O = MoO_4^{2-} + 4H^+ + 3Cl^-$$
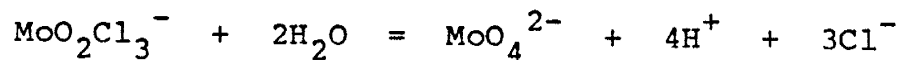
|      | PRESSURE (KB) | | | |
| TEMP | 0.5 | 1.0 | 1.5 | 2.0 |
| --- | --- | --- | --- | --- |
| 250 | -7.54 | -7.25 | -7.08 | -6.95 |
| 300 | -8.87 | -8.33 | -8.04 | -7.83 |
| 350 | -10.84 | -9.68 | -9.15 | -8.82 |
| 400 | -14.39 | -11.45 | -10.49 | -9.97 |
| 450 |  | -13.90 | -12.14 | -11.31 |
| 500 |  | -17.28 | -14.15 | -12.84 |
| 550 |  |  | -16.37 | -14.42 |
| 600 |  |  |  | -15.55 |

LOG K(T,P) FOR THE REACTION:

$$MoO_2^+ + 1.5H_2O + 0.25O_2 = MoO_4^{2-} + 3H^+$$
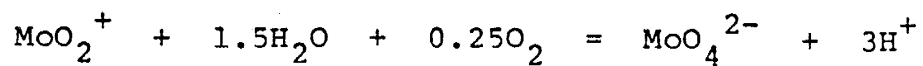
|  | PRESSURE (KB) | | | |
|---|---|---|---|---|
| TEMP | 0.5 | 1.0 | 1.5 | 2.0 |
| 250 | -4.74 | -4.57 | -4.47 | -4.40 |
| 300 | -6.13 | -5.82 | -5.65 | -5.53 |
| 350 | -7.84 | -7.17 | -6.87 | -6.68 |
| 400 | -10.41 | -8.72 | -8.17 | -7.87 |
| 450 |  | -10.61 | -9.61 | -9.13 |
| 500 |  | -13.01 | -11.22 | -10.47 |
| 550 |  |  | -12.92 | -11.80 |
| 600 |  |  |  | -12.85 |

LOG K(T,P) FOR THE REACTION:

$$MoOCl_3 + H_2O = MoO_2^+ + 2H^+ + 3Cl^-$$

|       | PRESSURE (KB) | | | |
| TEMP  | 0.5   | 1.0   | 1.5   | 2.0   |
|-------|-------|-------|-------|-------|
| 250   | -1.55 | -1.33 | -1.20 | -1.10 |
| 300   | -2.71 | -2.30 | -2.08 | -1.92 |
| 350   | -4.29 | -3.40 | -3.01 | -2.76 |
| 400   | -7.02 | -4.78 | -4.05 | -3.66 |
| 450   |       | -6.63 | -5.29 | -4.66 |
| 500   |       | -9.16 | -6.79 | -5.79 |
| 550   |       |       | -8.41 | -6.93 |
| 600   |       |       |       | -7.71 |

APPENDIX E

STOICHIOMETRIC INDIVIDUAL ION ACTIVITY COEFFICIENTS

The total molality of molybdenum, $\Sigma Mo$, is given by:

$$\Sigma Mo = (MoO_4^{2-}) + (HMoO_4^{-}) + (H_2MoO_4^{0}) + (MoO_2^{2+}) +$$

$$(MoO_2Cl^{+}) + (MoO_2Cl_2^{0}) + (MoO_2Cl_3^{-}) \qquad \text{E.1}$$

where the brackets denote the molal concentrations of the individual species.

Five hydrolysis reactions and corresponding mass action expressions may be written:

$$MoO_2(OH)_{4-n}^{n-2} + (n-2)H_2O = MoO_4^{2-} + H^{+} \qquad \text{E.2}$$
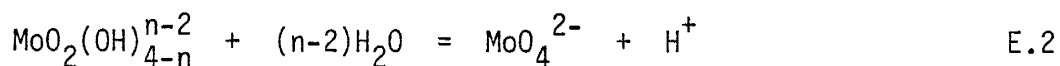
$$\frac{(MoO_4^{2-})(H^{+})^{n}}{(MoO_2(OH)_{4-n}^{n-2})} = K_{h,n} \qquad \text{for } n = 0 \text{ to } 4 \qquad \text{E.3}$$

where the parentesis denote the activity of the individual species (i.e., $(i) = \gamma_i \cdot (i)$). The species; $MoO_2(OH)_3^{-} - H_2O$ and $MoO_2(OH)_4^{2-}$ - $2H_2O$ are $HMoO_4^{-}$ and $MoO_4^{2-}$ respectively. The equilibrium constants $K_{h,n}$ are given in Appendices C and D, with $K_{h,0}$ being equal to one at all temperatures and pressures.

Three chloride dissociation reactions may be written as:

$$MoO_2Cl_m^{2-m} + 2H_2O = MoO_4^{2-} + 4H^{+} + mCl^{-} \qquad \text{E.4}$$
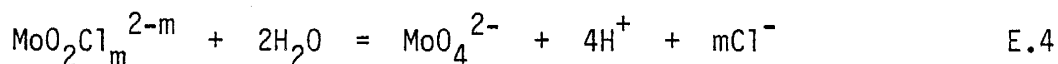
$$\frac{(MoO_4^{2-})(H^{+})^{4}(Cl^{-})^{m}}{(MoO_2Cl_m^{2-m})} = K_{Cl,m} \qquad \text{for } m = 1 \text{ to } 3 \qquad \text{E.5}$$

Substituting equations (E.3) and (E.5) into equation (E.1) using the relationship (i) = $\sum_i$ i yields:

$$\Sigma Mo = (MoO_4^{2-}) \cdot \left[ \sum_{n=0}^{4} \frac{(H^+)^n}{K_{h,n} \cdot \gamma_{h,n}} + \sum_{m=1}^{3} \frac{(H^+)^4 (Cl^-)^m}{K_{Cl,m} \cdot \gamma_{Cl,m}} \right] \qquad \text{E.6}$$

where $\gamma_{Cl,m}$ and $\gamma_{h,n}$ are the activity coefficients for the subscripted species $(\gamma_{h,n} = \gamma_{MoO_4^{2-}})$.

The stoichiometric individual ion activity coefficient for the molybdate ion is given by:

$$\dot{\gamma}_{MoO_4^{2-}} = \frac{(MoO_4^{2-})}{\Sigma Mo}$$

$$= \frac{1}{\displaystyle\sum_{n=0}^{4} \frac{(H^+)^n}{K_{h,n} \cdot \gamma_{h,n}} + \sum_{m=1}^{3} \frac{(H^+)^4 (Cl^-)^m}{K_{Cl,m} \cdot \gamma_{Cl,m}}} \qquad \text{E.7}$$

Similar expressions may be derived which include fluoride, sulfide and pentavalent molybdenum complexes.

APPENDIX F


EXPERIMENTAL TECHNIQUES FOR ANALYSES OF FLUID INCLUSION

VOLATILES BY MASS SPECTROMETERY


The analyses of fluid inclusion volatiles by mass spectrometery introduce two uncertainties not associated with typical gas analyses. These result from the small amounts of total volatiles available in the sample and the possibility of modifying the volatile composition during the analytical procedure.


EQUIPMENT

Mass Spectrometer - An Inficon IQ200 (Leybold-Heraeus, Inc.) quadrupole mass spectrometer equipped with an electron multiplier detection system was used in this study. The instrument was operated at an electron multiplier potential of 1200 volt, an emission current of 2 milliamps and in constant M mode.

Capacitance Manometer - Pressure measurements were made with a Baratron 221AHS Absolute Pressure Transducer (MKS Instruments, Inc.). The instrument has a reported sensitivity of 0.5 to 1.5% and a resolution of 0.001 torr.

Furnace - The furnace used to dry and decrepitate samples was a vertically mounted 1.5" x 8" (3.8 x 20 cm) resistance tube furnace which was closed at the lower end. A model 50 on-off temperature controller (Omega Engineering, Inc.) was used in conjunction with a Chromel-Alumel (type K) thermocouple to regulate the temperature.

Glass line - The vacuum line was all glass and is diagramed in Fig. F.1. The quartz sample container as well as the weighed capillary were attached to the line using 1/2" and 1/16" Cagon Ultratorr fittings (Cagon Company) respectively.

Chemicals - All chemical use in this study were reagent grade. The water used was distilled and deionized and had resitivities of greater than 250,000 ohm $cm^{-1}$.

## SAMPLE PREPARATION

Samples of quartz were crushed and hand picked to be as free from other mineral impurities as possible. These samples were fumed in concentrated perchloric acid for four hours to remove surface organics and oxidize any sulfide minerals. The perchloric acid was discarded and the samples were washed with ten portions of water. The samples were then twice treated with concentrated hydrofluoric acid for ten minutes to remove feldspars and clay minerals. They were again rinsed with water and were crushed in a precleaned alumna mortar and pestle. Sieving of the sample followed and the -8 to +30 fraction was collected. The sieved fractions were retreated with perchloric acid, rinsed with 10 portions of water, dried and stored in closed containers.

## SAMPLE ANALYSES

A previously cleaned sample (5 to 8 grams) was placed in a quartz furnace and attached to the gas line (see Fig. F.1). The sample was degassed to a pressure of $3 \times 10^{-6}$ torr at a temperature of 150°C. Liquid nitrogen baths were then placed on the traps ($T_1$ and $T_2$) and the valves ($V_2$, $V_3$ and $V_8$) to the vacuum pumps were shut. Decrepitation of

Fig. F.1

Diagram of high-vacuum glass line used in this study for the determination of the composition of fluid inclusion volatiles.
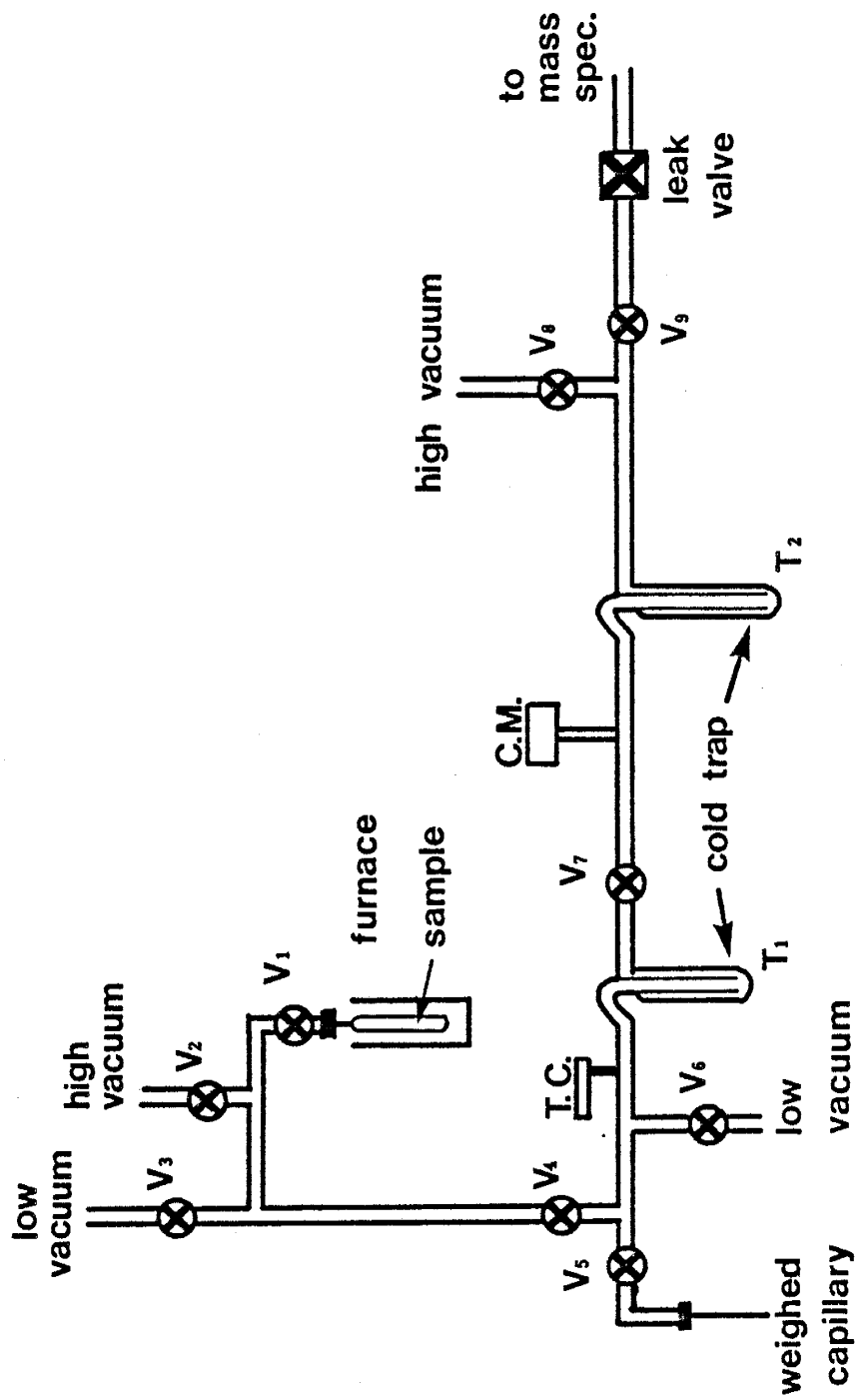
the inclusions was accomplished by heating the sample to 550°-600°C for five minutes. The volatiles, except for the noncondensable fraction ($H_2$, $N_2$, $CH_4$, and CO) were frozen into the traps. The pressure was measured and the gases introduced into the mass spectrometer. The system was re-evacuated, the liquid nitrogen bath were removed and an alcohol-dry-ice (solid $CO_2$) bath was placed on trap $T_1$ (see Fig. F.1). Only the water remained frozen in the trap ($T_1$ Fig. 1.1). The pressure of the condensable gas fraction ($CO_2$, $NH_3$, $H_2S$, $SO_2$ and light hydrocarbons) was measured and the gas fraction was introduced into the mass spectrometer. Finally, the system was re-evacuated, a liquid nitrogen bath was placed on the weighed capillary and the water was quantitatively transfered into the capillary by removing the alcohol-dry-ice bath. The capillary was sealed with a torch and weighed.

Net mass spectra were calculated by subtracting the measured backgrounds from the sample spectra. If a peak intensity in the sample spectra was not three times the background, the peak was not used. The composition of each gas fraction was determined using a computerized least squares routine which compared the spectra to previously determined spectras of known gases. The compositions were combined with the pressures, the know volumes of the glass line and the amount of water to calculate mole fractions of each gas.

ANALYTICAL UNCERTAINTIES

Pressure - Typical pressures for the noncondensable gas fraction were 0.006 torr. In light of the resolution of the capacitance manometer given above, this corresponds to an uncertainty of 17%. The condensable fractions had much higher pressures, typically 0.050 torr. This corresponds to an uncertainty of 2%.

Water measurements - The absolute uncertainty in measuring the water was 0.4 milligrams. Samples in this study yielded about 3.6 milligrams of water, corresponding to a relative uncertainty of 11%.

Interpretation of spectra - Replicate analyses of air dissolved in tap water by Norman and Bernhard (1982) indicated a relative uncertainty of approximately 10% for gases which made up greater than 2% of the total mass spectra. They also found that gases which make up a large portion of the spectra have uncertainties of less than 5%. The estimated relative uncertainty for solution of the spectra is 5% for carbon dioxide and hydrogen and 10% for hydrogen sulfide and sulfur dioxide. In the case of nitrogen and carbon monoxide spectral overlap precluded the accurate determination of either of these gases.

Over all uncertainties - Evaluation of the above uncertainties allows the analytical uncertainties associated with each gas to be estimated. These estimates result in relative uncertainties of 23% for $SO_2$ and $H_2S$, 16% for $CO_2$ and 31% for $H_2$. The uncertainties given above reflect only the analytical uncertainties and do not consider the modification of the gas composition by the decrepitation process.

REFERENCES


Akerman Th. (1958) The self-dissociation of water from measurements of molar heat of dissolved electrolytes. Zeits. Electrochem. 62, 411.

Ahluwalia J. C. and Cobble J. W. (1964) The thermodynamic properties of high temperature aqueous solutions. II. Standard partial molal heat capacities of sodium perrhenate and perrhenenic acid from 0 to 100°. J. Am. Chem. Soc. 86, 5377-5381.

Arnek R. and Szilard I. (1968) Thermochemical studies of hydrolytic reactions. 9. The reaction of $H^+$ and molybdate ions in 3 M $NaClO_4$. Acta Chem. Scand. 22, 1334-1338.

Arutyunyan L. A. (1966) Stability of water-soluble forms of molybdenum in sulfur bearing solutions at high temperatures (abs.). Geochem. Int. 3, 370.

Atwater A. (1970) Implications of plate tectonics for the Cenozoic tectonic evolution of western North America. Geol. Soc. Am. Bull. 81, 3513-3536.

Aveston J., Anacker E. W., and Johnson J. S. (1964) Hydrolysis of molybdenum (VI). Ultracentrifugation, acidity measurements and Ramam spectra of polymolybdates. Inorg. Chem. 3, 735-746.

Aziz A. and Lyle S. J. (1969) Applications of the fluoride-sensitive electrode to the study of metal-fluoride ion association constants. Anal. Chim. Acta 47, 49-56.

Baes C. F., Jr. and Mesmer R. E. (1976) The Hydrolysis of Cations. New York, Wiley-Interscience, 489 p.

Barnes H. L. (1979) Solubilities of ore minerals, in Geochemistry of Hydrothermal Ore Deposits, H. L. Barnes (ed.). New York, Wiley-Interscience, 404-460.

Barnes H. L., Romberger S. B., and Stemprok M. (1967) Ore solution chemistry II. Solubility of HgS in sulfide solutions. Econ. Geol. 62, 957-982.

Beane R. E. (1972) A thermodynamic analysis of the effect of solid solution on the hydrothermal stability of biotites. Ph.D. dissertation, Northwestern Univ., Evanston, Ill., 195 p.

_____ (1982) Hydrothermal alteration of silicate rocks, in: Advances in Geology of the Porphyry Copper Deposits, S. R. Titley (ed.). Tucson, Arizona, Univ. Arizona Press, 117-137.

_____ and Titley S. R. (1981) Porphyry copper deposits. Part II. Hydrothermal alteration and mineralization. Econ. Geol. 75th Annv. Vol., 214-269.

Bjerrum N. (1929) Neuer Anschauungen uber Elektolyte. Deutsche Chem. Gesell Ber. 62, 1091-1103.

Bloom M. S. (1981) Chemistry of inclusion fluids: Stockwork molybdenum deposits from Questa, New Mexico, Hudson Bay Mountain and Endako, British Columbia. Econ. Geol. 76, 1906-1920.

Boctor N. Z., Popp R. K., and Frantz J. D. (1980) Mineral - solution equilibria IV. Solubilities and the thermodynamic properties of $FeCl_2^o$ in the system $Fe_2O_3 - H_2 - H_2O - HCl$. Geochim. Cosmochim. Acta 44, 1509-1518.

Bodnar R. J. and Beane R. E. (1980) Temporal and spatial variations in hydrothermal fluid characteristics during vein filling in preore cover overlying deeply buried porphyry copper-type mineralization at Red Mountain, Arizona. Econ. Geol. 75, 876-893.

Born Von M. (1920) Volumen und Hydratationswarme der Ion. Zeits. Physik. 1, 45-48.

Bourcier W. L. and Barnes H. L. (1981) Stabilities of hydrothermal zinc chloride complexes (abs.). Geol. Soc. Am. An. Meeting 13, 414.

Broene H. H. and De Vries T. (1947) The thermodynamics of aqueous hydrofluoric acid solutions. J. Am. Chem. Soc. 69, 1644-1646.

Butler J. N. and Huston R. (1970) Potentiometric studies of multicomponent activity coefficients using the lanthanum fluoride membrane electrode. Anal. Chem. 42, 1308-1311.

Cadek J., Vesely J., and Sulcek Z. (1971) Bildung von Fluoridkomplexen mit Erdalkalimetallen. Collection Czechoslov. Chem. Commum. 36, 3377-3381.

Carpenter R. H. (1968) Geology and ore deposits of the Questa Molybdenum Mine are, Taos County, New Mexico, in: Ore Deposits of the United States, 1933-1967 (Granton-Sales Volume). New York, AIME, 1328-1350.

Christiansen R. L and Lipman P. W. (1972) Cenozoic volcanism and plate-tectonic evolution of the western United States, part 2. Late Cenozoic. Proc. Royal Soc. Lond. Philos. Trans. 271, 249-284.

Clark K. F. (1968) Structural controls in the Red River District, New Mexico. Econ. Geol. 63, 553-566.

_____ (1972) Stockwork molybdenum deposits in western cordillera of North America. Econ. Geol. 67, 731-758.

Cobble J. W. (1953a) Empirical considerations of entropies of the oxy-anions and related species. J. Chem. Phys. 21, 1443-1446.

_____ (1953b) Empirical considerations of entropy. II. The entropies of complex ions. J. Chem. Phys. 21, 1446-1450.

_____ (1964) The thermodynamic properties of high temperature aqueous solution. VI. Application of entropy correspondence to thermodynamics and kinetics. J. Am. Chem. Soc. 86, 5394-5401.

Coney P. J. and Reynolds S. J. (1977) Cordillerian Benioff zones. Nature 270, 403-406.

Connick R. E. and Paul A. D. (1957) The fluoride complexes of zinc, copper and lead ions in aqueous solutions. J. Am. Chem. Soc. 80, 2069-2071.

Cotton A. F. and Wilkinson G. (1980) Inorganic Chemistry. A Comprehensive Text. New York, Wiley-Interscience, 1369 p.

Craig H. (1957) Isotopic standard for carbon and oxygen and correction factors for mass spectrometric analysis of carbon dioxide. Geochim. Cosmochim. Acta 12, 133-149.

_____ (1961) Standard for reporting concentrations of deuterium and oxygen-18 in natural waters. Science 133, 1833-1834.

Crerar D. A. and Barnes H. L. (1976) Ore solution chemistry vs. solubilities of chalcopyrite and chalcocite assemblages in hydrothermal solutions at 200° to 350°. Econ. Geol. 71, 772-794.

_____, Susak H. J., Borcsik M., and Schartz S. (1978) Solubility of the buffer assemblage pyrite + pyrrhotite + magnetite in NaCl solutions from 200 to 350°C. Geochim. Cosmochim. Acta 42, 1427-1439.

Criss C. M. and Cobble C. W. (1964a) The thermodynamic properties of high temperature aqueous solutions. IV. Entropies of the ions up to 200° and the correspondence principle. J. Am. Chem. Soc. 86, 5385-5390.

_____ and _____ (1964b) The thermodynamic properties of high temperature aqueous solutions. V. The calculation of ionic heat capacities up to 200°. Entropies and heat capacities above 200°. J. Am. Chem. Soc. 86, 5390-5393.

Cuta F. and Strafelda F. (1954) The second dissociation constant of carbonic acid between 60 and 90°. Chem. Listy 48, 1308-1313.

Dellien I., Hall F. M. and Helper L. G. (1976) Chromium, molybdenum and tungsten: Thermodynamic properties, chemical equilibria and standard potentials. Chem. Rev. 76, 283-310.

Dunn L. A. and Marshall W. L. (1969) Electrical conductance of aqueous sodium iodide and the comparative thermodynamic behavior of aqueous sodium halide solutions to 800° and 4000 bars. J. Phys. Chem. 73, 723-728.

Elevatorski E. A. (1979) Molybdenum Resource Guide Book. MINOBRAS, 159 p.

Ellis A. J. (1959) The effects of pressure on the first dissociation constant of carbonic acid.  J. Chem. Soc. (Lond.), 3689-3699.

_____ (1963) The effects of temperature on the ionization of hydrofluoric acid.  J. Chem. Soc. (Lond.), 4300-4303.

_____ (1966) Partial molal volumes of alkali chlorides in aqueous solutions to 200°.  J. Chem. Soc. A (Lond.), 1579-1584.

_____ (1967) Partial molal volumes of $MgCl_2$, $CaCl_2$ and $BaCl_2$ in aqueous solution to 200°.  J. Chem. Soc. A (Lond.), 660-664.

_____ (1968) Partial molal volumes in high temperature water. part III. halides and oxyanion salts.  J. Chem. Soc. A (Lond.), 1138-1143.

_____ and Mahon W. A. J. (1964) Natural hydrothermal systems and experimental hot water/rock interactions.  Geochim, Cosmochim. Acta 28, 1323-1357.

_____ and McFadden I. M. (1968) The partial molal volume of hydrochloric acid in high temperature water.  Chem. Communications, 516.

Field C. W. (1966) Sulfur isotopic methods for discriminating between sulfates of hypogene and supergene origin.  Econ. Geol. 61, 1478-1485.

Flower G. C. (1979) Correction of Holloway's (1977) adaptation of the modified Redlich-Kwong equation of state for calculation of the fugacities of molecular species in supercritical fluids of geologic interest.  Contrib. Mineral. Petrol. 69, 315-318.

Franck E. U. (1961) Supercritical water as an electrolytic solvent. Angew. Chem. 73, 309-322.

Fredrickson D. R. and Chasanov M. G. (1971) The enthalpy of molybdenum disulfide to 1200 K by drop calorimetry.  J. Chem. Thermodynamics 3, 693-696.

Franks F. (1973) Water v. 3 Aqueous Solutions of Simple Electrolytes. New York, Plenum Press, 427 p.

Frantz J. D. and Popp R. K. (1979) Mineral-solution equilibria I. Experimental study of complexing and the thermodynamic properties of aqueous $MgCl_2°$ in the system $MgO - SiO_2 - H_2O - HCl$.  Geochim. Cosmochim. Acta 43, 1223-1239.

Friedman I., Redfield A. C., Schoen B. and Harris J. (1964) The variation of the deuterium content of natural waters in the hydrologic cycle.  Rev. Geophys. 2, 177-224.

Ganster M. W. (1976) Evidence for the localized accummulation of hydrothermal fluids at the Henderson molybdenum deposit, Colorado (abs.).  Geol. Soc. Am. An. Meeting 8, 880.

Gardner W. L. Jekel E. C. and Cobble J. W. (1969) The thermodynamic properties of high temperature aqueous solutions. IX. The standard partial molal heat capacities of sodium sulfate and sulfuric acid from 0 to 100°. J. Phys. Chem. 73, 2017-2020.

Graham R. L. and Helper L. G. (1956) Heats of formation of sodium molybdate, molybdic acid and aqueous molybdate ion. J. Am. Chem. Soc. 78, 4846-4848.

Griffith W. P. and Wickins T. D. (1967) Raman studies in aqueous solutions. part II. Oxy-species of metals of group VIA, VA, IVA. J. Chem. Soc. A (Lond.), 675-679.

Gunow A. W., Ludington P. and Munoz J. L. (1980) Fluorine in Micas from the Henderson molybdenite deposit, Colorado. Econ. Geol. 75, 1127-1137.

Haas J. L. and Fisher, J. R. (1976) Simultaneous evaluation and correlation of thermodynamic data. Am. J. Sci. 276, 525-545.

Hall W. E., Friedman I., and Nash J. T. (1974) Fluid inclusion and light stable isotope study of the Climax molybdenum deposits, Colorado. Econ. Geol. 69, 884-901.

Harned H. S. and Scholes S. R., Jr. (1941) The ionization constant of $HCO3^-$ from 0 to 50°. J. Am. Chem. Soc. 63, 1706-1709.

_____ and Davis R., Jr. (1943) The ionization of carbonic acid in water and the solubility of carbon dioxide in water and aqueous salt solutions from 0 to 50°. J. Am. Chem. Soc. 65, 2030-2037.

Helgeson H. C. (1964) Complexing and Hydrothermal Ore Deposits. Oxford, Pergamon Press, 128 p.

_____ (1967) Thermodynamics of complex dissociation in aqueous solutions at elevated temperatures. J. Phys. Chem. 71, 3121-3136.

_____ (1969) Thermodynamics of hydrothermal systems at elevated temperatures and pressures. Am. J. Sci. 267, 729-804.

_____ (1970) A chemical and thermodynamic model of ore deposition in hydrothermal systems, in: Fiftieth Annv. Symposia, B. A. Morgan (ed.). Min. Soc. Am. Spec. Paper 3, 133-186.

_____ (1971) Kinetics of Mass transfer among silicate and aqueous solutions. Geochim. Cosmochim. Acta 35, 421-469.

_____ (1982) Prediction of the thermodynamic properties of electrolytes at high pressure and temperatures, in: Chemistry and Geochemistry of Solutions at High Temperature and Pressures, D. Rickard and F. E. Wickman (eds.). Oxford, Pergamon Press, 133-177.

_____ and Aagaard P. (1979) A retroactive clock for geochemical processes (abs.). Geol. Soc. Am. An. Meeting 11, 442.

_____ and Kirkham D. H. (1974a) Theoretical prediction of the thermodynamic behavior of aqueous electrolytes at high pressure and temperatures: I. Summary of the thermodynamic/electrostatic properties of the solvent. Am. J. Sci. 274, 1089-1198.

_____ and _____ (1974a) Theoretical prediction of the thermodynamic behavior of aqueous electrolytes at high pressure and temperatures: II. Debeye-Huckel parameters for activity coefficients and relative partial molal properties. Am. J. Sci. 274, 1199-1261.

_____ and _____ (1976) Theoretical prediction of the thermodynamic behavior of aqueous electrolytes at high pressure and temperatures: III. Equation of state for aqueous species at infinite dilution. Am. J. Sci. 276, 97-240.

_____, _____ and Flower, G. (1981) Theoretical prediction of the thermodynamic behavior of aqueous electrolytes at high pressure and temperatures: IV. Calculation of activity and osmotic coefficients and apparent molal and standard and relative partial molal properties to 600°C and 5 Kb. Am. J. Sci. 281, 1249-1516.

_____, Brown T. H., Nigrini A., and Jones T. A. (1970) Calculation of mass transfer in geochemical processes involving an aqueous solution. Geochim. Cosmochim. Acta 34, 569-592.

_____, Delany J. M., Nesbitt H. W., and Bird D. K. (1978) Summary and critique of the thermodynamic properties of rock-forming minerals. Am. J. Sci. 278A, 229 p.

Hem J. D. (1968) Graphical methods for studies of aqueous aluminum hydroxide, fluoride and sulfate complexes. U. S. Geol. Survey Water-Supply Paper 1827B, 33 p.

Holland R. A. G., Bray C. J., and Spooner E. T. C. (1978) A method for preparing doubly polished thin sections suitable for microthermo-metric examination of fluid inclusions. Mineralogy Mag. 42, 407-408.

Holloway J. R. (1977) Fugacity and activity of molecular species in supercritical fluids, in: Thermodynamics in Geology, D. G. Frasher (ed.). Dordrecht, Holland, D. Reidel Publishing Co., 161-181.

Int. Crit. Tables of Numerical Data, Physics, Chemistry and Technology v. 4. (1928) E. W. Washburn (ed.), New York, McGraw-Hill, 481 p.

Ishihara S. (1967) Molybdenum mineralization in Questa mine New Mexico, U.S.A. Japan Geol. Survey Rept. 218, 64 p.

Isuk E. E. and Carnan J. H. (1981) The system $Na_2Si_2O_5 - K_2Si_2O_5 - MoS_2 - H_2$ with implications for molybdenum transport in silicate melts. Econ. Geol. 76, 2222-2235.

Ivanova G. F., Lavkina N. I., Nesterova L. A., Zhidikova A. P., and Khodakovskiy I. L. (1975) Equilibrium in the $MoO_3-H_2O$ system at 25-300°C. Geochem. Int. 12, no. 1, 163-176.

Jacob G. K. and Kerrick D. M. (1981) APL and FORTRAN programs for a new equation of state for $H_2O$, $CO_2$, and their mixtures at supercritical conditions. Computers and Geoscience 7, 131-143.

Karyakin Yu. V. and Kryachko E. N. (1967) Fluoro-complexes of Mo(VI) in dilute aqueous solutions. Russ. J. Inorg. Chem. 12, 1355-1357.

Keevil N. B. (1942) Vapor pressure of aqueous solutions at high temperatures. J. Am. Chem. Soc. 64, 841-850.

Kelley K. K. (1960) Contributions to the data on theoretical metallurgy. XIII, High temperature heat contents, heat capacity and entropy data for the elements and inorganic compounds. U.S. Bur. Mines Bull. 584, 232 p.

Kerker M. (1957) The ionization of sulfuric acid. J. Am. Chem. Soc. 79, 3664-3667.

Khitarov N. I., Arutyunyan L. A., and Ryzhenko B. N. (1965) The effects of hydrogen sulfide on the migration of molybdenum in the form of a silicomolybdenum complex under elevated temperatures. Geochem. Int. 2, 192-195.

Khodakovskiy I. L., Ryzhenko B. N., and Naumov G. B. (1968) Thermodynamics of aqueous electrolyte solutions at elevated temperater (Temperature dependence of the heat capacities of ions in aqueous solutions). Geochem. Int. 5, 1200-1219.

King E. G., Weller, W. W. and Christensen A. U. (1960) Thermodynamics of some oxides of molybdenum and tungsten. U.S. Bur. Mines Rept. Inv. 564, 29 p.

Klevtsov P. V. and Lemmlein G. G. (1959) Determination of minimum pressure of quartz formation as exemplified by crystals from the Pamir. Zap. Vses. Miner. Obshch. 85. 661-666.

Klotz I. M. and Rosenberg R. M. (1972) Chemical Thermodynamics, third ed. Reading, Mass., Benjamin/Cummings Publishing Co., 444 p.

Lagache M. and Weisbrod A. (1977) The system: two alkali feldspar - KCl - NaCl - $H_2O$ at moderate to high temperatures and pressures. Contr. Mineralogy Petrology, 62, 77-101.

Larsen E. S. and Ross C. S. (1920) The R. and S. molybdenum mine Taos County, New Mexico. Econ. Geol. 15, 567-573.

Larson H. R. and Elliott J. F. (1967) The standard free energies of formation of certain sulfides of some transition elements and zinc. Trans. AIME 293, 1713-1720.

Latimer W. M. (1954) The Oxidation State of the Elements and Their Potentials in Aqueous Solutions. Englewood, New Jersey, Prentice-Hall, Inc., 392 p.

Latimer W. M. and Jolly W. L. (1952) Heats and entropies of successive steps in the formation of $AlF_6^{3-}$. J. Am. Chem. Soc. 75, 1548-1550.

Laughlin A. W., Rehrig W. A. and Mauger R. L. (1969) K-Ar chronology and sulfur and strontium isotope ratios at the Questa Mine, New Mexico. Econ. Geol. 64, 903-909.

Lietzke M. H. and Stoughton R. W. (1961) The bisulfate acid constant from 25 to 225° as computed from solubility data. J. Phys. Chem. 65, 2247-2249.

Lipman P. W. (1981) Volcanic-tectonic setting of Tertiary ore deposits, southern Rocky Mountains, in: Relations of Tectonics to Ore Deposits in the Southern Cordillers, W. R. Dickinson and W. D. Payne (eds.). Ariz. Geol. Soc. Digest 14, 199-213.

Lyakhov Y. V. (1975) Errors in determining pressure of mineralization from gas - liquid inclusions with halite, their cause and ways of eliminating them. Zap. Vses. Miner. Obshch. 102, 385-393.

MacDonald A. J. and Spooner E. T. C. (1981a) Calibration of a Linkam TH 600 programmable heating - cooling stage for microthermometric examination of fluid inclusions. Econ. Geol. 76, 1248-1258.

_____ and _____ (1981b) Hydrothermal fluid flow and molybdenite transport in the Boss Mountain breccia pipe sheeted vein deposit, B. C. Geol. Assoc. Canada An. Meeting.

MacDonald G. A. (1972) Volcanoes. Englewood Cliffs, NJ, Prentice-Hall Inc., 510.

Maksinova I. N., Pravdiu N. N., and Razaraev V. E. (1976) Study of hydrolysis of sodium chromate, molybdate and tungstate in aqueous solutions at 15-90°. Uler. Khimii. Zh. 42, 1019-1023.

Martineau M. P., Heinemeyer G. R., Craig S. D., and McAndrews K. P. (1977) Geological Report: Questa Project 1975-1977. unpublished mine report, Questa Molybdenum Company.

Marshall W. L. (1967) Aqueous systems at high temperature. XX. The dissociation constants and thermodynamic functions for magnesium sulfate to 200°. J. Phys. Chem. 71, 3584-3588.

_____ (1972) Predictions of the geochemical behavior of aqueous electrolytes at high temperatures and pressures. Chem. Geol. 10, 59-68.

Mathews J. F. (1972) Critical constants of inorganic substances. Chem. Rev. 72, 71-100.

Matteoli E. (1980) Calculations of individual ionic partial molal volumes in water: A scaled particle theory approach. Zeits. Phys. Chem. 123, 141-149.

McGee K. A. and Hostetler P. B. (1975) Studies in the system $MgO-SiO_2-CO_2-H_2$ (IV): The stability of $MgOH^+$ from 10 to 90°C. Am. J. Sci. 275, 304-317.

McKinlay P. F. (1956) Geology of the Latir Peak and Costilla quadrangle, Taos County, New Mexico. N. Mex. Inst. Min. Tech., State Bur. Mines and Mineral Res. Bull. 42, 31 p.

_____ (1957) Geology of the Questa Quadrangle, Taos County, New Mexico. N. Mex. Inst. Min. Tech., State Bur. Mines and Mineral Res. Bull. 53, 31 p.

Mesmer R. E. and Baes C. F., Jr. (1974) Phosphoric acid dissociation equilibria in aqueous solutions to 300°C. J. Soln. Chem. 3, 307-322.

Miller G. R. and Kester D. R. (1976) Sodium fluoride ion pairs in sea water. Mar. Chem. 4, 67-82.

Millero F. J. (1971) The molal volume of electrolytes. Chem. Rev. 71, 147-176.

_____ (1972) The partial molal volumes of electrolytes in aqueous solutions, in: Water and Aqueous Solutions, R. A. Horne (ed.). New York, Wiley-Interscience. 519-595.

Munoz J. L. (1980) Determination of the relative HCl and HF activities in hydrothermal systems from biotite analyses (abs.). Geol. Soc. Am. An. Meeting 12, 489.

Nair V. K. S. and Nancollas G. H. (1958) Thermodynamics of ion association. Part V. Dissociation of the bisulfate ion. J. Chem. Soc. (Lond.), 4144-4147.

Nash J. T. (1976) Fluid inclusion petrology-data from porphyry copper deposits and applications to exploration. U.S. Geol. Survey Prof. Paper 907-D, 16 p.

Naumov G. B., Ryzhenko B. N. and Khodakovskiy (1974) Handbook of Thermodynamic Data (trans. from Russian original, 1971). Nat. Tech. Info. Services PB-226-722, 328 p.

Nazarenko V. A. and Shelikhina E. I. (1971) Spectrophotometric determination of the formation constants of mono-nuclear hydroxo-complexes of molybdenum (VI). Russ. J. Inorg. Chem. 16, 88-90.

Nordstrom D. K. and Jenne E. A. (1977) Fluorite solubility equilibrium in selected geothermal waters. Geochim. Cosmochim. Acta 41, 175-188.

Norman D. I. (1977) Geology and geochemistry of Tribag Mine, Batchawana Bay, Ontario. Ph.D. Thesis, Univ. of Minnesota, Minneapolis, Minn., 257 p.

_____ and Palin J. M. (1982) Volatiles in phyllosilicate minerals. Nature 296, 551-553.

Norton D. and Knight J. (1977) Transport phenomena in hydrothermal systems: Cooling plutons. Am. J. Sci. 277, 937-981.

Noyes A. A., Kato Y., and Sosmam R. B. (1910) The hydrolysis of ammonium acetate and the ionization of water at high temperatures. J. Am. Chem. Soc. 32, 159-178.

O'Hare P. A. G., Benn E., Cheng F. Y., and Kuzmyca G. (1970) A fluorine bomb calorimetric study of molybdenum disulfide. The standard enthalpies of formation of di- and sesquisulfide of molybdenum. J. Chem. Thermodynamics 2, 797-804.

_____ and Hoekstra H. R. (1974) Thermochemistry of molybdates. II. Standard enthalpies of formation of rubidium molybdate and the aqueous molybdate ion. J. Chem. Thermodynamics 6, 117-122.

Olofsson I. V., Spitzer J. J., and Helper, L. G. (1978) Apparent molar heat capacities and volumes of aqueous electrolytes at 25°C: $Na_2SO_4$, $K_2SO_4$, $Na_2S_2O_3$, $Na_2S_2O_8$, $K_2CrO_4$, $Na_2MoO_4$ and $Na_2WO_4$. Can. J. Chem. 56, 1871-1873.

Ohmoto H. (1979) Isotopes of sulfur and carbon, in Geochemistry of Hydrothermal Ore Deposits, H. L. Barnes (ed). New York, Wiley-Interscience, 509-567.

O'Neil J. R. and Taylor H. P., Jr. (1969) Oxygen isotope equilibrium between muscovite and water. J. Geophys. Res. 74, 6012-6022.

Pauling L. (1952) Interatomic distances and the bond character in oxygen acids and related substances. J. Phys. Chem. 56, 361-365.

Pillmore C. L., Obradovich J. D., Landreth J. O., and Pugh L. E. (1973) Mid-tertiary volcanism in the Sangre de Cristo Mountains of northern New Mexico (abs.). Geol. Soc. Am. Rocky Mount. Sect. Meeting 5, 502.

Popp R. K. and Frantz J. D. (1979) Mineral-solutions equilibria II. An experimental study of mineral solubility and thermodynamic properties of aqueous $CaCl_2$ in the system $CaO - SiO_2 - H_2 - HCl$. Geochim. Cosmochim. Acta 43, 1777-1790.

Potter R. W., Clynne M. A. and Brown D. L. (1978) Freezing point depression of aqueous sodium chloride solutions. Econ. Geol. 73, 284-285.

Powell R. E. and Latimer W. M. (1951) The entropy of aqueous solutes. J. Chem. Phys. 19, 1139-1142.

Putnam B. R., III (1980) Fluid inclusion and microchemical analysis of the Hansonburg Mississippi Valley - Type ore deposit in central New Mexico. M. S. Thesis, N. Mex. Inst. Min. Tech., Socorro, N. Mex., 126 p.

Quist A. S. and Marshall W. L. (1966) Electrical conductances of aqueous solutions at high temperatures and pressures. III. The conductance of potassium bisulfate solutions from 0 to 700° and pressures to 4000 bars. J. Phys. Chem. 70, 3714-3725.

_____ and _____ (1968a) Electrical conductances of aqueous sodium chloride solutions from 0 to 800° and pressures to 400 bars. J. Phys. Chem. 72, 684-703.

_____ and _____ (1968b) Ionization equilibria in ammonia - water solutions to 700°C and 4000 bars pressure. J. Phys. Chem. 72, 3122-3128.

_____ and _____ (1969) The electrical conductance of some alkali metal halides in aqueous solutions from 0 to 800°C and at pressures to 4000 bars. J. Phys. Chem. 73, 978-985.

_____ and _____ (1970) Electrical conductance of aqueous potassium nitrate and tetra-methylammonium bromide solutions to 800°C and 4000 bars. J. Chem. Engin. Data 15, 375-375.

_____, Franck E. U., Jolley H. R., and Marshall W. L. (1963) The electrical conductance of aqueous solutions at high temperature and pressure: I. The conductance of potassium sulfate solutions from 25 to 800° and at pressures up to 4000 bars. J. Phys. Chem. 67, 2453-2459.

_____, Marshall W. L., and Jolley H. R. (1965) Electrical conductance of aqueous solutions at high temperature and pressure. II. The conductance and ionization constants of sulfuric acid solutions from 0 to 800° and pressures up to 4000 bars. J. Phys. Chem. 69, 2726-2735.

Reed A. J. (1975) The first ionization constant of carbonic acid from 25 to 250°C and to 2000 bars. J. Sol. Chem. 4, 53-70.

Redlich O. and Kwong J. N. S. (1949) On the thermodynamics of solutions. V. An equation of state. Fugacities of gaseous solutions. Chem. Rev. 44, 233-244.

Richardson C. K. and Holland H. D. (1979a) The solubility of fluorite in hydrothermal solutions, an experimental study. Geochim. Cosmochim. Acta 43, 1313-1325.

_____ and _____ (1979b) Fluorite deposition in hydrothermal systems. Geochim. Cosmochim. Acta 43, 1327-1325.

Robie R. A., Hemingway B. S., and Fisher J. R. (1978) Thermodynamic properties of minerals and related substances at 298.15 K and 1 bar ($10^5$ pascals) pressure and at higher temperatures. U.S. Geol. Survey Bull. 1452, 456 p.

Roedder R. E. (1971) Fluid inclusion studies on porphyry type ore deposits at Bingham, Utah, Butte, Montana, and Climax, Colorado. Econ. Geol. 66, 98-120.

_____ (1979) Fluid inclusions as samples of ore fluids, in: Geochemistry of Hydrothermal Ore Deposits, H. L. Barnes (ed.). New York, Wiley-Interscience, 684-737.

_____ and Bodnar R. J. (1980) Geologic pressure determinations from fluid inclusion studies. Ann. Rev. Earth Planet. Sci. 8, 263-301.

Rogers P. S. Z. and Pitzer K. S. High temperature thermodynamic properties of aqueous sodium sulfate. J. Phys. Chem. 85, 2886-2895.

Romberger S. B. and Barnes H. L. (1970) Ore solution chemistry III. solubility of CuS in sulfide solutions. Econ. Geol. 65, 920-936.

Ryzhenko B. N. (1963) Determination of the dissociation constants of carbonic acid and the degree of hydrolysis of the $CO_3^{2-}$ and $HCO_3^-$ ion in solutions of alkali carbonates and bicarbonates at elevated temperatures. Geochem. no. 2, 151-164.

_____ (1964) Determination of the second dissociation constant of sulfuric acid and the precipitation of salts in the reciprocal system: $Ca^{2+}$, $Ba^{2+}$ $SO_4^{2-}$, $CO_3^{2-}$ under hydrothermal conditions. Geochem. Int. 1, 8-13.

_____ (1965) Determination of the dissociation constant of hydrofluoric acid and the conditions of replacement of calcite by fluorite. Geochim. Int. 2, 196-199.

Sasaki Y. and Sillen L. G. (1968) Equilibrium studies of polyanions XVI. Equilibriums of molybdates in 3 M sodium perchlorate medium at 25°C. Ark. Keni 29, 253-257.

Schaefer S. C. and Goken N. A. (1980) Electrochemical determination of thermodynamic properties of Molybdenite ($MoS_2$). High Temp. Sci. 12, 267-276.

Schilling J. H. (1956) Geology of the Questa molybdenum (Moly) Mine area, Taos County, New Mexico. N. Mex. Bur. Min. Mineral Resources Bull. 51, 87 p.

Seward T. M. (1976) The stability of chloride complexes of silver in hydrothermal solutions up to 350°C. Geochim. Cosmochim. Acta 40, 1329-1341.

Shepherd T. J. (1981) Temperature-programmable, Heating - Freezing stage for microthermometric analysis of fluid inclusions. Econ. Geol. 76. 1244-1247.

Sheppard S. M. F., Nielsen R. L. and Taylor H. P., Jr. (1971) Hydrogen and oxygen isotope ratios in minerals from porphyry copper deposits. Econ. Geol. 66, 515-542.

_____ and Taylor H. P., Jr. (1974) Hydrogen and oxygen isotope evidence for the origin of water in the Boulder Batholith and the Butte ore deposit, Montana. Econ. Geol. 69, 926-946.

Shieh Y. N. and Schawarcz H. P. (1974) Oxygen isoteope studies of granite and migmatite, Grenville Province of Ontario, Canada. Geochim. Cosmochim. Acta 38, 21-45.

Sillitoe R. H. (1980) Types of porphyry molybdenum deposits. Mining Mag. 142, 550-553.

Sillen L. and Martell A. E. (1964) Stability constants of metal-ion complexes. Chem. Soc. (Lond.) Spec. Paper 17, 754 p.

Skinner B. J. (1966) Thermal expansion, in: Handbook of Physical Constants, S. P. Clark, Jr. (ed.). Geol. Soc. Am. Mem. 97, 78-96.

Sokolova N. T. and Khodakovskiy, I. L. (1977) The mobility of aluminim in hydrothermal systems. Geochem. Int. 14 no. 3, 105-112.

Sourirajan S. and Kennedy G. C. (1962) The system $H_2O-NaCl$ at elevated temperatures and pressures. Am. J. Sci. 260, 115-141.

Smith R. M. and Martell A. E. (1976) Critical Stability Constants V. 4. New York, Plenum Press, 257 p.

Smith R. W., Norman D. I., and Popp C. J. (1980) Calculated solubility of molybdenite in hydrothermal solutions (abs.). Geol. Soc. Am. An. Meeting 12, 525.

_____ and Putnam B. R., III (1981) Stability of lead fluoride complexes at elevated temperatures (abs.). New Mexico Geol. 3, 45.

Stubbles J. R. and Richardson F. D. (1960) Equilibria in the system molybdenum + sulfur + hydrogen. Trans. Faraday Soc. 56, 1460-1466.

Stull D. R. and Prophet H. (1971) JANAF Thermochemical Tables. Nat. Stand. Ref. Data Ser. Nat. Bur. Stand. 37, 1141 p.

Tanner S. P., Walker J. B., and Choppin G. R. (1968) Thermodynamic parameters of the alkaline earth mono-fluorides. J. Inorg. Nucl. Chem. 30, 2067-2070.

Taylor H. P., Jr. (1974) The application of oxygen and hydrogen isotope studies to problems of hydrothermal alteration and ore deposition. Econ. Geol. 69, 843-883.

_____ (1979) Oxygen and hydrogen isotope relationships in hydrothermal mineral deposits, in: Geochemistry of Hydrothermal Ore Deposits, H. L. Barnes (ed.). New York, Wiley-Interscience, 236-277.

_____ and Magaritz M. (1978) Oxygen and hydrogen isotope studies of the Cordillerian batholiths of western North America, in: Stable Isotopes in the Earth Sciences, B. W. Robinson (ed.). N. Zealand Dept. Sci. Ind. Res. Bull. 220, 151-173.

Titley S. R. (1963) Some behavioral aspects of molybdenum in the supergene environment. Trans. AIME 226, 199-204.

Tugarinov A. I., Khodakovskiy, I. L., and Zhidikova A. P. (1973) Physicochemical conditions for molybdenite production in hydrothermal uranium-molybdenum deposits. Geochem. Int. 10, 731-739.

Urusova, M. A. (1975) Volume properties of aqueous solutions of sodium chloride at elevated temperatures and pressures. Russ. J. Inorg. Chem. 20, 1717-1721.

Vanderwilt J. W. (1938) Geology of the Questa molybdenite deposit, Taos County, New Mexico. Colo. Sci. Soc. Proc. 13, 599-643.

Vlek P. L. G. and Lindsay W. L. (1977) Thermodynamic stability of molybdenum minerals in soils. Soil Sci. Soc. Am. J. 41, 42-46.

Walther J. V. and Helgeson H. C. (1977) Calculations of the thermodynamic properties of aqueous silica and the solubility of quartz and its polymorphs at high pressures and temperatures. Am. J. Sci. 277, 1315-1351.

Wagman D. D., Evans W. H., Parker V. P., Halow I. Bailey S. M., and Schumm R. H. (1968) Selected values of chemical thermodynamic properties. Nat. Bur. Stand. Tech. Note 270-3.

Westra G. and Keith S. B. (1981) Classification and genesis of stockwork molybdenum deposits. Econ. Geol. 76. 844-897.

Westrich H. R. (1974) The solubility of molybdenite in pH buffered KCl-HCl fluids (abs.). EOS (Trans. Am. Geophys. Union) 56, 1200.

White W. H., Brookstrom A. A., Kamilli R. J., Ganster M. W., Smith R. P., Ranta D. E., and Steininger R. C. (1981) Character and origin of Climax-type molybdenum deposits. Econ. Geol. 75th Annv. Vol., 270-316.

Wissburn K. F., French D. M., and Paterson A., Jr. (1954) The true ionization constant of carbonic acid in aqueous solutions from 5 to 45°. J. Phys. Chem. 58, 693.

Yeatts L. B. and Marshall W. L. (1969) Apparent invariance of the activity coefficients of calcium sulfate at constant ionic strength and temperature in the system $CaSO_4$ - $Na_2SO_4$ - $NaNO_3$ - $H_2O$ to the critical temperature of water: association equilibria. J. Phys. Chem. 73, 81-90.

Zhidikova A. P. and Khodakovskiy I. L. (1971) The activity product of powellite at 25°C, (abs.). Geochem. Int. 8, 306.

_____ and Kuskov O. L. (1971) Determination of the thermodynamic constants of calcium molybdate (powellite) and sodium molybdate. Geochem. Int. 8, 722-724.

_____ and Malinin S. D. (1972) solubility of powellite, $CaMoO_4$, in aqueous NaCl at 50 to 300°C. Geochem. Int. 9, 21-27.

_____, Khodakovskiy I. L., Urusova M. A., and Valysashko V. M. (1973) Experimental determination of the activity coefficients of sodium molybdate in aqueous solutions at 25° and 300°C. Russ. J. Inorg. Chem. 18, 612-615.

Zhu J. and Barnes H. L. (1981) Geochemical conditions of tin mineralization. Geol. Soc. Am. An. Meeting 13, 587.